

**THE REPUBLIC OF TURKEY
HARRAN UNIVERSITY
GRADUATE SCHOOL OF
APPLIED AND NATURAL SCIENCES**

DOCTOR OF PHILOSOPHY (PhD) THESIS

**CLINICAL AND ENVIRONMENTAL APPLICATIONS OF
ELECTROCHEMICAL SENSORS BASED ON CARBON NANOTUBES**

Ayşegül KUTLUAY BAYTAK

DEPARTMENT OF CHEMISTRY

**ŞANLIURFA
2014**

CONTENTS

	Page No
ÖZET	i
ABSTRACT	iii
ACKNOWLEDGEMENT	v
LIST of FIGURES	vi
LIST of TABLES	xi
LIST of SCHEMES	xii
NOMENCLATURE	xiii
1. INTRODUCTION	1
2. REVIEW of LITERATURE	5
2.1. Clinical and Pharmaceutical Applications of Electrochemical Sensors Based on CNTs.....	5
2.2. Environmental Applications of Electrochemical Sensors Based on CNTs.....	20
3. MATERIAL and METHOD	27
3.1. Instrumentation.....	27
3.2. Reagents.....	28
3.3. The Samples Used for Analytical Applications	29
3.4. Preparation of Used Standard Stock Solutions.....	30
3.5. Preparation of Used Real Samples for Analytical Applications.....	31
3.6. Preparations of Carbon Nanotubes Based Modified Electrodes	33
3.6.1. Pre-treating of glassy carbon electrode	33
3.6.2. Preparation of MWCNT- modified electrodes.....	34
3.6.3. Preparation of poly(pivalic acid)/MWCNT modified electrodes.....	34
3.6.4. Preparation of poly(pivalic acid)/CoNPs/MWCNT modified electrodes	34
3.6.5. Preparation of CoNPs/MWCNT modified GCE	35
3.6.6. Preparation of NiNPs/MWCNT modified Pt electrode.....	36
3.6.7. Preparation of Chitosan-MWCNT modified GCE.....	37
4. RESULTS and DISCUSSIONS	39
4.1. Voltammetric Detection of Paracetamol (PAR) in the Presence of Ascorbic Acid (AA), Dopamine (DA) and Uric Acid (UA) with Using MWCNT Modified GCE	39
4.1.1. Surface characterizations of bare GCE and MWCNT modified GCE.....	41
4.1.2. Voltammetric behaviour of paracetamol at bare GCE and MWCNT modified GCE...	41
4.1.3. The effect of pH on the voltammetric behaviour of PAR at MWCNT modified GCE	45
4.1.4. Calibration equation for the determination of paracetamol.....	49
4.1.5. Reproducibility and stability of modified electrode.....	52
4.1.6. Detection of paracetamol in the presence of AA, DA and UA	53
4.1.7. Determination of paracetamol in pharmaceutical preparations.....	56
4.2. Selective Voltammetric Detection of Albuterol in the Presence of Uric Acid Using a Glassy Carbon Electrode Modified with MWCNTs and poly(pivalic acid).....	56
4.2.1. The characterization of SEM images	58
4.2.2. Voltammetric behaviour of albuterol and uric acid.....	59
4.2.3. The effect of pH on the voltammetric behaviour of uric acid and albuterol at PPA/MWCNT/GCE	65
4.2.4. Calibration equation for the determination of albuterol.....	68
4.2.5. Reproducibility and stability of modified electrode.....	72
4.2.6. Detection of albuterol in the presence of UA.....	72
4.2.7. Analytical Applications	75
4.3. MWCNTs/Electro-Copolymerized Cobalt Nanoparticles-Poly(pivalic acid) Composite Film Coated Glassy Carbon Electrode for the Voltammetric Determination of Methimazole	78
4.3.1. Surface characterization of the modified electrode.....	80
4.3.2. Voltammetric behaviour of methimazole.....	84
4.3.3. The effect of pH on the voltammetric behaviour of methimazole	89
4.3.4. Calibration equation for the determination of methimazole	91
4.3.5. Reproducibility and stability of modified electrode.....	92
4.3.6. Determination of methimazole in thyromazol tablets	93

4.4. Nickel Nanoparticles Functionalized Multi-Walled Carbon Nanotubes at Platinum Electrodes for the Detection of Bromhexine	94
4.4.1. Characterization of modified electrode	96
4.4.2. Voltammetric behavior of bromhexine	98
4.4.3. The effect of pH on the voltammetric behaviour of bromhexine	104
4.4.4. Calibration equation for the determination of bromhexine	105
4.4.5. Reproducibility and stability of modified electrode	106
4.4.6. Determination of bromhexine in tablets	107
4.5. Cobalt Nanoparticles Functionalized Multi-Walled Carbon Nanotubes at GCE for the Simultaneous Determination of Paracetamol and Dopamine.....	107
4.5.1. Surface characterization of the modified electrode	110
4.5.2. Voltammetric behaviour of paracetamol and dopamine	111
4.5.3. Determinations of PAR and DA.....	118
4.5.4. Reproducibility, stability and repeatability of modified electrode.....	127
4.5.5. Determination of drugs in pharmaceutical preparations	128
4.6. Simultaneous Determination of Cd(II) and Pb(II) at Chitosan-MWCNT modified Glassy Carbon Electrode by Square Wave Anodic Stripping Voltammetry	131
4.6.1. SEM images of modified electrodes	133
4.6.2. Procedure of detection for Cd(II) and Pb(II).....	134
4.6.3. Working mechanism of the CTS-MWCNT modified GC electrodes	134
4.6.4. Effects of electrolyte and pH.....	135
4.6.5. Effects of accumulation potential and accumulation time	136
4.6.6. Effect of the mass of the modifiers	137
4.6.7. Square wave anodic stripping voltammograms of Cd(II) and Pb(II).....	138
4.6.8. Calibration equation of Cd(II) in the absence of Pb(II)	140
4.6.9. Calibration equation of Pb(II) in the absence of Cd(II)	141
4.6.10. Simultaneous determination of Cd(II) and Pb(II)	143
4.6.10. Stability, reproducibility and repeatability of CTS-MWCNT/GCE	146
4.6.11. Interference studies.....	147
4.6.12. Analytical Applications	147
5. CONCLUSION and SUGGESTIONS	149
REFERENCES	154
CURRICULUM VITAE.....	173

ÖZET

Doktora Tezi

KARBON NANOTÜP TEMELLİ ELEKTROKİMYASAL SENSÖRLERİN KLİNİK VE ÇEVRE UYGULAMALARI

Ayşegül KUTLUAY BAYTAK

Harran Üniversitesi
Fen Bilimleri Enstitüsü
Kimya Anabilim Dalı

Danışman: Prof. Dr. Mehmet ASLANOĞLU
Yıl: 2014, Sayfa:175

Bu çalışmada, karbon nanotüp temelli elektrokimyasal sensörler kullanılarak klinik, farmasötik ve çevre örneklerinde bulunan bazı önemli maddelerin hızlı, güvenilir, duyarlı ve seçimli bir şekilde saptanması için elektroanalitik yöntemler geliştirilmiştir.

Parasetamolün askorbik asit, dopamin ve ürik asit varlığında seçimli bir şekilde saptanması için bir camlı karbon elektrot (GCE) çok duvarlı karbon nanotüp (MWCNT) ile modifiye edilmiştir. Bu modifiye elektrot 0.1 M pH 7.0 fosfat tampon çözeltisi içinde kare dalga voltametri kullanılarak parasetamolün saptanması için kullanılmıştır. Sonuçlar parasetamolün pik akımlarının 2.0×10^{-10} M ve 1.5×10^{-5} M derişim aralığında doğrusal ve saptama sınırının 9.0×10^{-11} M olduğunu göstermiştir. Bu metod ilaçlardaki parasetamolün saptanması için başarıyla uygulanmıştır.

MWCNT ve poly (pivalic acid) (PPA) ile modifiye edilen GCE, ilaçlarda ve doping kontrol amaçlı olarak idrar numunelerinde seçimli bir albuterol saptaması için kullanılmıştır. Bu modifiye elektrot

(PPA/MWCNT/GCE) idrar numunelerinin aşırı miktarda ürik asit (UA) ihtiva etmesi nedeniyle UA varlığında albuterolün saptanması için uygulanmıştır. Bu modifiye elektrot 0.1 M pH 8.0 fosfat tampon çözeltisi içinde kare dalga voltametri kullanılarak albuterolün saptanması için kullanılmıştır. Pik akımları 5.0×10^{-8} - 7.0×10^{-5} M aralığındaki albuterolün derişimiyle doğrusal olarak artmaktadır ve saptama sınırı 1.2×10^{-8} M'dir. Önerilen bu metod, farmasötik ve idrar numunelerinde bulunan albuterolün saptanması için uygulanmıştır.

Methimazolün saptanması için MWCNT/elektro-kopolimerizasyonla elde edilen kobalt nanoparçacık-poli (pivalik asit) kompozit ile modifiye edilen camlı karbon elektrot temelli tekrarlanabilir bir voltametrik metod geliştirilmiştir. Bu modifiye elektrot 0.1 M pH 7.2 PBS içinde methimazolün saptanması için kullanılmıştır. Pik akımları 1.0×10^{-7} - 3.0×10^{-4} M aralığındaki methimazolün derişimiyle doğrusal olarak artmaktadır ve korelasyon katsayısı 0.9996'dır. Saptama sınırı 9.36×10^{-9} M (S/N=3)'dir. Bu önerilen metod, thyramozol tabletlerinde bulunan methimazolün saptanması için başarıyla uygulanmıştır.

Nikel nanoparçacıklarıyla fonksiyonelleştirilen çok duvarlı karbon nanotüpler bir platin elektrodun modifikasyonu için kullanılmıştır. Bu modifiye elektrot 0.1 M pH 4.0 PBS içinde bromheksinin saptanması için kullanılmıştır. Pik akımları 5.0×10^{-6} - 2.3×10^{-4} M aralığındaki bromheksinin derişimiyle doğrusal olarak artmaktadır ve korelasyon katsayısı 0.9999'dır. Saptama sınırı 3.0×10^{-6} M (S/N=3)' dir. Bu önerilen metod, farmasötik formüllerde bulunan bromheksinin saptanması için başarıyla uygulanmıştır.

Kobalt nanoparçacıklarıyla fonksiyonelleştirilen çok duvarlı karbon nanotüpler bir GC elektrodun modifikasyonu için kullanılmıştır. Bu önerilen elektrot parasetamolün ve dopaminin eş zamanlı

olarak saptanması için uygulanmıştır. Bunun yanı sıra, potansiyel ilaç girişimcileri olan askorbik asit ve ürik asit parasetamolün ve dopaminin voltametrik yanıtını etkilememiştir. Yükseltgenme pik akımları $5.2 \times 10^{-9} \sim 4.5 \times 10^{-7} \text{ M}$ ($R^2 = 0.9987$) ve $5.0 \times 10^{-8} \sim 3.0 \times 10^{-6} \text{ M}$ ($R^2 = 0.9999$) derişim aralığında sırasıyla parasetamol ve dopamin için doğrusaldır. Saptama sınırları PAR ve DA için sırasıyla, $1.0 \times 10^{-9} \text{ M}$ ve $1.5 \times 10^{-8} \text{ M}$ 'dir. Bu önerilen metod, ilaç numunelerinde bulunan PAR ve DA'nın saptanması için başarıyla uygulanmıştır.

Cd(II) ve Pb(II)'nin eş zamanlı olarak saptanması için bir camı karbon elektrot Kitosan ve MWCNT kompozit ile modifiye edilmiştir. Cd(II) ve Pb(II) negatif bir potansiyelde (-1.2 V) ve CTS-MWCNT karışımıyla kompleksleşerek modifiye elektrot yüzeyinde bir ön deriştirme yapılı. Daha sonra indirgenen ürünler kare dalga sıyırma voltametri ile yükseltgenilmektedir. Uygun şartlar altında, kalibrasyon grafiđi Cd(II) ve Pb(II) için sırasıyla 0.1 nM-2.5 nM ve 0.1 nM-1.8 nM derişim aralığında doğrusaldır. S/N=3 ve ön deriştirmenin 120 s olduđu durumda, saptama sınırları Cd(II) için 0.035 nM ve Pb(II) için 0.030 nM olarak hesaplanmıştır. Geri kazanım çalışmaları su, idrar ve gıda örneklerinde gerçekleştirilmiştir.

ANAHTAR KELİMELELER; Elektrokimyasal sensör, karbon nanotüp, voltametri, modifiye elektrot, voltametrik saptama

ABSTRACT

PhD Thesis

CLINICAL AND ENVIRONMENTAL APPLICATIONS OF ELECTROCHEMICAL SENSORS BASED ON CARBON NANOTUBES

Ayşegül KUTLUAY BAYTAK

Harran University
Graduate School of Natural and Applied Sciences
Department of Chemistry

Supervisor: Prof. Dr. Mehmet ASLANOĞLU
Year: 2014, Page:175

In this study, electroanalytical methods were developed for rapid, reliable, sensitive and selective determination of some important analytes in clinical, pharmaceutical and environmental samples using electrochemical sensors based on multi-walled carbon nanotubes (MWCNTs).

A glassy carbon electrode (GCE) was modified with MWCNTs for selective detection of paracetamol (PAR) in the presence of ascorbic acid, dopamine and uric acid. The modified electrode was used for the determination of PAR using square wave voltammetry in 0.1 M phosphate buffer solution (PBS) at pH 7.0. The results showed that the peak currents were proportional to the concentrations of PAR with a linear dynamic range of 2.0×10^{-10} M to 1.5×10^{-5} M and a detection limit of 9.0×10^{-11} M was obtained. The method was successfully applied for the determination of PAR in pharmaceuticals.

A selective detection of albuterol was carried out in pharmaceuticals and urine samples for doping control purposes using a GCE modified with MWCNT and poly (pivalic acid) (PPA). The modified electrode (PPA/MWCNT/GCE) was applied for the detection of albuterol in the presence of uric acid (UA) since the urine samples contain excess amount of UA. The PPA/MWCNT/GCE was used for the determination of albuterol using square wave voltammetry in 0.1 M PBS at pH 8.0. The peak current increased linearly with the concentration of albuterol in the range of 5.0×10^{-8} - 7.0×10^{-5} M with a detection limit of 1.2×10^{-8} M. The proposed method was employed for the determination of Albuterol in pharmaceutical and urine samples.

A reproducible voltammetric method was developed for the determination of methimazole based on the modification of a glassy carbon electrode with MWCNT/electro-copolymerized cobalt nanoparticles-poly(pivalic acid) composite. The modified electrode was used for the determination of methimazole in 0.1 M PBS at pH 7.2. The peak current increased linearly with the concentration of methimazole in the range of 1.0×10^{-7} - 3.0×10^{-4} M with a correlation coefficient of 0.9996. The detection limit was 9.36×10^{-9} M (S/N=3). The proposed method was successfully applied to the determination of methimazole in thyramazol tablets.

MWCNTs functionalized by nickel nanoparticles was used for modification of a platinum electrode. The modified electrode was used for the determination of bromhexine in 0.1 M PBS at pH 4.0. The peak current increased linearly with the concentration of bromhexine in the range of 5.0×10^{-6} to 2.3×10^{-4} M with a correlation coefficient of 0.9999. The detection limit was 3.0×10^{-6} M (S/N=3). The proposed method was successfully applied to the determination of bromhexine in pharmaceutical formulations.

MWCNTs functionalized by cobalt nanoparticles was used for modification of a GC electrode. The proposed electrode has been applied for the simultaneous determination of PAR and Dopamine (DA). On the other hand, the presence of potential drug interfering compounds AA and UA does not affect the voltammetric responses of PAR and DA. The current of oxidation peaks

showed a linear dependent on the concentrations of PAR and DA in the range of $5.2 \times 10^{-9} \sim 4.5 \times 10^{-7}$ M ($R^2 = 0.9987$) and $5.0 \times 10^{-8} \sim 3.0 \times 10^{-6}$ M ($R^2 = 0.9999$), respectively. The detection limits of 1.0×10^{-9} M and 1.5×10^{-8} M were obtained for PAR and DA, respectively. The proposed method was successfully applied to the determination of PAR and DA in pharmaceuticals.

A glassy carbon electrode (GCE) was modified with Chitosan (CTS) and MWCNT composite for the simultaneous determination of Cd(II) and lead(II). Cd(II) and Pb(II) were preconcentrated on the surface of the modified electrode by complexing with CTS-MWCNT mixture and reduced at -1.2 V. Then the reduced products were oxidized by square wave anodic stripping voltammetry. Under the optimized working conditions, peak currents were linear in the concentration ranges 0.1 nM-2.5 nM for Cd(II) and 0.1 nM-1.8 nM for Pb(II) in the same solution. The detection limits were calculated as 0.035 nM for Cd(II) and 0.030 nM for Pb(II) using a preconcentration time of 120 s (S/N=3). The recovery studies were also carried out with samples of water, human urine and nutrition.

KEYWORDS: Electrochemical sensor, carbon nanotube, voltammetry, modified electrode, voltammetric detection

ACKNOWLEDGEMENT

I would like to express my thoughtful appreciation and regards my advisor, Prof. Dr. Mehmet ASLANOĞLU. His professional expertise, guidance and generous help during the process of my thesis have great effect to come out with this piece of research.

I am sincerely gratefull to Prof. Dr. M. İrfan YEŞİLNACAR and Assoc. Prof. Dr. Mahmut ULUSOY for their positive and critical feedbacks. I also like to thank Assoc. Prof. Dr. Sıtkı BAYTAK for his encouragements and constructive suggestions.

All my collagugaes and professors at the Chemistry Department also deserve many thanks for their helpful ideas.

I would like to thank HÜBAK, Research Center at Harran University for their support.

Throughout the duration of this thesis, I have especially thankfull to my beloved husband Ahmet Baytak, my lovely son Mahmut Etkä and upcoming son Hasan Eren.

I would not forget every kind of support from my father, my mother and my special sisters. Thank you all.

LIST of FIGURES

	Page No
Figure 3.1. Schematic illustration for the stepwise preparation of poly (pivalic acid)/ CoNPs/MWCNT/GCE	35
Figure 3.2. Schematic illustration for the stepwise preparation of functional MWCNTs and synthesis of CoNPs-MWCNTs composite.....	37
Figure 4.1. SEM images of bare GCE (a) and MWCNT modified GCE (b).....	42
Figure 4.2. Cyclic voltammograms of 1.0×10^{-6} M PAR at bare GCE in 0.1 M PBS at pH 7.0. Scan rates increasing from 25 mV/s to 150 mV/s. a) 25 mV/s; b) 50 mV/s; c) 75 mV/s; d) 100 mV/s; e) 125 mV/s; f) 150 mV/s. Equilibrium time: 5 s.....	43
Figure 4.3. A plot of anodic peak currents of PAR versus scan rates at the bare GCE.....	44
Figure 4.4. Cyclic voltammograms of 1.0×10^{-6} M PAR at 0.15 μ g MWCNT/GCE in 0.1 M PBS at pH 7.0. Scan rates increasing from (a) 25 to (g) 175 mV/s. Equilibrium time:5 s	45
Figure 4.5. Cyclic voltammograms of 1.0×10^{-6} M PAR in 0.1 M PBS at pH 7.0 at a GC electrode modified with 0.00 μ g (a), 0.025 μ g (b), 0.1 μ g (c) and 0.15 μ g (d) MWCNTs. Scan rate: 100 mV/s. Equilibrium time:5 s	46
Figure 4.6. Plot of peak potentials of 1.0×10^{-6} M PAR solution vs. mass of MWCNTs on the electrode surface.....	47
Figure 4.7. Cyclic voltammograms of 1.5×10^{-6} M PAR at 0.15 μ g MWCNT/GCE in 0.1 M PBS at different pH values. pH: 3.0; 4.0; 5.0; 6.0; 7.0; 8.0; 9.0. Scan rate: 100 mV/s. Equilibrium time: 5 s.....	48
Figure 4.8. A plot of anodic peak potentials of PAR vs. solution pH at 0.15 μ g MWCNT/GCE	49
Figure 4.9. Square wave voltammograms of increasing concentrations of PAR at 0.15 μ g MWCNT/GCE in 0.1 M PBS at pH 7.0. PAR concentrations: 0.00; 0.0002; 0.0015; 0.006; 0.010; 0.015; 0.020; 0.025; 0.125; 2.50; 5.50; 7.50; 10.0; 15.0 μ M. Frequency: 22 Hz. Step potential: 100 mV/s. Amplitude: 50 mV/s. Equilibrium time: 5 s.....	50
Figure 4.10. Plots of peak currents vs. increasing concentrations of PAR at 0.15 μ g MWCNT/GCE in 0.1 M PBS at pH 7.0.....	51
Figure 4.11. A cyclic voltammogram of the mixture of 1.25×10^{-4} M AA; 1.75×10^{-7} M DA; 2.0×10^{-4} M UA and 7.5×10^{-6} M PAR at bare GCE in 0.1 M PBS at pH 7.0. Scan rate: 100 mV/s. Equilibrium time: 5 s	53
Figure 4.12. Cyclic voltammograms of the mixture of 1.25×10^{-4} M AA, 1.75×10^{-7} M DA, 2.0×10^{-4} M UA and increasing concentrations of PAR at 0.15 μ g MWCNT/GCE in 0.1 M PBS at pH 7.0. Scan rate: 100 mV/s. Equilibrium time: 5 s. PAR concentrations: 0.00; 5.0×10^{-7} M; 7.5×10^{-7} M; 1.0×10^{-6} M; 1.2×10^{-6} M; 1.5×10^{-6} M; 3.0×10^{-6} M; 5.0×10^{-6} M; 7.5×10^{-6} M	54
Figure 4.13. Cyclic voltammograms of the mixture of simultaneously increasing concentrations of AA, DA, UA and PAR at 0.15 μ g MWCNT/GCE in 0.1 M PBS at pH 7.0. Scan rate: 100 mV/s. Equilibrium time: 5 s. (a) 2.5×10^{-5} M AA; 1.0×10^{-7} M DA; 1.0×10^{-4} M UA; 3.0×10^{-7} M PAR. (b) 5.0×10^{-5} M AA; 1.25×10^{-7} M DA; 1.25×10^{-4} M UA; 7.5×10^{-7} M PAR. (c) 1.0×10^{-4} M AA; 1.50×10^{-7} M DA; 1.5×10^{-4} M UA; 1.0×10^{-6} M PAR. (d) 1.25×10^{-4} M AA; 1.75×10^{-7} M DA; 2.0×10^{-4} M UA; 1.5×10^{-6} M PAR	55
Figure 4.14. Chemical structure of albuterol	57
Figure 4.15. SEM images of (a) MWCNT/GCE and (b) PPA/MWCNT/GCE.....	59
Figure 4.16. Cyclic voltammograms of the mixture 80 μ M UA and 35 μ M albuterol in 0.1 M PBS at pH 8.0 at bare GCE. Scan rate: 50 mV/s; Equilibrium time: 5 s	60
Figure 4.17. Cyclic voltammograms of the mixture 80 μ M UA and 35 μ M albuterol in 0.1 M PBS at pH 8.0 at MWCNT/GCE (a) and PPA/MWCNT/GCE (b). Scan rate: 50 mV/s; Equilibrium time: 5 s.....	61

Figure 4.18. Cyclic voltammograms of 2.0×10^{-5} M UA and 1.0×10^{-5} M albuterol at PPA/MWCNT/GCE in 0.1 M PBS at pH 8.0. Scan rate increasing from 50 mV/s to 300 mV/s; Equilibrium time: 5 s	62
Figure 4.19. Plot of anodic peak currents of uric acid vs. scan rates (A) and plot of anodic peak currents of albuterol vs. scan rates (B)	63
Figure 4.20. Plot of anodic peak potentials of albuterol vs. logarithm of scan rates	64
Figure 4.21. Cyclic voltammograms of 2.0×10^{-5} M albuterol at PPA/MWCNT/GCE in 0.1 M PBS at different pH values. Scan rate: 50 mV/s; Equilibrium time: 5 s	65
Figure 4.22. Plot of oxidation peak potential of albuterol vs. solution pH	66
Figure 4.23. Cyclic voltammograms of 9.0×10^{-5} M UA at PPA/MWCNT/GCE in 0.1 M PBS at different pH. Scan rate: 50 mV/s; Equilibrium time: 5 s	67
Figure 4.24. Plot of oxidation peak potentials of UA vs. solution pH	68
Figure 4.25. Cyclic voltammograms of increasing concentrations of albuterol at PPA/MWCNT/GCE in 0.1 M PBS at pH 8.0. Albuterol concentrations = 0.0; 0.15; 1.5; 4.5; 6.0; 9.0; 15.0; 24.0; 38.0; 65.0 μ M. Scan rate: 50 mV/s; Equilibrium time: 5 s	69
Figure 4.26. Plot of anodic peak currents vs. concentration of albuterol	70
Figure 4.27. Square wave voltammograms of increasing concentrations of albuterol at PPA/MWCNT/GCE in 0.1 M PBS at pH 8.0. Albuterol concentrations = (a) 0.05 μ M (b) 1.5 μ M (c) 5 μ M (d) 8 μ M (e) 15 μ M (f) 25 μ M (g) 40 μ M (h) 52 μ M (i) 70 μ M. Equilibrium time: 5 s, frequency: 8 Hz, step potential: 25 mV, amplitude: 10 mV	71
Figure 4.28. Plot of anodic peak currents vs. concentration of albuterol with the SWV	72
Figure 4.29. Cyclic voltammograms of the mixture of UA and increasing concentrations of albuterol PPA/MWCNT/GCE in 0.1 M PBS at pH 8.0 at. Scan rate: 50 mV/s; Equilibrium time: 5 s. UA concentration = 0.0, 85.0 μ M and albuterol concentrations = 0.0, 8.5, 20.0, 30.0, 36.0 μ M	73
Figure 4.30. Cyclic voltammograms of the mixture of albuterol and increasing concentrations of UA at PPA/MWCNT/GCE in 0.1 M PBS at pH 8.0. Scan rate: 50 mV/s; Equilibrium time: 5 s. Albuterol concentration=35.0 μ M and UA concentrations = 7.5, 20.0, 50.0, 100.0 μ M	74
Figure 4.31. Cyclic voltammograms of the mixture of increasing concentrations of UA and albuterol at PPA/MWCNT/GCE in 0.1 M PBS at pH 8.0. Scan rate: 50 mV/s; Equilibrium time: 5 s. UA concentrations = 7.5, 21.0, 40.0, 80.0, 90.0 μ M and albuterol concentrations : 4.5, 12.0, 22.0, 40.0, 60.0 μ M	75
Figure 4.32. Chemical structure of methimazole	78
Figure 4.33. Cyclic voltammograms of 10 mM pivalic acid and 30 mM Co(II) chloride at multi-walled carbon nanotube modified glassy carbon electrode in acetonitril including 50 mM LiClO ₄ Scan rate: 150 mV/s	81
Figure 4.34. Sem images of modified electrodes	82
Figure 4.35. Cyclic voltammograms of poly (pivalic acid)-CoNPs/MWCNT/GCE in 0.1 M PBS at pH 7.2. Scan rate increasing from (a) 50 mV/s to (g) 200 mV/s . Equilibrium time:5 s	83
Figure 4.36. Plot of background currents of poly(pivalic acid)-CoNPs/MWCNT/GCE versus scan rate	84
Figure 4.37. Cyclic voltammograms of 1.12×10^{-4} M methimazole at bare GCE (a), poly(pivalic acid)/GCE (b), MWCNT/GCE (c), poly(pivalic acid)/MWCNT/GCE (d) and poly(pivalic acid)-CoNP/MWCNT/GCE (e) in 0.1 M PBS at pH 7.2. Scan rate 50 mV/s. Equilibrium time:5 s	85
Figure 4.38. Cyclic voltammograms of 1.76×10^{-4} M methimazole at poly(pivalic acid)-CoNPs/MWCNT/ GCE in 0.1 M PBS at pH 7.2. Scan rate increasing from (a) 50 mV/s to (g) 200 mV/s. Equilibrium time:5 s	87
Figure 4.39. Plot of anodic peak currents of methimazole versus scan rate	88
Figure 4.40. Plot of anodic peak potentials of methimazole versus logarithm of scan rate	89
Figure 4.41. Cyclic voltammograms of 1.12×10^{-4} M methimazole at poly(pivalic acid)-CoNPs/MWCNT/GCE in 0.1 M PBS at different pH values. pH: 4.0; 5.0; 6.0; 7.2; 8.0; 9.0. Scan rate: 50 mV/s. Equilibrium time: 5 s	90
Figure 4.42. Plot of anodic peak potentials of methimazole versus solution pH	91

Figure 4.43. Cyclic voltammograms of increasing concentrations of methimazole at poly(pivalic acid)-CoNPs/MWCNT/GCE in 0.1 M PBS at pH 7.2. Methimazole concentrations: 0; 0.1; 2; 6; 8; 10; 16; 18; 20; 30; 45; 65; 100 μM . Scan rate: 50 mV s^{-1} . Equilibrium time: 5 s	92
Figure 4.44. Plot of anodic peak currents of methimazole versus increasing concentration of methimazole	93
Figure 4.45. Chemical structure of bromhexine	95
Figure 4.46. SEM images of MWCNT/Pt (A) and NiNPs/MWCNT/Pt (B)	97
Figure 4.47. EDX analysis of NiNPs/MWCNT/Pt.....	98
Figure 4.48. Cyclic voltammograms of NiNPs/MWCNT/Pt in 0.1 M PBS at pH 4.0 at different scan rates from 50 to 250 mV/s	99
Figure 4.49. Cyclic voltammograms of 1.5×10^{-5} M bromhexine at bare Pt electrode (a), NiNPs/Pt electrode (b), MWCNT/Pt electrode (c) and NiNPs/MWCNT/Pt (d) in 0.1 MPBS at pH 4.0. Scan rate: 50 mV/s . Equilibrium time: 5 s.....	100
Figure 4.50. Cyclic voltammograms of 1.0×10^{-5} M bromhexine at NiNPs/ MWCNT/Pt in 0.1 M PBS at pH 4.0. Scan rates: (a) 10 mV/s ; (b) 20 mV/s ; (c) 30 mV/s ; (d) 40 mV/s ;(e) 50 mV/s . Equilibrium time: 5 s.....	101
Figure 4.51. Plot of anodic peak currents of bromhexine versus scan rates.....	102
Figure 4.52. Plot of logarithm of peak currents of bromhexine versus logarithm of scan rates.....	102
Figure 4.53. Plot of anodic peak potentials of bromhexine versus logarithm of scan rate.....	103
Figure 4.54. Cyclic voltammograms of 8.0×10^{-6} M bromhexine at NiNPs/ MWCNT/Pt in 0.1 M PBS at different pH values. Scan rate: 50 mV/s . Equilibrium time: 5 s.....	104
Figure 4.55. Square wave voltammograms of increasing concentrations of bromhexine at NiNPs/MWCNT/Pt in 0.1 M PBS at pH 4.0. Bromhexine concentrations: (a) 5; (b) 30; (c) 55; (d) 80; (e) 105; (f) 130; (g) 155; (h) 180; (i) 205; (j) 230 μM . Frequency:20 Hz. Step potential: 100 mV/s . Amplitude: 50 mV/s . Equilibrium time: 5 s	105
Figure 4.56. Plot of anodic peak currents vs. concentration of bromhexine	106
Figure 4.57. SEM images of MWCNT/GCE (A) and CoNPs/MWCNT/GCE (B).....	110
Figure 4.58. EDX analysis of CoNPs/MWCNT/GCE.....	111
Figure 4.59. Cyclic voltammograms of a mixture of 5.0×10^{-7} M DA and 5.0×10^{-8} M PAR at bare GCE (a); MWCNT/GCE (b) and CoNPs/MWCNT/GCE (c) in 0.1 M PBS at pH 7.0. Scan rate: 50 mV/s . Equilibrium time: 5 s	112
Figure 4.60. Cyclic voltammograms of 2.5×10^{-8} M PAR at CoNPs/MWCNT/GCE in 0.1 M PBS at pH 7.0. Scan rate increasing from 25 mV/s to 175 mV/s (Each increment 25 mV/s). Equilibrium time: 5 s.....	113
Figure 4.61. Plot of anodic peak currents of PAR versus scan rate.....	114
Figure 4.62. Cyclic voltammograms of 1.5×10^{-7} M DA at CoNPs/MWCNT/GCE in 0.1 M PBS at pH 7.0. Scan rate increasing from 25 mV/s to 175 mV/s (Each increment 25 mV/s). Equilibrium time: 5 s.....	115
Figure 4.63. Plot of anodic peak currents of DA versus scan rate.....	115
Figure 4.64. Cyclic voltammograms of 2.5×10^{-8} M PAR at CoNPs/MWCNT/GCE in 0.1 M PBS at different pH values. Scan rate: 50 mV/s . Equilibrium time: 5 s	116
Figure 4.65. Cyclic voltammograms of 7.5×10^{-7} M DA at CoNPs/MWCNT/GCE in 0.1 M PBS at different pH values. Scan rate: 50 mV/s . Equilibrium time: 5 s	117
Figure 4.66. Plots of anodic peak potentials of PAR and DA versus solution pH	118
Figure 4.67. Square wave voltammograms of increasing concentrations of PAR in the presence of 1.3×10^{-6} M DA at CoNPs/MWCNT/GCE in 0.1 M PBS at pH 7.0. PAR concentrations; 5.0×10^{-8} M; 1.0×10^{-7} M; 1.5×10^{-7} M; 2.0×10^{-7} M; 2.5×10^{-7} M; 3.0×10^{-7} M; 3.5×10^{-7} M; 4.0×10^{-7} M; 4.5×10^{-7} M. Frequency: 22 Hz. Step potential: 100 mV/s . Amplitude: 50 mV/s . Equilibrium time: 5 s	119
Figure 4.68. Plot of peak currents of PAR versus concentration.....	120
Figure 4.69. Square wave voltammograms of increasing concentrations of DA in the presence of 2.8×10^{-7} M PAR at CoNPs/MWCNT/GCE in 0.1 M PBS at pH 7.0. DA concentrations; 2.8×10^{-7} M; 5.6×10^{-7} M; 8.4×10^{-7} M; 1.12×10^{-6} M; 1.4×10^{-6} M; 1.7×10^{-6} M; 2.0×10^{-6} M; 2.3×10^{-6} M. Frequency: 22 Hz. Step potential: 100 mV/s . Amplitude: 50 mV/s . Equilibrium time: 5 s	121
Figure 4.70. Plot of peak currents of DA versus concentration.....	121

Figure 4.71. Square wave voltammograms of simultaneously increasing concentrations DA and PAR at CoNPs/MWCNT/GCE in 0.1 M PBS at pH 7.0. DA concentrations: 5.0×10^{-8} M; 2.4×10^{-7} M; 5.1×10^{-7} M; 7.3×10^{-7} M; 9.4×10^{-7} M; 1.2×10^{-6} M; 1.5×10^{-6} M; 1.7×10^{-6} M. PAR concentrations: 5.2×10^{-9} M; 2.7×10^{-8} M; 6.0×10^{-8} M; 9.0×10^{-8} M; 1.2×10^{-7} M; 1.4×10^{-7} M; 1.8×10^{-7} M; 2.0×10^{-7} M. Frequency: 22 Hz. Step potential: 100 mV/s. Amplitude: 50 mV/s. Equilibrium time: 5 s	122
Figure 4.72. A) A plot of peak currents of PAR and B) A plot of peak currents of DA versus simultaneous increasing concentrations of PAR and DA, respectively	123
Figure 4.73. Square wave voltammograms of simultaneously increasing concentrations of DA and PAR in the presence of 1.0×10^{-4} M AA and 2.0×10^{-5} M UA at CoNPs/MWCNT/GCE in 0.1 M PBS at pH 7.0. DA concentrations: 5.0×10^{-7} M; 8.5×10^{-7} M; 1.25×10^{-6} M; 1.6×10^{-6} M; 2.0×10^{-6} M; 2.5×10^{-6} M; 3.0×10^{-6} M. PAR concentrations: 5.0×10^{-8} M; 1.0×10^{-7} M; 1.5×10^{-7} M; 2.0×10^{-7} M; 2.5×10^{-7} M; 3.0×10^{-7} M; 3.85×10^{-7} M. Frequency: 22 Hz. Step potential: 100 mV/s. Amplitude: 50 mV/s. Equilibrium time: 5 s. Inset A: A plot of peak currents versus the concentration of DA. Inset B: A plot of peak currents versus the concentration of PAR.	126
Figure 4.74. Square wave voltammograms of the mixture of simultaneously increasing concentrations of AA, DA, UA and PAR at CoNPs/MWCNT/GCE in 0.1 M PBS at pH 7.0. AA concentrations: 3.0×10^{-4} M; 3.5×10^{-4} M; 4.0×10^{-4} M; 4.5×10^{-4} M; 5.0×10^{-4} M; 5.5×10^{-4} M. DA concentrations: 5.0×10^{-7} M; 8.5×10^{-7} M; 1.25×10^{-6} M; 1.6×10^{-6} M; 2.5×10^{-6} M; 3.0×10^{-6} M. UA concentrations: 3.5×10^{-5} M; 4.0×10^{-5} M; 4.5×10^{-5} M; 5.0×10^{-5} M; 5.5×10^{-5} M; 6.0×10^{-5} M. PAR concentrations: 7.5×10^{-8} M; 1.0×10^{-7} M; 1.5×10^{-7} M; 2.0×10^{-7} M; 2.75×10^{-7} M; 3.25×10^{-7} M. Frequency: 22 Hz. Step potential: 100 mV/s. Amplitude: 50 mV/s. Equilibrium time: 5 s. Inset A: A plot of peak currents versus the concentration of DA. Inset B: A plot of peak currents versus the concentration of PAR.	127
Figure 4.75. SEM images of MWCNT/GCE (A) and CTS-MWCNT/GCE (B) surfaces.....	133
Figure 4.76. An illustration of CTS-MWCNT modifier acts as the ligand (L) and the metal ions (M^{2+})	134
Figure 4.77. Effects of solution pH on anodic stripping peak currents of 2 nM Cd(II) and 2 nM Pb(II) in 100 mM $NaNO_3$ solution at CTS-MWCNT/GCE. Accumulation time: 120 s. Accumulation potential: -1.2 V. Frequency: 22 Hz. Step potential: 100 mV/s. Amplitude: 50 mV/s. Equilibrium time: 5 s	136
Figure 4.78. Effects of accumulation time on anodic stripping peak currents of 2 nM Cd(II) and 2 nM Pb(II) at pH 7.0 in 100 mM $NaNO_3$ solution at CTS-MWCNT/GCE. Accumulation potential: -1.2 V. Frequency: 22 Hz. Step potential: 100 mV/s. Amplitude: 50 mV/s. Equilibrium time: 5 s.....	137
Figure 4.79. Effects of the amount of CTS in CTS-MWCNT mixture % (W/W) on the peak potential separations of 2 nM Cd(II) and 2 nM Pb(II) in 100 mM $NaNO_3$ solution at modified GCE. Accumulation time: 120 s. Accumulation potential: -1.2 V. Frequency: 22 Hz. Step potential: 100 mV/s. Amplitude: 50 mV/s. Equilibrium time: 5 s.....	138
Figure 4.80. Square wave anodic stripping voltammograms (SWASV) of 1.7 nM Cd(II) and 1.2 nM Pb(II) at pH 7.0 in 100 mM $NaNO_3$ solution at A) CTS-MWCNT/GCE and B) MWCNT/GCE. Accumulation time: 120 s. Accumulation potential: -1.2 V. Frequency: 22 Hz. Step potential: 100 mV/s. Amplitude: 50 mV/s. Equilibrium time: 5 s.....	139
Figure 4.81. Square wave anodic stripping voltammograms (SWASV) of increasing concentrations of Cd(II) at pH 7.0 in 100 mM $NaNO_3$ solution at CTS-MWCNT/GCE. Accumulation time: 120 s. Accumulation potential: -1.2 V. Frequency: 22 Hz. Step potential: 100 mV/s. Amplitude: 50 mV/s. Equilibrium time: 5 s. Cd(II) concentrations: 0.1 nM; 0.2 nM; 0.25 nM; 0.3 nM; 0.5 nM; 0.7 nM; 1.0 nM; 1.3 nM; 1.8 nM; 2.5 nM.....	140
Figure 4.82. A plot of peak currents versus increasing concentrations of cadmium(II) in lead(II) free solution.....	141

Figure 4.83. Square wave anodic stripping voltammograms (SWASV) of increasing concentrations of Pb(II) at pH 7.0 in 100 mM NaNO ₃ solution at CTS-MWCNT/GCE. Accumulation time: 120 s. Accumulation potential: -1.2 V. Frequency: 22 Hz. Step potential: 100 mV/s. Amplitude: 50 mV/s. Equilibrium time: 5 s. Pb (II) concentrations: 0.1 nM; 0.2 nM; 0.25 nM; 0.3 nM; 0.5 nM; 0.7 nM; 1.0 nM; 1.3 nM; 1.8 nM	142
Figure 4.84. A plot of peak currents versus increasing concentrations of lead(II) in cadmium(II) free solution	143
Figure 4.85. Square wave anodic stripping voltammograms (SWASV) of increasing concentrations of Cd(II) and Pb(II) at pH 7.0 in 100 mM NaNO ₃ solution at CTS-MWCNT/GCE. Accumulation time: 120 s. Accumulation potential: -1.2 V. Frequency: 22 Hz. Step potential: 100 mV/s. Amplitude: 50 mV/s. Equilibrium time: 5 s. Cd (II) concentrations: 0.1 nM; 0.2 nM; 0.4 nM; 0.7 nM; 1.2 nM; 1.7 nM; 2.0 nM; 2.5 nM. Pb (II) concentrations: 0.1 nM; 0.15 nM; 0.3 nM; 0.6 nM; 0.9 nM; 1.2 nM; 1.5 nM; 1.8 nM	144
Figure 4.86. A plot of peak currents versus increasing concentrations of lead(II) in the presence of simultaneously increasing concentrations of cadmium(II)	145
Figure 4.87. A plot of peak currents versus increasing concentrations of cadmium(II) in the presence of simultaneously increasing concentrations of lead(II)	145

LIST of TABLES

	Page No
Table 4.1. The application results of various electrodes for the determination of PAR.	52
Table 4.2. Results of the determination of PAR in tablets.....	56
Table 4.3. Voltammetric analysis of albuterol at PPA/MWCNT/GCE in albuterol tablets.....	76
Table 4.4. The application results of various electrodes for determining albuterol.....	77
Table 4.5. Voltammetric analysis albuterol at PPA/MWCNT/GCE in urine samples.....	78
Table 4.6. The oxidation peak potentials and peak heights of methimazole at various electrodes.....	86
Table 4.7. Results of the determination of methimazole in thyromazol tablets.....	94
Table 4.8. Results of the determination of bromhexine in tablets.....	107
Table 4.9. The application results of various electrodes for the determination of PAR.	124
Table 4.10. Analytical parameters of some modified electrodes for the determination of DA.....	125
Table 4.11. Results of the determination of PAR and DA in pharmaceuticals.....	129
Table 4.12. Results of recoveries of PAR and DA in pharmaceuticals.....	129
Table 4.13. Determinations of PAR and DA in mixtures.....	130
Table 4.14. Results of recoveries of PAR and DA in urine samples.....	130
Table 4.15. The application results of various electrodes for the determination of Cd(II) and Pb(II) simultaneously.....	146
Table 4.16. Possible interferences of some metal ions on the simultaneous determination of 2.0 nM cadmium(II) and 2.0 nM lead(II) with using the CTS-MWCNT/GCE	147
Table 4.17. The recoveries of Cd(II) and Pb(II) in different samples using proposed method.....	148

LIST of SCHEMES

	Page No
Scheme 4.1. Proposed PAR reaction at a GCE modified with MWCNTs.....	48
Scheme 4.2. Electrode reaction of albuterol at PPA/MWCNT/GCE.....	66
Scheme 4.3. Electrode reaction of UA at PPA/MWCNT/GCE.....	68
Scheme 4.4. Electrode reaction of methimazole at poly (pivalic acid)-CoNPs/ MWCNT/ GCE.....	90
Scheme 4.5. Electrode reaction of bromhexine at NiNPs/MWCNT/Pt.....	105
Scheme 4.6. Proposed PAR reaction at CoNPs/MWCNT/GCE.....	117
Scheme 4.7. Proposed DA reaction at CoNPs/MWCNT/GCE.....	118

NOMENCLATURE

AA	Ascorbic Acid
C	Concentration
CNT	Carbon Nanotube
CoNPs	Cobalt Nanoparticles
CTS	Chitosan
CV	Cyclic Voltammetry
DA	Dopamine
EDX	Energy Dispersive X-Ray
Ep	Peak Potential
Epa	Anodic Peak Potential
Epc	Cathodic Peak Potential
Eq	Equation
GCE	Glassy Carbon Electrode
Ip	Peak Current
Ipa	Anodic Peak Current
Ipc	Cathodic Peak Current
M	Molar
μ M	Mikromolar
min	Minute
mV	Milivolt
MWCNT	Multi-Walled Carbon Nanotube
n	Number of electron
NiNPs	Nickel Nanoparticles
nM	Nanomolar
PAR	Paracetamol
PBS	Phosphate Buffer Solution
PPA	Poly (Pivalic acid)
Pt	Platinum Electrode
R.S.D	Relative Standard Deviation
r^2	Correlation coefficient
SEM	Scanning Electron Microscopy
SWCNT	Single-Walled Carbon Nanotube
SWV	Square Wave Voltammetry
SWVAS	Square Wave Anodic Stripping Voltammetry
UA	Uric Acid
V	Volt
v	Scan rate

1. INTRODUCTION

Upgrading the standards of life quality is one of the highest priority purposes of the global research efforts. Accordingly, the standards of life quality are closely related to a better control of some illnesses, drug and food quality and safety, and so directly the quality of our environment we live in. In all these fields, a continuous, sensitive, fast and reliable monitoring is required to control some important key parameters (Castillo et al., 2004). Monitoring, controlling and preventing or at least minimizing the side effects of some dangerous substances or chemicals in drugs, foods and environment is the main important field of the scientific studies in the last decade.

Providing the safety of the drug therapy is closely linked to controlling and reducing the adverse effects of drugs. The risk of their contribution to the adverse effects of the drug materials can be controlled and minimized with quantitative determination of purity and degradation products (Görög, 2008). The design of novel sensitive devices for the simultaneous determination of several drugs have been the most popular field in pharmaceutical and clinical studies.

On the other hand, heavy metals have been used in many different areas especially in industries for thousands of years. The deposition of these heavy metals in soils, waters and plants has some quite dangerous threats to human health and ecosystem. The main risks to human health and ecosystem from heavy metals are associated with exposure to lead, cadmium, mercury and arsenic. These hazardous metals have been extensively investigated and their effects on human health regularly reviewed by international bodies such as the WHO (Järup, 2003). The quantitative detection and the removal of the heavy metals are very important subject since they are very persistent in the environment. They are toxic even in trace amounts and their deposition in the biological cells can cause severe pathologies (Săndulescu et al., 2011).

For this purposes, electroanalytical methods or electroanalysis have a lot of advantages over other analytical techniques. They provide outstanding facilities such as; low cost/economic, quick response, easy automation, miniaturization, portability, the ability to monitor *in-situ* and in real time, and no need for sample manipulation. They are based on the control of electrical signal and its correlation/relation to target analyte concentration in samples (ElKaoutit, 2012).

In this connection, the utilize of electrochemical sensors offer very promising devices for monitoring and controlling of a wide range of analytes as a result of their sensitivity, specificity and the ease of use, quick responses, low-cost, reliable and reproducible measurements with miniaturized and portable devices, the interest in their application in the clinical, pharmaceutical and environmental field substantially increased lately (Săndulescu et al., 2011).

Moreover the modification of electrodes for using as a sensor facilitated the following processes in electroanalytical chemistry (Alkire et al., 2009):

- Providing selectivity and sensitivity of electrodes
- Improving chemical or electrochemical stability
- Increasing as well as a larger usable potential range
- Resisting fouling
- Concentrating species
- Improving electrocatalytic properties
- Limiting access of interferences in complex samples
- Providing minimum limit of detection
- Clarification of the electrochemical mechanism.

Atoms, molecules, ions, biomolecules (enzymes, nucleic acids, proteins), conductive and semi-conductive polymers, and nanomaterials (metal nanoparticles, carbon nanotubes, nanowires etc.) are attached to the surface of materials to modify their electronic and structural properties, providing to changing their functionality.

In recent years, many scientists have focused on developing novel materials which are used for signal amplification methods in electrochemical sensors. Especially nanomaterials usually provide a lot of incredible advantage such as having a larger surface area for some molecules to be immobilized. This generally advances the number of binding sites available for the detection of a specific chemical analyte (Padigi et al., 2007).

Various types of nanomaterials are used in electrochemical sensors. Several kinds of nanomaterials including carbon nanotubes, metal nanoparticles and even composite nanomaterials, have been widely used in electroanalysis and electrochemical sensors. Carbon nanotubes (CNTs) are one of the most interesting materials because of their excellent physical properties.

Since the discovery of Multi Walled Carbon Nanotubes (MWCNTs) (Lijima, 1991), and the related Single Walled Carbon Nanotubes (SWCNTs) (Lijima and Ichihashi, 1993), carbon nanotubes have been the subject of numerous investigations in the areas of chemical, physical and material science due to their remarkable structural, mechanical, electronic and chemical properties (Ajayan, 1999; Odom et al., 1998). CNT can display high aspect ratio, electrical conductivity, chemical stability, and extremely high mechanical strength and Young's modulus (Ajayan, 1999; Sinnott et al., 2002). These remarkable mechanical and electrical properties of CNTs endow them with a wide range of potential and practical applications.

The primary aim of these thesis is improving carbon nanotubes-based novel, economic, simple, selective and sensitive electrochemical sensors in order to apply reliable, quick and reproducible for investigation of voltammetric characteristics and quantitative determination of various important analytes such as paracetamol, albuterol and uric acid, methimazole, dopamine and paracetamol, bromhexine, cadmium(II) and lead(II) under the optimum conditions and in the presence of some interferences such as ascorbic acid, uric acid, other organic or inorganic

interferences and other interferent drugs in pharmaceuticals, biological and environmental samples. So, carbon nanotubes based various composite modified electrodes were designed using various techniques and applied to different analytes for this purposes. Moreover, outstanding features of the results obtained in these studies have been compared to other various electrodes and methods in the literature.

2. REVIEW of LITERATURE

Electrochemical sensors based on CNTs represent a new and interesting alternative for the quantification of different analytes (Gooding, 2005; Wildgoose et al., 2006 and Kachoosangi et al., 2008). There are numerous studies done on carbon nanotubes based electrochemical sensors and their applications. In this review of the literature, clinical, environmental and pharmaceutical applications have been studied since this current thesis is only focused on newly designed carbon nanotubes based electrochemical sensors and their analytical applications. The cited literature is mainly the newest studies and the most popular applications have been made in recent years in this field.

2.1. Clinical and Pharmaceutical Applications of Electrochemical Sensors Based on CNTs

Carbon nanotubes was used firstly as an electrode to study the electrochemical behaviour of dopamine by Britto et al. (1996), In this study, carbon nanotube electrodes were constructed using bromoform as a binder, and the oxidative behaviour of dopamine was investigated at these electrodes. At carbon nanotube electrode in PBS at pH 7.4, DA showed an oxidation peak at $E_{pa}=0.22$ V and a corresponding reduction peak at $E_{pc}=0.19$ V. The separation in peak potential was about $\Delta E_p=0.030$ V. The peak potential difference suggested that dopamine showed ideal reversibility in cyclic voltammetry, and was significantly superior to that observed at other carbon electrodes. They reported the achievement of a high degree of reversibility in the oxidation of dopamine using a carbon nanotube electrode without any pretreatment to induce surface activation. The peak current (i_p) was proportional to the square root of sweep rate ($v^{1/2}$) over the range of 20–200 mV/s. The constancy of the current function suggested that dopamine was undergoing a diffusion-controlled process. They investigated the electrochemical oxidation of dopamine at a nanotube electrode after treating the electrode with goat's brain homogenate.

Luo et al. (2001), reported the electrochemical properties of a film of single-walled carbon nanotubes (SWCNTs) functionalized with carboxylic acid groups was studied on a GCE. In this study, SWCNTs were treated with nitric acid for purification and the carboxylic acid groups were created on the SWCNTs surface. A known amount of purified SWCNTs was dispersed in of N,N-dimethylformamide (DMF) to give a black solution. The SWCNT film was prepared by dropping a solution of SWCNT on the GC electrode surface. The SWCNT film was showed very stable electrochemical behavior. It was used as a modified electrode for investigations of some biological molecules such as dopamine, epinephrine and ascorbic acid and their analytical applications. The results showed that the SWCNT modified electrode had excellent electro-catalytic activity with the biomolecules. At the SWCNT film-modified GC electrode in Britton-Robinson Buffer Solution at pH 6.9, DA showed an anodic peak at 0.182 V and a cathodic peak at 0.129 V and compared with that a bare electrode the peak current increased significantly. In the range of $1.0 \times 10^{-6} \sim 2.0 \times 10^{-4}$ M, the anodic peak current increased linearly with the concentration of dopamine. Epinephrine and ascorbic acid were also showed a similar catalytic behavior on the SWCNT film modified electrode.

Wang et al. (2001), demonstrated that the SWCNT-modified electrode provided high electrocatalytic activity towards the electrochemical oxidation of 3,4-dihydroxy phenylacetic acid (DOPAC). One well-defined redox couple with $\Delta E_p = 49$ mV was obtained in 0.1 M Hac-NaAc Buffer Solution at pH 4.4 using the SWCNT-modified electrode. Compared with that a bare electrode the peak current increased significantly also. The peak current increased linearly with the concentration of DOPAC in the range of $1.0 \times 10^{-6} \sim 1.2 \times 10^{-4}$ M. The detection limit was 4.0×10^{-7} M. This SWCNT-modified electrode separated the electrochemical responses of DOPAC and 5-hydroxytryptamine (5HT).

Wu et al. (2003), reported that simultaneous determination of dopamine (DA) and serotonin (5-HT) on the carbon nanotube film-coated glassy carbon electrode (GCE). In this study the modified electrode was prepared with multi-walled carbon nanotube (MWCNT) and dihexadecyl hydrogen phosphate (DHP). The GCE was

coated with a known amount of MWCNT–DHP suspension and evaporated at room temperature. Compared with that at a bare GCE, the oxidation peak potential shifted negatively to 0.18 V, and the reduction peak potential shifts positively to 0.151 V in 0.1 M PBS at pH 7.0. The separation between peak potentials (ΔE_p) was 30 mV, indicating that two electrons are involved in the redox process of DA. At the same conditions the voltammetric behaviors of DA and 5-HT were investigated by cyclic voltammetry (CV). DA and 5-HT showed two well-defined oxidation peaks, whose potentials are 0.18V and 0.36 V, at the MWCNT–DHP film–coated GCE. The linear working range of Dopamine was $5.0 \times 10^{-8} \sim 5.0 \times 10^{-6}$ mol/L with $r=0.9989$ and the detection limit of 1.1×10^{-8} mol/L was obtained with the accumulation of 2 min using differential pulse voltammetry. The modified electrode was applied for the assay of 5-HT and DA in human blood serum.

Ye et al. (2003), reported that selective voltammetric detection of uric acid in the presence of ascorbic acid at well-aligned carbon nanotube electrode. Compared to glassy carbon, carbon nanotube electrode catalyzed oxidation of UA and L-AA, so it reduced the overpotentials by about 0.028 V and 0.416 V, respectively. Based on its differential catalytic function toward the oxidation of UA and L-AA, the carbon nanotube electrode resolved the overlapping voltammetric response of UA and L-AA into two well-defined voltammetric peaks in applying both cyclic voltammetry (CV) and differential pulse voltammetry (DPV), which can be used for a selective determination of UA in the presence of L-AA. The peak current obtained from DPV was linearly dependent on the UA concentration in the range of 0.2 μ M to 80 μ M. The detection limit for UA was found to be 0.1 μ M. Finally, the carbon nanotube electrode was successfully applied as an electrochemical sensor to the determination of UA in human urine samples.

Wu et al. (2004), reported that electrocatalysis of tryptophan at multi-walled carbon nanotube modified electrode. The electrocatalytic response of the modified electrode towards tryptophan (Trp) was investigated by cyclic voltammetry (CV) and differential pulse voltammetry (DPV). The results showed that the modified electrode exhibited an excellent catalytic activity towards the oxidation of Trp. An

oxidation peak was obtained at 978 mV in 0.1 M PBS at pH 3.5 at the MWNT-modified electrode. Under the conditions, the DPV peak current was linear to the concentration of Trp in the range of 2.5×10^{-7} to 1.0×10^{-4} mol/L and the detection limit was 2.7×10^{-8} mol/L.

Lü (2004), studied that electrochemical determination of 8-azaguanine in human urine at a multi-walled carbon nanotubes-(Dicetyl phosphate) DCP modified electrode. The electrochemical properties of 8-azaguanine at the modified electrode were investigated by cyclic voltammetry, and an anodic peak was observed at approximately 0.86 V in 0.1 M PBS at pH 7.0. The oxidation peak current was linear to the concentration of 8-azaguanine over the range from 2.5×10^{-8} to 1.0×10^{-5} M, and the limit of detection was 1.0×10^{-8} M at 2 min open-circuit accumulation. The proposed method was demonstrated by using human urine samples obtained from cancer patients following intravenous administration of 8-azaguanine.

Qu et al. (2004), described that voltammetric determination of pyridoxine (Vitamin B6) by use of a carbon nanotube-modified glassy carbon electrode. The MWCNT-modified glassy carbon electrode showed an obvious electrocatalytic activity to the oxidation of pyridoxine. The oxidation peak appeared at 0.80 V in 0.1 M PBS at pH 6.0. A sensitive linear voltammetric response for pyridoxine was obtained in the concentration range of 5.0×10^{-7} ~ 1.0×10^{-4} mol/L, and the detection limit was 2.0×10^{-7} mol/L by using DPV. The proposed method was applied to pyridoxine drugs.

Salimi et al. (2005), reported that amperometric detection of morphine at preheated glassy carbon electrode modified with multi-walled carbon nanotubes. The CNT-coated electrode exhibited an oxidation peak at 0.3 V and no reduction signal was observed in the reversed scan in 0.1 M PBS at pH 7.0. Under the optimized conditions the calibration plots were linear in the concentration range 0.5 – 150 μ M with the calculated detection limit (S/N=3) of 0.2 μ M. Finally, the modified electrode was applied for simultaneous determination of morphine and codeine.

Wu and Hu (2005), investigated determination of cytochrome-*c* using colloidal gold-carbon nanotubes-dihexadecylphosphate (DHP) composite film on a gold electrode. The composite film modified gold electrode was used to detect cytochrome-*c* and a pair of well-defined redox waves was obtained the anodic and cathodic peaks at 0.0 and 0.05V, respectively in 0.06 M PBS at pH 7.0. A linear regression equation was obtained over a cytochrome-*c* concentration range of 1.5–45 μM .

Xu and Wang (2005), studied electrocatalytic oxidation and direct determination of L-tyrosine by square wave voltammetry at multi-wall carbon nanotubes modified glassy carbon electrodes. Cyclic voltammetry was used to investigate L-tyrosine at the MWNTs-modified GCE. It showed that L-tyrosine only had an oxidation peak in the cyclic voltammograms from 0.20 to 1.20V, suggesting that the electrochemical process of L-tyrosine was totally irreversible. Under the optimum conditions the SWASV peak height was linearly correlated to the L-tyrosine concentration over the range 2.0×10^{-6} to 1.0×10^{-4} mol/L. The detection limit was 4.0×10^{-7} mol/L. The method was applied for quantitative determination of L-tyrosine in pharmaceutical preparations.

Zhu et al. (2005), researched electrochemical oxidation of theophylline at multi-wall carbon nanotube modified glassy carbon electrodes. In this study, MWCNTs were treated with nitric acid/ sulphuric acid so the carboxylic acid groups were created on the MWCNTs surface. It showed that theophylline only had an oxidation peak in the cyclic voltammograms at 26 mV in 0.1 M PBS at pH 5.8. The anodic peak current increased linearly with the square root of scan rate which indicated a diffusion controlled oxidation process occurring at the modified GCE. Under optimal conditions there was a good linear relationship between anodic peak current and TP concentration in the range from 3.0×10^{-7} to 1.0×10^{-5} mol/L, and a detection limit of was 5.0×10^{-8} mol/L after 2 min of open-circuit accumulation. The MWCNT modified electrode was applied to determination of TP in drug.

Xiang et al. (2006), proposed a new method for determination of L-Dopa by the adsorption stripping voltammetry (ASV) using a multiwalled carbon nanotubes (MWNTs)–Nafion modified glassy carbon electrode (GMGCE). In this experimental study, a sensitive oxidation peak was observed and the anodic peak potential was ca. 0.374V (vs. SCE). There was a linear correlation between the peak current (i_p) and L-dopa concentration in the range of 3.5×10^{-7} – 1.5×10^{-5} mol/L, with the limit of detection 5.0×10^{-8} mol/L. The method has been applied to the determination of L-dopa in samples.

Wang et al. (2006), reported application of a single-wall carbon nano-tube film electrode to the determination of trace amounts of folic acid. Cyclic voltammetry (CV) and linear sweep voltammetry (LSV) were used in investigation of the electrochemical reduction of folic acid with the film electrode. Two couples of redox peaks between 0.4 and -1.4 V observed at the film electrode except for an irreversible reduction peak. The reduction peak current was linearly related to folic acid concentration over the range of 1.0×10^{-8} to 1.0×10^{-4} mol/L with a detection limit of 1.0×10^{-9} mol/L after 5 min accumulation. The proposed method was successfully used for determination of folic acid in tablets.

Zeng et al. (2006), reported voltammetric behavior and determination of rutin at a single-walled carbon nanotubes modified gold electrode. In this research, the anodic (E_{pa}) and cathodic peak potentials (E_{pc}) were 0.375 V and 0.328 V (versus SCE), respectively, and the ratio of i_{pa}/i_{pc} was about 1 in a 0.1 M phosphate buffer solution at pH 5.0. The peak current was linear to the rutin concentration over the range of 2.0×10^{-8} M to 5.0×10^{-6} M, and the detection limit was 1.0×10^{-8} M. The method has been applied to the determination of rutin in drug tablets.

Duan et al. (2007), investigated electrochemical behaviour of acetaminophen on multi-walled carbon nanotubes modified electrode and its analytical applications. In this work, cyclic voltammetry (CV) was used to explore the electrochemical redox mechanism of acetaminophen (ACOP) on the MWNTs/GCE and differential pulse voltammetry (DPV) was used to determine ACOP in samples, respectively. on

the MWNTs/GCE there was a couple of quasi-reversible reduction and oxidation peak at $E_{pa}= 0.404$ mV, $E_{pc}=0.324$ mV, and $\Delta E_p=80$ mV in 0.1 M PBS at pH 6.0. The results showed that the oxidative peak currents were linear with the concentration of ACOP in the range of $4.0 \times 10^{-7} \sim 1.5 \times 10^{-4}$ M with the detection limit 1.2×10^{-7} M. The MWNTs/GCE was used to quantify ACOP in effervescent dosage real samples.

Li and Jing (2007), investigated electrochemical behavior of acetaminophen and its detection on the PANI–MWCNTs composite modified electrode. A polyaniline–multi-walled carbon nanotubes (PANI–MWCNTs) composite modified electrode exhibited excellent electrocatalytic effects on the electrochemical reaction of acetaminophen. At the PANI–MWCNTs electrode a pair of well-defined redox waves of acetaminophen were observed and the oxidative peak potentials at 58 and 41 mV, respectively in 0.2 M HAc–NaAc buffer solutions (ABS) at pH 5.5. The oxidation peak current was proportional to the concentration of acetaminophen from 1.0×10^{-6} to 1.0×10^{-4} mol/L and 2.5×10^{-4} to 2.0×10^{-3} mol/L, respectively. The detection limit was 2.5×10^{-7} mol/L. The proposed method was applied to detect acetaminophen in tablets.

Yogeswaran et al. (2007), reported nanocomposite of functionalized multiwall carbon nanotubes with nafion, nano Platinum, and nano gold biosensing film for simultaneous determination of ascorbic acid, epinephrine, and uric acid. In this report, a unique bimetallic, nano Platinum (Pt) with nano gold (Au) on nafion (NF) incorporated with functionalized multiwall carbon nanotubes (f-MWCNTs) composite film (f-MWCNTs–NF–PtAu) was developed by the potentiostatic method. The novel composite film exhibited catalytic activity towards the oxidation of mixture of biochemical compounds and simultaneous measurement of ascorbate anion, epinephrine and urate anion in 0.5 M H_2SO_4 aqueous buffer solution at pH 6.75. Well-separated voltammetric peaks were obtained for ascorbate, epinephrine and urate anions at $E_{pa}= 0.07$; 0.29 and 0.42 V respectively, The peak separation between AA and EP was 0.222 V, and the peak separation between EP and UA was 0.131 V. The calibration curves for AA, EP, and UA were linear with the

concentrations: 1.2 to 4.8 mM for AA and 0.06 to 0.24 mM for EP and UA. The limit of detections were calculated as 0.02–0.16 mM for EP and UA respectively.

Shahrokhian and Mehrjardi (2007), reported simultaneous voltammetric determination of uric acid (UA) and ascorbic acid (AA) using a carbon-paste electrode modified with multi-walled carbon nanotubes/nafion and cobalt(II)- 5-nitro-salophen. The best peak resolution for these compounds using the modified electrode was obtained in solutions with pH 4.0 using cyclic voltammetry. The ΔE_p for UA and AA in these method was about 315 mV. A linear dynamic range of 1.0×10^{-7} to 1.0×10^{-4} M with a detection limit of 6.0×10^{-8} M was calculated for UA in 0.1 M acetate buffer solutions at pH 4.0. The voltammetric response characteristics for AA was obtained as, the linear range of 5.0×10^{-7} to 1.0×10^{-4} M with the detection limit of 1.0×10^{-7} M. The designed modified electrode was applied for the determination of AA and UA in mixture samples.

Rezaei and Zare (2008), investigated determination of leucine in biological and pharmaceutical samples using modified glassy carbon electrode with multiwall carbon nanotubes as a voltammetric sensor. The cyclic voltammetric results showed that MWNTs significantly increased electrocatalytic activity toward the oxidation of leucine. At the modified electrode, two anodic peaks and one cathodic were observed in the peak potential of 0.275; 1.025; and -0.350 V in 0.1 M universal buffer solution (boric acid, phosphoric acid, acetic acid, and sodium hydroxide) at pH 10.0. The calibration curve was linear in the concentration range 9.0×10^{-6} ~ 1.5×10^{-3} mol/L, with the detection limit of 3.0×10^{-6} mol/L. The improved method was employed to determine leucine in plasma and urine samples.

Fei et al. (2008), demonstrated electrochemical determination of diethylstilbestrol by a single-walled carbon nanotube/Platinum nanoparticle composite film electrode. The glassy carbon (GC) electrode modified with SWNT/Pt nano composite film was used for determine diethylstilbestrol (DES) using by linear sweep voltammetry and cyclic voltammetry in optimized 0.1 M PBS at pH 7.0. Under optimal conditions, a linear response of DES was obtained in the

range from 1.0×10^{-7} to 2.0×10^{-5} M and with a limit of detection (LOD) was 1.5×10^{-8} M. The proposed method was applied to determine DES in tablets.

Goyal et al. (2008), described that novel sensors for determination of 5-hydroxytryptamine and 5-hydroxyindole acetic acid based on nanomaterial modified electrodes. Simultaneous voltammetric determination of serotonin and 5-hydroxyindole acetic acid has been studied at single walled carbon nanotube modified glassy carbon electrode and gold nanoparticles modified indium tin oxide electrode. In this method, detection limits were calculated as low as 32 nM for 5-hydroxytryptamine (5-HT) at single-walled carbon nanotube modified glassy carbon electrode and 27 nM for 5-hydroxyindole acetic acid (5-HIAA) at gold nanoparticles modified indium tin oxide electrode. Linear working range was obtained 0.1–100 μ M for 5-HT and 5-HIAA. Application of the method for determination of this compounds was applied in urine samples.

Huang et al. (2008), investigated that electrochemical behavior and voltammetric determination of norfloxacin using glassy carbon electrode modified with multi walled carbon nanotubes/Nafion. The MWCNTs/Nafion film-coated glassy carbon electrode (GCE) was fabricated and the electrochemical behavior of norfloxacin at the electrode was investigated using cyclic voltammetry. Linear sweep voltammetry was also used for quantitative determination of norfloxacin in 0.5 M acetate buffer solution at pH 4.4 as optimal condition. Under the condition the concentration calibration range and detection limit (S/N=3) were 0.1–100 mol/L and 5×10^{-8} mol/L for NFX. The proposed method was successfully applied to NFX determination in pharmaceutical tablets.

Lai et al. (2008), demonstrated that electrocatalytic oxidation and voltammetric determination of dopamine at a Nafion/carbon-coated iron nanoparticles-chitosan composite film modified electrode. In this method, a known amount of homogeneous carbon-coated iron nanoparticles-chitosan (CCINPs-CS) dispersion and Nafion solution were successively dropped on the surface of a glassy carbon electrode (GCE) to fabricate a Nafion/CCINPs-CS modified GCE. The

modified electrode exhibited good electrocatalytic activity for electrochemical oxidation of dopamine (DA) in the pH 5.5, 0.1 M phosphate buffer solution. The oxidation peak currents showed a linear relation on the DA concentration in the range from 2.0×10^{-6} to 6.0×10^{-5} M by differential pulse voltammetry. The detection limit was calculated to be 8.3×10^{-7} M. This method was also used for the detection of DA in an injection sample.

Liu et al. (2008), showed that simultaneous determination of adenine and guanine in DNA using polythionine/NPAu/MWNTs modified electrode. In this research, for the fabrication of polythionine/gold nanoparticles/multi-wall carbon nanotubes (PTH/NPAu/MWNTs) modified electrode was proposed via a two-step process. First, the gold nanoparticles/multi-wall carbon nanotubes (NPAu/MWNTs) composites, which were synthesized by ultrasonic method, were deposited on the glassy carbon electrode to prepare the NPAu/MWNTs electrode. Then, the thionine was electropolymerized on the surface of NPAu/MWNTs modified electrode to prepare the PTH/NPAu/MWNTs modified electrode. The experimental parameters were optimized and a direct electrochemical method for the simultaneous determination of guanine and adenine was developed. The detection limit (S/N=3) for guanine and adenine was calculated as 1.0×10^{-8} M and 8.0×10^{-9} M, respectively. This method was also applied for the measurement of guanine and adenine in calf thymus DNA.

Shahrokhian and Asadian (2009), investigated that electrochemical determination of L-dopa in the presence of ascorbic acid using the glassy carbon electrode modified by a bilayer of multi-walled carbon nanotube and poly-pyrrole doped with tiron. In here, a new type of the modified electrodes were prepared in a layer-by-layer process by using multi-walled carbon nanotube (MWCNT) and poly-pyrrole. The electrochemical behavior of L-dopa was investigated on the surface of the modified electrode using cyclic voltammetry (CV). Under the optimized conditions, the DPV of various concentrations L-dopa in 0.1 M phosphate buffer solutions of pH 7.0 were studied. The working linear range was 1.0×10^{-6} to 1.0×10^{-4} M and its low detection limit was calculated 0.1 μ M by DPV. This

composite film electrode was successfully applied to plasma samples for determination of L-dopa.

Tashkhourian et al. (2009), researched that silver nanoparticles modified carbon nanotube paste electrode for simultaneous determination of dopamine and ascorbic acid. Differential pulse voltammetry was used for the simultaneous determination of DA and AA. The peak separation between DA and AA was 67 mV in 0.1 M PBS at pH 2.0. The calibration curves for DA and AA were obtained in the range of 8.0×10^{-7} – 6.4×10^{-5} M and 3.0×10^{-5} – 2.0×10^{-3} M, respectively. The lowest detection limits (S/N=3) were 3.0×10^{-7} M and 1.2×10^{-5} M for DA and AA, respectively. This method was applied to the determination of DA and AA in real samples.

Shahrokhian et al. (2009), investigated that sensitive voltammetric determination of thioridazine (TR) using multi-walled carbon nanotubes with immobilised cobalt nanoparticle modified glassy carbon electrode. In this research, Differential pulse voltammetry was applied for the determination of sub-micromolar amounts of TR. A linear working range of 5.0×10^{-7} to 1.0×10^{-4} M with a detection limit of 5.0×10^{-8} M in 0.1 M PBS at pH 7.0. TR was obtained. The modified electrode was applied to determination of minor amounts of TR in pharmaceutical and clinical preparations.

Shen and Wang (2009), investigated that simultaneous determination of adenine, guanine and thymine a novel modified electrode based on β -cyclodextrin/MWCNTs. In this research, novel nanocomposites of β -cyclodextrin and multi-wall CNT (MWCNTs) were prepared and deposited on the glassy carbon electrodes to form the β -CyDex/MWCNT modified electrodes. These novel modified electrodes used for the simultaneous determination of guanine (G), adenine (A) and thymine (T). Well separated voltammetric peaks were obtained between G and A: 330 mV, A and T : 170 mV, present in the analyte mixture in 0.1 M PBS at pH 7.0. The detection limits of A, T and G for individual analysis was calculated to be 0.75, 6.76 and 33.67 ± 7.8 % nM, respectively.

Lin et al. (2009), researched that sensitive amperometric immunosensor for α -feto-protein (AFP) based on carbon nanotube/gold nanoparticle doped chitosan film. The immunosensor was prepared by immobilizing AFP antigen onto the glassy carbon electrode (GC) modified by gold nanoparticles and carbon nanotubes doped chitosan (GNP/CNT/Ch) film. GNP/CNT hybrids were produced by one-step synthesis based on the direct redox reaction. Under the optimized experimental conditions, the resulting immunosensor was detected AFP in a linear range from 1 to 55 ng/mL with a detection limit of 0.6 ng/mL in 0.1 M Britton-Robinson Buffer solution at pH 9.0, using cyclic voltammetry.

Zhang et al. (2010), proposed a new electrochemical sensor for determination of procaine based on a glassy carbon electrode modified with poly-amidosulfonic acid and multi-walled carbon nanotubes. In this study, a glassy carbon electrode was prepared that was coated with a composite film containing electropolymerized poly(amidosulfonic acid) and multi-walled carbon nanotubes. It was used to study the electrochemical properties of procaine by differential pulse voltammetry. The peak current was proportional to the concentration of procaine from 80 nM to 1.0 μ M. The detection limit was calculated as 25 nM (S/N=3). The modified electrode was applied to determination of procaine in pharmaceutical formulations.

A glassy carbon electrode modified with poly (3-methylthiophene) (P3MT) and coated with multiwall carbon nanotubes (MWNTs) film was fabricated and used for determination of hydroquinone and catechol by Zhang et al. (2010). The peaks for hydroquinone and catechol were separated by about 101 mV in pH 6.4 phosphate buffer solution using cyclic voltammetry. A linear relationships between the peak current and concentration were obtained for single solution of hydroquinone (or catechol) by differential pulse voltammetry. The detection limits were 12 nM and 40 nM. When simultaneously changing the concentration of both hydroquinone and catechol, the linear responses were in the range from 0.5 to 200 μ M, for hydroquinone, and from 0.5 to 150 μ M for catechol, and the detection limits were estimated as 50 nM for both hydroquinone and catechol.

Ran et al. (2010), proposed a sensitive amperometric immunosensor for determination of alpha-fetoprotein based on carbon nanotube/DNA/Thi/nano-Au modified glassy carbon electrode. In the electrode design, firstly, multiwall carbon nanotubes (MWCNT) dispersed in poly(diallyldimethylammonium chloride) (PDDA) were immobilized on the nano-Au film which was electrochemically deposited on the surface of glassy carbon electrode. Then a negatively charged DNA film was absorbed on the positively charged PDDA. Subsequently, thionine was attached to the electrode via the electrostatic interaction between thionine and the DNA. Finally, the nano-Au was retained on the thionine film for immobilization of AFP antibody (anti-AFP). Under optimal conditions, the proposed immunosensor exhibited good electrochemical behavior to AFP in a two concentration ranges: 0.01–10.0 and 10.0–200.0 ng/mL with a relatively low detection limit of 0.04 ng/mL in 0.1 M PBS at pH 7.0.

Hu et al. (2011), reported that electrochemical determination of L-phenylalanine at polyaniline modified carbon electrode based on cyclodextrin incorporated carbon nanotube composite material. In this study, the electrochemical behavior of the sensor towards L-phenylalanine was investigated by cyclic voltammetry (CV), differential pulse voltammetry (DPV). A linear calibration plot was obtained including the concentration range from 5.0×10^{-7} to 1.0×10^{-4} mol L⁻¹ in 0.2 M PBS at pH 7.0 with a detection limit of 1.0×10^{-9} mol L⁻¹. The modified electrode was also used to detect L-phenylalanine in blood plasma samples successfully.

Benvidi et al. (2011), investigated that electrocatalytic oxidation of hydrazine using a Co(II) complex multi-wall carbon nanotube modified carbon paste electrode. The electrocatalytic current increased linearly with the hydrazine concentration in the range of 0.3–70.0 μM in 0.1 M PBS at pH 7.0, and detection limit was 0.1 μM. The modified electrode (Co(II)BBAEDI-MWCNT-MCPE) showed good reproducibility (RSD < 3.3%). This method was applied to determine hydrazine in water samples.

Wei et al. (2011), proposed a new sensor based on CeO₂ nanoparticles decorated multi-walled carbon nanotubes for electrochemical determination of guanine and adenine. In this study, cyclic voltammetry (CV) and differential pulse voltammetry (DPV) were used to investigate the electrocatalytic activity toward the electrochemical oxidation of guanine and adenine. The detection limit for adenine and guanine was found to be 20 and 10 nM in 0.1 M PBS at pH 7.0, respectively. The linear working ranges were 5-50 µM and 5-35 µM, respectively.

Beitollahi and Sheikhshoae (2011), suggested a novel modified electrode based on molybdenum (VI) complex-carbon nanotube for simultaneous determination of isoproterenol (IP), uric acid and folic acid. Differential pulse voltammetry (DPV) in 0.1 M phosphate buffer solution (PBS) at pH 7.0 was used to determine IP in the range from 0.7 to 600.0 µM, with a detection limit of 35.0 nM. The modified electrode was also performed to determine IP in an excess amount of uric acid (UA) and folic acid (FA) by DPV. This proposed method was also employed for the determination of IP in some real samples such as IP injections, urine and human blood serum.

Cao et al. (2011), proposed a novel electrochemical immunosensor for the determination of casein based on gold nanoparticles and poly(L-Arginine)/multi-walled carbon nanotubes (P-L-Arg/MWCNTs) composite film. Under optimal conditions, the peak currents observed by DPV decreased linearly with the increasing casein concentrations in the range from 1×10^{-7} to 1×10^{-5} gmL⁻¹ and low detection limit was calculated to be 5×10^{-8} gmL⁻¹. The novel modified electrode was successfully applied to the determination of casein in cheese samples.

Manjunatha et al. (2011), reported that direct electrochemical determination of cholesterol oxidase on MWCNTs. Well defined redox peaks were observed in cyclic voltammogram of the modified graphite electrode in phosphate buffer solution at pH 7.0. These peaks were corresponding to direct electron transfer of FAD/FADH₂ of ChOx and carboxylic groups of multi walled nanotubes. The reduction current of oxygen at the modified electrode decreased linearly with the cholesterol in the

concentration range of 0.2–1 mM using cyclic voltammetry with the lower detection limit of 3.0×10^{-6} M.

Wang et al. (2012), investigated electrochemical oxidation behavior of methotrexate using a sensor based on DNA/SWCNT/Nafion composite film-modified glassy carbon electrode. In this research, glassy carbon electrode modified with DNA functionalized single-walled carbon nanotube (DNA/SWCNT) and Nafion composite film was constructed for the detection of methotrexate. Under the optimal conditions, the modified electrode in pH 2.78 Britton–Robinson buffer solutions showed a linear voltammetric response within the methotrexate's concentration range of 2.0×10^{-8} – 1.5×10^{-6} M, with the detection limit of 8.0×10^{-9} M. The method was also applied to detect methotrexate in medicinal tablets and spiked human blood serum samples.

Hu et al. (2012), proposed that a novel sensitive and selective imprinted electrochemical sensor for the determination of oleanic acid was fabricated on a carbon electrode by stepwise modification of functional multi-walled carbon nanotubes, cobalt hexacyanoferrate nanoparticles and a thin imprinted sol–gel film. In this work, the construction of a homogeneous porous poly (sodium 4-styrenesulfonate-co-acrylic acid)-grafted multi-walled carbon nanotubes/SiO₂-chitosan nanocomposite film was conducted using controllable electrodeposition technique. This sensor showed high sensitivity and selectivity for electrochemical behaviour of oleanic acid. A linear working range was obtained from 1.0×10^{-8} to 1.0×10^{-3} M with a detection limit of 2.0×10^{-9} M. This improved sensor was also applied to the determination of oleanic acid in real capsule samples.

Wang et al. (2012), suggested a new electrochemical sensor based on Fe₃O₄/MWCNTs/β-CD modified electrode. In here, this sensor was used for investigation of the electrochemical oxidation behaviour of hypoxanthine in phosphate buffer solution by cyclic voltammetry and linear sweep voltammetry. Under the optimal conditions, the log oxidation peak current was proportional to log hypoxanthine concentration in the range from 5.0×10^{-8} to 1.0×10^{-5} M with a

detection limit of 3.0×10^{-9} M. The modified electrode were used for the determination of hypoxanthine in meat samples.

Fathirad et al. (2013), demonstrated that fabrication of a new carbon paste electrode modified with multi-walled carbon nanotube for determination of bismuth(III). In this study, a selective and sensitive carbon paste electrode modified with multi-walled carbon nanotubes and 4-[1-(4-methoxyphenyl) methyldene]-3-methyl-5-isoxazolone was performed for accumulation and determination of trace amounts of bismuth by the differential pulse anodic stripping voltammetric method. An anodic peak related to the oxidation of accumulated Bi(0) on the electrode surface was observed at about -0.05 V. The linear working range was from $1 \mu\text{g/L}$ to $400 \mu\text{g/L}$. The limit of detection was $0.2 \mu\text{g/L}$. The modified electrode was also applied for the determination of bismuth in pharmaceutical, biological and several water samples.

2.2. Environmental Applications of Electrochemical Sensors Based on CNTs

Lü (2003), reported that a multi-walled carbon nanotubes (MWCNT) film coated glassy carbon electrode (GCE) was developed for the determination of 1-naphthyl-acetic acid (NAA) in soil samples. In this study, the voltammetric behaviors of NAA at the MWCNT-DHP film coated GCE were investigated using cyclic voltammetry (CV). At the modified electrode, NAA showed an oxidation peak at 1.03 V in 0.1 M MacIlvaine buffer solution at pH 4.0 and no corresponding reduction peak was observed on the reverse scan, so the electrode reaction of NAA was totally irreversible. The oxidation peak current was proportional to the concentration of NAA over the range from 1×10^{-8} to 2×10^{-6} mol/L, and the detection limit was 2.5×10^{-9} mol/L after 2 min accumulation using differential pulse voltammetry. The MWCNT-film modified GCE was applied to detect NAA in soil samples.

Wu et al. (2003), investigated that a multi-wall carbon nanotube (MWNT) modified glassy carbon electrode (GCE) was used for the simultaneous

determination of trace levels of cadmium(II) and lead(II) by anodic stripping voltammetry (ASV). In this study, Cd^{2+} and Pb^{2+} first was adsorbed onto the surface of a MWNT film coated GCE and then reduced at -1.20 V in containing 0.02 M KI NaAc-Hac buffer solution at pH 4.5. During the positive potential sweep, reduced cadmium and lead were oxidized, and two well-defined stripping peaks appeared at -0.88 and -0.62 V. The stripping peak currents increased linearly with the concentration of Cd^{2+} from 2.5×10^{-8} to 1×10^{-5} mol/L and with that of Pb^{2+} from 2×10^{-8} to 1×10^{-5} mol/L. The detection limits of Cd^{2+} and Pb^{2+} were obtained to 6×10^{-9} and 4×10^{-9} mol/L, respectively.

Yi (2003), described that an electrochemical method for the determination of trace levels of mercury based on a multi-walled carbon nanotubes film coated glassy carbon electrode. In this method, Hg^{2+} was firstly preconcentrated in 0.1 mol/L HCl solution containing 0.02 mol/L KI at the MWNT film and then reduced at -0.60 V. During the anodic potential sweep, reduced mercury was oxidized, and then a sensitive and well-defined stripping peak at about -0.20 V appeared. The stripping peak current was proportional to the concentration of Hg(II) over the range $8 \times 10^{-10} \sim 5 \times 10^{-7}$ M. The detection limit of of Hg^{2+} was 2.0×10^{-10} mol/L at 5 min accumulation. This method was successfully applied to detect Hg(II) in some water samples.

Gao et al. (2006), proposed a novel method for determination of trace heavy metal ions using carbon nanotubes/poly(1,2-diaminobenzene) nanoporous composite film electrode. In this study, the multi-walled carbon nanotubes (MWNTs) and poly(1,2-diaminobenzene) were deposited simultaneously on the electrode surface by multipulse potentiostatic electropolymerization. The nanoporous composite film modified glassy carbon electrode was applied successfully for the simultaneously voltammetric determination of trace level of Cd^{2+} and Cu^{2+} at first-time. Under the optimal conditions, the limit of detections were obtained 0.25 and 0.33 ppb for Cd^{2+} and Cu^{2+} , respectively. The calibration graphs were linear in the concentration range of $5 - 100$ ppb. The improved method was used for determination of Cd^{2+} and Cu^{2+} in real metallurgy waste water sample.

Hrapovic et al. (2006), reported metallic nanoparticle-carbon nanotube composites for electrochemical determination of explosive nitroaromatic compounds. Pt, Au and Cu nanoparticles together with multiwalled (MWCNT) and single-walled carbon nanotubes (SWCNT) solubilized in Nafion were used to form nanocomposites for electrochemical detection of trinitrotoluene (TNT) and several other nitroaromatics. An excellent signal effect was observed for the nanocomposite modified glassy carbon electrode (GC) containing Cu nanoparticles and SWCNT solubilized in Nafion. This combination material provided the best sensitivity for detecting TNT and other nitroaromatic compounds. Adsorptive stripping voltammetry for TNT resulted in a detection limit of 1 ppb. The Cu-SWCNT-modified GC electrode was used for analysis of TNT in tap water, river water, and contaminated soil samples.

Sun et al. (2007), reported voltammetric determination of Cd^{2+} based on the bi-functionality of single-walled carbon nanotubes–Nafion film. In this study, an electrochemical method was developed for the determination of trace levels of Cd^{2+} by anodic stripping voltammetry (ASV). In 0.1 M NaAc–HAc buffer at pH 5.0, Cd^{2+} was firstly exchanged and adsorbed onto SWNTs/Nafion film surface, and then reduce at -1.10 V. During the positive potential sweep, reduced cadmium was oxidized, and a well-defined stripping peak appeared at -0.84 V. The linear range was found to be from 4.0×10^{-8} to 4.0×10^{-6} M, and the lowest detectable concentration was calculated as 4.0×10^{-9} M. Finally, this method was successfully employed to detect Cd^{2+} in water samples.

Xu et al. (2008), reported that ultrasensitive voltammetric detection of trace lead(II) and cadmium(II) using MWCNTs-Nafion/bismuth composite electrodes. In this work, Multiwall carbon nanotubes were dispersed in Nafion (MWCNTs-NA) solution and used in combination with bismuth (MWCNTs-NA/Bi) for constructing composite sensors to detect trace Pb(II) and Cd(II) by differential pulse anodic stripping voltammetry (DPASV). Linear calibration curves ranged from 0.05 to 100 mg/L for Pb(II) and 0.08 to 100 mg/L for Cd(II) in 0.2 M KCl. The determination limits ($S/N=3$) were calculated as 25 ng/L for Pb (II) and 40 ng/L for Cd (II). The

MWCNTs-NA/Bi composite film electrodes were successfully employed to determine Pb (II) and Cd (II) in real tap water samples.

Sun and Sun (2008), reported electrochemical determination of Pb^{2+} using a carbon nanotube/Nafion composite film-modified electrode. In this study, the anodic stripping peak current of Pb^{2+} was proportional to its concentration over the range 8.0×10^{-8} to 6.0×10^{-6} M in optimized conditions as pH 5.0 0.1 M NaAc–HAc buffer solution. The limit of detection (S/N=3) was calculated as 5.0×10^{-9} M. Finally, this improved method was used to determine Pb^{2+} in waste water samples.

Hwang et al. (2008), reported that determination of trace metals (lead, cadmium and zinc) by anodic stripping voltammetry using a bismuth-modified carbon nanotube electrode. The simultaneous determination of lead, cadmium and zinc was performed by square wave anodic stripping voltammetry in 0.1 M acetate buffer solution at pH 4.5 as optimum experimental media. The peak current response increased linearly with the metal concentration in a range of 2–100 $\mu\text{g/L}$. The limit of detection was 1.3 $\mu\text{g/L}$ for lead, 0.7 $\mu\text{g/L}$ for cadmium and 12 $\mu\text{g/L}$ for zinc (S/N=3). The Bi-CNT electrode was applied to analysis of the trace metals in real environmental samples.

Tian et al. (2009), reported that simultaneous determination of trace zinc(II) and cadmium(II) by differential pulse anodic stripping voltammetry using a MWCNTs–NaDBS modified stannum film electrode. In this work, the Sn/MWCNTs–NaDBS film electrode was prepared by applying MWCNTs–NaDBS suspension to the surface of the GCE, while the Sn film was plated *in situ* simultaneously with the target metal ions. Under optimal conditions, linear calibration curves were obtained in a range of 5.0 -100.0 mg/L with detection limits of 0.9 mg/L for zinc(II) and 0.8 mg/L for cadmium(II), respectively. This film electrode was successfully applied to the determination of Zn(II) and Cd(II) in tap water samples.

Tu et al. (2009), reported that a sensitive electrochemical method was developed for the determination of bisphenol A (BPA) at a glassy carbon electrode (GCE) modified with a multiwalled carbon nanotubes (MWCNTs)-gold nanoparticles (GNPs) hybrid film. Under the optimal conditions, the differential pulse voltammetric anodic peak current of BPA was linear with the BPA concentration from 2.0×10^{-8} to 2.0×10^{-5} M, with a limit of detection of 7.5 nM. The proposed method was applied to determine BPA in real plastic samples.

Zhang et al. (2009), reported that gold nanoparticles-carbon nanotubes modified sensor for electrochemical determination of organophosphate pesticides. Cyclic voltammetry was used for electrodeposition of gold nanoparticles. Organophosphate pesticides (e.g. parathion) were determined using linear scan voltammetry. A linear working range was obtained for parathion from 6.0×10^{-5} to 5.0×10^{-7} M with a detection limit of 1.0×10^{-7} M. The method was applied to the analysis of parathion in river water samples.

Deng et al. (2010), proposed a new method for determination of Hg(II) using thiol functionalized chitosan-multiwalled carbon nanotubes nanocomposite film electrode. In this work, a glassy carbon electrode modified with a nanocomposite made from thiol-functionalized chitosan (CS-SH) and multiwalled carbon nanotubes was constructed for square wave voltammetric determination of Hg(II). The procedure comprised the steps of (I) chemical accumulation of Hg(II) under open-circuit condition and (II) electrochemical determination of Hg(II). Linear working range were obtained from 10 to 140 nM, with a limit of detection of 3 nM under optimized conditions. The electrode was also applied to the determination of Hg(II) in water samples.

Jia et al. (2010), improved a new electrode system based on the carbon nanotubes-(CNTs-PSS/Bi) composite film for determination of Lead(II) and Cadmium(II). In this method, the bismuth modified carbon nanotubes (CNTs)-poly(sodium 4-styrenesulfonate) composite film electrode (CNTs-PSS/Bi) was used with DPASV. Well defined and sharp stripping peaks at -0.77 V for Cd^{2+} and -0.55

V for Pb^{2+} , respectively, were observed on the electrode in 0.1 M acetate buffer solution at pH 4.5. The detection limits were calculated to be 0.04 ppb for lead(II) and 0.02 ppb for cadmium(II) with a preconcentration time of 120 s, respectively. The linear responses of Cd^{2+} and Pb^{2+} were obtained in the ranges of 0.5 – 50 ppb and 0.5 – 90 ppb, respectively. Finally, the proposed method was employed in the real water samples.

Li et al. (2011), investigated voltammetric determination of bisphenol A in food package using a glassy carbon electrode modified with carboxylated multi-walled carbon nanotubes as a sensor. In this research, a sensitive oxidation peak was found at 550 mV in linear sweep voltammograms at pH 7.0. Trace levels of bisphenol A was determined over a concentration range from 10 nM to 104 nM, and the detection limit was calculated as 5.0 nM. The method was successfully applied to the determination of BPA in food package.

Luo et al. (2013), reported that sensitive determination of Cd(II) by square wave anodic stripping voltammetry using bismuth-modified multiwalled carbon nanotubes doped carbon paste electrodes. The modified electrode showed a good electrocatalytic activity towards electrochemical oxidation of Cd(II) because of good electrical conductivity of MCNTs and excellent electroanalytical performance of bismuth film. Under optimum conditions, the linear working range was from 1.0 to 60 $\mu\text{g/L}$ with a detection limit of 0.3 $\mu\text{g/L}$. The Bi/MCNTs-CPE was successfully applied to the determination of Cd(II) in tap water samples.

Fathirad et al. (2013), demonstrated that fabrication of a new carbon paste electrode modified with multi-walled carbon nanotube for determination of bismuth(III). In this study, a selective and sensitive carbon paste electrode modified with multi-walled carbon nanotubes and 4-[1-(4-methoxyphenyl) methylidene]-3-methyl-5-isoxazolone was performed for accumulation and determination of trace amounts of bismuth by the differential pulse anodic stripping voltammetric method. An anodic peak related to the oxidation of accumulated Bi(0) on the electrode surface was observed at about -0.05 V. The linear working range was from 1 $\mu\text{g/L}$

to 400 µg/L. The limit of detection was 0.2 µg/L. The modified electrode was also applied for the determination of bismuth in pharmaceutical, biological and several water samples.

3. MATERIAL and METHOD**3.1. Instrumentation**

For this current study, there are several instruments have been used. Some of them are listed below;

- Electrochemical experiments were performed using an Eco-Chemie Autolab PGSTAT 12 potentiostat/galvanostat (Utrecht, The Netherlands) with the electrochemical software package 4.9.
- A three-electrode system was used: a glassy carbon electrode [3 mm in diameter (Bioanalytical Systems, Lafayette, USA)] or a Pt electrode [1.6 mm in diameter (Bioanalytical Systems, Lafayette, USA)] as working electrode, a Pt wire counter electrode and a Ag/AgCl (saturated KCl) reference electrode (Metrohm, Switzerland).
- The pH measurements were made with Metrohm 744 pH Meter (Metrohm, Switzerland).
- Scanning Electron Microscope and energy dispersive X-ray analysis (EDX) (ZEIS EVO 50) was used for the characterization of multi walled carbon nanotubes, polymer film layers, metal nanoparticles and composite materials on the electrode surfaces.
- KUDOS (SK3301OHP) model ultrasonic bath was used for dispersing carbon nanotubes and synthesis of carbon nanotubes-metal nanoparticles composites.
- NUVE (MK-418) model magnetic stirrer was used to mix the solutions.
- SHIMADZU (AY-220) model balances was used for analytical weighing.

3.2. Reagents

All reagents were of analytical reagent grade or equivalent. All chemicals were obtained from Sigma–Aldrich, Fluka or Merck with highest grade available and used without further purification.

- Acetic acid ($\geq 99.8\%$, Merck, Germany),
- Acetone ($\geq 99.8\%$, Merck, Germany),
- Acetonitrile (99.9% , Merck, Germany),
- Amonium oxalate ($\geq 99.5\%$, Sigma Aldrich, Germany),
- Albuterole (99.0%, Alfa Aesar, Hungary),
- Alumina powder, (0.05; 0.3; 1.0 micron, Buehler, USA),
- Ascorbic acid (99.7%, Sigma Aldrich, Germany),
- Bromhexine ($\geq 98.0\%$, Fluka, China),
- Cadmium (II) nitrate tetra hydrate ($\geq 99.06\%$, Sigma Aldrich, Germany),
- Caffeine (99.9%, Sigma, Germany),
- Calcium chloride (99.5%, Merck, Germany),
- Chitosan (Sigma Aldrich, Iceland),
- Chloroform (99.0%, Merck, Germany),
- Cobalt (II) chloride hexahydrate (99.0%, Merck, Germany),
- Cupper (II) nitrate threehydrate (99.5%, Merck, Germany),
- D-Glucose anhydrous (99.0%, Fluka, USA)
- Disodium monohydrogen phosphate dihydrate (99.5%, Merck, Germany),
- Dopamine hydrochloride (99.0%, Merck, Germany),
- Ethanol ($\geq 99.5\%$, Merck, Germany),
- Hydrochloric acid, (37-38%, Merck, Germany),
- Lactic acid ($\geq 98.0\%$, Sigma Aldrich, USA),
- Lead (II) nitrate (99.0%, Alfa Aesar),
- Lithium perchlorate, LiClO_4 ($\geq 98.0\%$, Fluka, Germany),
- Methimazole (98.0%, Sigma, Germany),
- Multiwalled carbon nanotubes (MWCNTs) (95.0%, NanoLab, USA),
- Nickel (II) chloride tetrahydrate (99.0%, Merck, Germany),

- Nickel (II) nitrate hexahydrate (99.9 %, Sigma Aldrich, Germany),
- Nitric acid (65.0 %, Merck, Germany),
- Paracetamol (98.0%, Alfa Aesar, Germany),
- Perchloric acid (70-72 %, Merck, Germany),
- Pivalic acid (99.9 %, Sigma Aldrich, Netherlands),
- Potassium chloride (99.5 %, Merck, Germany),
- Potassium dihydrogen phosphate (99.5 %, Merck, Germany),
- Sodium hydroxide (≥ 99.0 %, Merck, Germany),
- Sodium nitrate (≥ 99.0 %, Sigma Aldrich, USA),
- Uric acid (≥ 98.0 Fluka, Germany),

3.3. The Samples Used for Analytical Applications

The samples which are used in these experiments were drugs, urine samples, water samples, and nutrition samples.

The drug tablets and injections were purchased from the local pharmacy.

- PAROL[®] Tablet, 500 mg paracetamol/tablet (Atabay Pharm. Co., Turkey.,).
- THYROMAZOL[®] Tablet, 5 mg Metil-1-Merkapto-2-İmidazol (Metimazol)/tablet (Abdi Ibrahim Pharm. Co., Turkey.,).
- VENTOLIN[®] Tablet, 2 mg salbutamol (albuterole)/tablet (Glaxo Smithkline Pharm. Co.).
- DOPAMINE FRESENIUS[®] ampul, 200 mg dopamine hydrochloride/5 mL (Fresenius Kabi Pharm. Co., France)
- BROMEK[®] Tablet, 8 mg bromhexine hydrochloride/tablet (Kocak Pharm. Co., Turkey).

All real samples were taken according to the rules of sample collection.

- Urine samples were obtained from healthy and voluntry people who use no any drugs for determination of albuterol, dopamine and paracetamol, and heavy metals.
- Tap water samples were obtained from Sanliurfa city water network, Turkey for determination of lead(II) and cadmium(II).
- The river water samples were obtained from agricultural irrigation channel of Fırat River, Osmanbey Village region of Sanliurfa, Turkey for determination of lead(II) and cadmium(II).
- The artificial lake water samples were collected from the artificial lake of Osmanbey Campus, Harran University, Sanliurfa, Turkey for determination of lead(II) and cadmium(II).
- Different brands with similar content, commercial and bottled drinking water samples were purchased from local supermarket for determination of lead(II) and cadmium(II).
- Other used nutrition samples were purchased from local supermarket.

3.4. Preparation of Used Standard Stock Solutions

- Phosphate buffer saline solutions (PBS) were prepared from potassium dihydrogen phosphate, KH_2PO_4 (6.8 g/L), disodium monohydrogen phosphate dihydrate, $\text{Na}_2\text{HPO}_4 \cdot 2\text{H}_2\text{O}$ (8.8 g/L) and potassium chloride, KCl (0.75 g/L) as a saline and then adjusted in the pH range from 3 to 9 with adding 0.1 M HCl or 0.1 M NaOH solutions. Ionic strength was kept nearly constant for each buffer solution as 0.1 M. All buffer solutions were prepared from analytical grade reagents and in ultrapure water.
- Paracetamol 1 mM stock solution was prepared with 0.1 M phosphate buffer solution at pH 7.0.

- Albuterol 1 mM and Uric acid 10 mM stock solution were prepared with 0.1 M phosphate buffer solution at pH 8.0.
- Methimazole 1mM stock solution was prepared with 0.1 M phosphate buffer solution (PBS) at pH 7.2.
- Dopamine 1 mM, Paracetamol 1 mM, Ascorbic acid 10 mM and Uric acid 10 mM stock solutions were prepared with 0.1 M phosphate buffer solution at pH 7.0.
- Bromhexine 1 mM stock solution was prepared with 0.1 M phosphate buffer solution at pH 4.0.
- Cadmium(II) nitrate tetra hydrate 1 mM, and lead(II) nitrate 1 mM stock solution was prepared in 0.1 M NaNO₃ solution at pH 7.0.

All of the standard stock solutions were prepared freshly before each use and the all stock solutions were kept in amber bottles in order to protect from light. The standard stock solutions were also diluted before use when it was needed. All experiments were carried out at room temperature. Oxygen-free nitrogen was bubbled through the cell prior to each experiment.

3.5. Preparation of Used Real Samples for Analytical Applications

- Five THYROMAZOL[®] tablets were weighed and crushed to a fine powder in a mortar. A mass of powder equivalent to the average mass of one tablet was dissolved in 25 mL of 0.1 M PBS at pH 7.2. It was then introduced to an ultrasonic bath for 5 min, filtered and diluted with 0.1 M PBS in a calibrated 100 mL flask. Appropriate dilutions were made from the supernatant solution with 0.1 M PBS. Then the tablet solution was subjected to cyclic voltammetry. The methimazole content of drug was determined referring to the regression equation.

- Several VENTOLIN[®] tablets were weighed and crushed to a fine powder in a mortar. A mass of powder equivalent to the average mass of one tablet was dissolved in 25 mL of 0.1 M PBS at pH 8.0. It was then introduced to an ultrasonic bath for 8-10 min, filtered and diluted with 0.1 M PBS in a calibrated 100 mL flask. Appropriate dilutions were made from the supernatant solution with 0.1 M PBS. Square wave voltammetric determination of albuterol in pharmaceutical formulations was referred to the regression equation.
- Urine samples that obtained healthy and voluntry people who use no any drug were filtered and diluted 50 times in a calibrated flask by 0.1 M PBS at pH 8.0 and subjected to the square wave voltammetric analysis for determination of albuterol by the regression equation.
- Five BROMEK[®] tablets were weighed and crushed to a fine powder in a mortar. A mass of powder equivalent to the average mass of one tablet was dissolved in 25 mL of 0.1 M PBS at pH 4.0. It was then introduced to an ultrasonic bath for 10 min, filtered and diluted with 0.1 M PBS in a calibrated 100 mL flask. Appropriate dilutions were made from the supernatant solution with 0.1 M PBS. Then the tablet solution was subjected to square wave voltammetry. The bromhexine content of drug was determined referring to the regression equation.
- Five PAROL[®] tablets were weighed and crushed to a fine powder in a mortar. A mass of powder equivalent to the average mass of one tablet was dissolved in 25 mL of 0.1 M PBS at pH 7.0. It was then introduced to an ultrasonic bath for 10 min, filtered and diluted with 0.1 M PBS in a calibrated 100 mL flask. Appropriate dilutions were made from the supernatant solution with 0.1 M PBS. Then the tablet solution was subjected to square wave voltammetry. The paracetamol content of drug was determined referring to the regression equation.
- 1 mL DOPAMINE FRESENIUS[®] ampoule drug was taken by a micropipette and then diluted with 0.1 M PBS at pH 7.0 in a calibrated 50 mL flask. Appropriate dilutions were made from the prepared solution with 0.1 M PBS.

Then the ampoule drug solution was subjected to square wave voltammetry. The dopamine content of drug was determined referring to the regression equation.

- Urine samples that obtained healthy and voluntry people who use no any drug were filtered and diluted 50 times in a calibrated flask by 0.1 M PBS at pH 7.0 and subjected to the square wave voltammetric analysis for calculation of recoveries of dopamine and paracetamol by the regression equation.
- Urine samples that obtained healthy and voluntry people who use no any drug were filtered and diluted 50 times in a calibrated flask by 0.1 M NaNO₃ at pH 7.0 and subjected to the square wave voltammetric analysis for calculation of recoveries of Cd (II) and Lead (II). Different standard concentrations of Cd(II) and Lead(II) were added to the diluted UA samples for testing recovery.
- Various water samples filtered and diluted 50 times with 0.1 M NaNO₃ at pH 7.0 in a calibrated flask. Appropriate dilutions were made from the prepared solution with 0.1 M NaNO₃ solution at pH 7.0. Then, the sample solution was subjected to square wave voltammetry. The cadmium (II) and lead (II) content of water samples were determined referring to the regression equation.
- Other used nutrition samples filtered and diluted 50 times with 0.1 M NaNO₃ at pH 7.0 in a calibrated flask. Appropriate dilutions were made from the prepared solution with 0.1 M NaNO₃ solution at pH 7.0 and the sample solution subjected to the square wave voltammetric analysis for calculation of recoveries of Cd (II) and Lead (II).

3.6. Preparations of Carbon Nanotubes Based Modified Electrodes

3.6.1. Pre-treating of glassy carbon electrode

Prior to the modification, the bare glassy carbon electrode was polished with 1 micron, 0.3 micron and 0.05 micron alumina slurry on a polishing pad respectively. The electrode rinsed with water and sonicated with 1:1 HNO₃ and acetone and water for 10 min or sonicated in ethanol for 5 min respectively. After being cleaned, the electrode was activated by 10 cyclic sweeping from -1.0 to 1.5 V in PBS at studied pH.

3.6.2. Preparation of MWCNT- modified electrodes

Multiwalled carbon nanotubes were first dispersed in chloroform (1 mg in 5 mL). This was placed into an ultrasonic bath for 10 min, after which an aliquot of known volume was cast onto the glassy carbon electrode and the solvent allowed to evaporate.

3.6.3. Preparation of poly(pivalic acid)/MWCNT modified electrodes

After being cleaned, as mentioned before, the electrode was activated by 10 cyclic sweeping from -1.0 to 1.5 V in PBS at pH 8.0. 5 mg of MWCNT was dispersed in 5 mL chloroform and ultrasonicated 30 min resulting in a homogeneous black suspension. Then 20 µL of the MWCNT suspension was dropped directly onto the GCE surface and dried at ambient conditions to obtain MWCNT/GCE. The electropolymerization of PA on MWCNT/GCE was carried out using cyclic sweeps between -1.0 V and 1.5 V for 15 cycles with a scan rate of 150 mV/s by immersing the MWCNT/GCE into a solution of 10 mM PA in acetonitrile containing 50 mM LiClO₄ as supporting electrolyte. Finally, the PPA/MWCNTs/GCE was washed double-distilled water and stored in 0.1 M PBS.

3.6.4. Preparation of poly(pivalic acid)/CoNPs/MWCNT modified electrodes

After being cleaned, as mentioned before, the electrode was activated by 10 cyclic sweeping from -1.0 to 1.5 V in PBS at pH 7.2. Multiwalled carbon nanotubes were first dispersed in chloroform (5 mg in 5 mL). This was placed in an ultrasonic

bath for 30 min, after which an aliquot of known volume was cast on the glassy carbon electrode and the solvent was allowed to evaporate. The simultaneous electropolymerization of pivalic acid and deposition of cobalt on MWCNT/GCE was carried out using cyclic sweepings from -1.0 V to 1.5 V for 40 cycles at a scan rate of 0.15 V/s by immersing the carbon nanotubes modified electrode into a solution of 10 mM pivalic acid and 30 mM cobalt (II) chloride hexahydrate in acetonitrile containing 50 mM LiClO_4 as supporting electrolyte. Then the modified electrode was washed with ultra pure water and stored in 0.1 M PBS. A simple illustration for the stepwise preparation of poly(pivalic acid)-CoNPs/MWCNT/GCE is also shown in Figure 3.1.

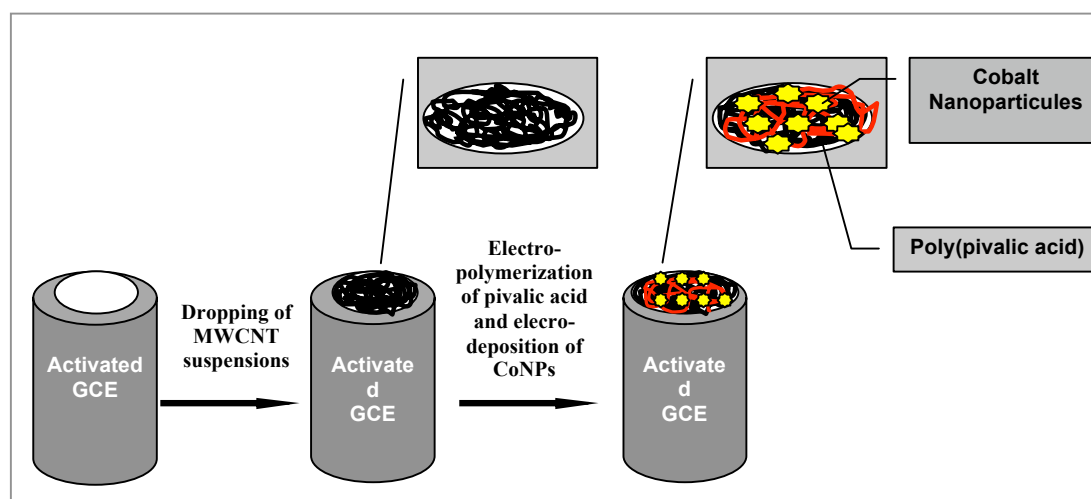


Figure 3.1. Schematic illustration for the stepwise preparation of poly (pivalic acid)/CoNPs/MWCNT/GCE

3.6.5. Preparation of CoNPs/MWCNT modified GCE

Cobalt nanoparticles were synthesized onto the surface of CNTs using the following protocol: The MWCNTs were sonicated in concentrated $\text{HClO}_4 + \text{HNO}_3$ (3:7, v:v) for 7 h in order to oxidize their surface, they were then filtered and extensively washed with deionized water to pH 7.0, and dried in air. Then, 2.7 mg

CoCl₂ and 2.0 mg oxidized CNTs were added to 60 mL of acetonitrile in an airtight glass flask. The mixture was sonicated for one hour. 4.0 mg of L- ascorbic acid was then added in the flask and the pH was adjusted to 5.2 using 1 M NaOH. The reaction was allowed to proceed for 5 min at 65 °C under sonication. Finally, the products were separated by centrifugation, washed with acetonitrile and deionized water to remove any unreacted species. The multi-walled carbon nanotubes decorated with cobalt nanoparticles (CoNPs /MWCNTs) were allowed to air-dry for 24 h prior to use. A simple illustration for the stepwise preparation of ultrasonic synthesis of cobalt nanoparticles on MWCNTs is also shown in Figure 3.2.

The synthesized CoNPs-MWCNTs composite products were first dispersed in chloroform (1 mg in 5 mL). This was placed into an ultrasonic bath for 30 min, after which an aliquot of known volume was cast onto the glassy carbon electrode and the solvent allowed to evaporate. Then the CoNPs-MWCNT modified electrode was washed with ultra pure water and stored in 0.1 M PBS.

3.6.6. Preparation of NiNPs/MWCNT modified Pt electrode

Multiwalled carbon nanotubes (MWCNTs) were sonicated in concentrated HClO₄ + HNO₃ (3:7, v:v) for 7 h in order to oxidize their surface, they were then filtered and extensively washed with deionized water to pH 7.0, and dried in air. Then, 2.9 mg NiCl₂ and 2.0 mg oxidized MWCNTs were added to 60 mL of acetonitrile in an airtight glass flask. The mixture was sonicated for 1 h. 4.0 mg of L-ascorbic acid was then added in the flask and the pH was adjusted to 5.2 using 1 M NaOH. The reaction was allowed to proceed for 5–6 min at 65 °C under sonication. Finally, the products were separated by centrifugation, washed with acetonitrile and deionized water to remove any unreacted species. The multiwalled carbon nanotubes functionalized with nickel nanoparticles (NiNPs/MWCNTs) were allowed to air-dry for 24 h prior to use.

The synthesized NiNPs-MWCNTs composite products were first dispersed in chloroform (1 mg in 5 mL). This was placed into an ultrasonic bath for 30 min, after

which an aliquot of known volume was cast onto a Platinum electrode polished with 0.05 micron alumina and the solvent allowed to evaporate. Then the NiNPs-MWCNT modified electrode was washed with ultrapure water and stored in 0.1 M PBS.

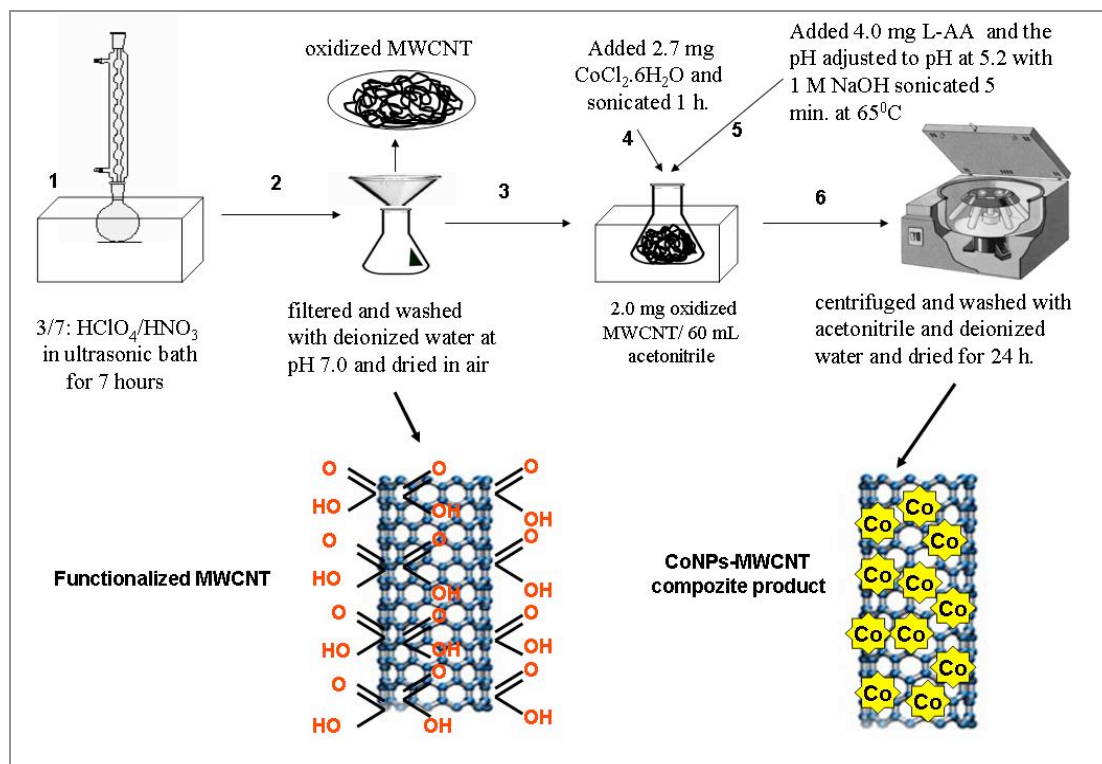


Figure 3.2. Schematic illustration for the stepwise preparation of functional MWCNTs and synthesis of CoNPs-MWCNTs composite

3.6.7. Preparation of Chitosan-MWCNT modified GCE

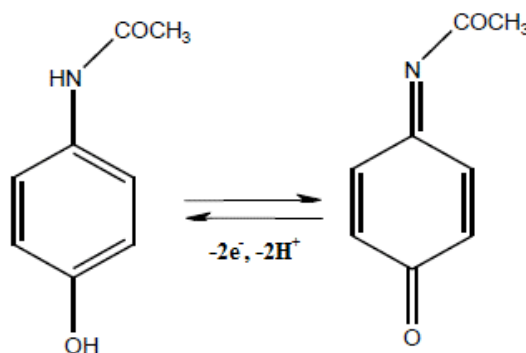
Functionalized multiwalled carbon nanotubes (as mentioned in section 3.6.5) were first dispersed in chloroform (1 mg in 5 mL). This was placed into an ultrasonic bath for 30 min, after which an aliquot of known volume was cast onto the glassy carbon electrode and the solvent allowed to evaporate. Chitosan solution was prepared in 3% acetic acid solution (1 mg in 5 mL) in an ultrasonic bath for 30 min, Then an aliquot of known volume cast onto the multiwalled carbon nanotubes modified GCE and the solvent was evaporated at room temperature. Then the modified electrode was washed deionized water and stored in 0.1 M PBS.

4. RESULTS and DISCUSSIONS

4.1. Voltammetric Detection of Paracetamol (PAR) in the Presence of Ascorbic Acid (AA), Dopamine (DA) and Uric Acid (UA) with Using MWCNT Modified GCE

In this study, we report experiments for the detection of PAR in the presence of AA, DA and UA at a glassy carbon electrode modified with multi-walled carbon nanotubes (MWCNTs).

Voltammetric detection provides a highly sensitive approach to the electroanalysis of a wide range of analytes (Kachoosangi and Compton, 2007; Wildgoose et al., 2006; Ensafi et al., 2009). However, this approach can sometimes be restricted by limitations of selectivity due to the interference from the other redox active molecules which may undergo electrolysis at similar potentials to the target species in the medium (Streeter et al., 2008; Kachoosangi et al., 2008). Such an example arises in the determination of the analgesic drug, paracetamol (PAR), by means of two electron oxidation: using carbon based electrodes,



since molecules such as ascorbic acid (AA), dopamine (DA) and uric acid (UA) all display redox behaviour at potentials close to those required for the oxidation of PAR. The most important strategy to overcome such problems is to modify the surface of the electrode to produce a chemically modified electrode, that aims to

alter the electrode kinetics of both target species and the interfering species so that the potential under which the target species undergo oxidation becomes shifted from that required to electrolyse the interfering species (Walcarius, 2008; Jones and Compton, 2008; Griese et al., 2008; Gooding, 2008; Chow and Gooding, 2006).

Voltammetric nanosensors based on CNTs represent a new and interesting alternative for the quantification of different analytes (Jain and Sharma, 2012; Geto et al., 2013; Gupta et al., 2013; Li et al., 2012). The performance of CNT modified electrodes has been found to be much superior to those of other carbon electrodes in terms of response time, increased sensitivity, resistance to surface fouling, decreased overpotentials, reuseability and limits of detection (Wang, 2005).

Paracetamol, also known as acetaminophen is an effective pain killer used for the widespread relief of pains associated with many parts of the body (Carvalho et al., 2004). The overdose of PAR can lead to the accumulation of toxic metabolites which may cause hepatotoxicity and nephrotoxicity (Martin and MacLean, 1998). Therefore controlling the amount of PAR in pharmaceuticals is of great importance for the general public health.

A number of analytical procedures have been reported for the analysis of PAR in pharmaceutical forms or biological fluids including chromatography (Ravinsankar et al., 1998), spectrophotometry (Hanaee, 1997), chemiluminescence (Easwaramoorthy et al., 2001), capillary electrophoresis (Zhao et al., 2006), FTIR and Raman spectrometry (Zhoubi et al., 2002), and flow injection analysis using various methods of detection (Knochen et al., 2003; Silva et al., 2006). However, these techniques are expensive and require time-consuming derivatization step and also in some cases low sensitivity and selectivity makes them unsuitable for a routine analysis.

On the other hand, voltammetric methods have several advantageous owing to their simplicity, high sensitivity and rapidness (Walcarius, 2008; Li et al., 2012). The development and application of electrochemical sensors for the determination of

PAR has received considerable interest in last few decades since PAR is an electroactive compound which can be oxidized electrochemically. Most electrochemical methods rely on the modification of electrodes such as MWCNT modified pyrolytic graphite electrode (Kachoosangi et al., 2008), carbon nanoparticles modified GCE (Ghorbani-Bidkorbeh et al., 2010), SWCNT-graphene modified GCE (Chen et al., 2012), carbon nanotube modified screen printed electrode (Fanjul-Bolado, 2009), SWCNT modified ceramic electrode (Habibi et al., 2011), and D50wx2-GNP-modified carbon paste electrode (Sanghavi and Srivastava et al., 2011).

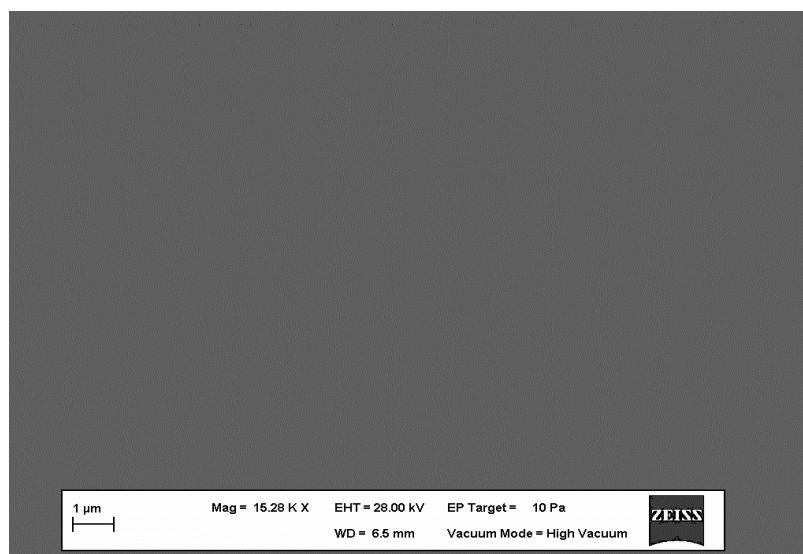
4.1.1. Surface characterizations of bare GCE and MWCNT modified GCE

Surface characterizations of bare GCE and MWCNT modified GCE were performed with a scanning electron microscope (SEM) at Harran University Central Laboratory. SEM images of bare GCE (a) and MWCNT/GCE (b) are given in Figure 4.1. It can be seen that MWCNT modified GCE have a rough surface and this can provide larger specific surface area than bare GCE for electrochemical oxidation.

4.1.2. Voltammetric behaviour of paracetamol at bare GCE and MWCNT modified GCE

Cyclic voltammetry was performed at a bare glassy carbon electrode for a 1.0×10^{-6} M solution of PAR in 0.1 M phosphate buffer solution at pH 7.0. The oxidation of PAR shows a quasi-reversible response on a naked glassy carbon electrode at which an appreciable overpotential is required to drive the two electron oxidation. Figure 4.2. shows cyclic voltammograms of PAR recorded at different scan rates. The anodic peak current (I_{pa}) was proportional to the square root of the scan rate ($v^{1/2}$) over the range of 25-150 mV/s (in Figure 4.3.) and also Log of peak current against log of scan rate showed slope close to 0.5, suggesting that the redox wave is diffusional in nature.

(a)



(b)

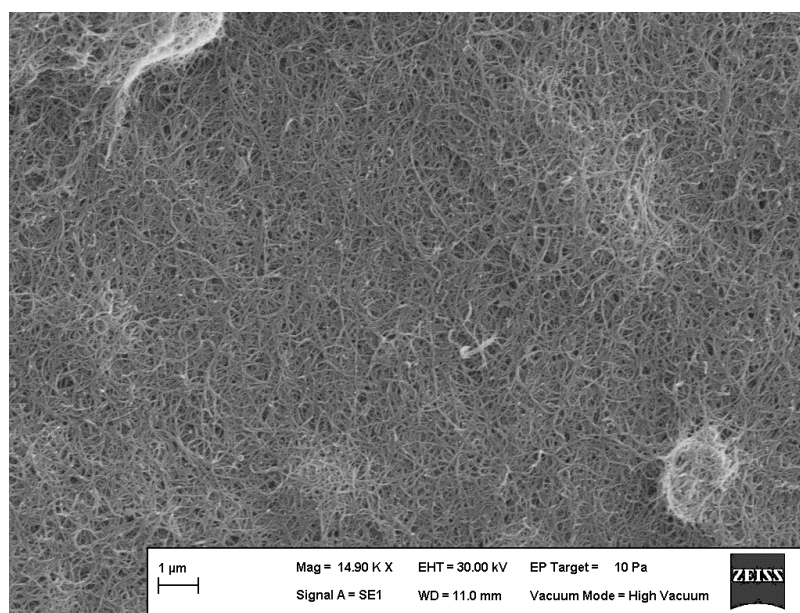


Figure 4.1. SEM images of bare GCE (a) and MWCNT modified GCE (b)

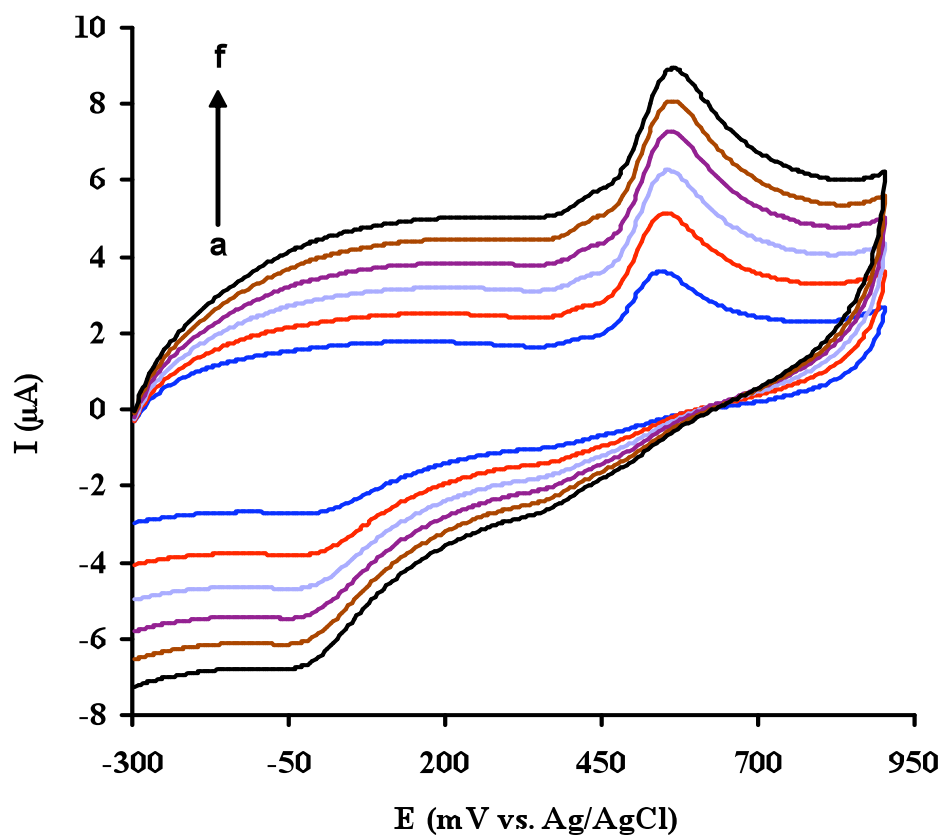


Figure 4.2. Cyclic voltammograms of 1.0×10^{-6} M PAR at bare GCE in 0.1 M PBS at pH 7.0. Scan rates increasing from 25 mV/s to 150 mV/s. a) 25 mV/s; b) 50 mV/s; c) 75 mV/s; d) 100 mV/s; e) 125 mV/s; f) 150 mV/s. Equilibrium time: 5 s

The cyclic voltammograms of 1.0×10^{-6} M PAR recorded at different scan rates using a GCE modified with MWCNTs are shown in Figure 4.4. The peak current was observed to vary linearly with scan rate for an electrode modified with $0.15 \mu\text{g}$ MWCNTs. The change in the peak current response from a square root to a linear dependence on scan rate is attributed to the transition from planar diffusion to thin layer behaviour (Streeter et al., 2008; Henstridge et al., 2010). As the signals were seen immediately on exposure of the electrode to solution, and changed only a little over a period of ca. 10 min from which it was inferred that adsorption effects were considerably less than solution-phase signals. Although, the distinction between thin layer diffusion and adsorption effects are not easy to make, especially where the adsorption is rapidly reversible we infer that thin layer effects may dominate in the oxidation of PAR as strong oxidative signals are seen immediately

on exposure to the solution, changing relatively little with prolonged immersion of the electrode prior to oxidation (Henstridge et al., 2010).

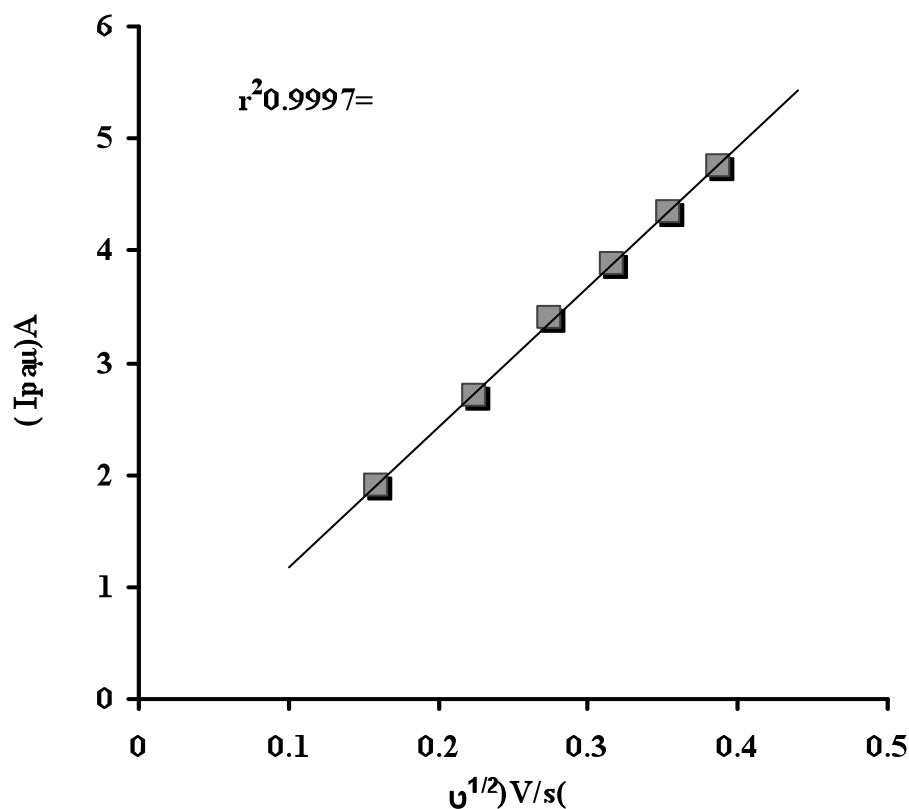


Figure 4.3. Plot of anodic peak currents of PAR versus scan rates at the bare GCE

The effect of the mass of MWCNTs on the electrode surface was then examined. Cyclic voltammograms were recorded at a glassy carbon electrode modified with varying amounts of MWCNTs, shown in Figure 4.5. The peak-to-peak separation is seen to reduce and the electrochemical signal appears more reversible as the glassy carbon electrode is modified with an increasingly thick layer of MWCNTs. A plot of peak potential vs. mass of MWCNTs is shown in Figure 4.6. The results indicate that both anodic and cathodic peaks occur at lower overpotential with increasing layer thickness on the electrode surface, and that the overall peak-to-peak separation decreases as a result. The data are consistent with a transition from planar diffusion to a thin layer character as the potential required for the oxidation of

PAR shifts to lower potentials (Streeter et al., 2008; Henstridge et al., 2010; Keeley et al., 2009; Xiao et al., 2009).

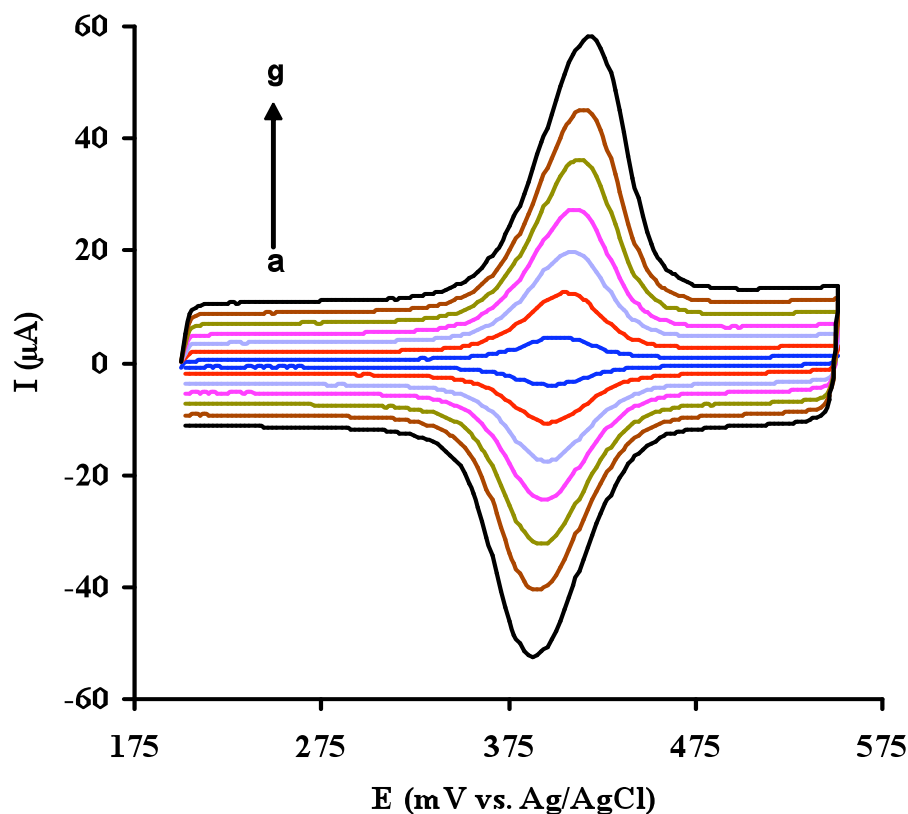


Figure 4.4. Cyclic voltammograms of 1.0×10^{-6} M PAR at $0.15 \mu\text{g}$ MWCNT/GCE in 0.1 M PBS at pH 7.0. Scan rates increasing from (a) 25 to (g) 175 mV/s. Equilibrium time: 5 s

4.1.3. The effect of pH on the voltammetric behaviour of PAR at MWCNT modified GCE

Figure 4.7. shows that the effect of pH on the peak potential of PAR using cyclic voltammetry at GCEs modified with $0.15 \mu\text{g}$ MWCNTs in 0.1 M PBS at pH 7.0. The results show that the oxidation peak potential shifts towards negative potential with increasing pH. This shows that the redox couple of PAR includes transfer of protons in oxidation and reduction process. The slope of oxidation peak potential (E_{pa}) vs. pH is 56.9 mV/pH (Figure 4.8.). The linear regression equation is

E_{pa} (mV) = 820.0714 - 56.8929 pH with a correlation coefficient of 0.9920. This indicated that the proportion of electrons and protons involved in the reaction is 1:1. Since equal numbers of electrons and protons should be involved in the electrode reaction, the number of hydrogen ions involved in the whole electrode reaction is 2. The proposed PAR reaction at a GCE modified with MWCNTs is given in Scheme 4.1.

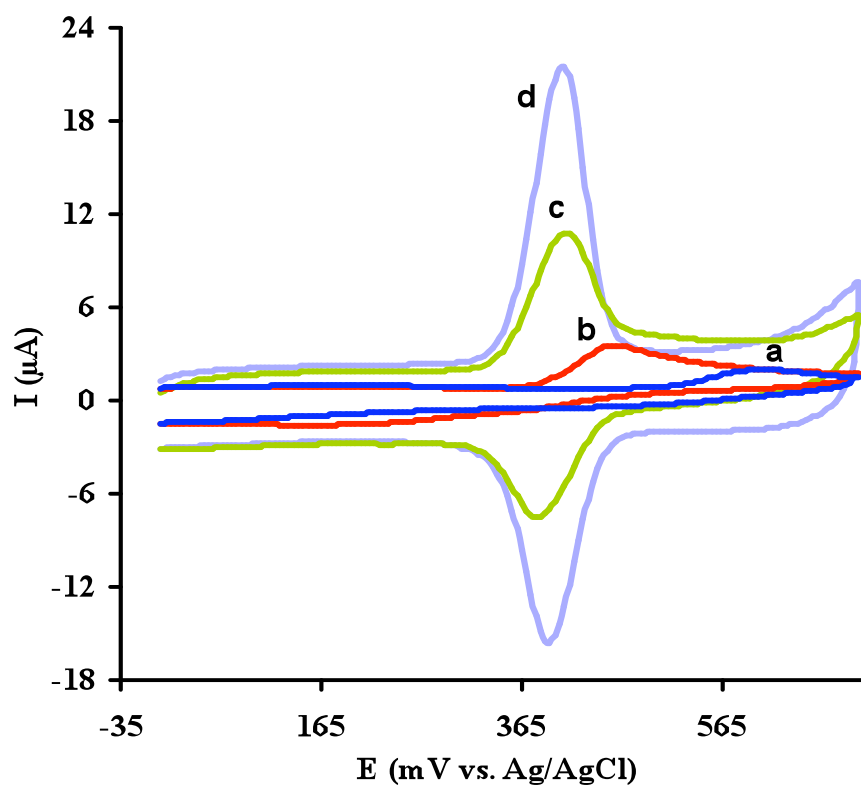


Figure 4.5. Cyclic voltammograms of 1.0×10^{-6} M PAR in 0.1 M PBS at pH 7.0 at a GC electrode modified with 0.00 μg (a), 0.025 μg (b), 0.1 μg (c) and 0.15 μg (d) MWCNTs. Scan rate: 100 mV/s. Equilibrium time: 5 s

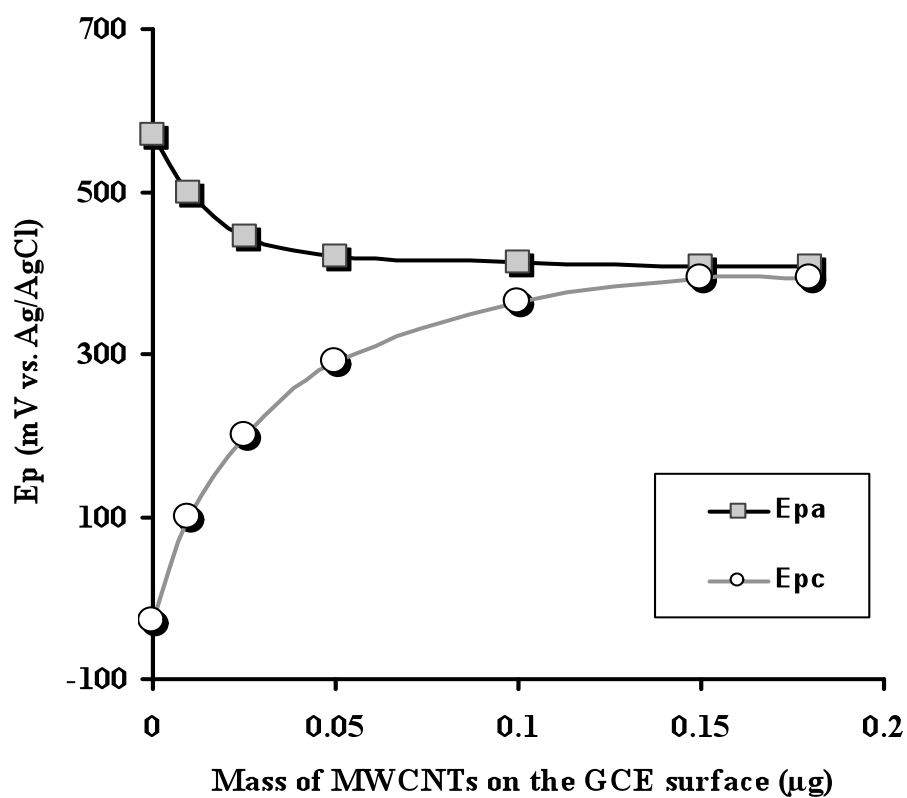


Figure 4.6. Plot of peak potentials of 1.0×10^{-6} M PAR solution vs. mass of MWCNTs on the electrode surface

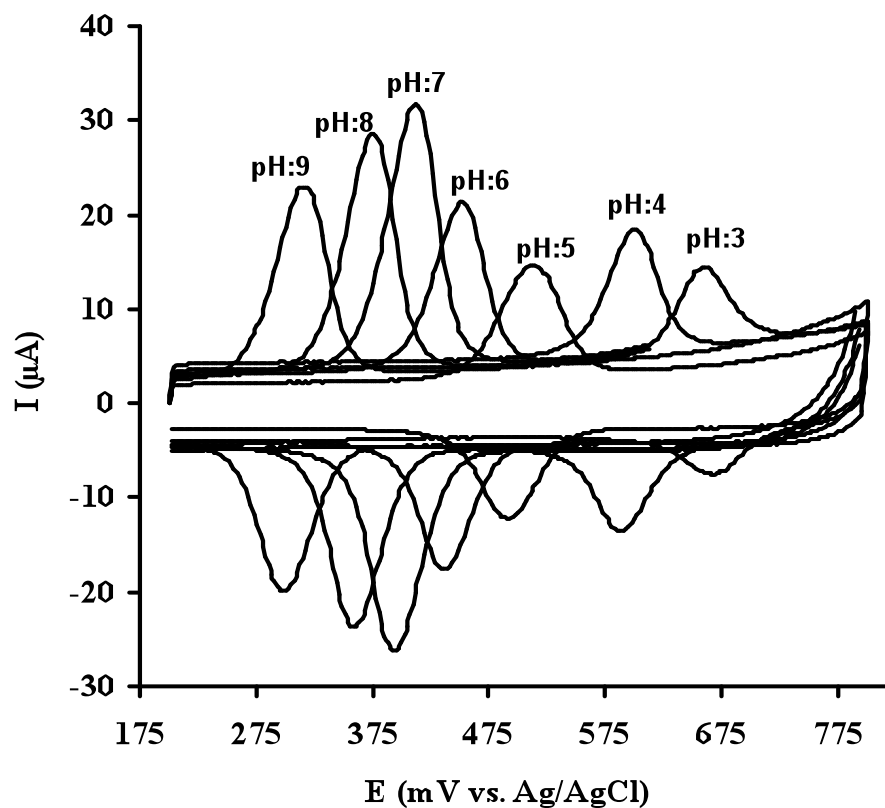
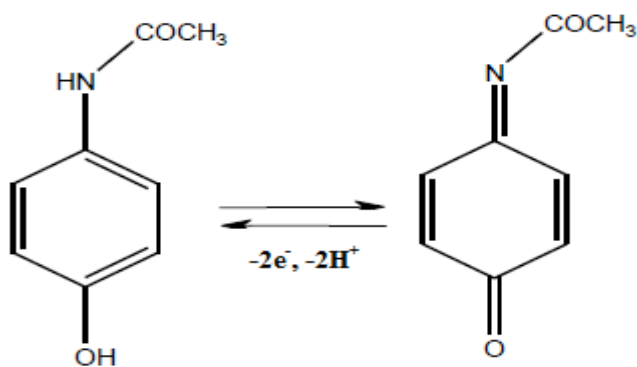


Figure 4.7. Cyclic voltammograms of 1.5×10^{-6} M PAR at $0.15 \mu\text{g}$ MWCNT/GCE in 0.1 M PBS at different pH values. pH: 3.0; 4.0; 5.0; 6.0; 7.0; 8.0; 9.0. Scan rate: 100 mV/s. Equilibrium time: 5 s



Scheme 4.1 Proposed PAR reaction at a GCE modified with MWCNTs

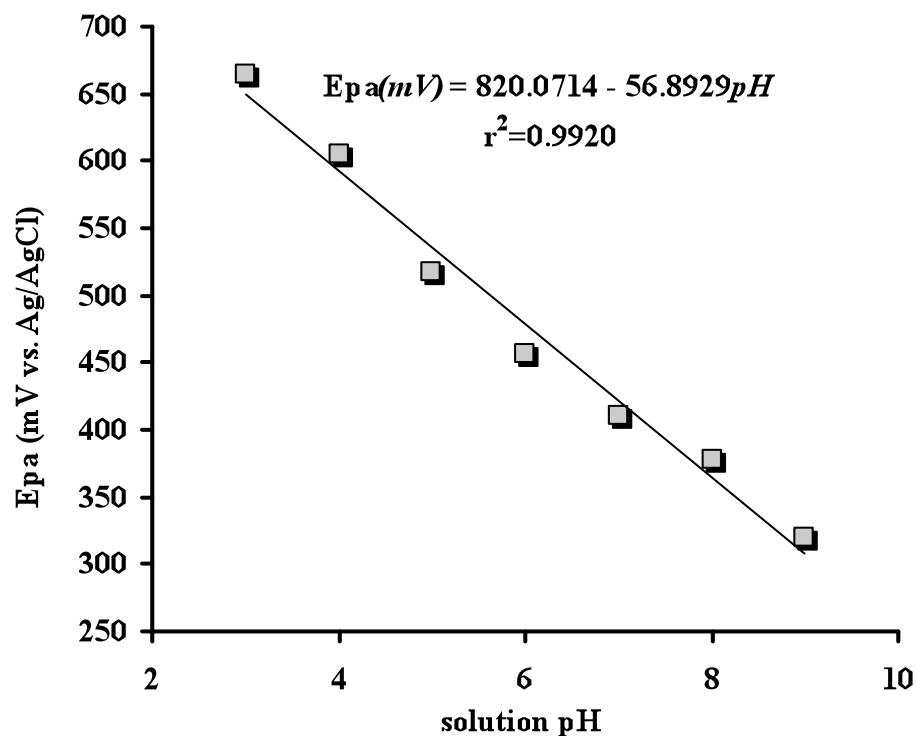


Figure 4.8. Plot of anodic peak potentials of PAR vs. solution pH at 0.15 μg MWCNT/GCE

4.1.4. Calibration equation for the determination of paracetamol

The square voltammetric determination of the concentration of PAR at glassy carbon electrodes modified with 0.15 μg MWCNTs was performed in 0.1 M PBS at pH 7.0 (Figure 4.9.). The anodic peak currents were plotted against the concentration of PAR as shown in Figure 4.10 (A and B). The anodic peak currents were linear with the concentrations of PAR over two intervals in the range of 2.0×10^{-10} M - 2.5×10^{-8} M (A) and 2.5×10^{-8} M - 1.5×10^{-5} M (B). The first linear regression equation was $I_{pa} (\mu\text{A}) = -0.06185 + 202.1743C (\mu\text{M})$ with a correlation coefficient of 0.9993. The second was $I_{pa} (\mu\text{A}) = 6.7992 + 0.6025C (\mu\text{M})$ with a correlation coefficient of 0.9962. The detection limit was 9.0×10^{-11} M (S/N=3). Also, the analytical parameters obtained by the proposed method are well compared with several methods for the determination of PAR as shown in Table 4.1.

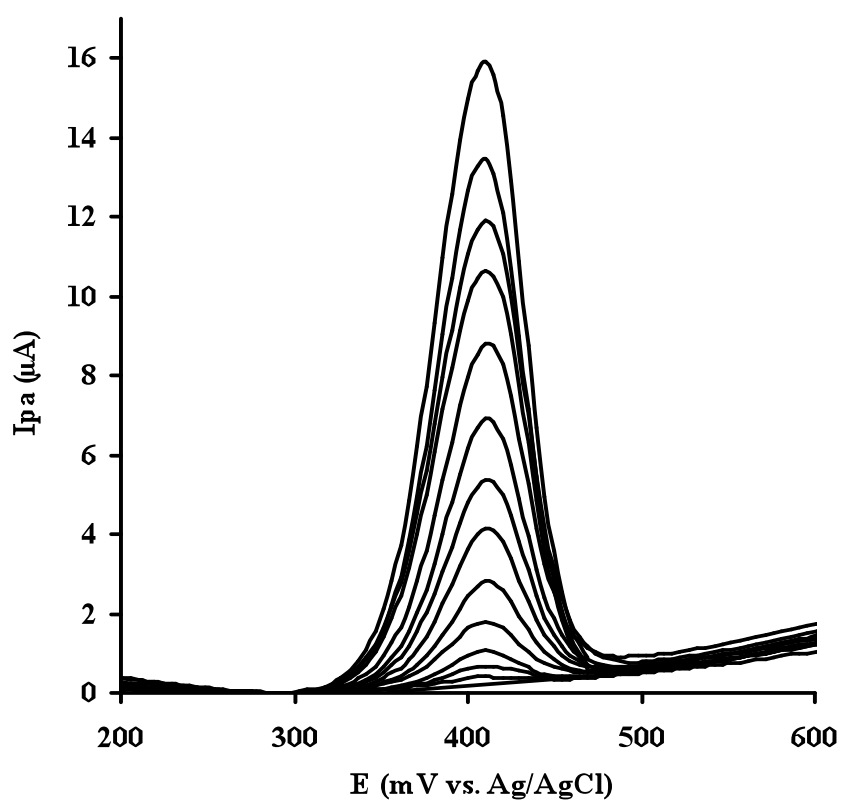


Figure 4.9. Square wave voltammograms of increasing concentrations of PAR at 0.15 μg MWCNT/GCE in 0.1 M PBS at pH 7.0. PAR concentrations: 0.00; 0.0002; 0.0015; 0.006; 0.010; 0.015; 0.020; 0.025; 0.125; 2.50; 5.50; 7.50; 10.0; 15.0 μM . Frequency: 22 Hz. Step potential: 100 mV/s. Amplitude: 50 mV/s. Equilibrium time: 5 s

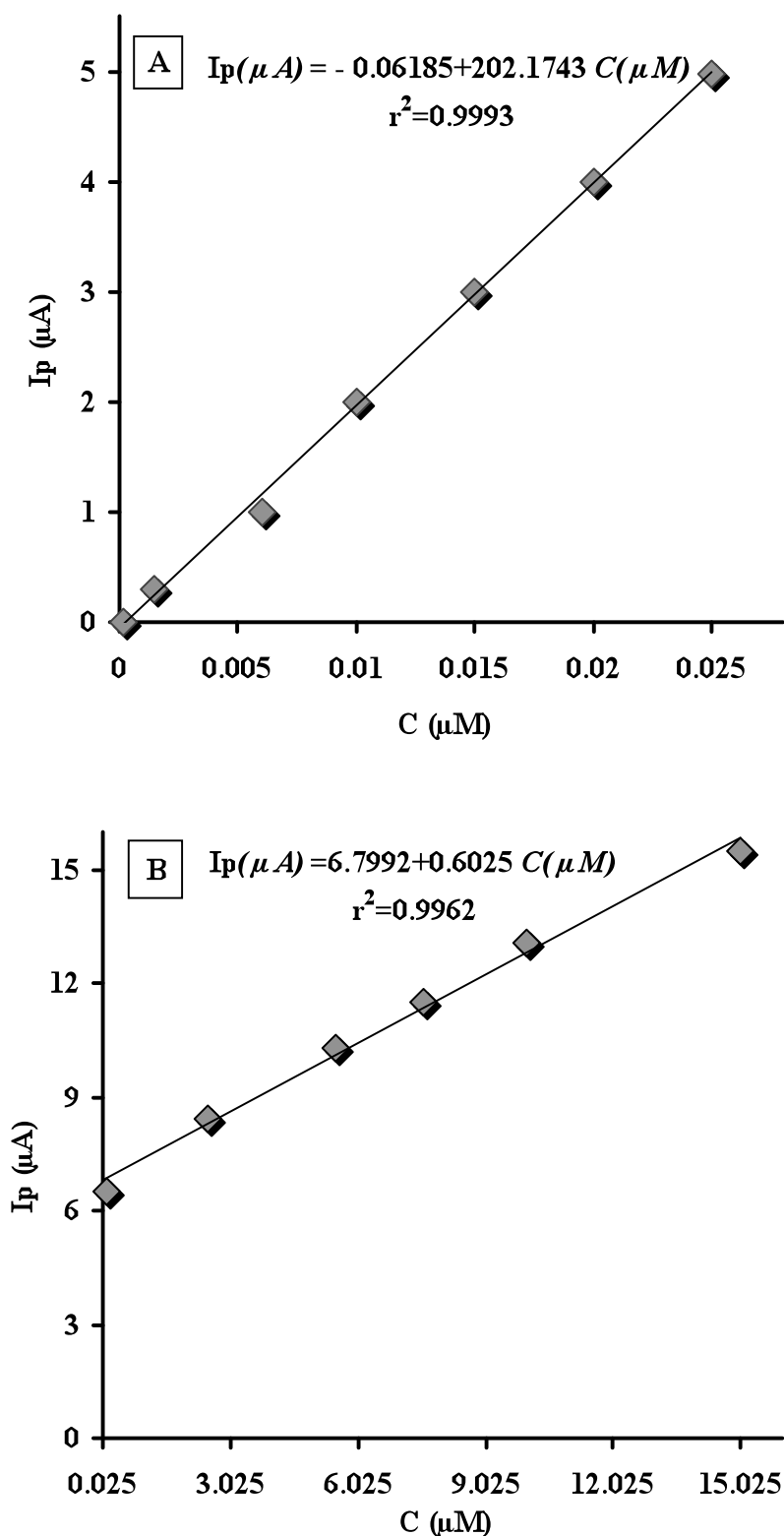


Figure 4.10. Plots of peak currents vs. increasing concentrations of PAR at 0.15 μg MWCNT/GCE in 0.1 M PBS at pH 7.0

Table 4.1. The application results of various electrodes for the determination of PAR

Electrode	pH used	Linear range (μM)	Detection limit (nM)	Reference
C ₆₀ /GCE	7.2	50-1500	50000	(Goyal and Singh, 2006)
N-DHPB-MWCNT/CPE	7.0	15-270	10000	(Ensafi et al., 2011)
PANI-MWCNT/GCE	5.5	1-100	2500	(Li and Jing, 2007)
PAY/nano-TiO ₂ /GCE	7.0	12-120	2000	(Kumar et al., 2008)
PEDOT/SPE	5.0	4-400	1390	(Su and Cheng, 2010)
ZrO ₂ /CPE	7.0	1- 2500	912	(Mazloum-Ardakani et al., 2010)
C-Ni/GCE	3.0	2-230	600	(Wang et al., 2007)
f-MWCNT/GCE	8.0	3-300	600	(Alothman et al., 2010)
PR/MCPE	5.0	0.7-100	530	(Thomas et al., 2013)
IL/CNTPE	7.0	1-600	500	(Tavana et al., 2012)
PSS-PDDA/GE	7.0	25-400	500	(Manjunatha et al., 2011)
Poly(taurin)-MWCNT/GCE	7.3	1-100	500	(Wan et al., 2009)
CoO _x /CCE	13	5-35	370	(Razmi and Habibi, 2010)
Carbon ionic liquid electrode	4.6	1-2000	300	(Shang-Guan et al., 2008)
Nafion/TiO ₂ -graphene	7.0	1-100	210	(Fan et al., 2011)
Chitosan-MWCNT/GCE	7.0	1-145	100	(Babaei et al., 2010)
Ppyox/AZ/Au	2.8	0.2-100	80	(Gholivand and Amiri, 2012)
MWCNT-ACS/GCE	9.0	0.05-2	50	(Lu and Tsai, 2011)
MWCNT/CPE	4.0	0.1 – 100	50	(Shahrokhian and Asadian, 2010)
Carbon NP/GCE	7.0	0.1-100	50	(Ghorbani-Bidkorbeh et al., 2010)
Graphite oxide/GCE	2.0	0.165-26.5	40	(Song et al., 2011)
SWCNT-DPF/GCE	6.5	0.1-20	40	(Sun and Zhang, 2007)
SWCNT-Graphene/GCE	7.0	0.05-64.5	38	(Chen et al., 2012)
Graphene/GCE	9.3	0.1-20	32	(Kang et al., 2010)
ISSM-CNT/PE	7.0	0.112– 69.4	25.8	(Sanghavi et al., 2010)
MWCNT/BPPGE	7.5	0.01-20	10	(Kachosangi et al., 2008)
Poly(CCA)/GCE	6.0	0.1-10	10	(Liu et al., 2012)
D50wx2-GNP/GCPE	6.0	0.0334-45.5	4.71	(Sanghavi and Srivastava, 2011)
MWCNT/GCE	7.0	0.0002- 15	0.09	This work

4.1.5. Reproducibility and stability of modified electrode

The relative standard deviation (RSD) of 10 successive scans was 2.5% for 1.5×10^{-6} M PAR. This indicated that the reproducibility of the modified electrode

was excellent. However, the modified electrode should be well treated to maintain its reproducibility. It was found that 20 cycles of scanning in 0.1 M PBS in the potential range 0.0~0.8 V could regenerate clean background CV curves and the modified electrode was ready for the next experiment or storage in 0.1 M PBS. Also, the current response decreased only by 5-6% over a week for storage in 0.1 M PBS.

4.1.6. Detection of paracetamol in the presence of AA, DA and UA

Electrochemical detection provides a sensitive approach to the detection of a wide range of analytes (Kachosangi et al., 2007; Wildgoose et al., 2006; Ensafi et al., 2009). However, this approach is sometimes restricted due to the interference from the other redox active molecules which may undergo oxidation/reduction at similar potentials to the target species in the medium as shown in Figure 4.11. where only one broad oxidation peak is observed for a mixture of AA, DA, UA and PAR at a naked glassy carbon electrode in 0.1 M PBS at pH 7.0.

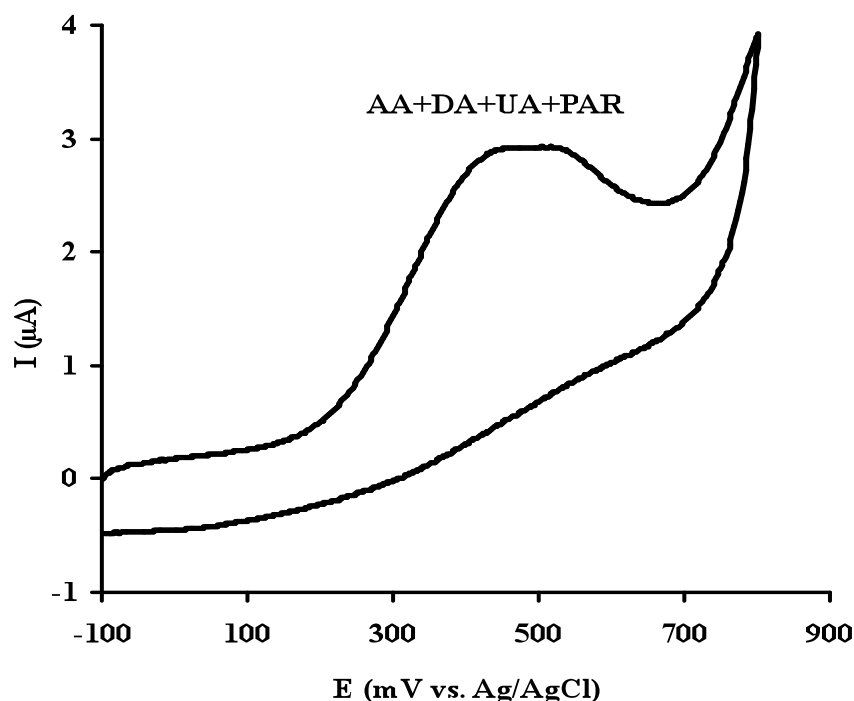


Figure 4.11. A cyclic voltammogram of the mixture of 1.25×10^{-4} M AA; 1.75×10^{-7} M DA; 2.0×10^{-4} M UA and 7.5×10^{-6} M PAR at bare GCE in 0.1 M PBS at pH 7.0. Scan rate: 100 mV/s. Equilibrium time: 5 s

However, 4 well-defined peaks were observed for a mixture of AA, DA, UA and PAR at a GCE modified with 0.15 μg MWCNTs (Figure 4.12.). The peak current increases linearly with the concentration of PAR in the presence of AA, DA and UA indicating that these three potential interfering molecules do not interfere with the determination of PAR. It is clearly shown that modification of glassy carbon electrodes using conductive porous layers enables selective detection of PAR in the presence of AA, DA and UA.

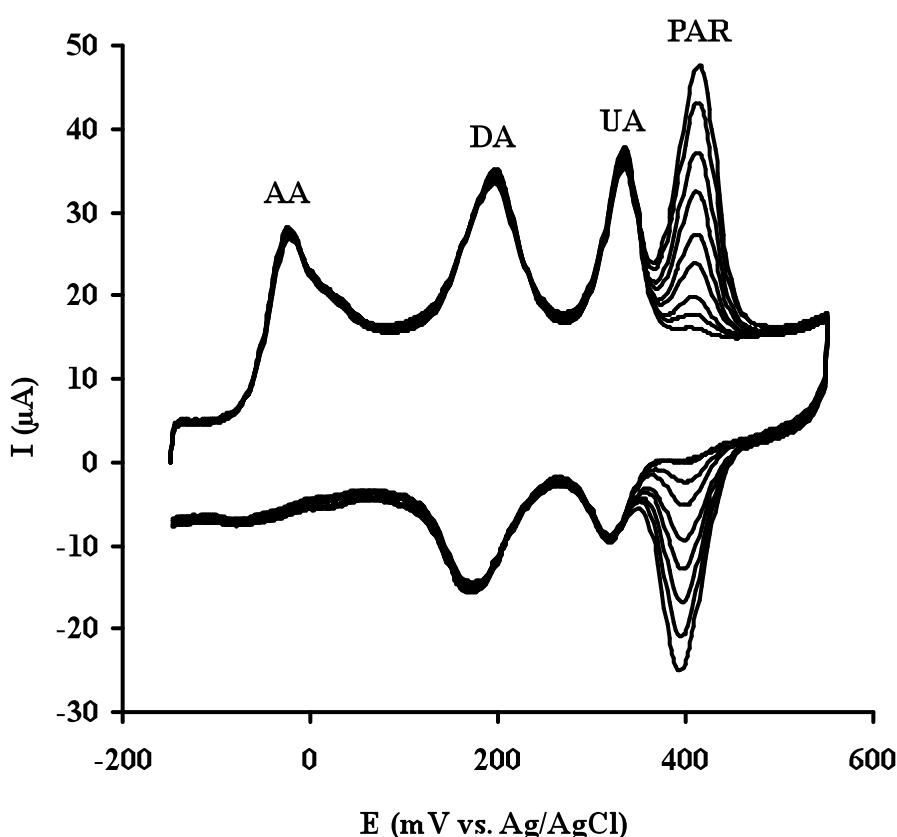


Figure 4.12. Cyclic voltammograms of the mixture of 1.25×10^{-4} M AA, 1.75×10^{-7} M DA, 2.0×10^{-4} M UA and increasing concentrations of PAR at 0.15 μg MWCNT/GCE in 0.1 M PBS at pH 7.0. Scan rate: 100 mV/s. Equilibrium time: 5 s. PAR concentrations: 0.00; 5.0×10^{-7} M; 7.5×10^{-7} M; 1.0×10^{-6} M; 1.2×10^{-6} M; 1.5×10^{-6} M; 3.0×10^{-6} M; 5.0×10^{-6} M; 7.5×10^{-6} M

The modified electrode also exhibits a high electrocatalytic effect towards AA, DA and UA with a distinct shift of the oxidation potential of AA, DA and UA in the cathodic direction and a marked enhancement of the current response and also

provides larger peak to peak separation between AA, DA, UA and PAR for their easier simultaneous determination. Therefore, the proposed electrode is selective not only for the detection of PAR in the presence of AA, DA and UA but also selective for the simultaneous determination of these four species present in a mixture as shown in Figure 4.13. These results indicate that covering electrode surfaces with porous layers can modify the mass transport regime from planar diffusion to a thin layer character and this alteration can in favourable circumstances facilitate the voltammetric discrimination between species in the target medium (Streeter et al., 2008; Henstridge et al., 2010; Keeley and Lyons, 2009; Xiao et al., 2009). This study presents an experiment to show that the modification of an electrode with porous layers of conducting material can shift voltammetric peaks in an analytically useful manner (Henstridge et al., 2010).

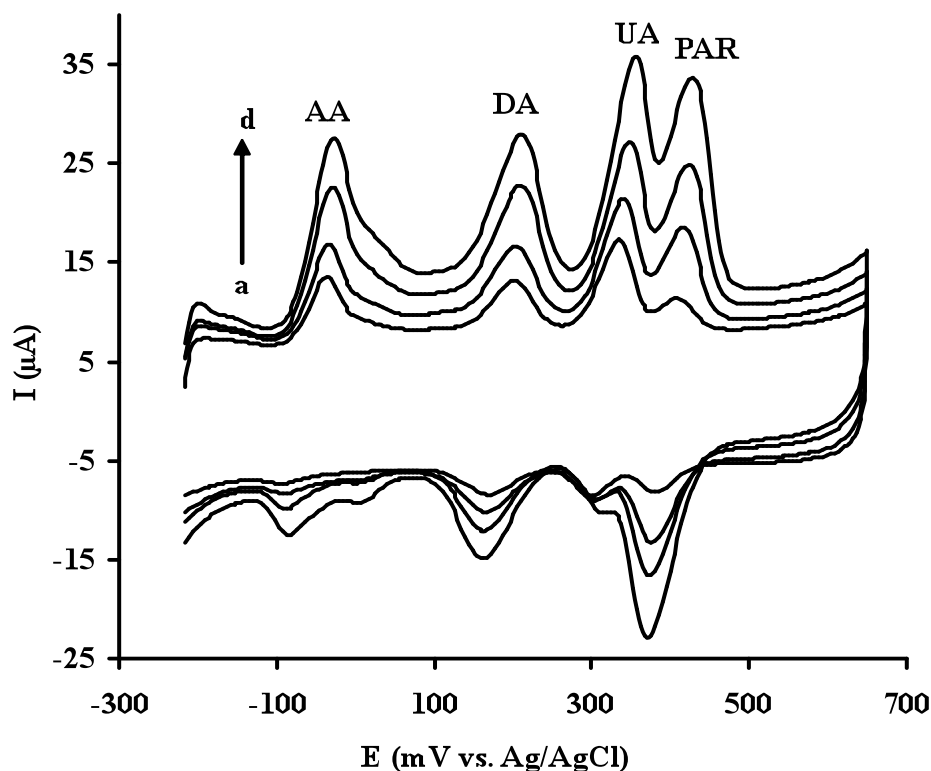


Figure 4.13. Cyclic voltammograms of the mixture of simultaneously increasing concentrations of AA, DA, UA and PAR at 0.15 μg MWCNT/GCE in 0.1 M PBS at pH 7.0. Scan rate: 100 mV/s. Equilibrium time: 5 s. (a) 2.5×10^{-5} M AA; 1.0×10^{-7} M DA; 1.0×10^{-4} M UA; 3.0×10^{-7} M PAR. (b) 5.0×10^{-5} M AA; 1.25×10^{-7} M DA; 1.25×10^{-4} M UA; 7.5×10^{-7} M PAR. (c) 1.0×10^{-4} M AA; 1.50×10^{-7} M DA; 1.5×10^{-4} M UA; 1.0×10^{-6} M PAR. (d) 1.25×10^{-4} M AA; 1.75×10^{-7} M DA; 2.0×10^{-4} M UA; 1.5×10^{-6} M PAR

4.1.7. Determination of paracetamol in pharmaceutical preparations

Square wave voltammetric determination of PAR in tablets on a glassy carbon electrode modified with 0.15 μg MWCNTs was referred to the regression equation. The analysis of tablets using the proposed method is summarised in Table 4.2. A mean recovery of 99.0% with RSD of 1.6% was obtained using the proposed method for the voltammetric analysis of tablets. The results of the drug analysis obtained from the proposed method are in close agreement with the claimed value. The results obtained are also comparable with the results obtained from square wave voltammetry at multiwalled carbon nanotube-alumina coated silica nanocomposite electrode with a recovery of 98.2% (Lu and Tsai, 2011), differential pulse voltammetry at nafion/TiO₂-graphene modified electrode with a recovery of 98.6% (Fan et al., 2011). However, the experimental results indicate that the proposed procedure is more precise and accurate for the determination of PAR in drug samples.

Table 4.2. Results of the determination of PAR in tablets

Content (mg)	Found (mg)	Recovery%	R.S.D%
500.0	495.0 \pm 7.2	99.0	1.6

Mean \pm standard deviation (n = 5)

4.2. Selective Voltammetric Detection of Albuterol in the Presence of Uric Acid Using a Glassy Carbon Electrode Modified with MWCNTs and poly(pivalic acid)

The main goal of this work is to develop a selective and rapid voltammetric sensor for the direct quantification of albuterol in pharmaceuticals for monitoring its therapeutic use and urine samples as it can easily detect the cases of doping in sporting competitions. For this purpose, a glassy carbon electrode has been modified with multi-walled carbon nanotubes and poly(pivalic acid) for the determination of albuterol in pharmaceutical formulations and urine samples. However, the determination of albuterol has been carried out in the presence of uric acid since the

urine samples contain a high amount of uric acid and to observe its effect on the determination of albuterol.

Albuterol [2-(tert-butylamino)-1-(4-hydroxy-3-hydroxymethyl) phenylethanol] also known as salbutamol, (Figure 4.14.) is one of the most widely used β_2 -adrenoceptor agonists in the treatment of bronchial asthma, chronic obstructive pulmonary disease and other allergic diseases associated with respiratory pathway (Spyridaki et al., 2006). It is known that albuterol may reduce premature labour in pregnancy (Dol and Knochen, 2004). However, high concentration of albuterol is prohibited in sports because of its abuse as a stimulant (Pichon et al., 2006). Albuterol is also utilized as a tocolytic agent (Vela et al., 2001). However, its residues which are the most abundant in liver can be toxic to humans (Koole et al., 1999). Thus, the quantification of albuterol is especially important for monitoring its therapeutic use as well as controlling doping cases of athletes in sporting competitions.

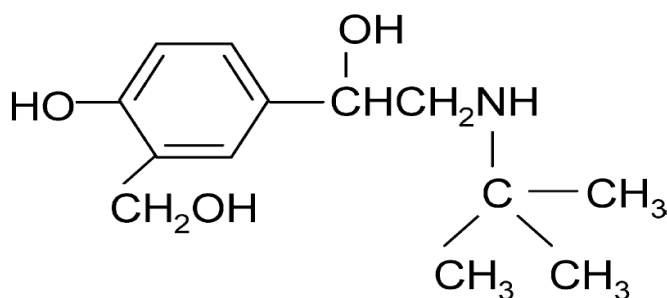


Figure 4.14. Chemical structure of albuterol

A number of methods have been used for the determination of albuterol including spectrophotometry (Satinsky et al., 2002), chemiluminescence (Lindino and Bulhoes, 2007) chromatography (El-Gindy et al., 2007), capillary electrophoresis (Sirichai and Khanatharana, 2008), amperometric detection (Quitino and Angnes, 2004) and voltammetry (Yilmaz et al., 1998; Sagar et al., 1993; Boyd et al., 1994). Spectrophotometry and chromatography are the two most widely employed techniques for the determination of albuterol. However, these techniques are expensive and require time-consuming derivatization step. The voltammetric

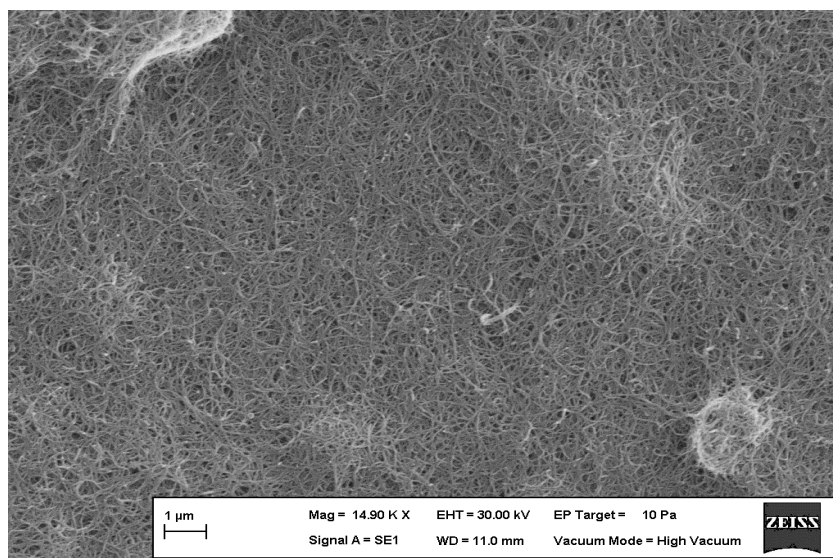
methods have several advantageous owing to their simplicity, high sensitivity and rapidness. Various electrodes including Platinum (Yilmaz et al., 1998), glassy carbon (Yilmaz et al., 1998; Sagar et al., 1993), carbon paste (Sagar et al., 1993; Boyd et al., 1994) have been applied for the detection of albuterol in biological samples. As albuterol causes strong electrode fouling, it is necessary to find an adequate surface for its determination. It is known that modification of conventional electrodes has attracted much attention in last 2 decades because it provides powerful means to bring new qualities to the electrode surface which exploited for electrochemical purposes (Walcarious, 2001).

Chemically modified electrodes can be obtained by either attaching molecules on electrode surfaces or by immobilizing multimolecular layer films on electrodes. They found applications in various fields including electroanalysis and electrocatalysis (Yang et al., 2012; Xu et al., 2012; Henstridge et al., 2010). Among the wide range of electrode modifiers, polymers and carbon nanotubes have been focus of attention for electrochemists because of advantageous features such as excellent long term stability, response time, increased sensitivity, resistance to surface fouling, decreased overpotentials, limits of detection, conductivity, nanometer size and providing large surface area (Goyal et al., 2008; Karuwan et al., 2009; Lijun et al., 2007; Goyal et al., 2011 and Huang et al., 2011).

4.2.1. The characterization of SEM images

Figure 4.15. shows the SEM images of the bare GCE, MWCNT/GCE and PPA/MWCNT/GCE. It can be seen from Figure 4.15.(a) that the MWCNT/GCE has a rough surface. It should be noted that, the MWCNTs formed on the electrode surface big bundles that cannot be totally and efficiently used for electrochemical sensors. However, it can be seen from Figure 4.15.(b) that the small bundles and single tubes are packaged in the polymeric membrane, which indicates the immobilization of the PPA film on the surface of MWCNT/GCE.

(a)



(b)

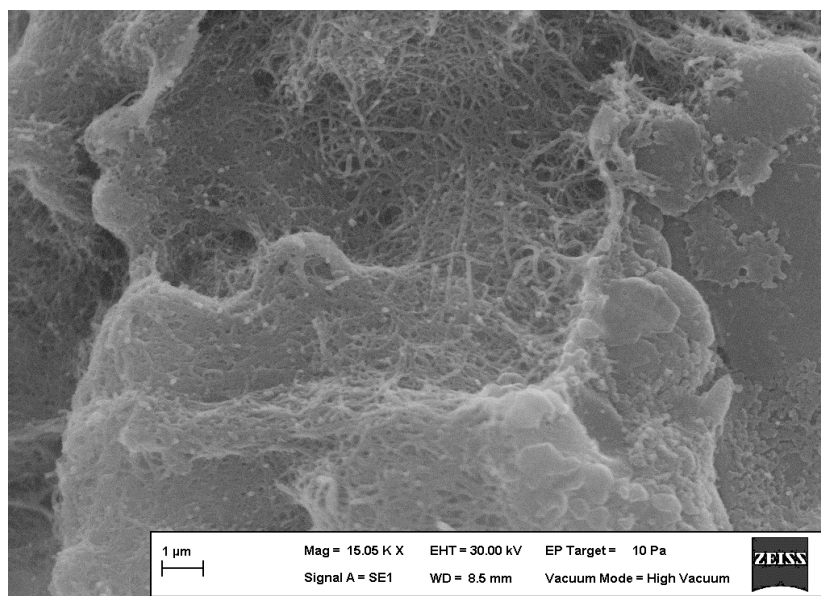


Figure 4.15. SEM images of (a) tMWCNT/GCE and (b) PPA/MWCNT/GCE

4.2.2. Voltammetric behaviour of albuterol and uric acid

A cyclic voltammogram of the mixture of 35 μM albuterol and 80 μM UA in 0.10 M PBS at pH 8.0 at bare GCE is given in Figure 4.16. At bare GCE, two poor

anodic waves were appeared at 0.450 V and 0.651 V for the oxidation of UA and albuterol, respectively. The electrochemical oxidation of both albuterol and UA were totally irreversible at bare GCE. Peak to peak separation between UA and albuterol is about 201 mV at bare GCE.

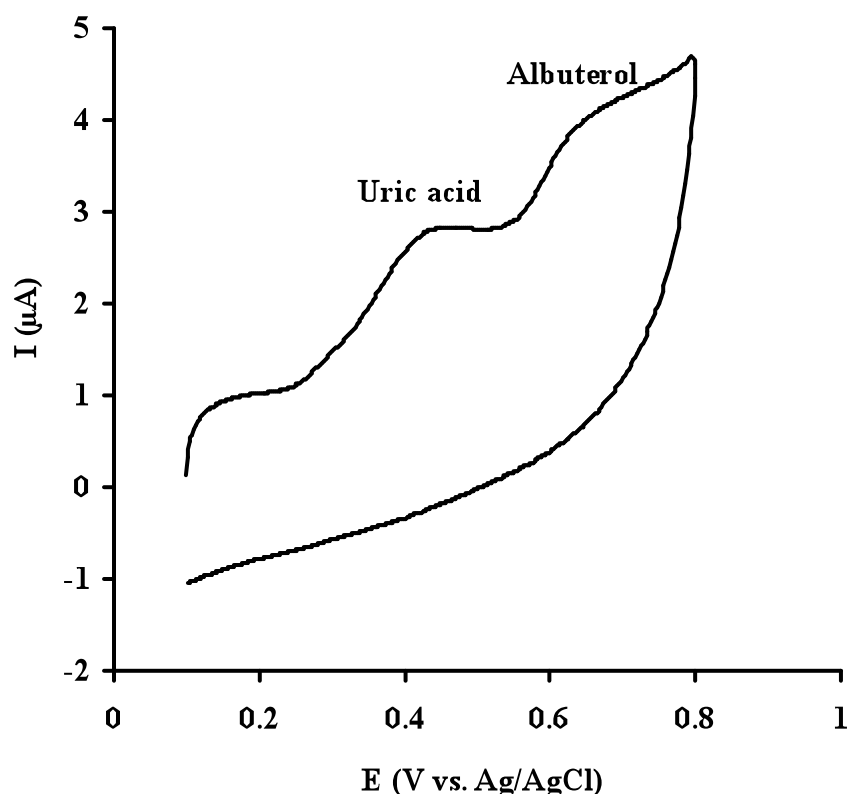


Figure 4.16. Cyclic voltammograms of the mixture 80 μM UA and 35 μM albuterol in 0.1 M PBS at pH 8.0 at bare GCE. Scan rate: 50 mV/s; Equilibrium time: 5 s

Also, cyclic voltammograms of the mixture of albuterol and UA at the MWCNT/GCE and PPA/MWCNT/GCE are given in Figure 4.17. Two anodic peaks were appeared at 0.360 V and 0.620 V for UA and albuterol with a peak to peak separation of 260 mV at MWCNT/GCE (Figure 4.17a). However, at PPA/MWCNT/GCE, UA and albuterol exhibits two well-defined anodic peaks at 312 mV and 590 mV with a peak to peak separation of 278 mV (Figure 4.17b). The separation of anodic peaks at PPA/MWCNT/GCE was large enough for simultaneous determination of UA and albuterol in a mixture. No peaks are observed in the cathodic branch indicating that the electrochemical process of

albuterol at PPA/MWCNT/GCE is totally irreversible. However, UA exhibits a small cathodic peak at 0.280 V. The ΔE_p is 32 mV indicating a quasi-reversible two-electron transfer process. It is clearly shown that the PPA/MWCNT/GCE exhibits an efficient electrocatalytic effect towards the oxidation of albuterol and UA with sharp peaks and enhancement in current responses and also good selectivity with large peak separations between UA and albuterol. This indicated that the electrochemical responses of UA and albuterol have greatly been increased at PPA/MWCNT/GCE. Intensive increases in peak currents of both albuterol and UA are observed owing to the improvement in the electron transfer process and the larger real area of the film at the surface.

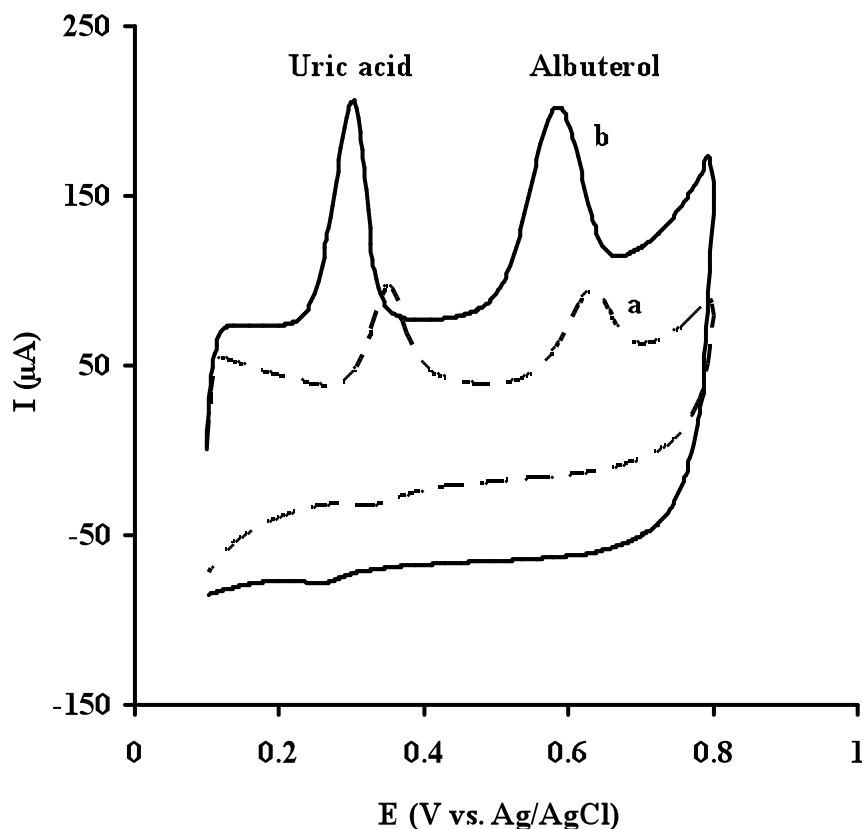


Figure 4.17. Cyclic voltammograms of the mixture 80 μM UA and 35 μM albuterol in 0.1 M PBS at pH 8.0 at MWCNT/GCE (a) and PPA/MWCNT/GCE (b). Scan rate: 50 mV/s; Equilibrium time: 5 s

In order to understand the mechanisms responsible for the oxidation of both UA and albuterol at PPA/MWCNT/GCE, cyclic voltammograms of UA and albuterol were simultaneously recorded at various scan rates. Figure 4.18. shows the effect of the scan rate on the electrochemical responses of UA and albuterol at PPA/MWCNT/GCE using cyclic voltammetry in 0.1 M PBS at pH 8.0.

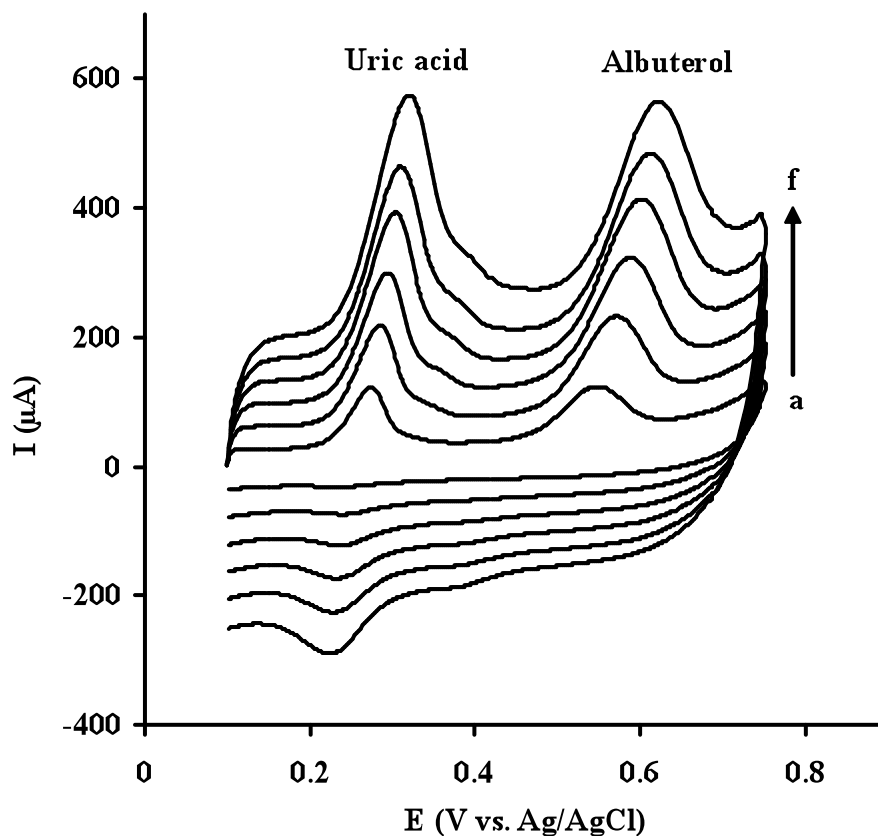


Figure 4.18. Cyclic voltammograms of 2.0×10^{-5} M UA and 1.0×10^{-5} M albuterol at PPA/MWCNT/GCE in 0.1 M PBS at pH 8.0. Scan rate increasing from 50 mV/s to 300 mV/s; Equilibrium time: 5 s

The anodic peak currents (I_p) were proportional to the scan rates (ν) over the range of 50-300 mV/s for both species in Figure 4.19. (A and B). The results indicated that the electrode processes of both species, UA and albuterol, are controlled by adsorption.

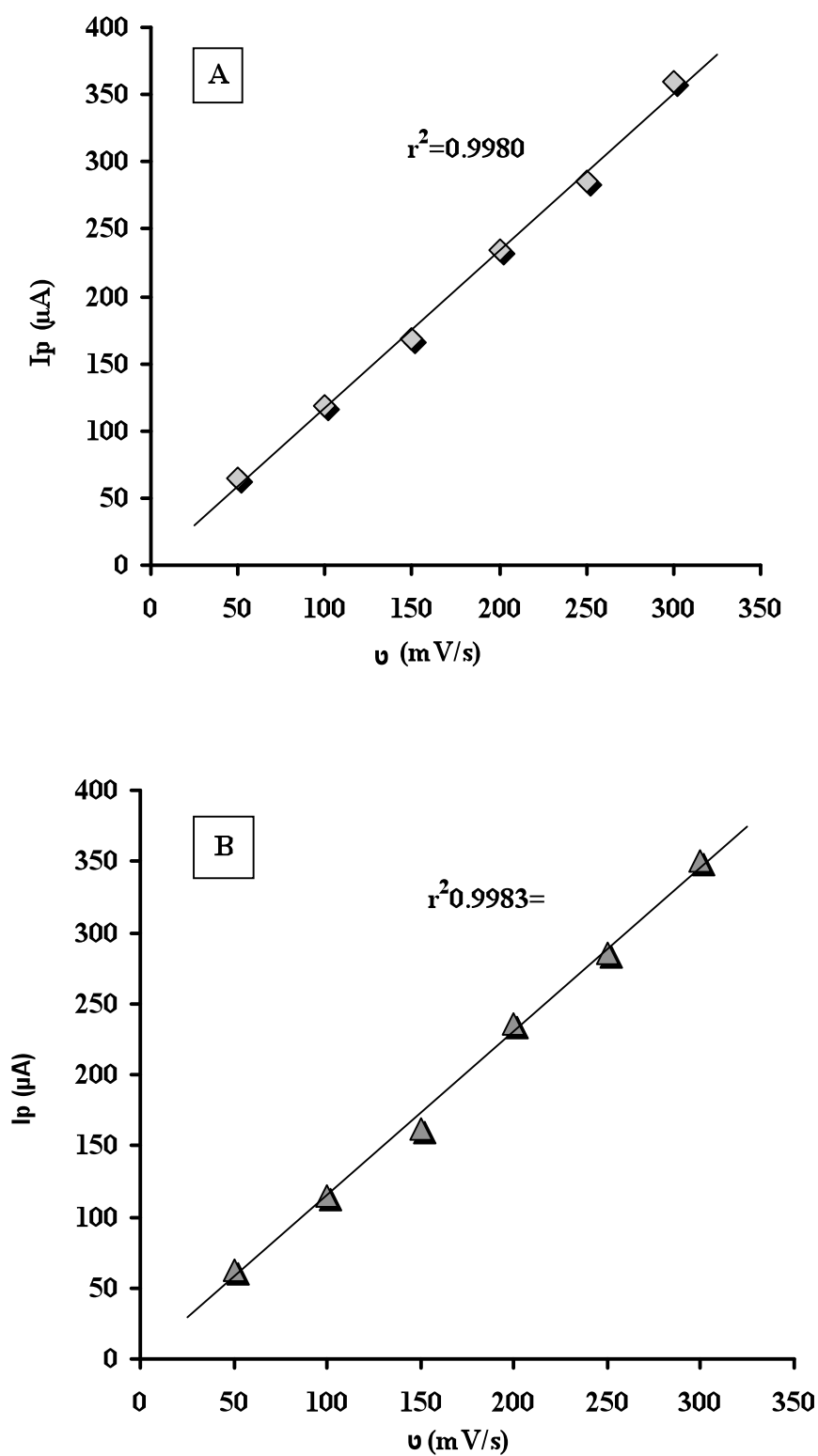


Figure 4.19. Plot of anodic peak currents of uric acid vs. scan rates (A) and plot of anodic peak currents of albuterol vs. scan rates (B)

In order to get information about the number of electrons involved in the oxidation of albuterol, the value of αn for the electrocatalytic oxidation of albuterol was acquired. The Tafel plot was determined using the following equation.

$$E_{pa} = (2.303RT/\alpha nF)(1/2) \log v + \text{constant} \quad \text{Eq.(4.1)}$$

where α is the transfer coefficient, n is the number of electrons transferred, v is the scan rate, F is the Faraday's constant (96487 C/mol), R is the rate gas constant (8.314 J/K mol) and T is the absolute temperature. The anodic peak potential of albuterol is proportional to $\log v$ with a slope of 0.04833 as shown in Figure 4.20. The oxidation of albuterol is a one-electron transfer process assuming the electron transfer coefficient α is approximately 0.5 in a totally irreversible electrode process. In addition, as shown in Figure 4.18. the cathodic peak for UA becomes more evident at high scan rates suggesting an EC process.

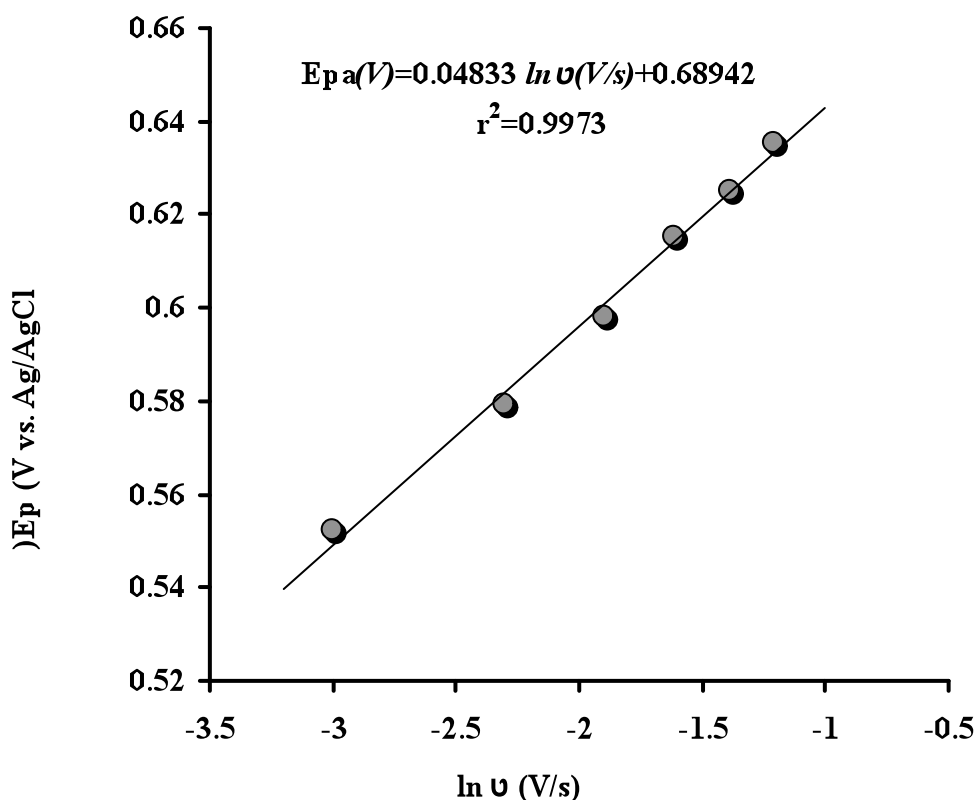


Figure 4.20. Plot of anodic peak potentials of albuterol vs. logarithm of scan rates

4.2.3. The effect of pH on the voltammetric behaviour of uric acid and albuterol at PPA/MWCNT/GCE

In addition, the effect of the pH value of the PBS buffer solution on peak potential of albuterol and UA at PPA/MWCNT/GCE was also investigated. Figure 4.21. shows that the effect of pH on the peak potential of albuterol using cyclic voltammetry at PPA/MWCNT/GCE in 0.1 M PBS at different pH values.

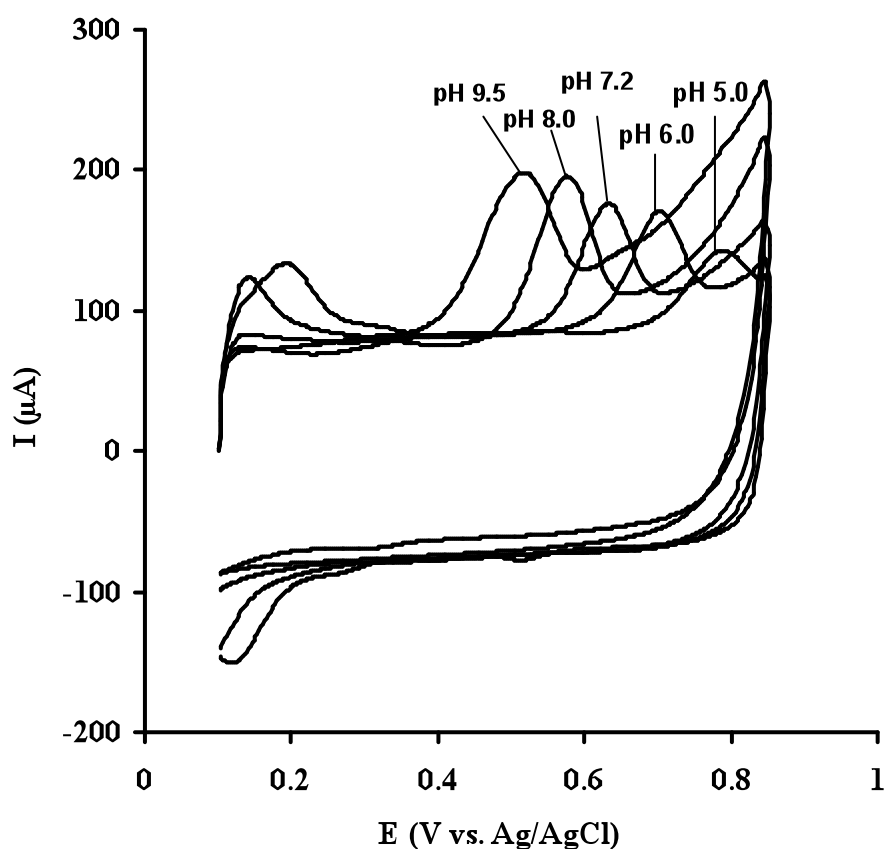


Figure 4.21. Cyclic voltammograms of 2.0×10^{-5} M albuterol at PPA/MWCNT/GCE in 0.1 M PBS at different pH values. Scan rate: 50 mV/s; Equilibrium time: 5 s

The results show that the oxidation peak potential of albuterol shifts towards the negative potentials with increasing pH. This indicates that the electrochemical process of albuterol includes transfer of protons. The slope of oxidation peak potential (E_p) vs. pH is 0.05962 V/pH in Figure 4.22. This indicated that the identical numbers of electrons and protons are involved in the oxidation process of

albuterol at PPA/MWCNT/GCE. Thus, the number of hydrogen ions involved in the whole electrode reaction of albuterol at PPA/MWCNT/GCE is 1. The electrode mechanism of albuterol at PPA/MWCNT/GCE is shown in Scheme 4.2. (Goyal et al., 2007).

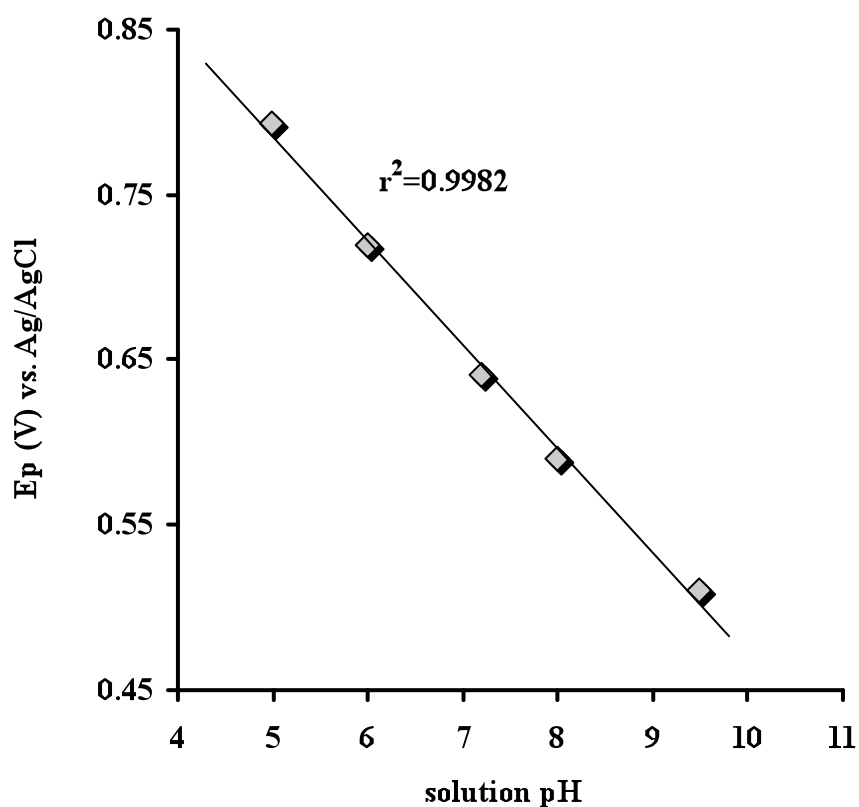
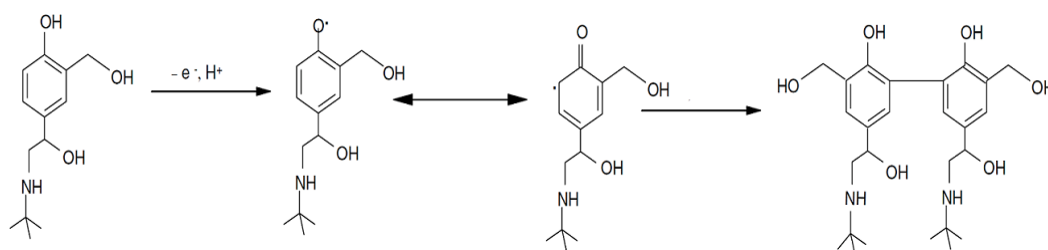


Figure 4.22. Plot of oxidation peak potential of albuterol vs. solution pH



Scheme 4.2. Electrode reaction of albuterol at PPA/MWCNT/GCE

Figure 4.23. shows that the effect of pH on the peak potential of UA using cyclic voltammetry at PPA/MWCNT/GCE in 0.1 M PBS at different pH values. The results show that oxidation peak potential of UA also shifts towards negative potentials with increasing pH. This shows that the redox of UA also includes transfer of protons in electrode process. The slope of oxidation peak potential (E_p) vs. pH is 0.05912 V/pH in Figure 4.24. This indicated that the proportion of electrons and protons involved in the reaction is also 1:1. Since equal numbers of electrons and protons should be involved in the electrode reaction, the number of hydrogen ions involved in the whole electrode reaction is 2. The electrode mechanism of UA at PPA/MWCNT/GCE is shown in Scheme 4.3.

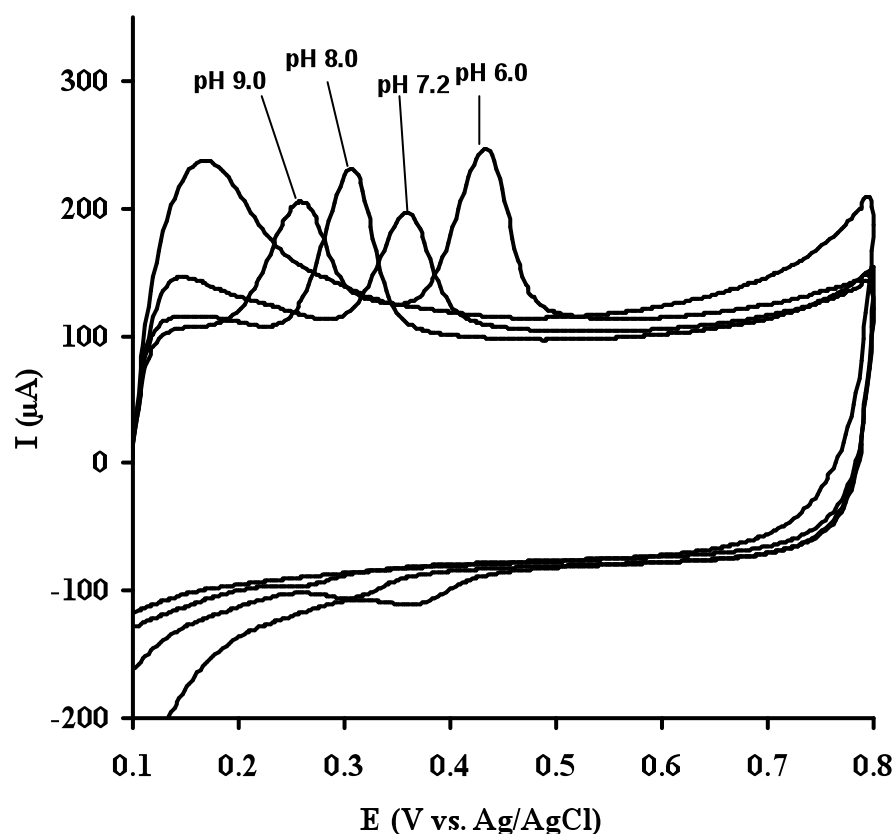


Figure 4.23. Cyclic voltammograms of 9.0×10^{-5} M UA at PPA/MWCNT/GCE in 0.1 M PBS at different pH. Scan rate: 50 mV/s; Equilibrium time: 5 s

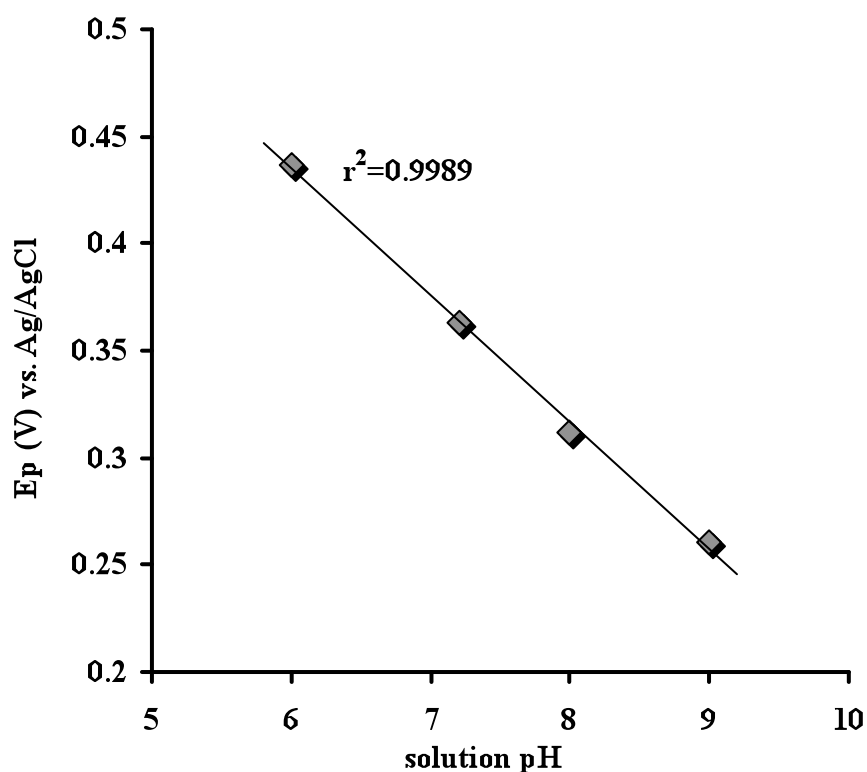
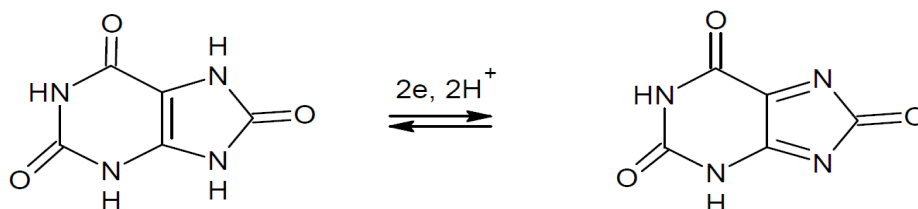


Figure 4.24. Plot of oxidation peak potentials of UA vs. solution pH



Scheme 4.3. Electrode reaction of UA at PPA/MWCNT/GCE

4.2.4. Calibration equation for the determination of albuterol

Cyclic voltammetric determination of the concentration of albuterol at PPA/MWCNT/GCE was performed in 0.1 M PBS at pH 8.0. Cyclic voltammograms of increasing concentrations of albuterol at PPA/MWCNT/GCE are given in Figure 4.25. The anodic peak currents were plotted against the concentration of albuterol after the background subtraction (in Figure 4.26.). The response of anodic peak currents of albuterol at PPA/MWCNT/GCE was linear with the concentration of

albuterol in the range of $1.5 \times 10^{-7} \sim 6.5 \times 10^{-5}$ M. The linear regression equation was $I_{pa} (\mu A) = 4.22139C (\mu M) + 0.36438$ with a correlation coefficient of 0.9998. The detection limit was 3.0×10^{-8} M (S/N=3).

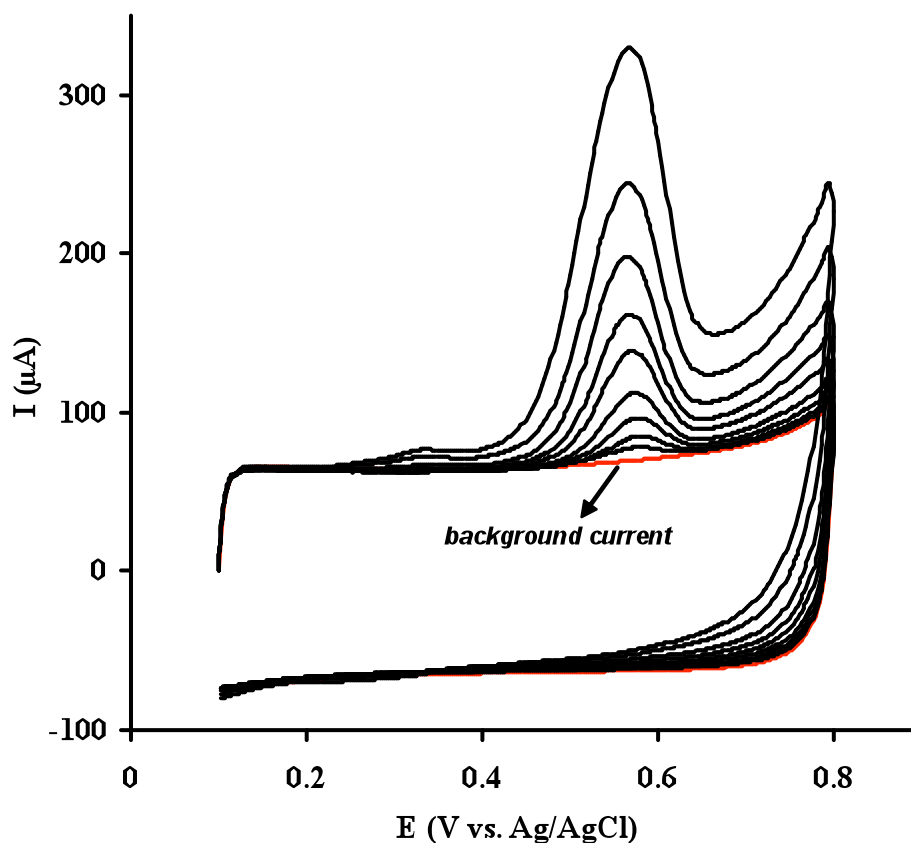


Figure 4.25. Cyclic voltammograms of increasing concentrations of albuterol at PPA/MWCNT/GCE in 0.1 M PBS at pH 8.0. Albuterol concentrations = 0.0; 0.15; 1.5; 4.5; 6.0; 9.0; 15.0; 24.0; 38.0; 65.0 μM . Scan rate: 50 mV/s; Equilibrium time: 5 s

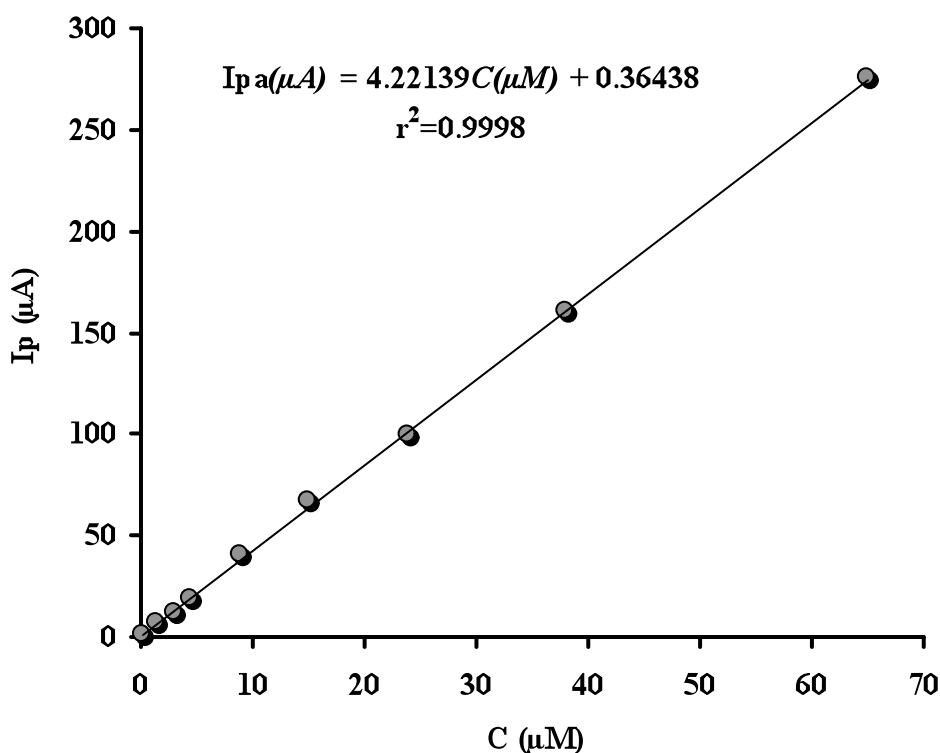


Figure 4.26. Plot of anodic peak currents vs. concentration of albuterol

Square voltammetric determination of the concentration of albuterol at PPA/MWCNT/GCE was also performed in 0.1 M PBS at pH 8.0. Square voltammograms of increasing concentrations of albuterol at PPA/MWCNT/GCE are given in Figure 4.27. The anodic peak currents were plotted against the concentration of albuterol in Figure 4.28. The response of anodic peak currents of albuterol at PPA/MWCNT/GCE was linear with the concentration of albuterol in the range of $1.5 \times 10^{-8} \sim 7.0 \times 10^{-5}$ M. The linear regression equation was $I_{pa} (\mu A) = 0.05447 + 0.13221 C (\mu M)$ with a correlation coefficient of 0.9995. The detection limit ($3\sigma/s$, where σ was the standard deviation of the intercept and s was the slope of the calibration curve) was 1.2×10^{-8} M. The results obtained by SWV are comparable with that of CV in the determination of albuterol in this study.

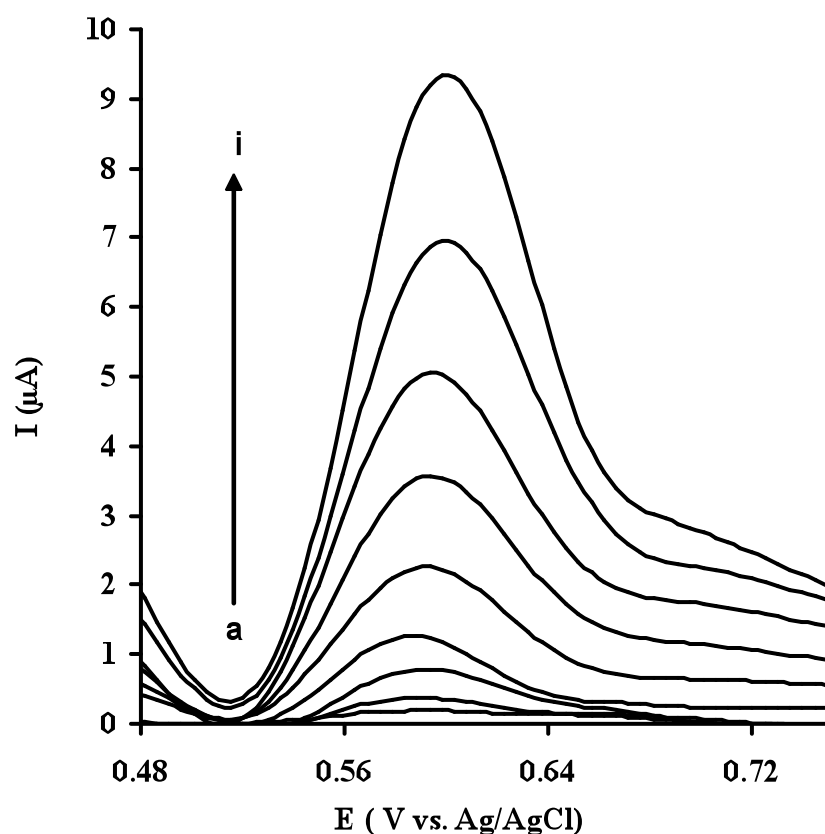


Figure 4.27. Square wave voltammograms of increasing concentrations of albuterol at PPA/MWCNT/GCE in 0.1 M PBS at pH 8.0. Albuterol concentrations = (a) 0.05 μM (b) 1.5 μM (c) 5 μM (d) 8 μM (e) 15 μM (f) 25 μM (g) 40 μM (h) 52 μM (i) 70 μM . Equilibrium time: 5 s, frequency: 8 Hz, step potential: 25 mV, amplitude: 10 mV

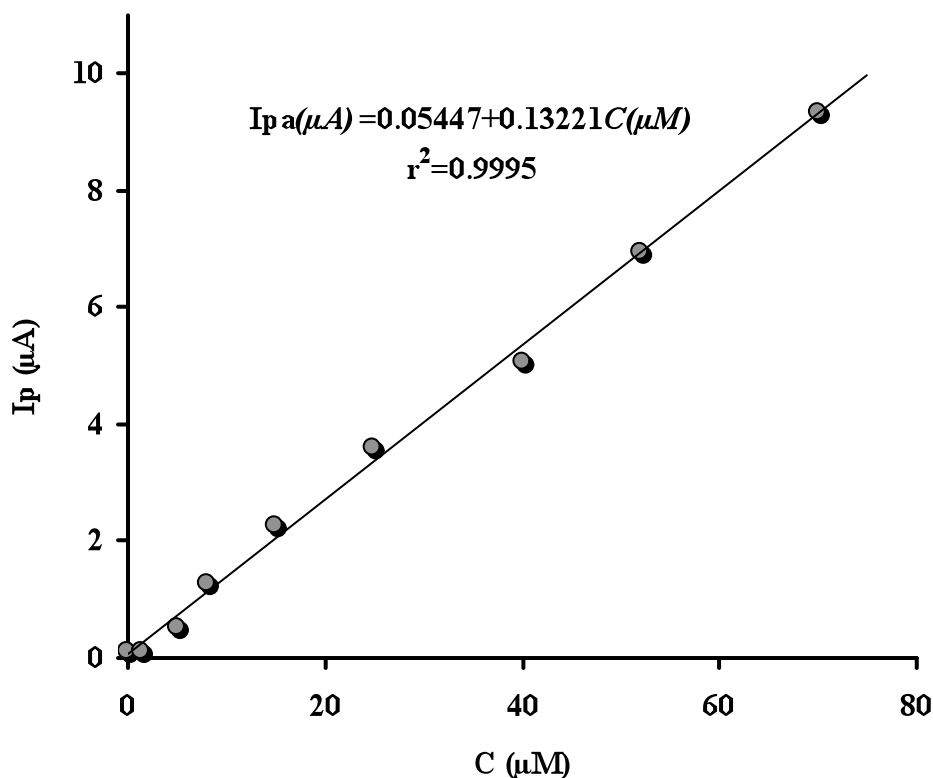


Figure 4.28. Plot of anodic peak currents vs. concentration of albuterol with the SWV

4.2.5. Reproducibility and stability of modified electrode

The relative standard deviation (RSD) of 10 successive scans was 2.5% for 10 μM albuterol. This indicated that the reproducibility of the PPA/MWCNT/GCE was excellent. However, the modified electrode should be well treated to maintain its reproducibility. It was found that 20 cycles of scanning in 0.1 M PBS in the potential range 0.0~0.8 V could regenerate clean background CV curves and the modified electrode was ready for the next experiment or storage in 0.1 M PBS. Also, the current response decreased only by 5-6% over a week for storage in 0.1 M PBS.

4.2.6. Detection of albuterol in the presence of UA

Figure 4.29. shows the cyclic voltammograms of increasing concentrations of albuterol where the concentration of UA was kept constant. In the presence of UA,

the anodic peak currents of albuterol increased linearly with its concentration. This indicates that the electrochemical response of UA do not interfere with the electrochemical response of albuterol. Therefore, the PPA/MWCNT/GCE could be used for the determination of albuterol in the presence of the UA. In other words, the PPA/MWCNT/GCE could be utilized for the selective determination of albuterol in urine samples.

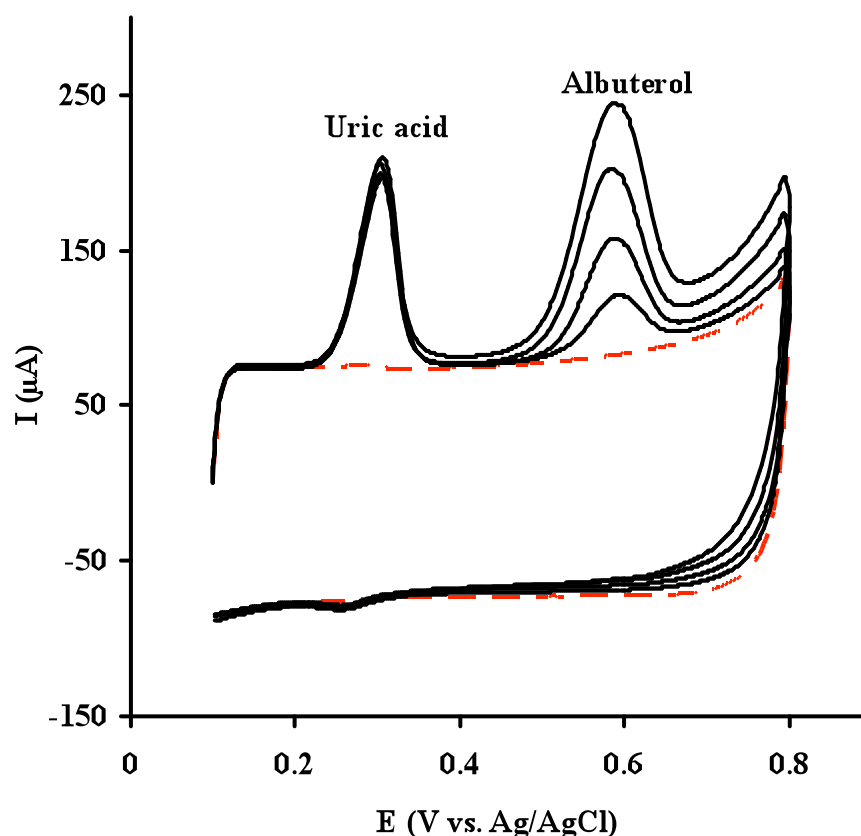


Figure 4.29. Cyclic voltammograms of the mixture of UA and increasing concentrations of albuterol PPA/MWCNT/GCE in 0.1 M PBS at pH 8.0 at. Scan rate: 50 mV/s; Equilibrium time: 5 s. UA concentration = 0.0, 85.0 μM and albuterol concentrations = 0.0, 8.5, 20.0, 30.0, 36.0 μM

Figure 4.30. shows that cyclic voltammograms of increasing concentrations of UA where the concentration of albuterol was kept constant. Overall facility of the PPA/MWCNT/GCE system for the simultaneous determination of albuterol and UA was demonstrated by changing their concentrations.

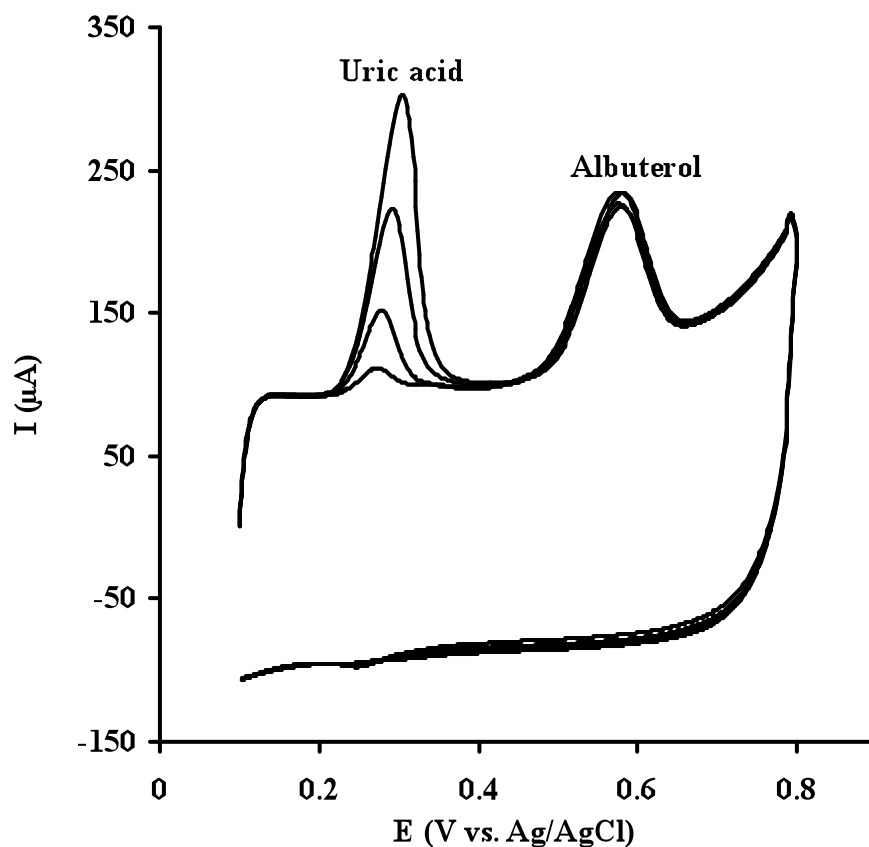


Figure 4.30. Cyclic voltammograms of the mixture of albuterol and increasing concentrations of UA at PPA/MWCNT/GCE in 0.1 M PBS at pH 8.0. Scan rate: 50 mV/s; Equilibrium time: 5 s. Albuterol concentration=35.0 μM and UA concentrations = 7.5, 20.0, 50.0, 100.0 μM

Figure 4.31. depicts the cyclic voltammograms obtained for albuterol and UA coexisting at various concentrations. The results indicated that no evidence of interference of UA was observed for the determination of albuterol. It is remarkable that the excess amount of UA does not interfere with the concentration of albuterol. This also indicates that the PPA/MWCNT/GCE could be used for the simultaneous determination of albuterol and UA owing to the large peak to peak separation.

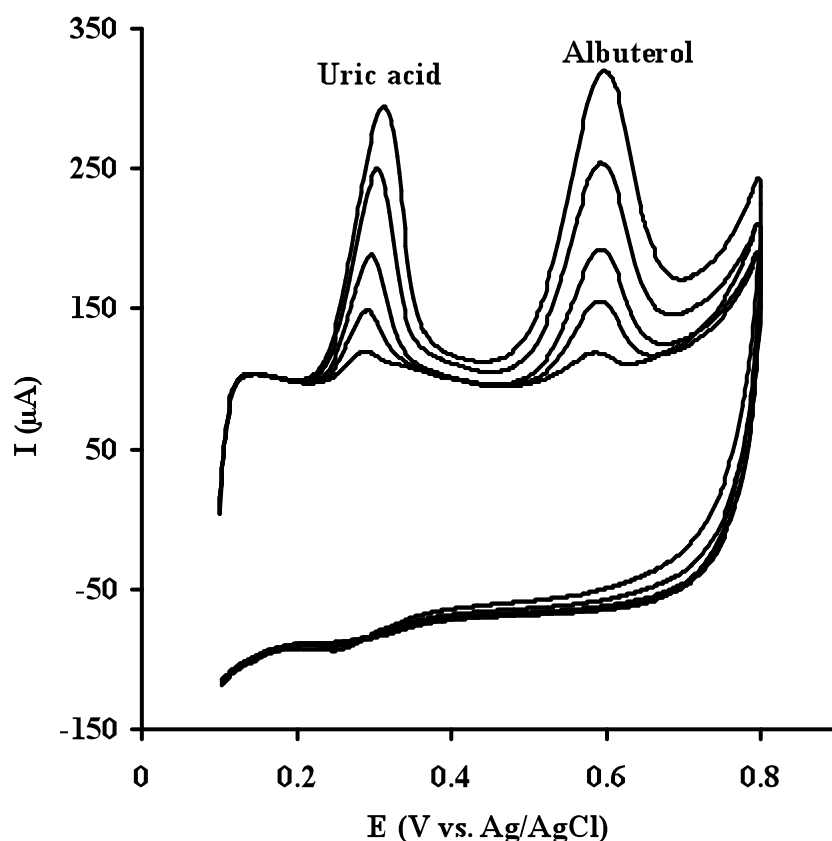


Figure 4.31. Cyclic voltammograms of the mixture of increasing concentrations of UA and albuterol at PPA/MWCNT/GCE in 0.1 M PBS at pH 8.0. Scan rate: 50 mV/s; Equilibrium time: 5 s. UA concentrations = 7.5, 21.0, 40.0, 80.0, 90.0 μM and albuterol concentrations : 4.5, 12.0, 22.0, 40.0, 60.0 μM

4.2.7. Analytical Applications

Square wave voltammetric determination of albuterol in pharmaceutical formulations was referred to the regression equation. The analysis of albuterol tablets using the proposed method is summarised in Table 4.3. The relative standard deviation (RSD) was 2.5 % using the proposed method for the voltammetric analysis of albuterol tablets. The validity of the proposed procedure applied to albuterol tablets was also assured by the recovery of standard additions. The data obtained at PPA/MWCNT/GCE are in close agreement with the claimed value. The average recovery of 99.0% with mean standard deviation of 0.05 was obtained by employing the proposed method for the five different determinations of albuterol tablets. However, the data obtained by the proposed method are comparable with standard

method of US Pharmacopoeia with an average recovery of 105.5% (The United States Pharmacopeia XXII Revision, 1990). At the same time, the results obtained are also comparable with the results obtained from fourier transform cyclic voltammetry at gold electrode with a recovery of 102.0% (Ganjali et al., 2005), capillary zone electrophoresis with a recovery of 96.5% (Sirichai and Khanatharana, 2008), voltammetry at nanogold modified indium tin oxide (ITO) electrode with a recovery of 95.0% to 105.0% (Goyal et al., 2007), voltammetry at glassy carbon electrode (GCE) with a recovery of 95.0% (Sagar et al., 1993) and multi-walled carbon nanotubes modified glassy carbon electrode with a recovery of 98.4% to 102.6 % (Wei et al., 2010). The results obtained by the proposed method are compared with several electrochemical methods for the determination of albuterol as shown in Table 4.4. The results indicated that the proposed method could be easily used for the determination of albuterol in pharmaceuticals.

The validity of the proposed method was assured by the recovery of albuterol in urine samples (Table 4.5.). The mean recovery of the two urine samples was 98.05% with RSD of 2.45%. However, the results obtained from the proposed method indicate that this method is more precise and accurate for the determination of albuterol in drug and urine samples.

Furthermore, any possible interference from some molecules and common ions on the determination of 1.0×10^{-5} M albuterol were also examined. Under the same experimental conditions, results have shown that 100-fold concentrations of ascorbic acid, dopamine, glucose, caffeine, oxalate, citric acid, lactic acid, sodium, potassium and chloride had no distinct influence on the peak current of albuterol indicating good selectivity of the proposed method for the determination of albuterol.

Table 4.3. Voltammetric analysis of albuterol at PPA/MWCNT/GCE in albuterol tablets.

Content (mg)	Found (mg)	Recovery%	R.S.D%
2.0	1.98±0.05	99.0	2.5

Mean ± standard deviation (n = 5)

Table 4.4. The application results of various electrodes for determining albuterol

Method/Electrode Construction	Linear range (μM)	Detection limit (nM)	Reproducibility (R.S.D%)	Pharmaceutical applications (Recovery%)	Referance
Spectrophotometry	1.73~26.00	173.6	1.7	102.0	(Satinsky et al., 2002)
Chemiluminescence	10~100	400	1.3	97.8-103.8	(Lindino and Bulhoes, 2007)
Chromatography	1.73~5.00	29.5	0.39	99.7	(El-Gindy et al., 2007)
Capillary electrophoresis	3.47~52.08	868	2.5	96.5	(Sirichai and Khanatharana, 2008)
Amperometric detection	0.80~200	250	0.92	95.8-103.8	(Quitino and Angnes, 2004)
A composite of polystyrene and polythiophene modified screen printed carbon electrode	5~550	1250	4.5	93.0	(Huang et al., 2011)
Nanogold modified ITO	0.20~8.35	310	2.02	95.0-105.0	(Goyal et al., 2007)
Bare GCE	0.80~80	200	2.4	95.0	(Sagar et al., 1993)
MWCNT/GCE	0.80~10	200	4.2	98.4-102.6	(Wei et al., 2010)
PPA/MWCNT/GCE	0.05~70	12	2.5	99.0	This work

Table 4.5. Voltammetric analysis albuterol at PPA/MWCNT/GCE in urine samples.

Sample	Added (μM)	Found (μM)	Recovery%	R.S.D%
1	20	19.52 \pm 0.51	97.6	2.6
2	50	49.25 \pm 1.13	98.5	2.3

Mean \pm standard deviation (n = 5)

4.3. MWCNTs/Electro-Copolymerized Cobalt Nanoparticles-Poly(pivalic acid) Composite Film Coated Glassy Carbon Electrode for the Voltammetric Determination of Methimazole

In this study, we aim to take the advantage of the combination of a polymer film, cobalt nanoparticles and multi-walled carbon nanotubes for the determination of methimazole.

Methimazole (2-mercapto-1-methylimidazole) (Figure 4.32.) used in the treatment of hyperthyroid by the production of thyroxin, a hormone excreted by the thyroid gland, inhibits the formation of thyroid hormones (Aletrari et al., 1998).

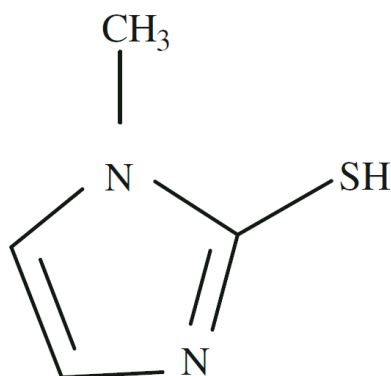


Figure 4.32. Chemical structure of methimazole

Methimazole is adsorbed by the gastrointestinal tract and concentrated in the thyroid gland (Reynolds, 1989; Aboul-Enein et al., 1979). It has been reported that methimazole may also cause side effects such as nephritis, liver cirrosis, irritation of the skin, allergies and pharyngitis with fever (Edward, 1992). The determination of

methimazole is important in many areas including clinical chemistry and pharmaceutical formulations.

Several analytical procedures have been described for the determination of methimazole including thin layer chromatography (Aletrari et al., 1998), coulometry (Nikolic and Velasevic, 1987), conductometry (Berka et al., 1989), high-performance liquid chromatography with ultraviolet detection (Moretti et al., 1993), spectroscopy (Elbardicy et al., 1991; Sanchezpedreno et al., 1995; Garcia et al., 1995), electrochemistry with a silver-silver sulphide solid-state electrode (Pinzanti et al., 1983), liquid chromatography with amperometric detection at a nafion/indium hexacyanoferrate film modified electrode (Zhang et al., 1999), capillary zone electrophoresis with amperometric detection at a carbon electrode (Wang et al., 2000), potentiometric and voltammetric methods (Aslanoglu and Peker, 2003).

Electrochemical methods have been useful for the determination of electroactive species in pharmaceuticals and body fluids due to its simplicity and low cost. Only a limited number of articles have been published in the literature on the use of chemically modified glassy carbon electrodes for the determination of methimazole including acetylene black/chitosan film modified glassy carbon electrode (Yazhen, 2011), multi-walled carbon nanotube modified GCE (Xi et al., 2010) and a carbon paste electrode modified with a schiff base complex of cobalt (Shahrokhian and Ghalkhani, 2008).

Electrochemical sensors based on CNTs represent a new and interesting alternative for the quantification of different analytes (Musameh et al., 2002; Gooding, 2005; Wildgoose et al., 2006; Kachoosangi et al., 2008; Rodriguez et al., 2008). The performance of CNT modified electrodes has been found to be much superior to those of other carbon electrodes in terms of response time, increased sensitivity, resistance to surface fouling, decreased overpotentials, reuseability and limits of detection (Wang, 2005). Also, nanoparticles of metals can display four advantages over macroelectrodes when used for electroanalysis: enhancement of mass transport, catalysis, high effective surface area and control over electrode

microenvironment (Xu et al., 2004; Wang et al., 2005; Wang et al., 2006; Laocharoensuk et al., 2007; Streeter et al., 2008).

However, conducting polymers have been applied for a wide area of practical applications, such as, for solar cells, lightweight batteries and chemical sensors (Zengin and Kalayci, 2010). Compared to other techniques, polymer film modified electrodes provide certain advantageous such as long term stability, sensitivity and homogeneity in electrochemical deposition (Roy et al., 2003; Ohnuki et al., 1983; Selvaraju and Ramaraj, 2003). So

4.3.1. Surface characterization of the modified electrode

The simultaneous electropolymerization of pivalic acid and deposition of cobalt on MWCNT/GCE was carried out using cyclic sweepings from -1.0 V to 1.5 V for 40 cycles at a scan rate of 0.15 V/s by immersing the carbon nanotubes modified electrode into a solution of 10 mM pivalic acid and 30 mM cobalt (II) chloride hexahydrate in acetonitrile containing 50 mM LiClO₄ as supporting electrolyte in Figure 4.33.

Figure 4.34. shows the SEM images of the bare GCE, MWCNT/GCE, poly(pivalic acid)/MWCNT/GCE and the poly (pivalic acid)-CoNPs/MWCNT/GCE. It can be seen from Figure 4.34a. that the MWCNT/GCE has a rough surface. It should be noted that, the MWCNTs formed on the electrode surface big bundles that cannot be totally and efficiently used for electrochemical sensors. However, it can be seen from Figure 4.34b. that the small bundles and single tubes are packaged in the polymeric membrane, which indicates the immobilization of the poly(pivalic) film on the surface of MWCNT/GCE. These images indicate that the significant modification of glassy carbon electrode surface morphology is observed. Figure 4.34c. shows the SEM image poly(pivalic acid)-CoNPs/MWCNT/GCE. It can be clearly seen that cobalt nanoparticles are non-agglomerated and well dispersed in the polymer film.

Figure 4.35. shows cyclic voltammograms of the poly(pivalic acid)-CoNPs/MWCNT/GCE in the range of -0.0 V to 0.8 V at various scan rates in 0.1 M PBS at pH 7.2. The anodic peak current (I_{pa}) was proportional to the scan rates over the range 50-200 mV/s in Figure 4.36. Therefore, a surface controlled process played a more important role in the electrochemical process.

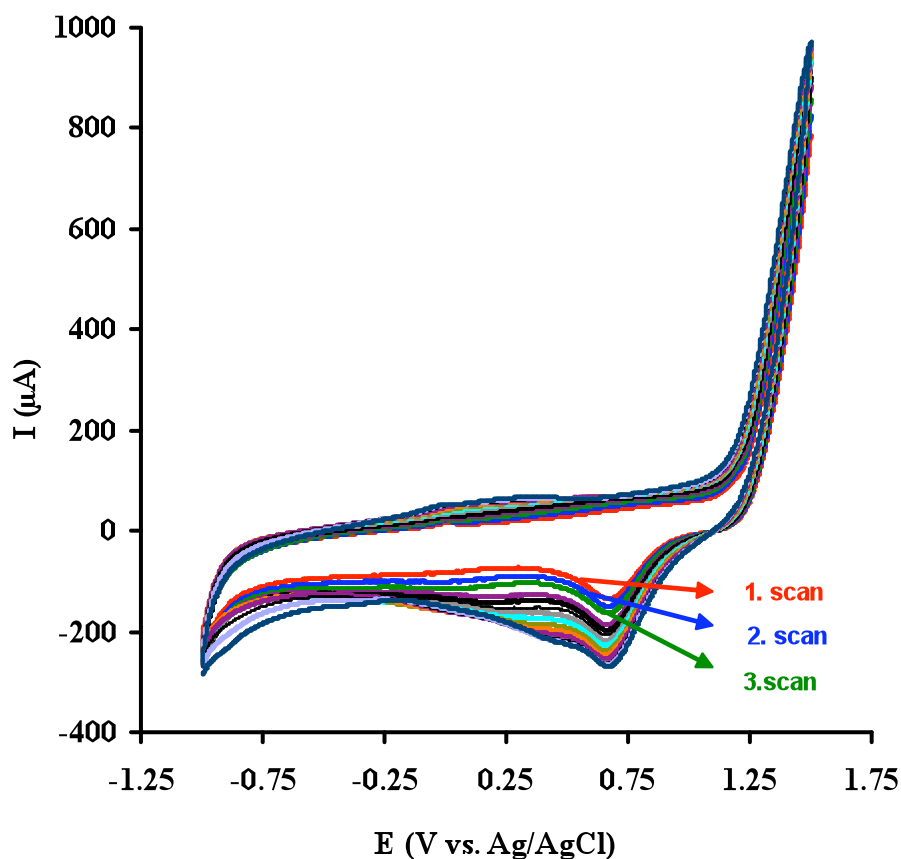
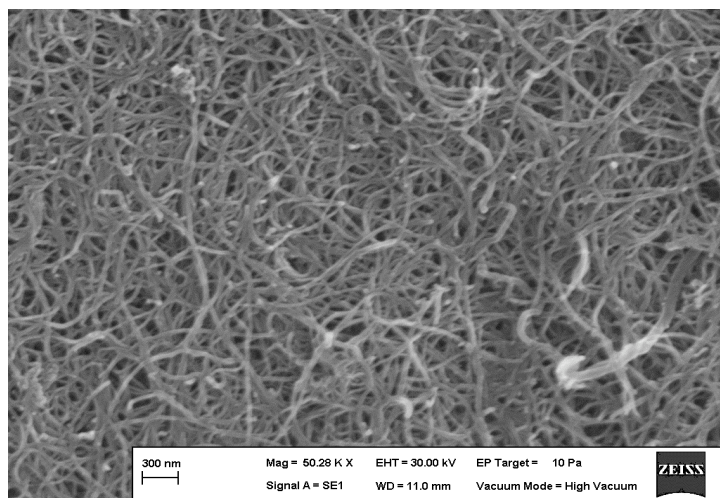
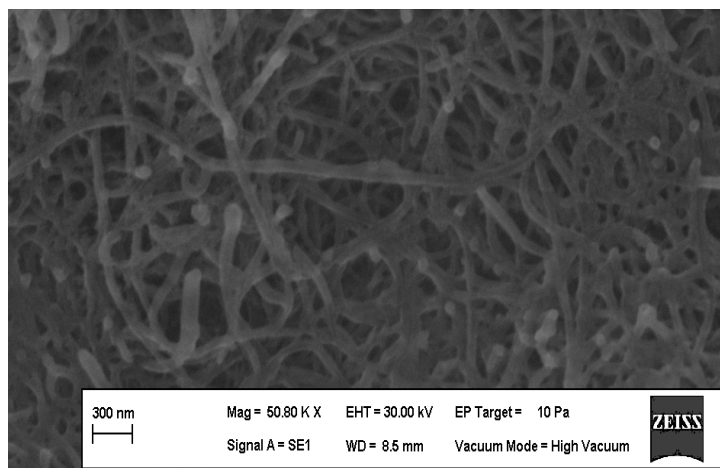


Figure 4.33. Cyclic voltammograms of 10 mM pivalic acid and 30 mM Co(II) chloride at multi-walled carbon nanotube modified glassy carbon electrode in acetonitril including 50 mM LiClO₄ Scan rate: 150 mV/s

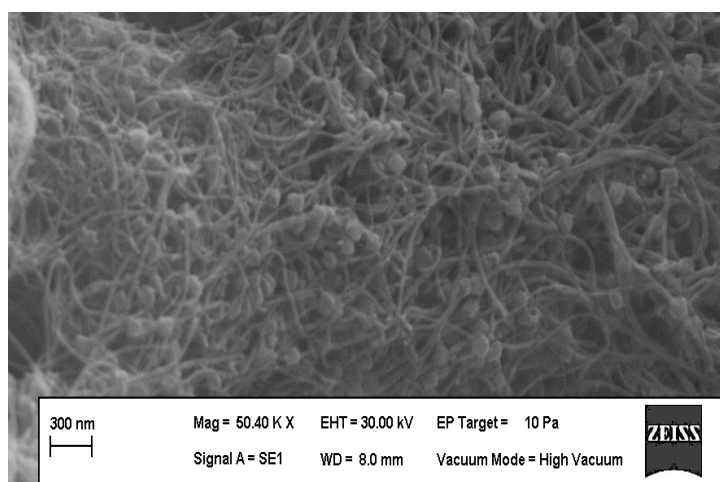
a) MWCNT/GCE



b) PPA/MWCNT/GCE



c) PPA/CoNPs/MWCNT/GCE

**Figure 4.34.** Sem images of modified electrodes

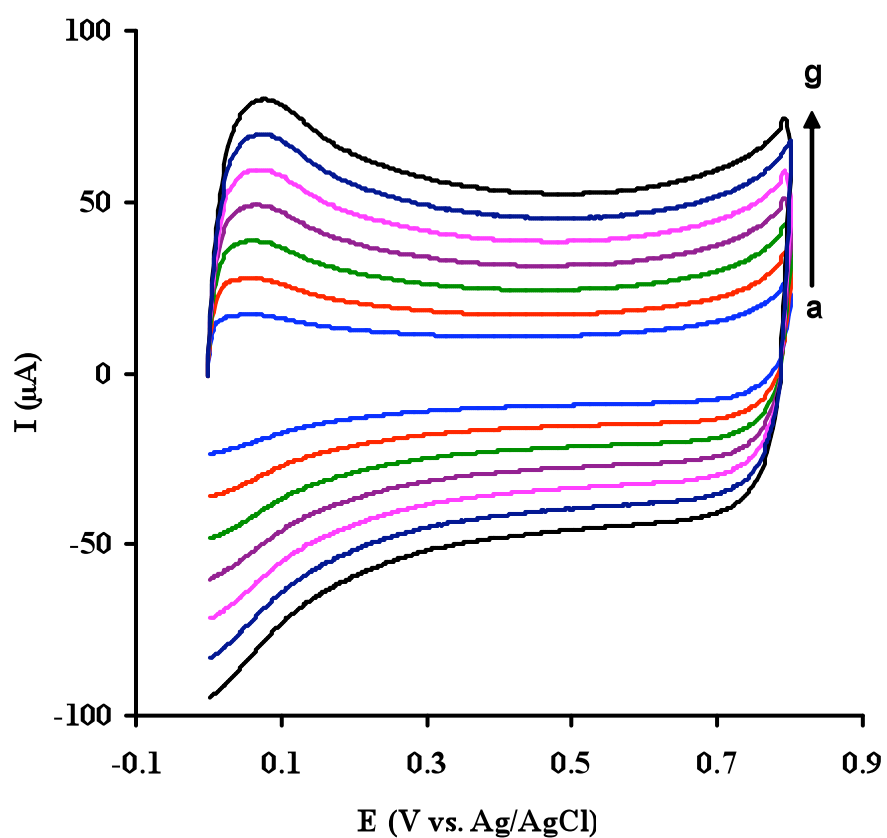


Figure 4.35. Cyclic voltammograms of poly (pivalic acid)-CoNPs/MWCNT/GCE in 0.1 M PBS at pH 7.2. Scan rate increasing from (a) 50 mV/s to (g) 200 mV/s . Equilibrium time:5 s

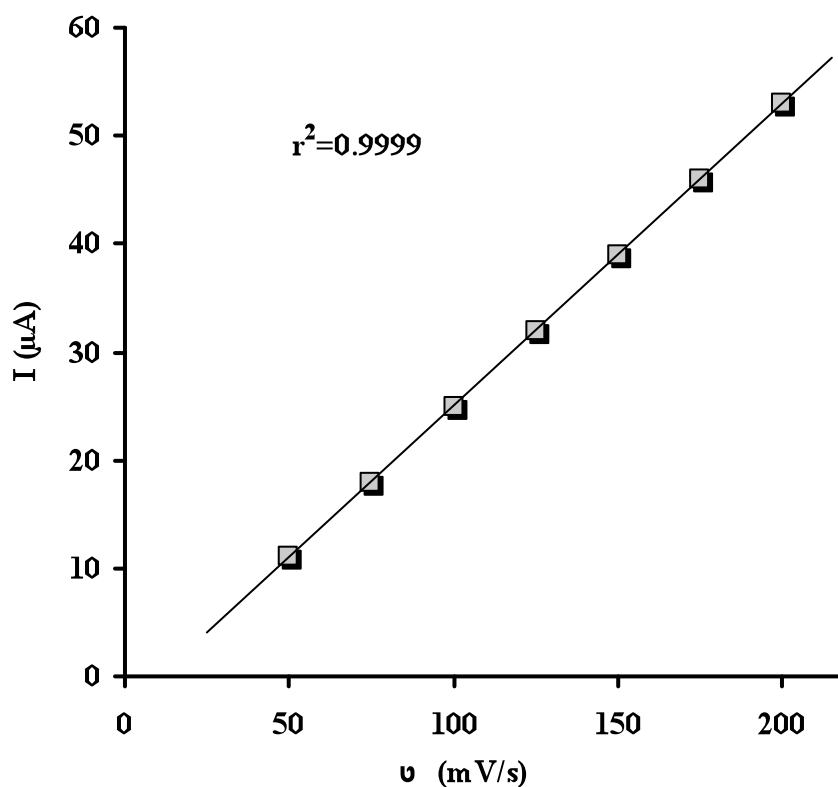


Figure 4.36. Plot of background currents of poly(pivalic acid)-CoNPs/MWCNT/GCE versus scan rate

4.3.2. Voltammetric behaviour of methimazole

Figure 4.37. exhibits the cyclic voltammograms of methimazole at bare GCE and various modified electrodes in 0.1 M PBS at pH 7.2. Methimazole exhibits an oxidation peak at *ca.* 0.665 V at a bare GCE, 0.440 V at poly(pivalic acid)GCE, 0.400 V at MWCNT/GCE and 0.273 V at poly(pivalic acid)/MWCNT/GCE. As shown in Figure 4.37., the voltammetric response of methimazole is rather broad due to a slow electron transfer, which is caused by fouling of the electrode surface especially at bare GCE. However, methimazole exhibits a sharp and well-defined anodic wave at 0.255 V at poly(pivalic acid)-CoNPs/MWCNT/GCE. This indicated that poly(pivalic acid)-CoNPs/MWCNT/GCE has exhibited an effective electrocatalytic effect towards the oxidation of methimazole.

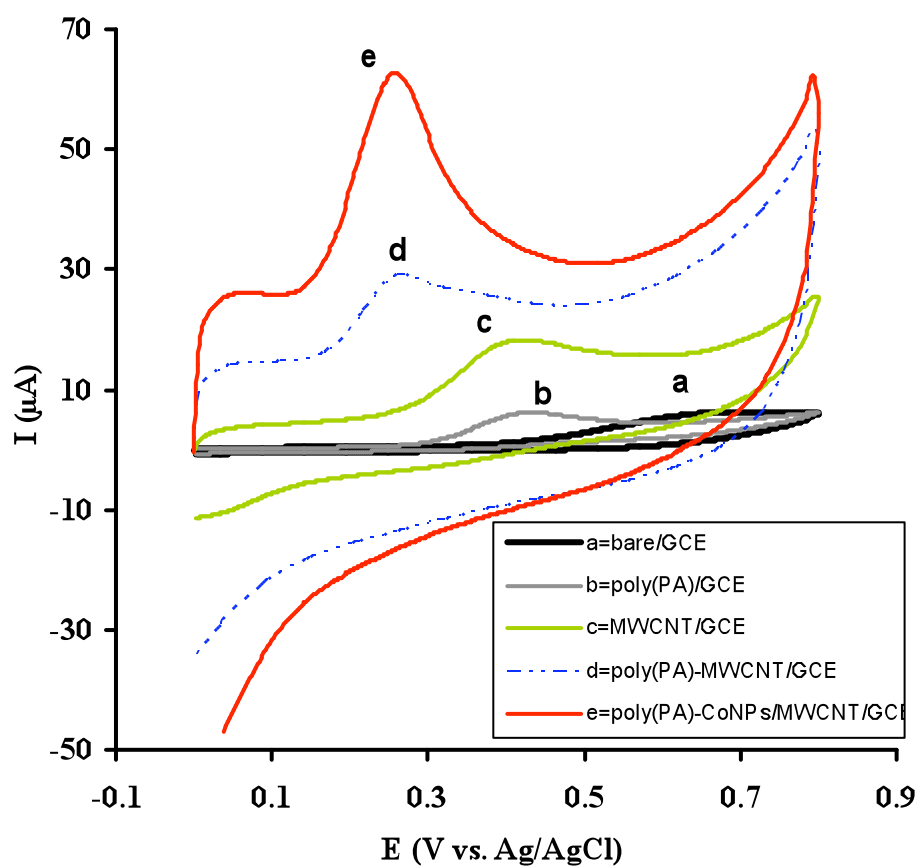


Figure 4.37. Cyclic voltammograms of 1.12×10^{-4} M methimazole at bare GCE (a), poly(pivalic acid)/GCE (b), MWCNT/GCE (c), poly(pivalic acid)/MWCNT/GCE (d) and poly(pivalic acid)-CoNPs/MWCNT/GCE (e) in 0.1 M PBS at pH 7.2. Scan rate 50 mV/s. Equilibrium time:5 s

Table 4.6. summarizes the electrochemical behaviour of methimazole at various electrodes. Compared with bare glassy carbon and other three modified electrodes, the electrochemical response of methimazole has greatly been increased on the poly(pivalic acid)-CoNPs/MWCNT/GCE. Intensive increase in peak current is observed owing to the improvement in the electron transfer process and the larger real area of the film at the surface. No peaks are observed in the cathodic branch indicating that the methimazole oxidation is an irreversible process. The anodic peak can be attributed to the thiol moiety of methimazole.

Table 4.6. The oxidation peak potentials and peak heights of methimazole at various electrodes

Voltammogram symbol	Electrode type	Peak potential of methimazole (E/mV)	Peak height of methimazole (I/μA)
a	Bare GCE	665	2
b	Poly(pivalic acid)/GCE	440	3
c	MWCNT/GCE	400	9
d	Poly(pivalic acid)/MWCNT/GCE	273	10
e	Poly(pivalic acid)CoNPs/MWCNT/GCE	255	36

In order to understand the mechanisms responsible for the oxidation of methimazole at poly(pivalic acid)-CoNPs/MWCNT/GCE, cyclic voltammograms of methimazole were recorded at various scan rates (Figure 4.38.). The peak potential shifted to more positive values on increasing the scan rate which confirms the irreversibility of the oxidation process. The anodic peak current (I_{pa}) was proportional to the scan rate (ν) over the range of 50–200 mV/s (Figure 4.39.). The results indicated that the electrochemical oxidation of methimazole at poly(pivalic acid)-CoNPs/MWCNT/GCE is a surface-controlled process.

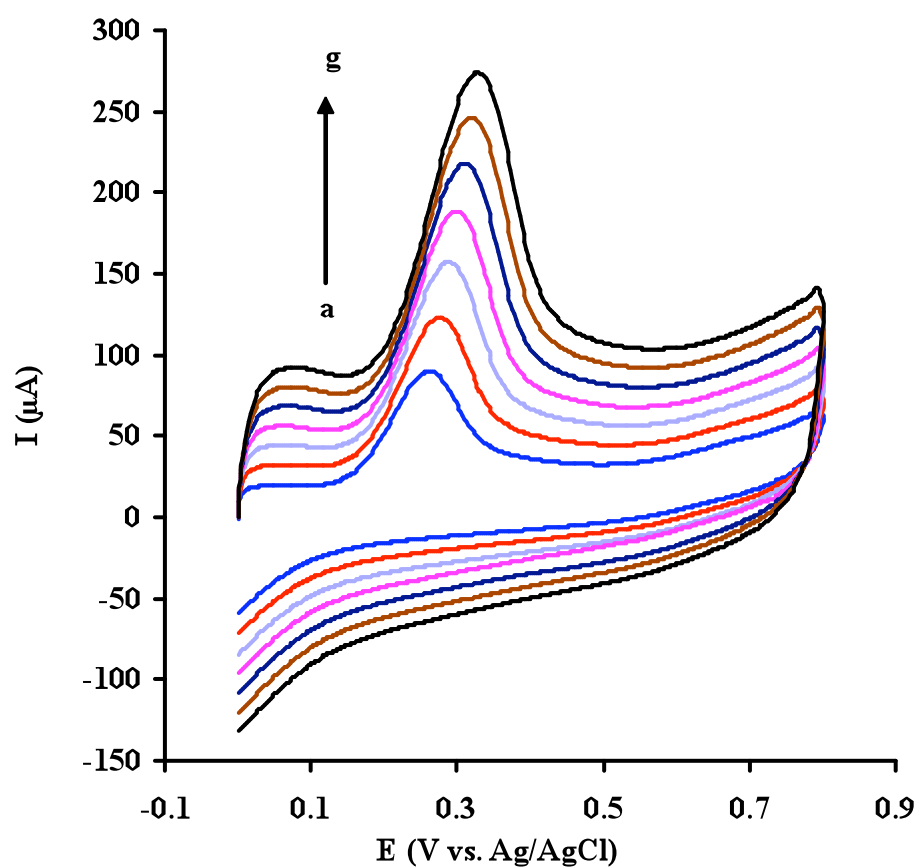


Figure 4.38. Cyclic voltammograms of 1.76×10^{-4} M methimazole at poly(pivalic acid)-CoNPs/MWCNT/ GCE in 0.1 M PBS at pH 7.2. Scan rate increasing from (a) 50 mV/s to (g) 200 mV/s. Equilibrium time: 5 s

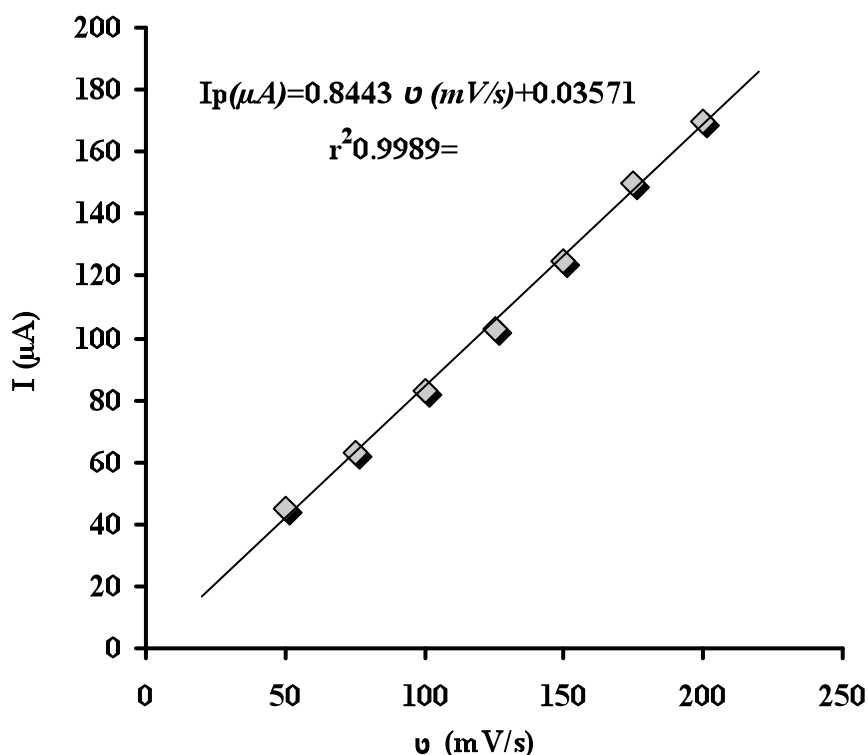


Figure 4.39. Plot of anodic peak currents of methimazole versus scan rate

In order to get information about the number of electrons involved in the oxidation of methimazole, the value of αn for the electrocatalytic oxidation of methimazole was determined. The Tafel plot was determined using the following equation.

$$E_{pa} = (2.303 RT / \alpha n F) (1/2) \log v + \text{constant} \quad \text{Eq. (4.2)}$$

The catalytic oxidation peak potential of methimazole is proportional to $\log v$ with a slope of 0.048663 as shown in Figure 4.40. The oxidation of methimazole is a one-electron transfer process assuming the electron transfer coefficient α is approximately 0.5 in a totally irreversible electrode process.

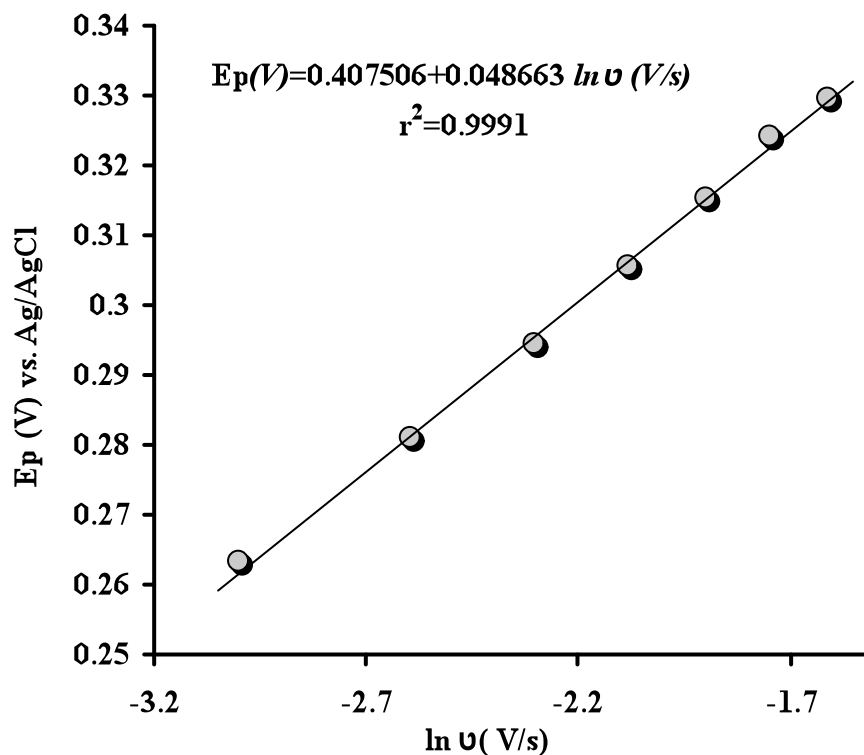
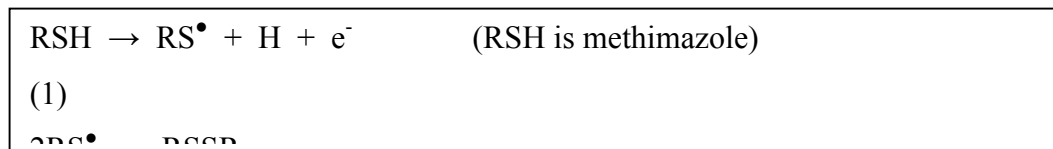


Figure 4.40. Plot of anodic peak potentials of methimazole versus logarithm of scan rate

4.3.3. The effect of pH on the voltammetric behaviour of methimazole

In addition, the effect of the pH value of the PBS buffer solution on peak potential of methimazole at poly(pivalic acid)-CoNPs/MWCNT/GCE was also investigated. The anodic peak potential of methimazole shifted in the negative direction with increasing pH (Figure 4.41.). Also a plot of numerical values of shifts in oxidation peak potential of methimazole with the solution pH is also shown as inset in Figure 4.42. The shift in E_p with pH refers to a proton transfer in the electrochemical oxidation of methimazole. It has also been reported that the identical numbers of electrons and protons are involved in the oxidation process of methimazole (Xi et al., 2010). Combining the fact that identical numbers of electrons and protons should be involved in the electrode process, it might be concluded that the electrochemical reaction of methimazole at poly(pivalic acid)-CoNPs/MWCNT/GCE could be realized the oxidation of disulfhydryl group in the

molecule as shown in Scheme 4.4. (Xi et al., 2010; Shahrokhian and Ghalkhani, 2008).



Scheme 4.4. Electrode reaction of Methimazole at poly(pivalic acid)-CoNPs/MWCNT/GCE

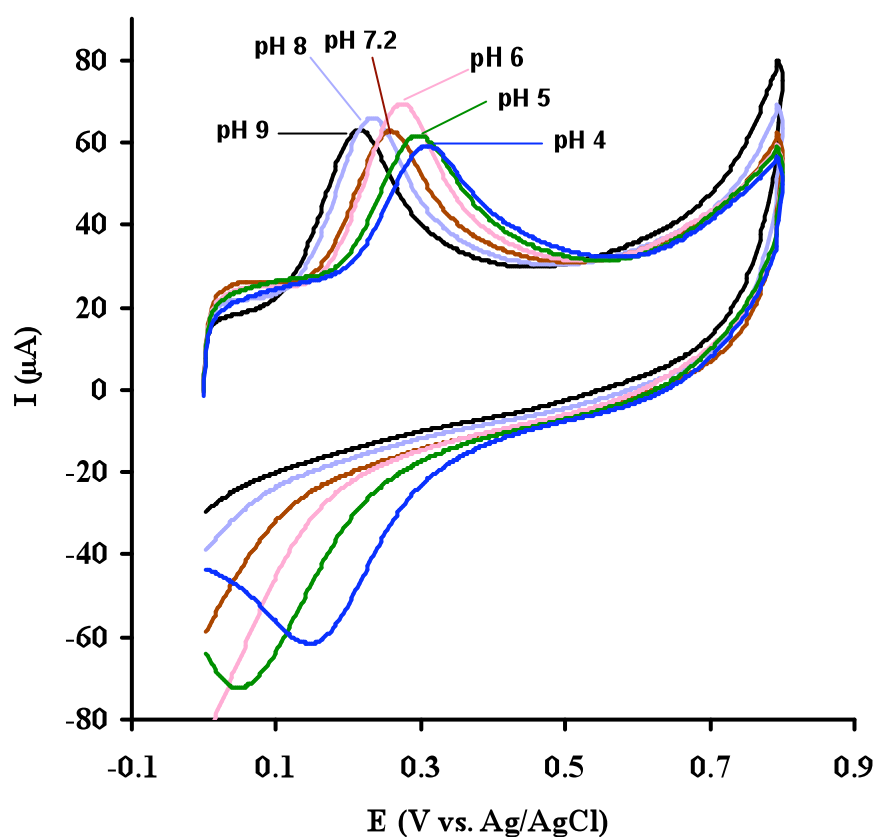


Figure 4.41. Cyclic voltammograms of 1.12×10^{-4} M methimazole at poly(pivalic acid)-CoNPs/MWCNT/GCE in 0.1 M PBS at different pH values. pH: 4.0; 5.0; 6.0; 7.2; 8.0; 9.0. Scan rate: 50 mV/s. Equilibrium time: 5 s

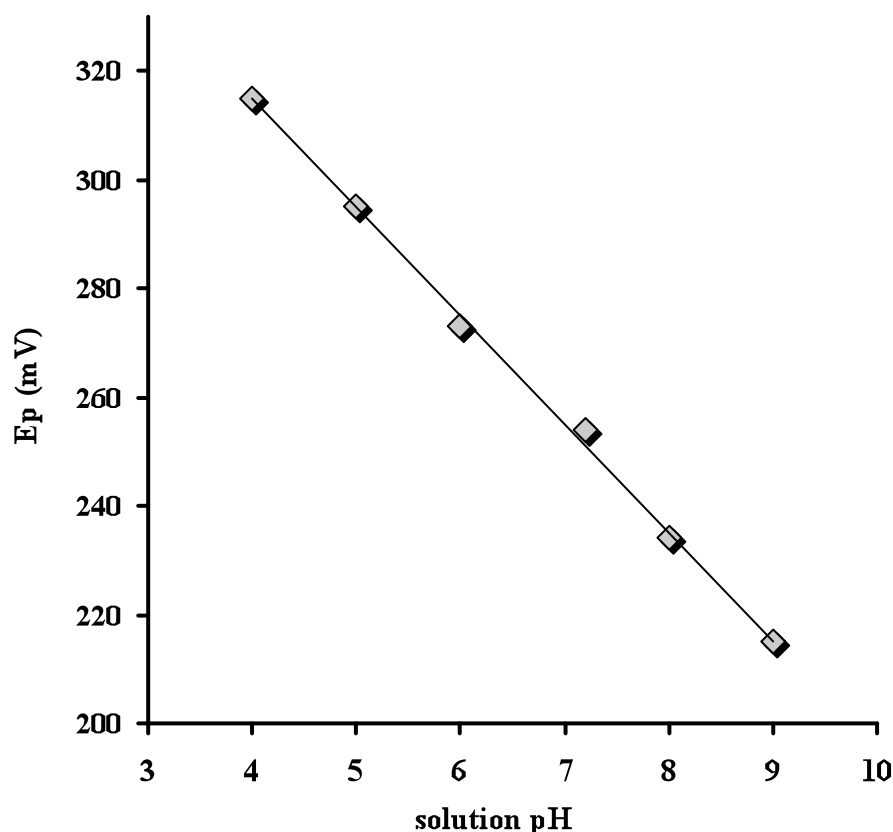


Figure 4.42. Plot of anodic peak potentials of methimazole versus solution pH

4.3.4. Calibration equation for the determination of methimazole

Determination of the concentration of methimazole at poly(pivalic acid)-CoNPs/MWCNT/GCE was performed at pH 7.2. Cyclic voltammograms of various concentrations of methimazole at poly(pivalic acid)-CoNPs/MWCNT/GCE are given in Figure 4.43. The anodic peak currents were plotted against the bulk concentration of methimazole after the background subtraction (Figure 4.44.). The response of anodic peak currents of methimazole at poly(pivalic acid)-CoNPs/MWCNT/GCE was linear with the concentration of methimazole in the range of $1.0 \times 10^{-7} \sim 3.0 \times 10^{-4}$ M. The linear regression equation was $I_{pa} (\mu A) = 0.00136 + 0.32399C (\mu M)$ with a correlation coefficient of 0.9995. The detection limit was 9.36×10^{-9} M (S/N=3).

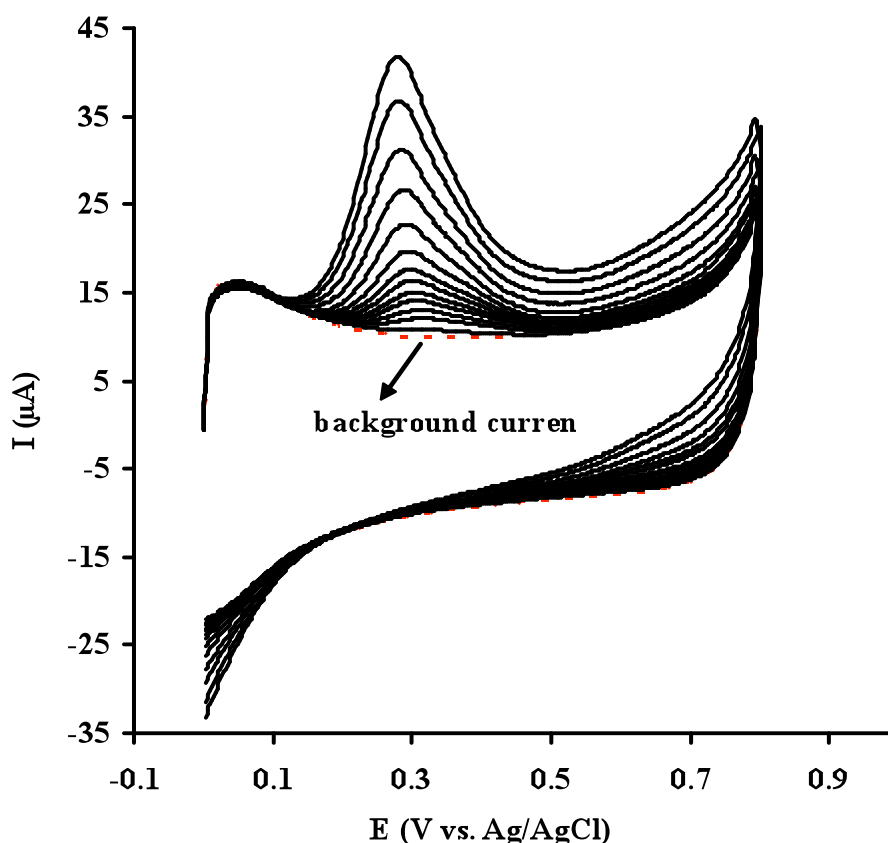


Figure 4.43. Cyclic voltammograms of increasing concentrations of methimazole at poly(pivalic acid)-CoNPs/MWCNT/GCE in 0.1 M PBS at pH 7.2. Methimazole concentrations: 0; 0.1; 2; 6; 8; 10; 16; 18; 20; 30; 45; 65; 100 μM . Scan rate: 50 mV s^{-1} . Equilibrium time: 5 s

4.3.5. Reproducibility and stability of modified electrode

The relative standard deviation (RSD) of 10 successive scans was 1.6% for 20 μM methimazole. This indicated that the reproducibility of the poly(pivalic acid)-CoNPs/MWCNT/GCE was excellent. However, the modified electrode should be well treated to maintain its reproducibility. It was found that 20 cycles of scanning in 0.1 M PBS in the potential range 0.0~0.8 V could regenerate clean background CV curves and the modified electrode was ready for the next experiment or storage in 0.1 M PBS. Also, the current response decreased only by 5% over a week for storage in 0.1 M PBS.

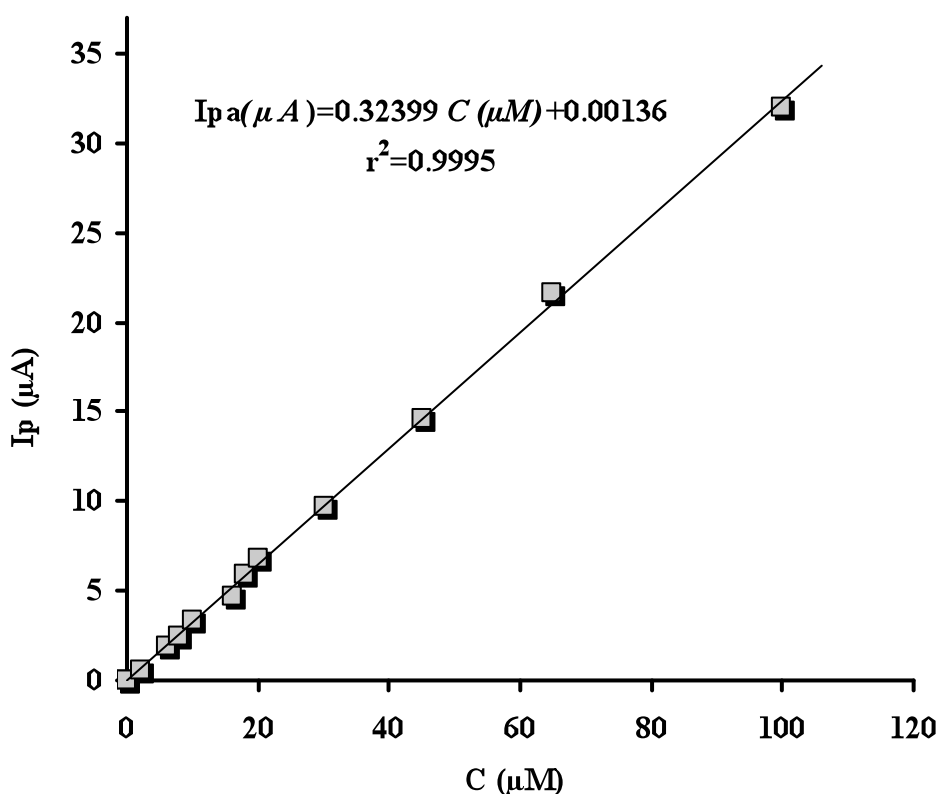


Figure 4.44. Plot of anodic peak currents of methimazole versus increasing concentration of methimazole

4.3.6. Determination of methimazole in thyromazol tablets

The tablet solution was subjected to cyclic voltammetry. Voltammetric determination of methimazole on a poly(pivalic acid)-CoNPs/MWCNT/GCE in the content of thyromazol tablets was referred to the regression equation. The analysis of thyromazol tablets using the proposed method is summarised in Table 4.7. The relative standard deviation (RSD) was 1.02 % using the proposed method for the voltammetric analysis of thyromazol tablets. The validity of the proposed procedures applied to thyromazol tablets was also assured by the recovery of standard additions. A mean recovery of 99.2% with RSD of 0.81 was obtained. The results of the drug analysis obtained from the proposed method are in close agreement with the claimed value. At the same time, the results obtained are also comparable with the results obtained from liquid chromatography and capillary zone electrophoresis (Zhang et al., 1999; Wang et al., 2000). Also, the results obtained

using the proposed method in this study are well compared with several electrochemical methods for the determination of methimazole in literature. However, the results obtained from the proposed method indicate that this method is more precise and accurate for the determination of methimazole in drug samples.

Table 4.7. Results of the determination of methimazole in thyromazol tablets

Sample No	Original (μg)	Added (μg)	Found	Recovery%	RSD%
1	5	0	4.89 \pm 0.05	98.8	1.02
2	5	5	9.90 \pm 0.08	99.2	0.81

Mean \pm Standard deviation (n =5)

4.4. Nickel Nanoparticles Functionalized Multi-Walled Carbon Nanotubes at Platinum Electrodes for the Detection of Bromhexine

In this study, a voltammetric nanosensor has been prepared by one-pot synthesis of multi-walled carbon nanotube-supported nickel nanoparticles in an ultrasonic bath. The nanocomposite material was immobilized on a Pt electrode surface for the detection of bromhexine. The surface modification with MWCNT and nanoparticles of nickel served to reduce the potential required to oxidize species, improve voltammetric behavior and enables are producible detection for bromhexine.

Bromhexine (Figure 4.45.) is a mucolytic drug used in the treatment of respiratory disorders (Grange and Snell, 1996). It is rapidly absorbed by oral route and spreads to the tissues including the bronchial epithelium (Parvez et al., 1996). Since mucolytics may disrupt the gastric mucosal barrier, bromhexine should be used with caution in patients with a history of gastric ulceration. The quantification of bromhexine is important in many areas including clinical chemistry and pharmaceutical formulations.

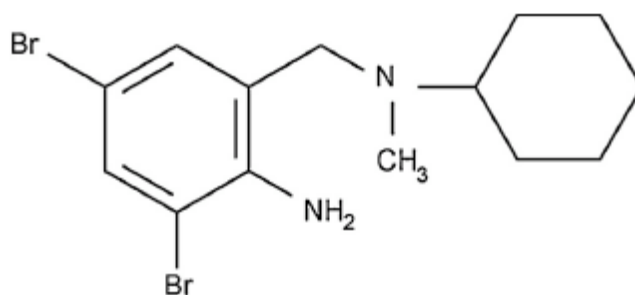


Figure 4.45. Chemical structure of bromhexine

A number of analytical methods have been utilized for the determination of bromhexine in pharmaceuticals and biological fluids including UV–visible spectrophotometry (Habib et al., 2005; Dias et al., 2003), flow injection analysis with ion selective electrodes (Abdel-Ghani et al., 2006), liquid chromatography (Bazylak and Nagels, 2003), inductively coupled plasma mass spectrometry (Jensen et al., 2005), capillary isotachopheresis (Pospisilova et al., 2001), electrokinetic chromatography (Okamoto et al., 2005), liquid-gas chromatography (Lau and Cheung, 1990) gas chromatography with mass detection (Uboh et al., 1991) and differential pulse voltammetry (Turchan et al., 2007). Spectrophotometry and chromatography are the two most widely employed techniques for the determination of bromhexine. However, these techniques are expensive and require time-consuming derivatization step. The electrooxidation of bromhexine has been studied in solution using a glassy carbon electrode (Turchan et al., 2007). However, it is necessary to find an adequate surface for a reproducible and sensitive determination of bromhexine in order to overcome electrode fouling. The modification of conventional electrodes has attracted much attention in last two decades because it provides powerful means to bring new qualities to the electrode surface which exploited for electrochemical purposes (Walcarus, 2001).

Chemically modified electrodes can be obtained by either attaching molecules on electrode surfaces or by immobilizing multimolecular layers on electrodes. They found applications in various fields including electroanalysis and electrocatalysis (Yang et al., 2012; Xu et al., 2012 and Henstridge et al., 2010). Among the wide range of electrode modifiers carbon nanotubes and metal nanoparticles have been focus of attention for electrochemists because of advantageous features such as

excellent long term stability, response time, increased sensitivity, resistance to surface fouling, decreased overpotentials, limits of detection, conductivity, nanometersize and providing large surface area (Goyal et al., 2008; Karuwan et al., 2009; Lijun et al., 2007; Goyal et al., 2011, and Huang et al., 2011). Furthermore, no articles have appeared in the literature on the use of chemically modified electrodes for the determination of bromhexine.

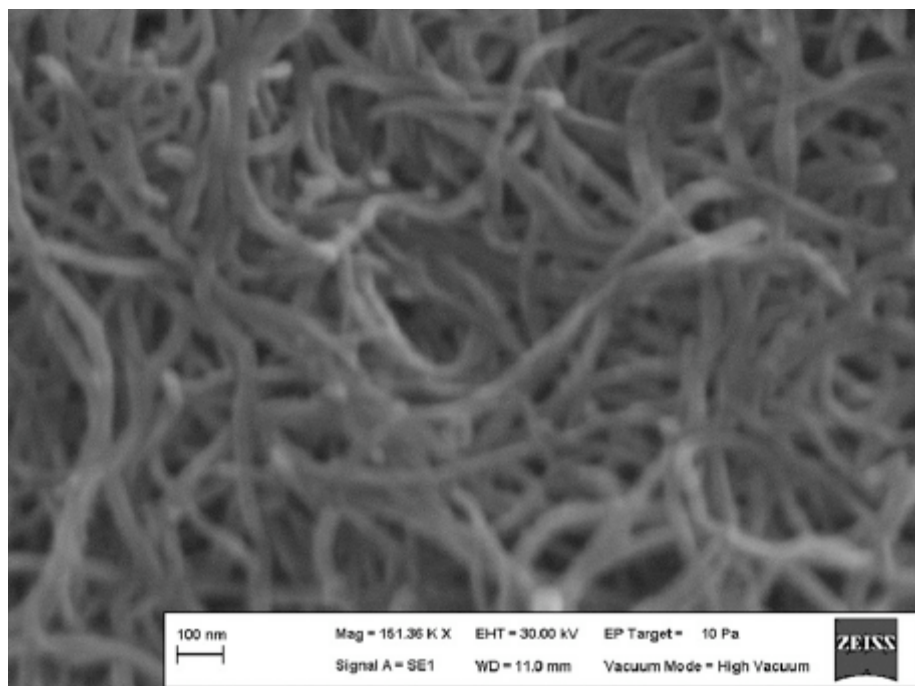
4.4.1. Characterization of modified electrode

The surface morphology of the NiNPs/MWCNT/GCE was characterized by SEM. As shown in Figure 4.46.(A) a MWCNT layer without aggregation was observed on the electrode surface, indicating that the MWCNTs were homogeneously dispersed on the surface of Pt electrode. As can be seen in Figure 4.46.(B), the NiNPs deposited on the MWCNTs were spherical and well distributed. The average size of nickel nanoparticles was *ca.* 100 nm.

The EDX results exhibited in Figure 4.46. show that Ni, C and Au were the major elements on the electrode surface. The Au was obtained from the gold coating of the NiNPs/MWCNT/Pt during SEM analysis. The EDX results clearly show that Ni is electrodeposited on the surface of MWCNT layer. The surface loading has been calculated to be 6.2 ng using the table obtained from the EDX measurement as provided under Figure 4.47.

The cyclic voltammograms of the modified electrode are given in Figure 4.48. in which nickel is clearly seen in the cathodic region. Also, no waves are observed in the potential region where bromhexine undergoes oxidation.

A)



B)

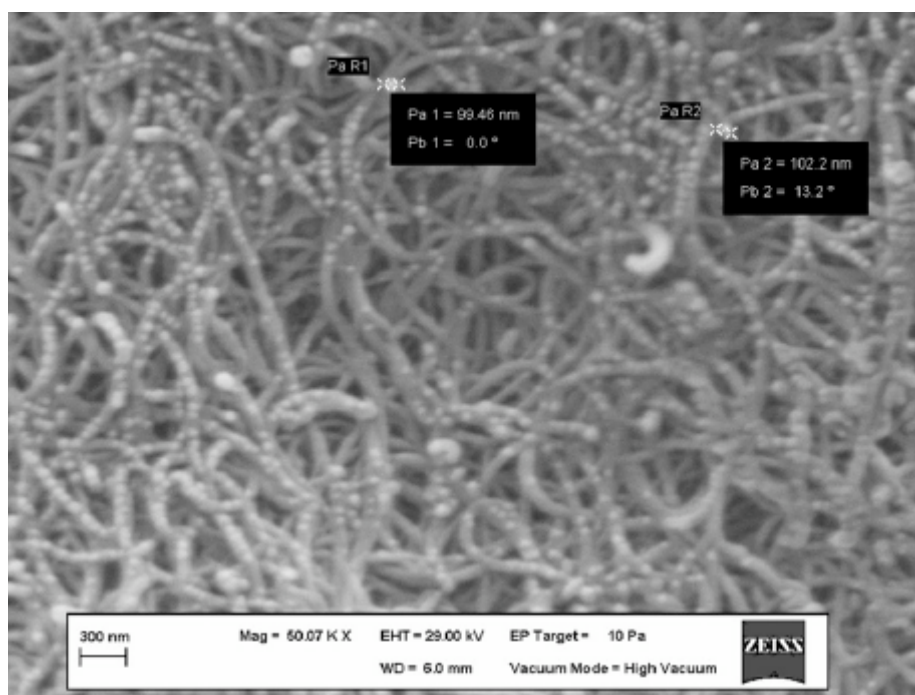
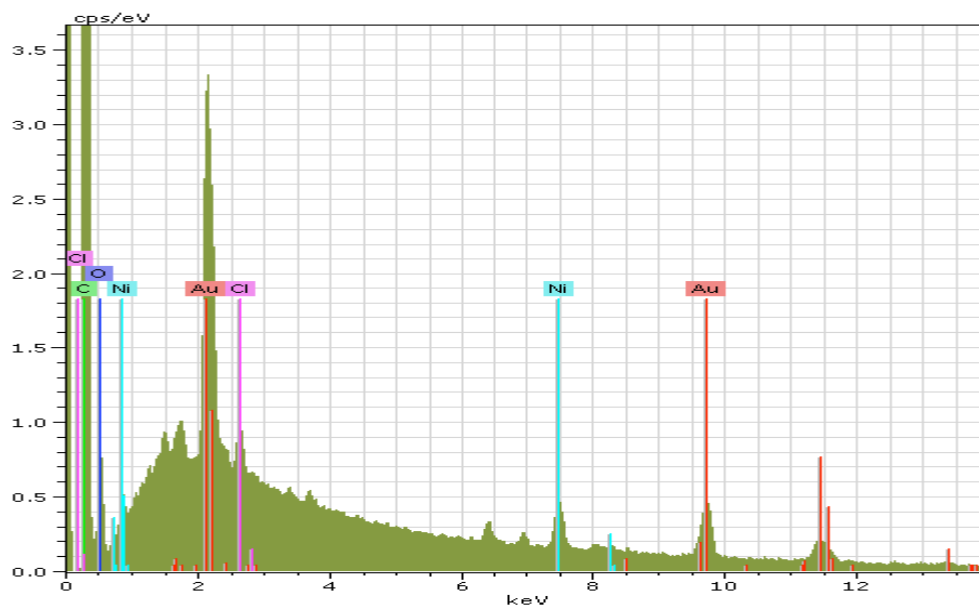


Figure 4.46. SEM images of MWCNT/Pt (A) and NiNPs/MWCNT/Pt (B)



El	AN	Series	unn. [wt.-%]	C norm. [wt.-%]	C Atom. [at.-%]	C error [%]
C	6	K	47.92	47.92	57.26	14.8
Au	79	L	4.28	4.28	0.31	0.1
Ni	28	K	0.62	0.62	0.15	0
Cl	17	K	0.11	0.11	0.04	0
O	8	K	47.08	47.08	42.23	0
Total	-	-	100	100	100	15.9

Figure 4.47. EDX analysis of NiNPs/MWCNT/Pt

4.4.2. Voltammetric behavior of bromhexine

Figure 4.49. exhibits the cyclic voltammograms of bromhexine at bare Pt and MWCNT/Pt and NiNPs/MWCNT/Pt electrodes in 0.1 M PBS at pH 4.0. Bromhexine exhibits a poor oxidation peak at ca. 1025 mV at bare Pt (Figure 4.49a.) and a broad oxidation peak at 1010 mV at MWCNT/Pt (Figure 4.49c.). The cyclic voltammogram of bromhexine at nickel nanoparticles modified Platinum electrode is also shown in Figure 4.49b. An oxidation peak is obtained at 1015 mV. It is

clearly shown that nickel nanoparticles offer a marked improvement in electron transfer compared to a bare Pt electrode and a MWCNT modified Pt electrode alone. However, bromhexine exhibits a sharp and well-defined anodic wave at 997 mV at NiNPs/MWCNT/Pt (Figure 4.49d.). This indicated that voltammetry of bromhexine has greatly been improved at NiNPs/MWCNT/Pt. Compared with bare Pt and MWCNT modified electrode, the electrochemical response of bromhexine has also been increased at NiNPs/MWCNT/Pt. Intensive increase in peak current is observed owing to the improvement in the electron transfer process and the larger real area of the film at the surface. No peaks are observed in the cathodic branch indicating that the bromhexine oxidation is an irreversible process. Also, another oxidation peak is observed at 1120 mV with a lower intensity of current.

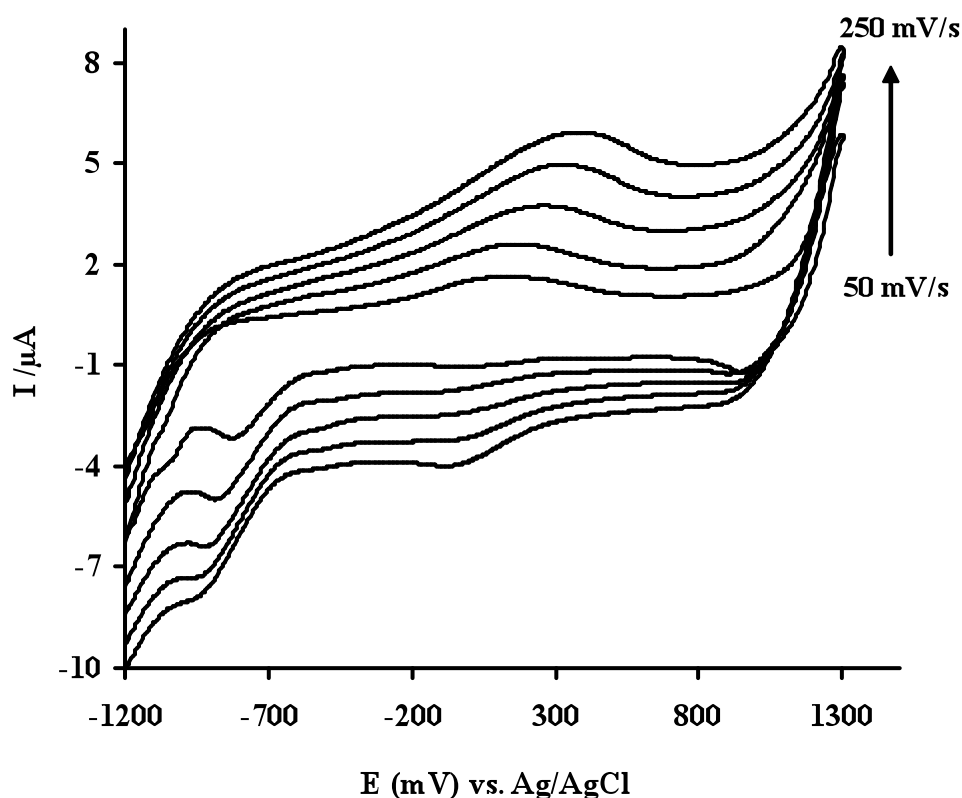


Figure 4.48. Cyclic voltammograms of NiNPs/MWCNT/Pt in 0.1 M PBS at pH 4.0 at different scan rates from 50 to 250 mV/s

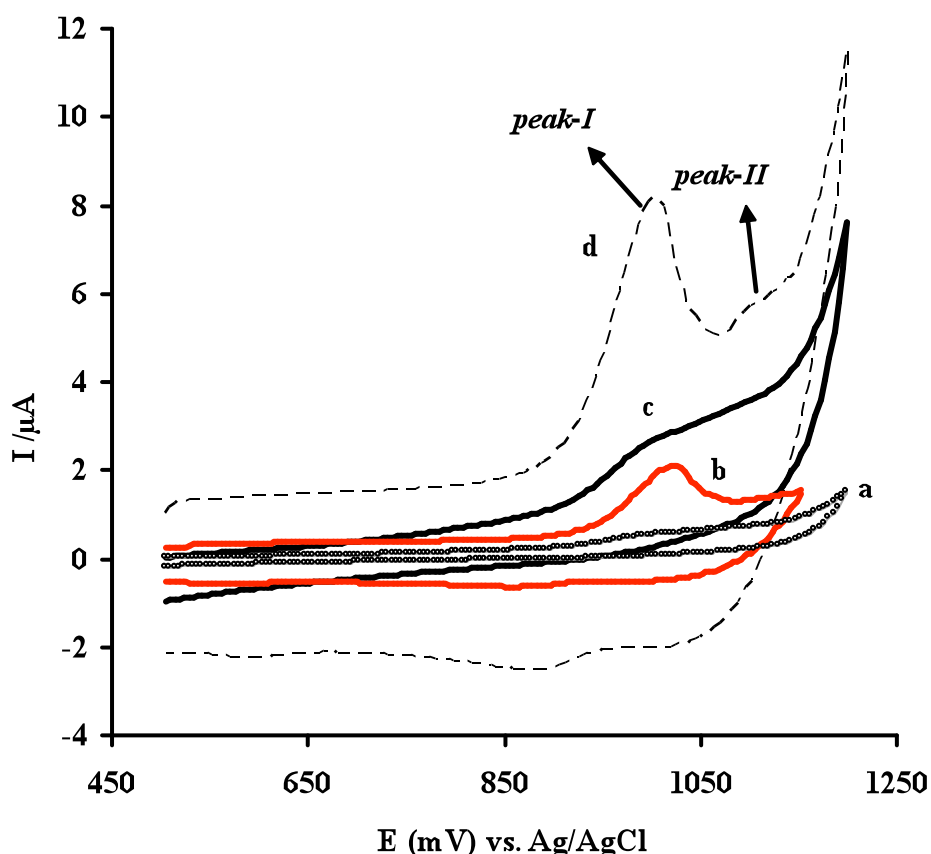


Figure 4.49. Cyclic voltammograms of 1.5×10^{-5} M bromhexine at bare Pt electrode (a), NiNPs/Pt electrode (b), MWCNT/Pt electrode (c) and NiNPs/MWCNT/Pt (d) in 0.1 MPBS at pH 4.0. Scan rate: 50 mV/s. Equilibrium time: 5 s

In order to understand the mechanisms responsible for the oxidation of bromhexine at NiNPs/MWCNT/Pt, cyclic voltammograms of bromhexine were recorded at various scan rates (Figure 4.50.).

The peak potential shifted to more positive values on increasing the scan rate which confirms the irreversibility of the oxidation process. The anodic peak current (I_{pa}) was proportional to the scan rate (ν) over the range of 10–50 mV/s (Figure 4.51.). Also, log of peak current against log of scan rate (Figure 4.52.) showed slope close to 1, suggesting that electrochemical oxidation of bromhexine at NiNPs/MWCNT/Pt is a surface-controlled process.

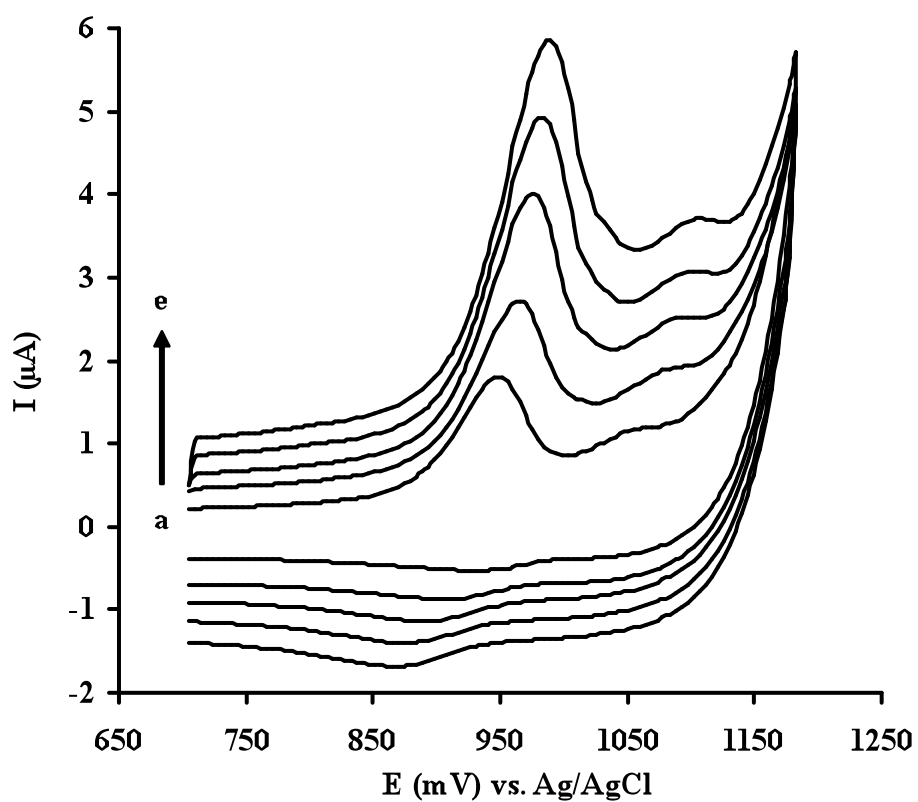


Figure 4.50. Cyclic voltammograms of 1.0×10^{-5} M bromhexine at NiNPs/ MWCNT/Pt in 0.1 M PBS at pH 4.0. Scan rates: (a) 10 mV/s; (b) 20 mV/s; (c) 30 mV/s; (d) 40 mV/s; (e) 50 mV/s. Equilibrium time: 5 s

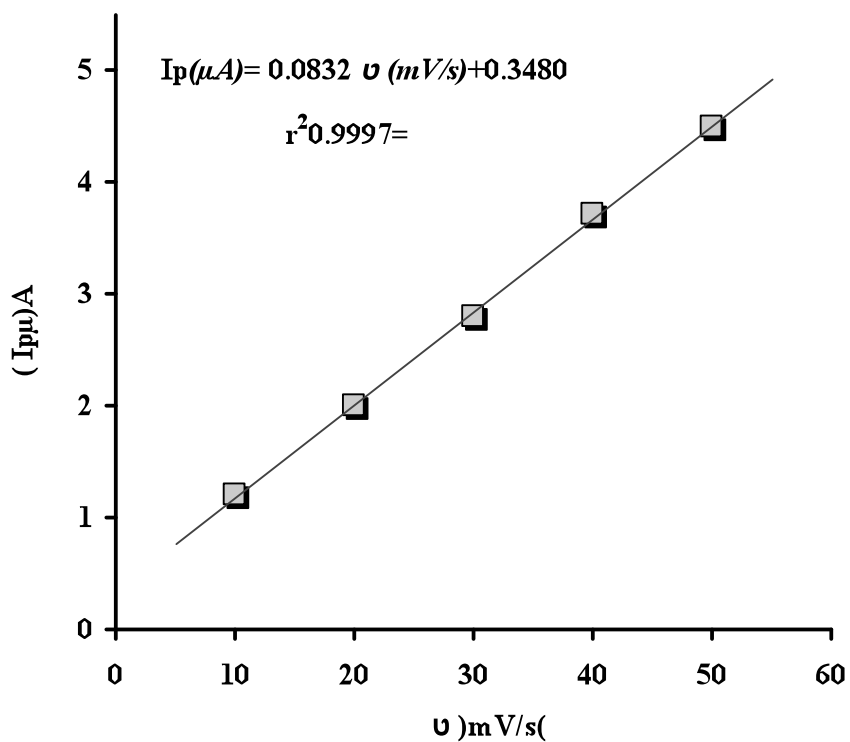


Figure 4.51. Plot of anodic peak currents of bromhexine versus scan rates

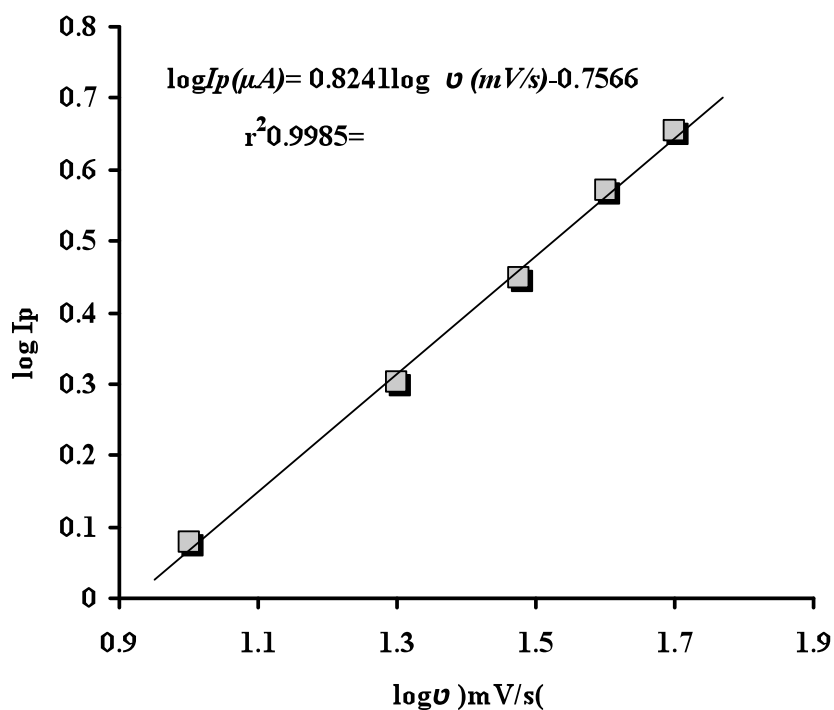


Figure 4.52. Plot of logarithm of peak currents of bromhexine versus logarithm of scan rates

In order to get information about the number of electrons involved in the oxidation of bromhexine, the value of αn for the electrocatalytic oxidation of bromhexine was determined. The Tafel plot was determined using the following equation.

$$E_{pa} = (2.303 RT / \alpha n F) (1/2) \log v + \text{constant} \quad \text{Eq. (4.3)}$$

The catalytic oxidation peak potential of bromhexine is proportional to the logarithm of scan rate with a slope of 0.02380 in Figure 4.53. The oxidation of bromhexine is a two-electron transfer process assuming the electron transfer coefficient is approximately 0.5 in a totally irreversible electrode process. Controlled potential electrolysis of bromhexine also yielded that the oxidation involved a two electron transfer (Turchan et al., 2007).

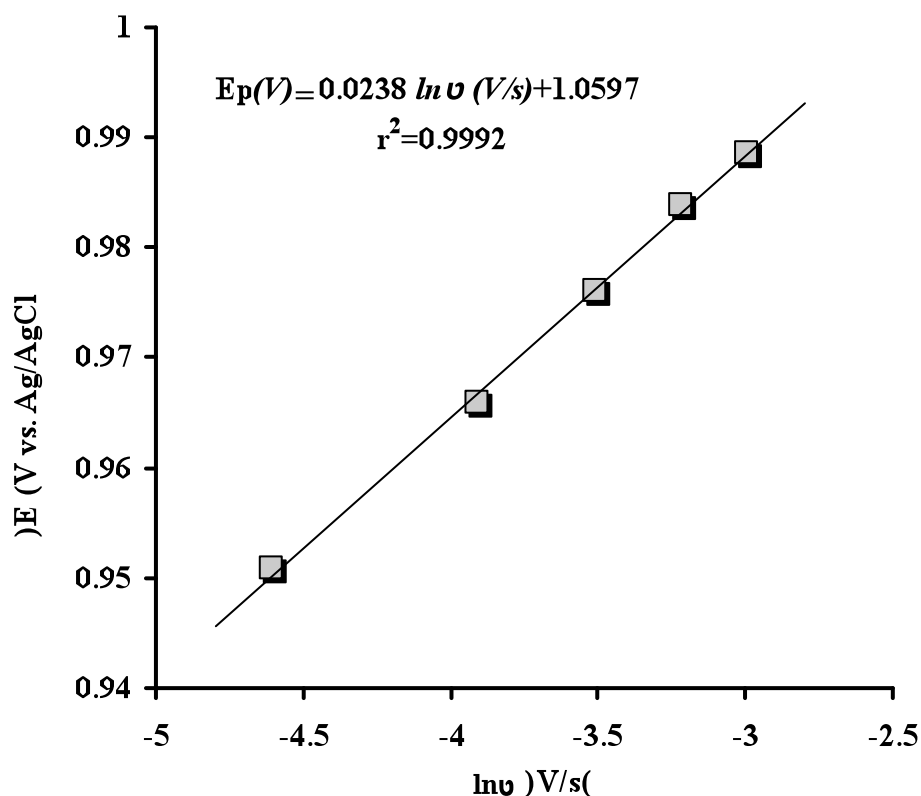


Figure 4.53. A plot of anodic peak potentials of bromhexine versus logarithm of scan rate

4.4.3. The effect of pH on the voltammetric behaviour of bromhexine

In addition, the effect of the pH value of the phosphate buffer solution on peak potential of bromhexine at NiNPs/MWCNT/Pt was also investigated. The anodic peak potential of bromhexine shifted in the negative direction with increasing pH (Figure 4.54.). The shift in E_p with pH refers to a proton transfer in the electrochemical oxidation of bromhexine. The slope of oxidation peak potential (E_p) vs. pH is 35.5 mV/pH with 0.9999 correlation coefficient. This indicated that the proportion of electrons and protons involved in the reaction is also $2e^-/H^+$ at over the range of pH 3–5. However, a break in the E_p versus pH plot above pH 5.0 is observed. This break might be attributed to the pK_a value of bromhexine (Turchan et al., 2007). On the other hand, the second oxidation peak also shows to be pH-dependent with alower intensity. The results indicate that the reaction involves a two electron transfer, accompanied by two protons in total. Electrode reaction of bromhexine is given in Scheme 4.5.(Turchan et al., 2007).

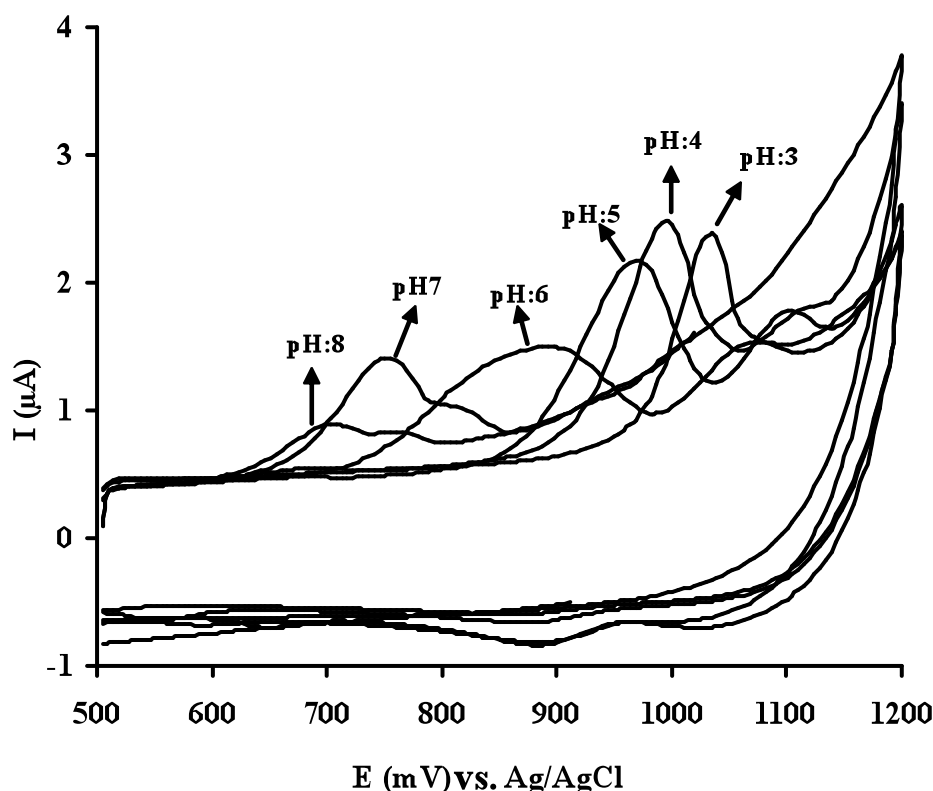
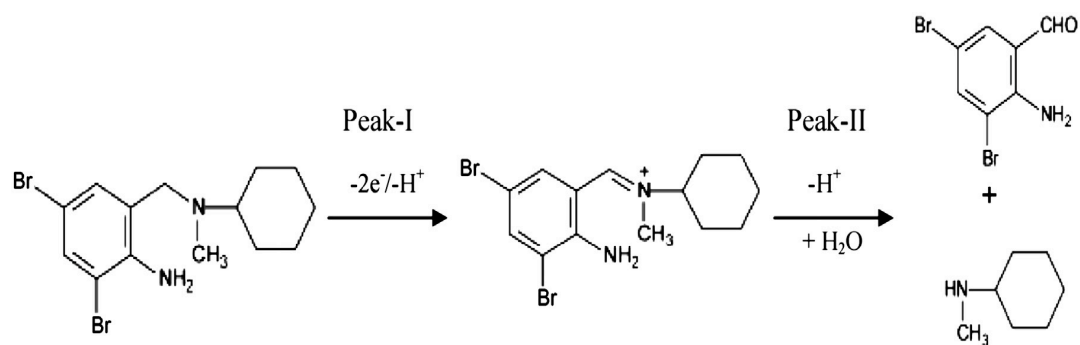


Figure 4.54. Cyclic voltammograms of 8.0×10^{-6} M bromhexine at NiNPs/ MWCNT/Pt in 0.1 M PBS at different pH values. Scan rate: 50 mV/s. Equilibrium time: 5 s



Scheme 4.5. Electrode reaction of bromhexine at NiNPs/MWCNT/Pt

4.4.4. Calibration equation for the determination of bromhexine

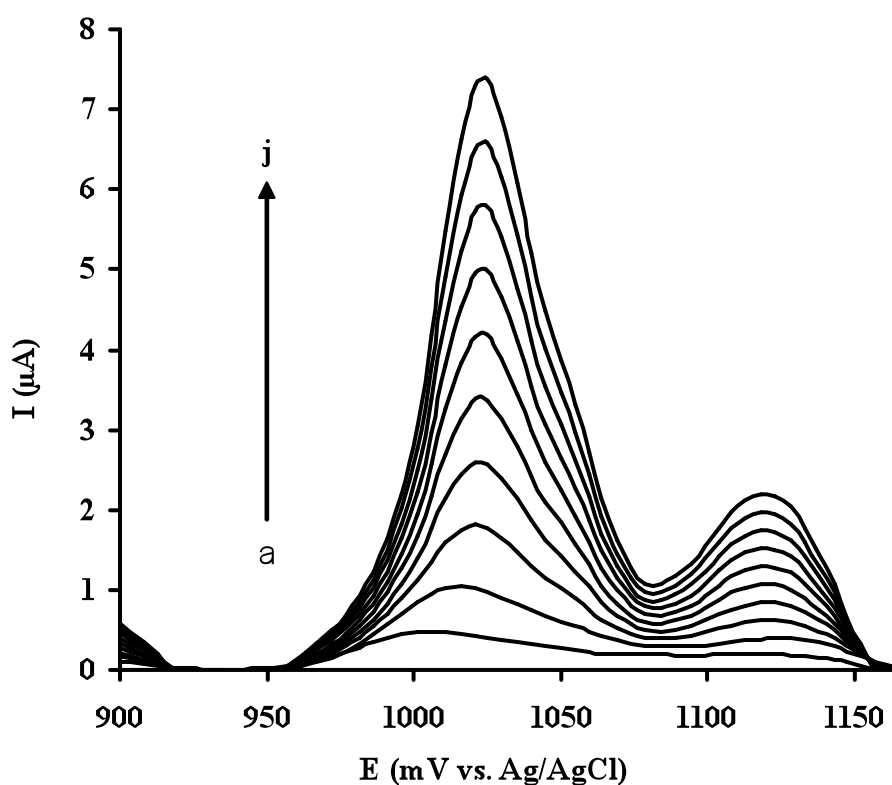


Figure 4.55. Square wave voltammograms of increasing concentrations of bromhexine at NiNPs/MWCNT/Pt in 0.1 M PBS at pH 4.0. Bromhexine concentrations: (a) 5; (b) 30; (c) 55; (d) 80; (e) 105; (f) 130; (g) 155; (h) 180; (i) 205; (j) 230 μ M. Frequency: 20 Hz. Step potential: 100 mV/s. Amplitude: 50 mV/s. Equilibrium time: 5 s

Determination of the concentration of bromhexine at NiNPs/MWCNT/Pt was performed at pH 4.0. Square wave voltammograms of various concentrations of bromhexine at NiNPs/MWCNT/Pt are given in Figure 4.55. The response of peak currents of bromhexine at NiNPs/MWCNT/Pt was linear with the concentration of bromhexine in the range of 5.0×10^{-6} to 2.3×10^{-4} M in Figure 4.56. The linear regression equation was $I_{pa} (\mu A) = 0.0947 + 0.031579 C (\mu M)$ with a correlation coefficient of 0.9999. The detection limit was 3.0×10^{-6} M (S/N=3).

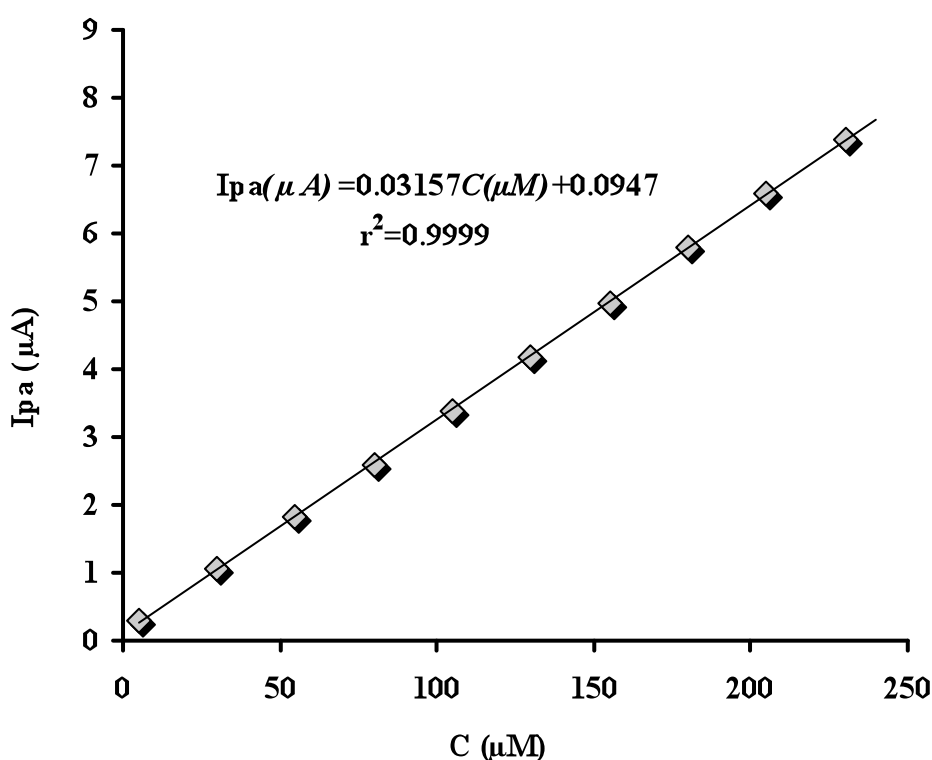


Figure 4.56. Plot of anodic peak currents vs. concentration of bromhexine

4.4.5. Reproducibility and stability of modified electrode

The relative standard deviation (RSD) of 10 successive scans was 1.5% for 30 μM bromhexine. This indicated that the reproducibility of NiNPs/MWCNT/Pt electrode system was excellent. However, the proposed electrode should be well treated to maintain its reproducibility. It was found that 20–25 cycles of scanning in 0.1 M PBS in the potential range 0.0–0.8 V could regenerate clean background CV

curves and the modified electrode was ready for the next experiment or storage in 0.1 M PBS. Also, the current response decreased only by 5% over a week for storage in 0.1 M PBS.

4.4.6. Determination of bromhexine in tablets

Voltammetric determination of bromhexine at NiNPs/MWCNT/Pt in bromhexine tablets was referred to the regression equation. The analysis of 8.0 mg bromhexine tablets using the proposed method is summarized in Table 4.8. A mean recovery of 98.9% with RSD of 1.01% was obtained. The results of the drug analysis obtained from the proposed method are in close agreement with the claimed value. The results obtained are also comparable with the results obtained from differential pulse voltammetry at unmodified glassy carbon macroelectrodes with a recovery of 94.5% (Turchan et al., 2007) and capillary isotachopheresis with a recovery of 101.2% (Pospisilova et al., 2001). However, the experimental results indicate that the proposed procedure is more precise and accurate for the determination of bromhexine in drug samples.

Table 4.8. Results of the determination of bromhexine in tablets

Content (mg)	Found (mg)	Recovery%	R.S.D%
8.0	7.91±0.08	98.9	1.01

Mean±Standard deviation (n =5)

4.5. Cobalt Nanoparticles Functionalized Multi-Walled Carbon Nanotubes at GCE for the Simultaneous Determination of Paracetamol and Dopamine

In this study, a voltammetric nanosensor has been prepared by one-pot synthesis of multi-walled carbon nanotube-supported cobalt nanoparticles in an ultrasonic bath for the simultaneous determination of PAR and DA. The surface modification with MWCNT and nanoparticles of cobalt served to improve peak separation from interfering compounds such as AA and UA, reduce the potential required to oxidize species and improve the detection limit.

Voltammetric nanosensors based on CNTs represent a new and interesting alternative for the quantification of different analytes (Jain and Sharma, 2012; Geto et al., 2013; Gupta et al., 2013; Li et al., 2012). The performance of CNT modified electrodes has been found to be much superior to those of other carbon electrodes in terms of response time, increased sensitivity, resistance to surface fouling, decreased overpotentials, reuseability and limits of detection (Wang, 2005). Also, nanoparticles of metals can display four advantages over macroelectrodes when used for electroanalysis: enhancement of mass transport, catalysis, high effective surface area and control over electrode microenvironment (Knochen et al., 2003; Silva et al., 2006a; Silva et al., 2006b; Kachoosangi et al., 2008 and Ghorbani-Bidkorbeh et al., 2010)

Paracetamol, also known as acetaminophen is an effective pain killer used for the widespread relief of pains associated with many parts of the body (Carvalho et al., 2004). The overdose of PAR can lead to the accumulation of toxic metabolites which may cause hepatotoxicity and nephrotoxicity (Martin and MacLean, 1998). Therefore controlling the amount of PAR in pharmaceuticals is of great importance for the general public health.

A number of analytical procedures have been reported for the analysis of PAR in pharmaceutical forms or biological fluids including chromatography (Ravinsankar et al., 1998), spectrophotometry (Hanaee, 1997), chemiluminescence (Easwaramoorthy et al., 2001), capillary electrophoresis (Zhao et al., 2006), FTIR and Raman spectrometry (Zhoubi et al., 2002), and flow injection analysis using various methods of detection (Knochen et al., 2003; Silva et al., 2006). However, these techniques are expensive and require time-consuming derivatization step and also in some cases low sensitivity and selectivity makes them unsuitable for a routine analysis.

On the other hand, voltammetric methods have several advantageous owing to their simplicity, high sensitivity and rapidness (Walcarius, 2008 and Li et al., 2012). The development and application of electrochemical sensors for the determination of

PAR has received considerable interest in last few decades since PAR is an electroactive compound which can be oxidized electrochemically. Most electrochemical methods rely on the modification of electrodes such as MWCNT modified pyrolytic graphite electrode (Kachoosangi et al., 2008), carbon nanoparticles modified GCE (Ghorbani-Bidkorbeh et al., 2010), SWCNT-graphene modified GCE (Chen et al., 2012), carbon nanotube modified screen printed electrode (Fanjul-Bolado, 2009), SWCNT modified ceramic electrode (Habibi et al., 2011), and D50wx2-GNP-modified carbon paste electrode (Sanghavi and Srivastava et al., 2011).

On the other hand, dopamine (DA) is one of the most typical catecholamine neurotransmitters, which mainly exists in mammalian brain tissues and fluids, and plays a very important role in the central nervous system (CNS). When present in low concentrations it is likely to give rise to neurodegenerative diseases such as Parkinson and Alzheimer among others (Avendo et al., 2007).

A number of electrodes have been utilized for the detection of DA such as poly(3-(5-chloro-2-hydroxyphenylazo)-4,5-dihydroxynaphthalene-2,7-disulfonic acid) (Ensafi et al., 2009), carbon paste electrode modified with carbon nanotubes and molybdenum (VI) complex (Beitollahi and Sheikshoae, 2012), poly(ethylene dioxythiophene) film modified electrode (Atta et al., 2011), poly(calmagite) modified electrode (Chandra et al., 2010), CNTs dispersed in polyethylenimine on GC (Rubianes and Rivas, 2007), Co phthalocyanine modified MWCNTs on GC (Moraes et al., 2008), graphite-polyurethane composite (Toledo et al., 2005), Pd/poly(3,4 ethylenedioxythiophene) (Harish et al., 2008), SiO₂-coated graphene oxide and molecularly imprinted polymers modified electrode (Zeng et al., 2013).

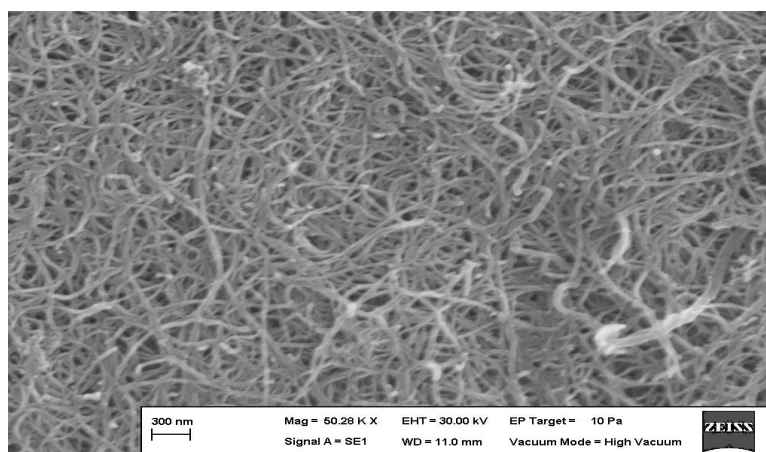
However, it has been reported that low concentration PAR significantly prevented DA neurodegeneration while high concentration of PAR did not protect DA neurons 6-hydroxydopamine-induced degeneration (Locke et al., 2008). Therefore, the simultaneous detection of PAR and DA is of great importance for both scientific and therapeutic reasons. A number of electrodes have been applied

for the simultaneous determination of PAR and DA including, multiwalled carbon nanotubes modified electrode (Allothman et al., 2010), SWCNT modified carbon - ceramic electrode (Habibi et al., 2011), polypyrrole-azsophloxine modified gold electrode (Gholivand and Amiri, 2012) molybdenum (VI) complex/carbon nanotubes modified carbon paste electrode (Beitollahi and Sheikhshoaie, 2012).

4.5.1. Surface characterization of the modified electrode

The surface morphology of the CoNPs/MWCNT/GCE was characterized by SEM. As shown in Figure 4.57A., a MWCNT layer without aggregation was observed on the electrode surface, indicating that the MWCNTs were homogeneously dispersed on the surface of the GCE. As can be seen in Figure 4.57B., the CoNPs deposited on the MWCNTs were spherical and well distributed.

A)



B)

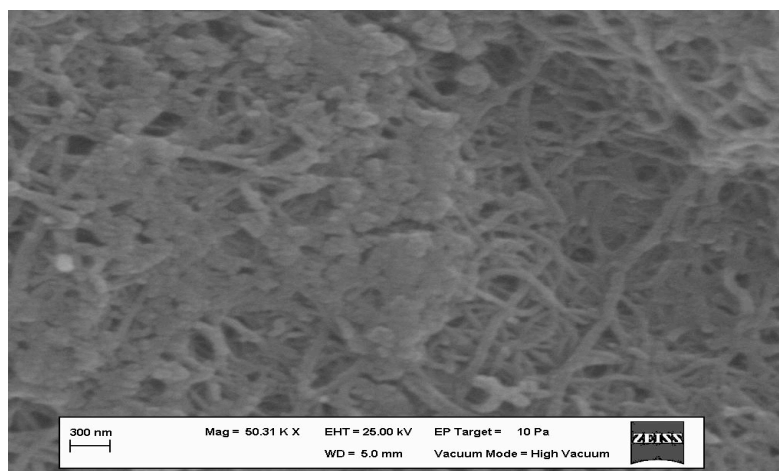


Figure 4.57. SEM images of MWCNT/GCE (A) and CoNPs/MWCNT/GCE (B)

The EDX results exhibited in Figure 4.58. show that Co, C, Pd and Au were the major elements on the electrode surface. The Au and Pd were obtained from the gold-palladium coatings of the CoNPs/MWCNT/GC during SEM analysis. The EDX results clearly show that Co is electrodeposited on the surface of MWCNT layer.

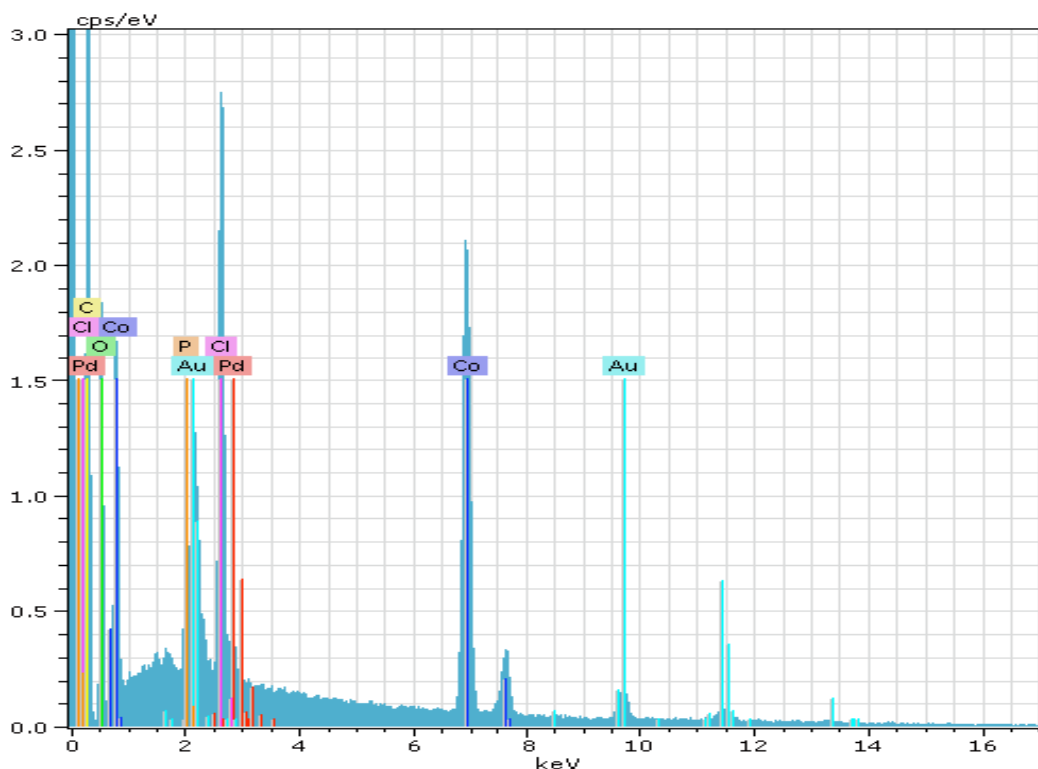


Figure 4.58. EDX analysis of CoNPs/MWCNT/GCE

4.5.2. Voltammetric behaviour of paracetamol and dopamine

Cyclic voltammograms of the mixture of 0.5 μM DA and 50 nM PAR in 0.10 M PBS at pH 7.0 at bare GCE (a), MWCNT/GCE (b) and CoNPs/MWCNTs/GCE (c) are given in Figure 4.59. At bare GCE, a broad anodic wave was observed at $E_p = 600$ mV for the oxidation of the mixture of DA and PAR and a poor cathodic wave was appeared at 450 mV for the reduction of the mixture of the two species. Two anodic peaks were appeared for DA and PAR at MWCNTs/GCE indicating that modification of electrodes with carbon nanotubes can resolve the voltammetric signals of DA and PAR (Figure 4.59b.). However, voltammetry of DA and PAR was

greatly improved at a glassy carbon electrode modified with both multiwalled carbon nanotubes (MWCNTs) and cobalt nanoparticles (CoNPs). DA and PAR exhibits two well defined anodic peaks at 207 mV and 410 mV with a peak to peak separation of 203 mV (Figure 4.59c.). The separation of anodic peaks at CoNPs/MWCNTs/GCE was large enough for simultaneous determination of DA and PAR in a mixture.

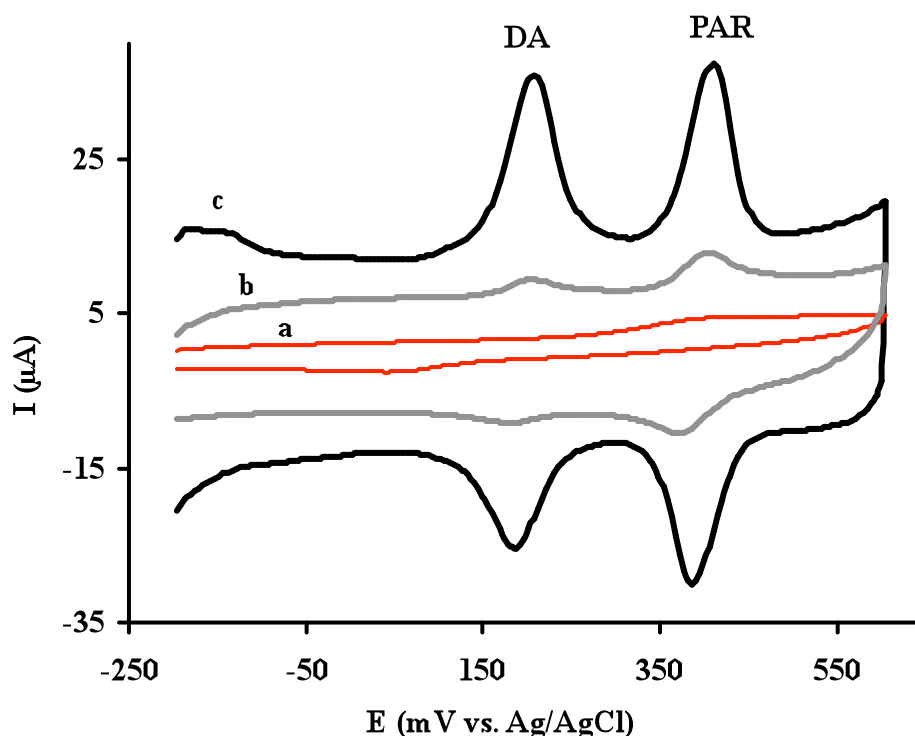


Figure 4.59. Cyclic voltammograms of a mixture of 5.0×10^{-7} M DA and 5.0×10^{-8} M PAR at bare GCE (a); MWCNT/GCE (b) and CoNPs/MWCNT/GCE (c) in 0.1 M PBS at pH 7.0. Scan rate: 50 mV/s. Equilibrium time: 5 s

It is clearly shown that the CoNPs/MWCNTs/GCE exhibits an efficient electrocatalytic effect towards the oxidation of DA and PAR with sharp peaks and enhancement in current responses and also good selectivity with large peak separations between DA and PAR. Also, two well defined peaks at $E_{pc} = 178$ mV, $E_{pc} = 381$ mV are observed in the cathodic branch for the reduction of DA and PAR at CoNPs/MWCNTs/GCE. The ΔE_p is 29 mV for the electrochemical process of both DA and PAR indicating a reversible two-electron transfer process for both species. This indicated that the electrochemical responses of DA and PAR have

greatly been increased at CoNPs/MWCNTs/GCE. Intensive increases in peak currents of both DA and PAR are observed owing to the improvement in the electron transfer process and the larger real area of the layer at the surface.

In order to understand the mechanisms responsible for the oxidation of both DA and PAR at CoNPs/MWCNTs/GCE, cyclic voltammograms of PAR and DA were recorded at various scan rates. Figure 4.60. shows the effect of the scan rate on the electrochemical responses of PAR at CoNPs/MWCNTs/GCE using cyclic voltammetry in 0.1 M PBS at pH 7.0. The anodic peak currents (I_p) were proportional to the scan rates (v) over the range of 25-175 mV/s for PAR (Figure 4.61.).

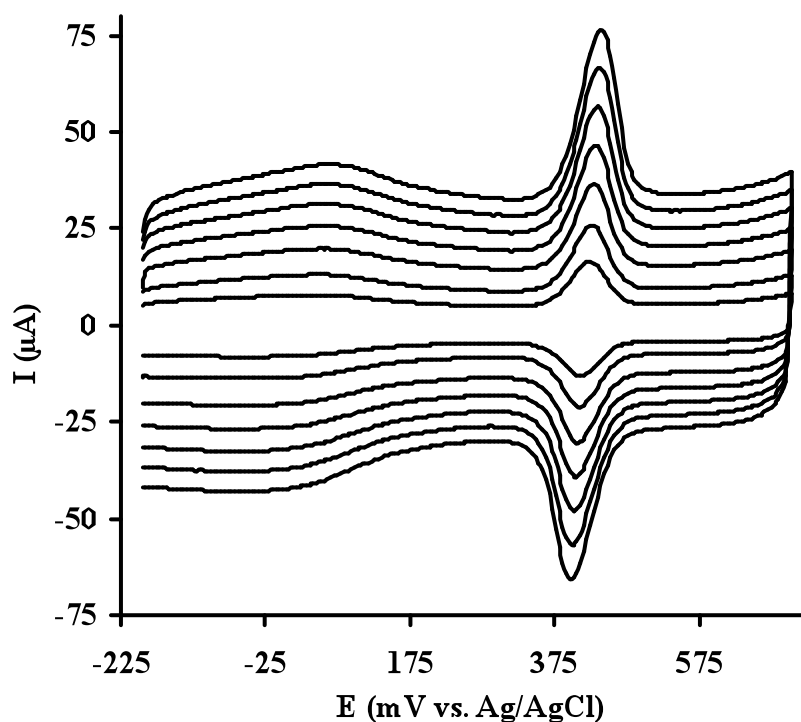


Figure 4.60. Cyclic voltammograms of 2.5×10^{-8} M PAR at CoNPs/MWCNT/GCE in 0.1 M PBS at pH 7.0. Scan rate increasing from 25 mV/s to 175 mV/s (Each increment 25 mV/s). Equilibrium time: 5 s

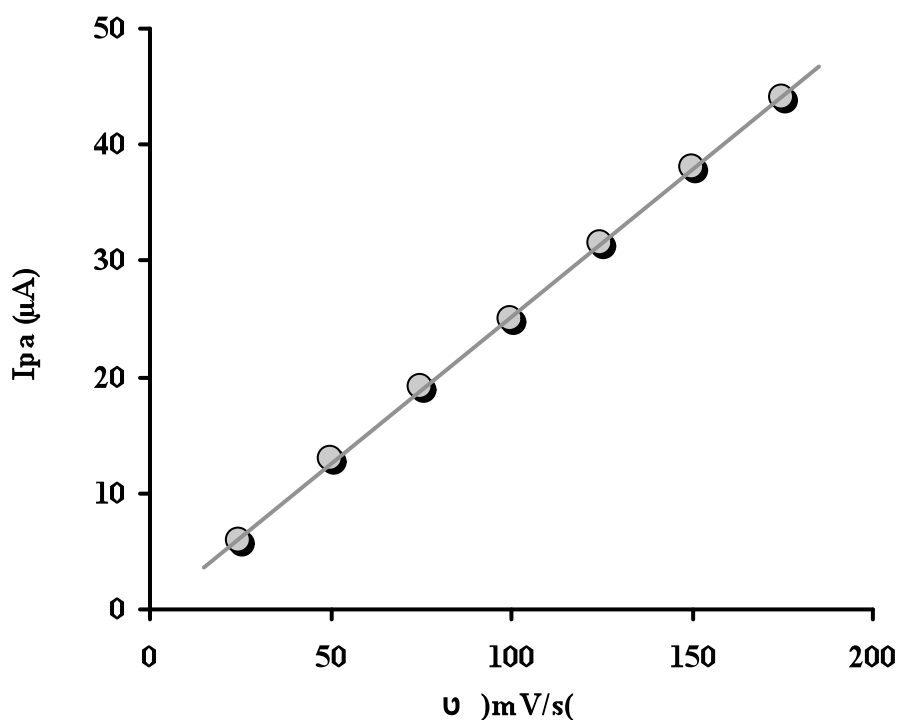


Figure 4.61. Plot of anodic peak currents of PAR versus scan rate

The electrochemical response of DA at CoNPs/MWCNTs/GCE using cyclic voltammetry at various scan rates is given in Figure 4.62. The experimental results showed that the anodic peak currents (I_p) were directly proportional to the scan rates (v) over the range of 25-175 mV/s for DA (Figure 4.63.). The results indicated that the electrode processes of both PAR and DA are controlled by adsorption.

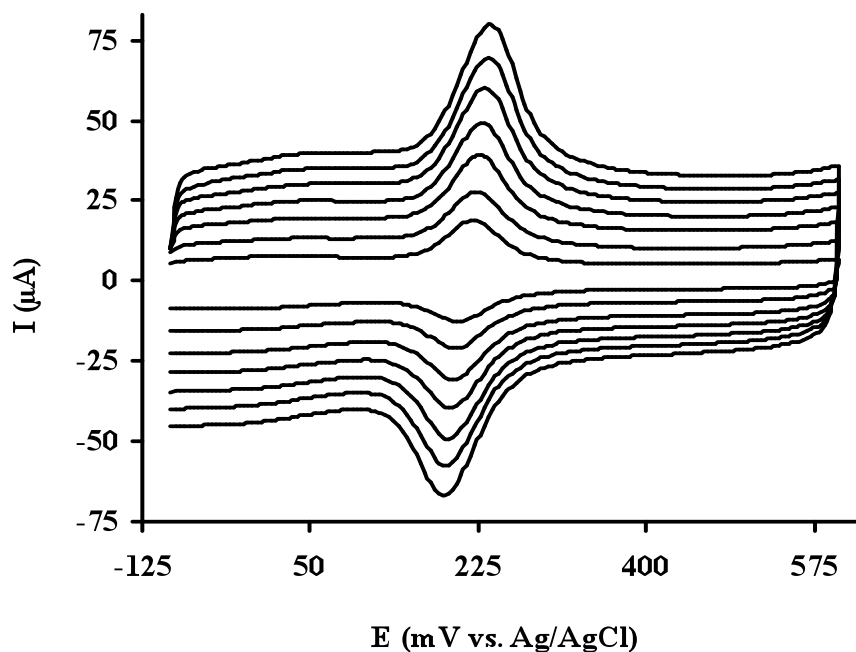


Figure 4.62. Cyclic voltammograms of 1.5×10^{-7} M DA at CoNPs/MWCNT/GCE in 0.1 M PBS at pH 7.0. Scan rate increasing from 25 mV/s to 175 mV/s (Each increment 25 mV/s). Equilibrium time: 5 s

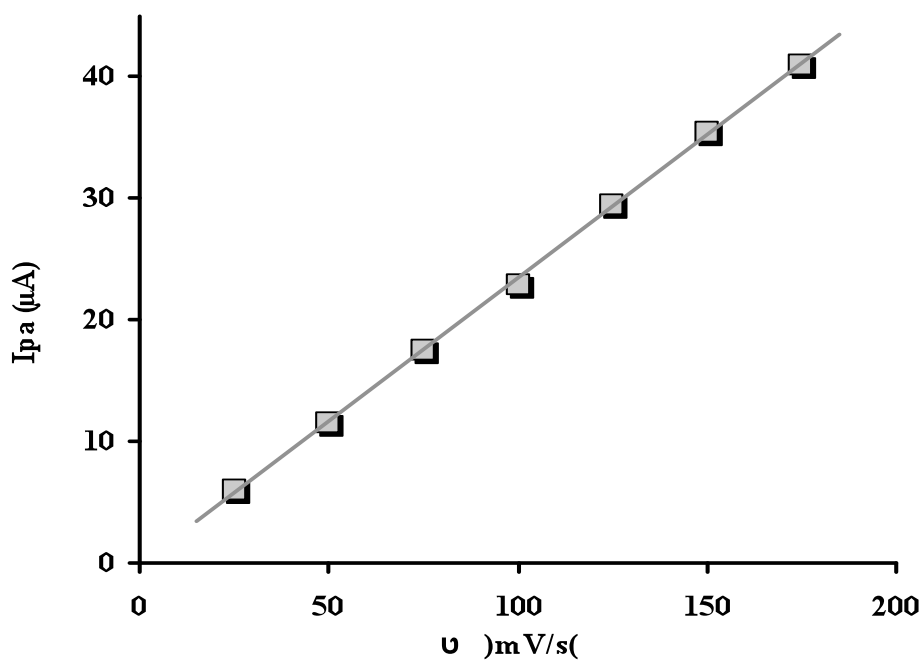


Figure 4.63. Plot of anodic peak currents of DA versus scan rate

In addition, the effect of the pH value of the PBS buffer solution on peak potential of PAR and DA at CoNPs/MWCNTs/GCE was also investigated. The effect of pH on the peak potential of PAR and DA using cyclic voltammetry at CoNPs/MWCNTs/GCE in 0.1 M PBS at different pH values is given in Figure 4.64. and Figure 4.65., respectively. The results show that the oxidation peak potential of PAR shifts towards the negative potentials with increasing pH. This indicates that the electrochemical process of PAR includes transfer of protons. The slope of oxidation peak potential (E_p) vs. pH is 58.17 mV/pH (Figure 4.66.). This indicated that the identical numbers of electrons and protons are involved in the oxidation process of PAR at CoNPs/MWCNTs/GCE. Thus, the number of hydrogen ions involved in the whole electrode reaction of PAR at CoNPs/MWCNTs/GCE is 2. The electrode mechanism of PAR at CoNPs/MWCNTs/GCE is shown in Scheme 4.6.

The oxidation peak potential of DA also shifts towards the negative potentials with increasing pH. The slope was calculated to be 58.03 mV/pH indicating that the number of electrons and protons are also identical (Fig. 10). This indicates that the electrochemical process of DA also includes transfer of protons. The electrode mechanism for DA is given in Scheme 4.7.

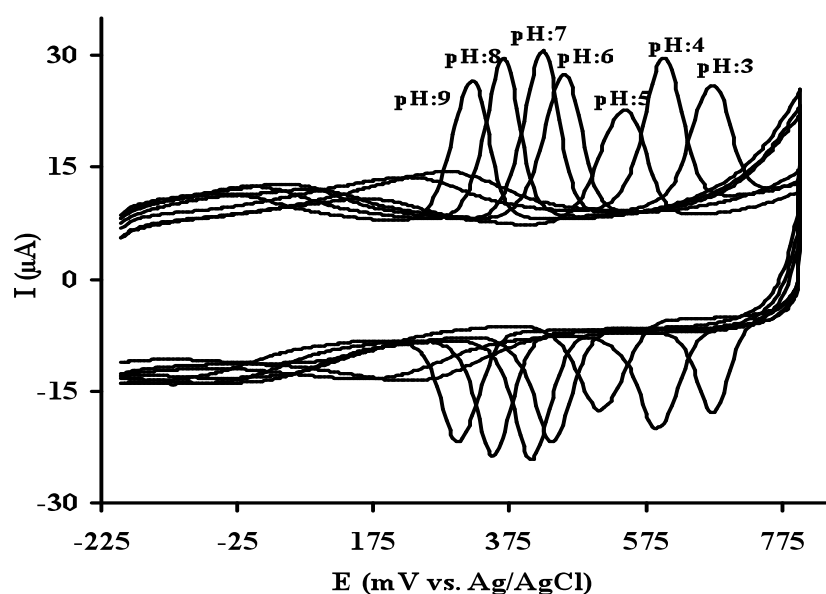
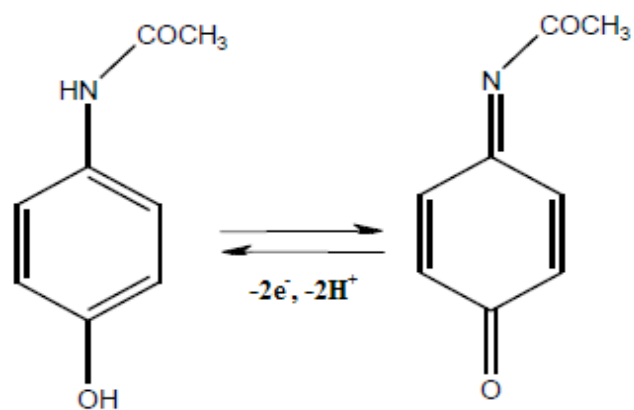


Figure 4.64. Cyclic voltammograms of 2.5×10^{-8} M PAR at CoNPs/MWCNT/GCE in 0.1 M PBS at different pH values. Scan rate: 50 mV/s. Equilibrium time: 5 s



Scheme 4.6. Proposed PAR reaction at CoNPs/MWCNT/GCE

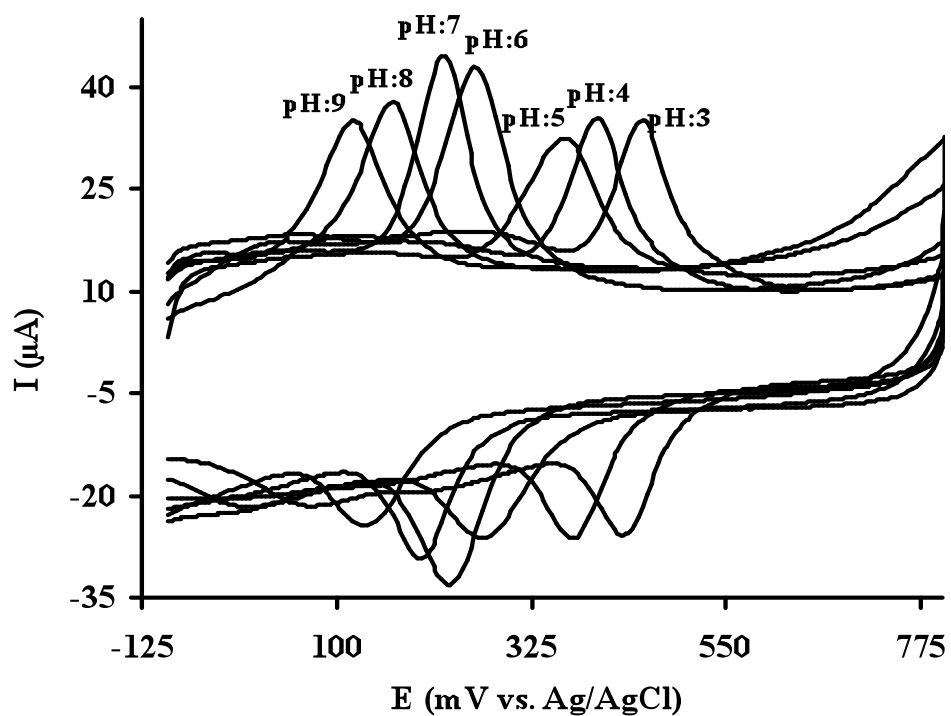
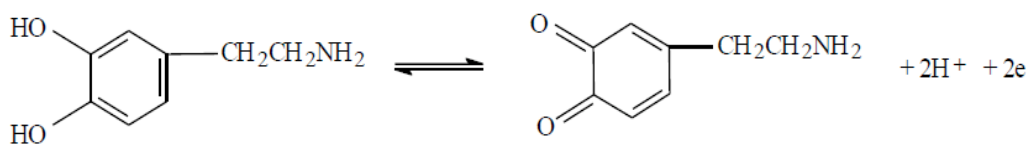


Figure 4.65. Cyclic voltammograms of 7.5×10^{-7} M DA at CoNPs/MWCNT/GCE in 0.1 M PBS at different pH values. Scan rate: 50 mV/s. Equilibrium time: 5 s



Scheme 4.7. Proposed DA reaction at CoNPs/MWCNT/GCE

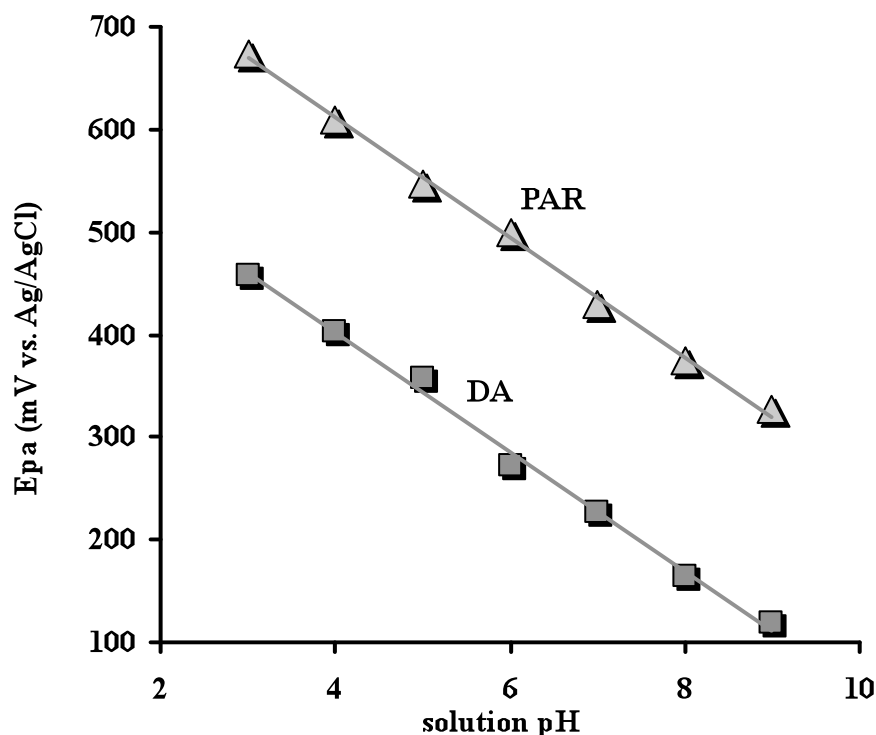


Figure 4.66. Plots of anodic peak potentials of PAR and DA versus solution pH

4.5.3. Determinations of PAR and DA

Square wave voltammetric determination of the concentration of PAR at CoNPs/MWCNTs/GCE was performed in the presence of DA in 0.1 M PBS at pH 7.0. Figure 4.67. shows the voltammograms of increasing concentrations of PAR where the concentration of DA was kept constant. In the presence of DA, the peak currents of PAR increased linearly with its concentration (Figure 4.68.). This indicates that the electrochemical response of DA do not interfere with the electrochemical response of PAR. Therefore, the CoNPs/MWCNTs/GCE could be used for the determination of PAR in the presence of the DA. In other words, the

CoNPs/MWCNTs/GCE could be utilized for the selective determination of PAR in samples.

The response of peak currents of PAR at CoNPs/MWCNTs/GCE was linear with the concentration of PAR in the range of $5.2 \times 10^{-9} \sim 4.5 \times 10^{-7}$ M. The linear regression equation was $I_{pa} (\mu A) = 26.98958C (\mu M) - 0.00551$ with a correlation coefficient of 0.9987. The detection limit was 1.0×10^{-9} M (S/N=3). Also, the analytical parameters obtained by the proposed method are well compared with several methods for the determination of PAR as shown in Table 4.9.

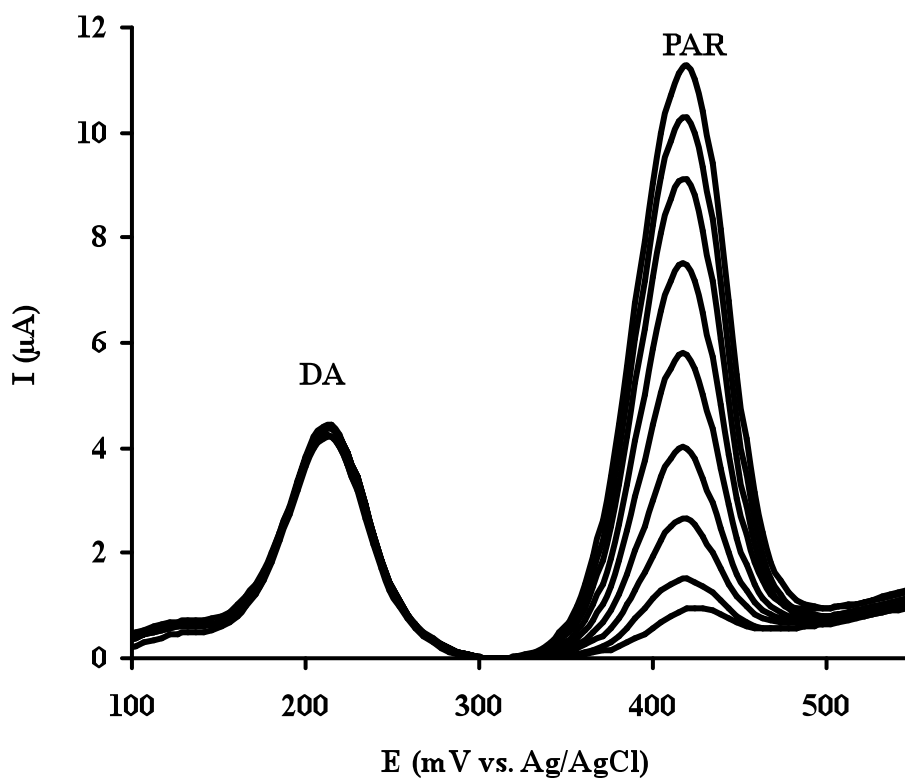


Figure 4.67. Square wave voltammograms of increasing concentrations of PAR in the presence of 1.3×10^{-6} M DA at CoNPs/MWCNT/GCE in 0.1 M PBS at pH 7.0. PAR concentrations; 5.0×10^{-8} M; 1.0×10^{-7} M; 1.5×10^{-7} M; 2.0×10^{-7} M; 2.5×10^{-7} M; 3.0×10^{-7} M; 3.5×10^{-7} M; 4.0×10^{-7} M; 4.5×10^{-7} M. Frequency: 22 Hz. Step potential: 100 mV/s. Amplitude: 50 mV/s. Equilibrium time: 5 s

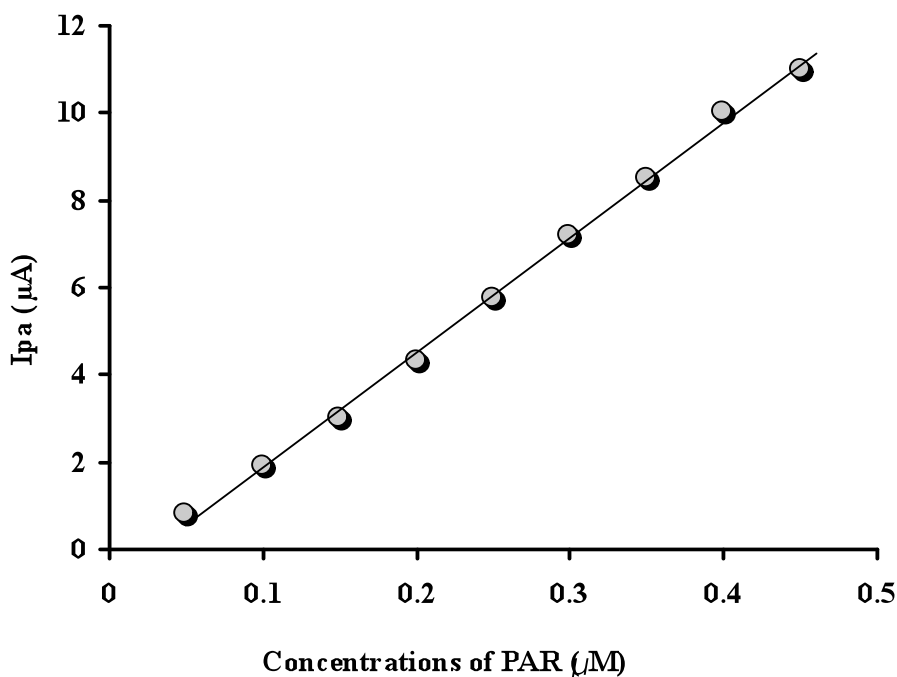


Figure 4.68. Plot of peak currents of PAR versus concentration

Figure 4.69. shows that voltammograms of increasing concentrations of DA where the concentration of PAR was kept constant. In the presence of PAR, the peak currents of DA increased linearly with its concentration (Figure 4.70.). This shows that the electrochemical response of DA also do not interfere with the electrochemical response of PAR. The response of peak currents of DA at CoNPs/MWCNTs/GCE was linear with the concentration of DA in the range of $5.0 \times 10^{-8} \sim 3.0 \times 10^{-6}$ M. The linear regression equation was $I_{pa} (\mu\text{A}) = 3.24118C (\mu\text{M}) + 0.001593$ with a correlation coefficient of 0.9999. The detection limit was 1.5×10^{-8} M (S/N=3). Table 4.10. shows the analytical parameters of some modified electrodes for the determination of DA.

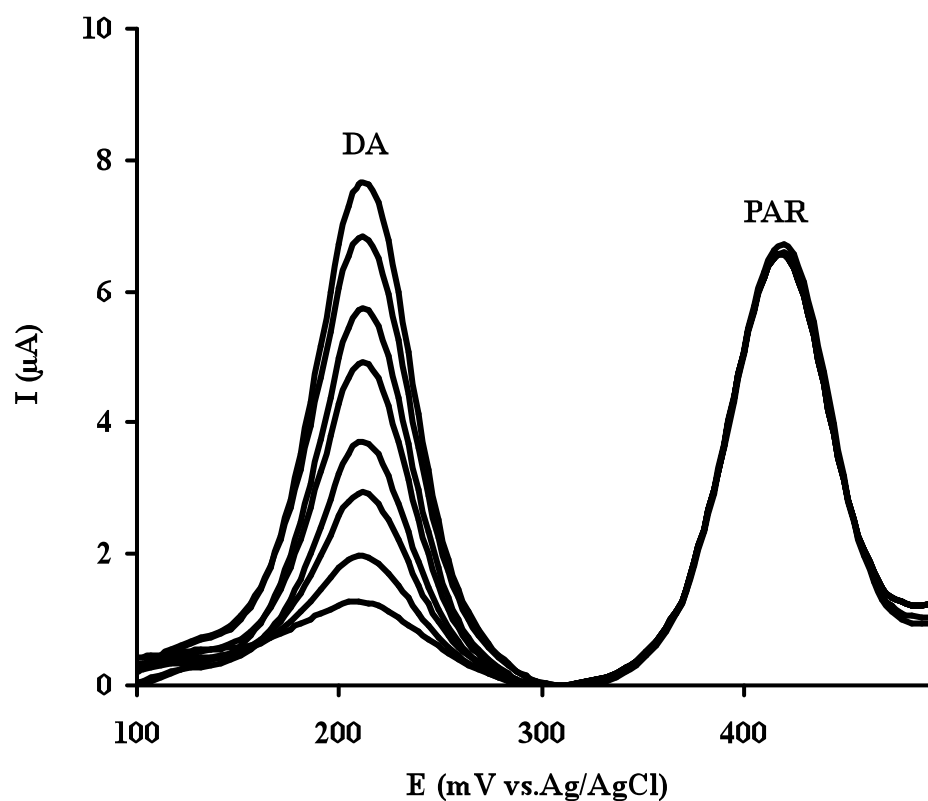


Figure 4.69. Square wave voltammograms of increasing concentrations of DA in the presence of 2.8×10^{-7} M PAR at CoNPs/MWCNT/GCE in 0.1 M PBS at pH 7.0. DA concentrations; 2.8×10^{-7} M; 5.6×10^{-7} M; 8.4×10^{-7} M; 1.12×10^{-6} M; 1.4×10^{-6} M; 1.7×10^{-6} M; 2.0×10^{-6} M; 2.3×10^{-6} M. Frequency: 22 Hz. Step potential: 100 mV/s. Amplitude: 50 mV/s. Equilibrium time: 5 s

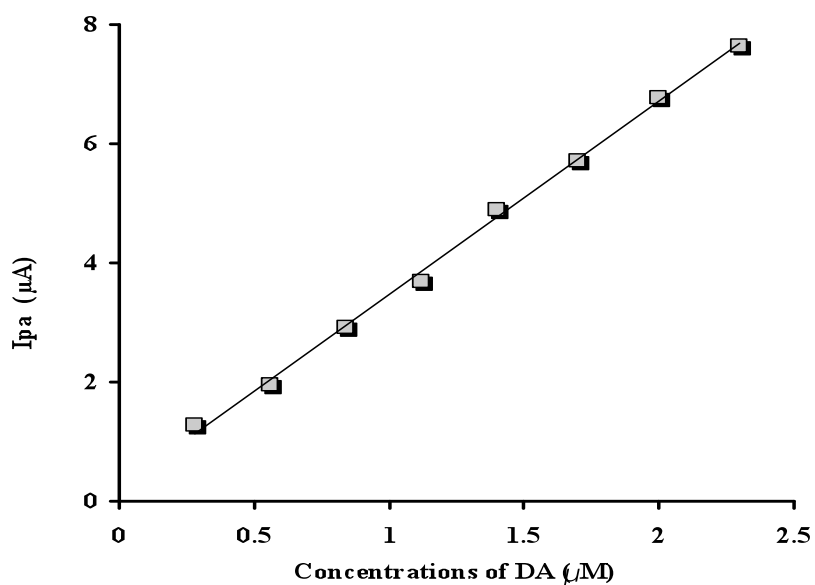


Figure 4.70. Plot of peak currents of DA versus concentration

Figure 4.71. shows the square wave voltammograms of simultaneously increasing concentrations DA and PAR in 0.1 M PBS at pH 7.0. The electrochemical responses of both DA and PAR have increased with their concentrations. The results indicate that the proposed electrode enables the simultaneous determination of DA and PAR owing to the large peak to peak separation.

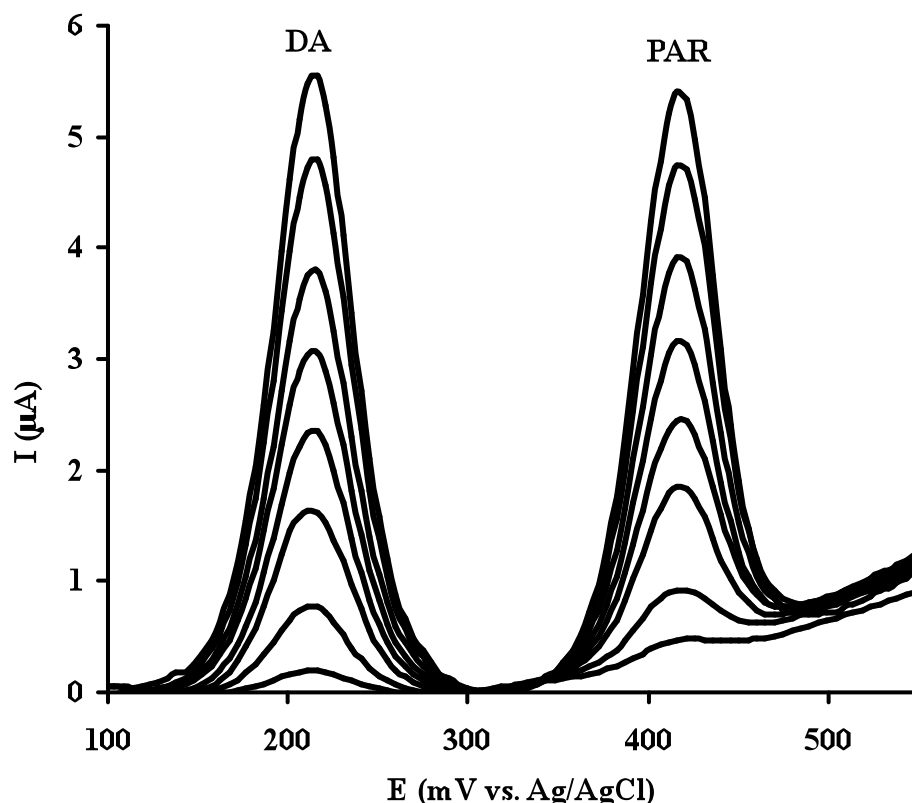


Figure 4.71. Square wave voltammograms of simultaneously increasing concentrations DA and PAR at CoNPs/MWCNT/GCE in 0.1 M PBS at pH 7.0. DA concentrations: 5.0×10^{-8} M; 2.4×10^{-7} M; 5.1×10^{-7} M; 7.3×10^{-7} M; 9.4×10^{-7} M; 1.2×10^{-6} M; 1.5×10^{-6} M; 1.7×10^{-6} M. PAR concentrations: 5.2×10^{-9} M; 2.7×10^{-8} M; 6.0×10^{-8} M; 9.0×10^{-8} M; 1.2×10^{-7} M; 1.4×10^{-7} M; 1.8×10^{-7} M; 2.0×10^{-7} M. Frequency: 22 Hz. Step potential: 100 mV/s. Amplitude: 50 mV/s. Equilibrium time: 5 s

The response of peak currents of PAR at CoNPs/MWCNTs/GCE was linear with the concentration of PAR in the range of $5.2 \times 10^{-9} \sim 4.5 \times 10^{-7}$ M (Figure 4.72A.). The linear regression equation was $I_{pa} (\mu A) = 26.98958C (\mu M) - 0.00551$ with a correlation coefficient of 0.9987. The detection limit was 1.0×10^{-9} M (S/N=3). Also, the analytical parameters obtained by the proposed method are well compared with several methods for the determination of PAR as shown in Table 4.9.

The response of peak currents of DA at CoNPs/MWCNTs/GCE was linear with the concentration of DA in the range of $5.0 \times 10^{-8} \sim 3.0 \times 10^{-6}$ M (Figure 4.72B.). The linear regression equation was $I_{pa} (\mu A) = 3.24118C (\mu M) + 0.001593$ with a correlation coefficient of 0.9999. The detection limit was 1.5×10^{-8} M (S/N=3). Table 4.10. shows the analytical parameters of some modified electrodes for the determination of DA.

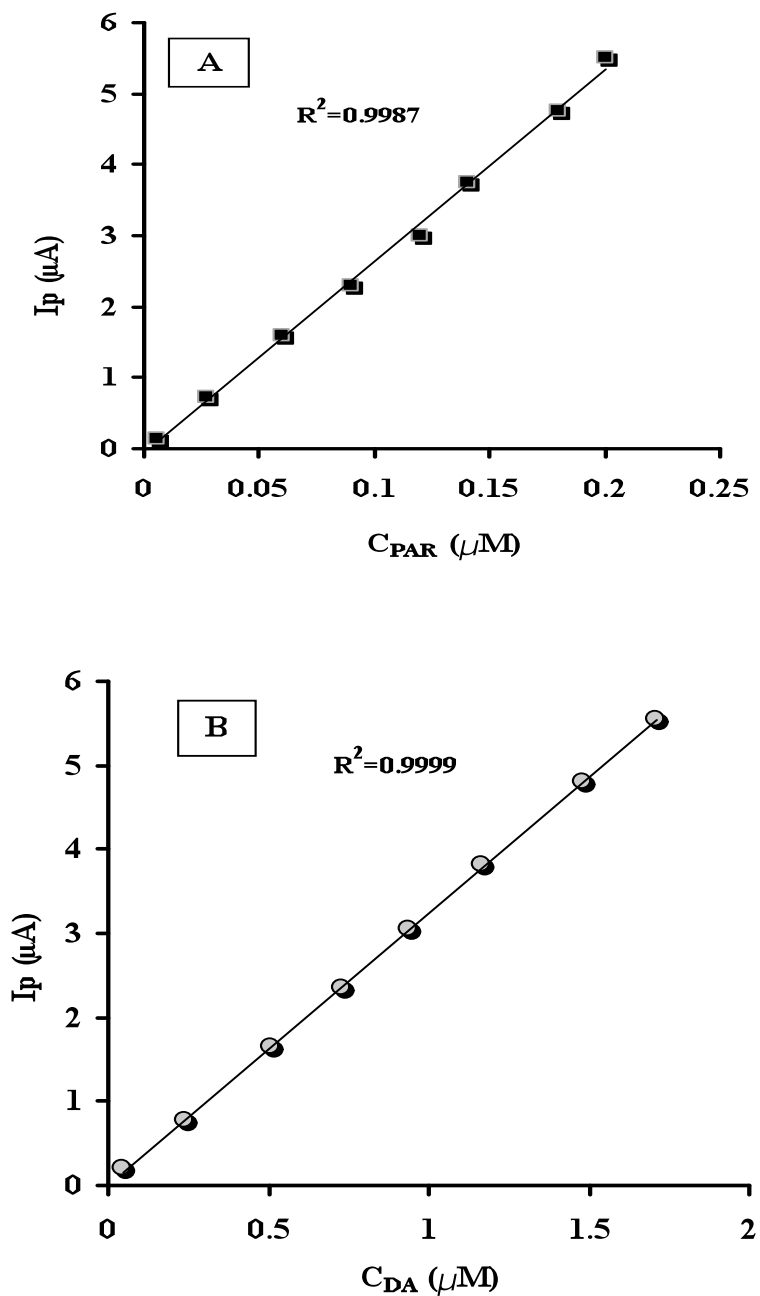


Figure 4.72. A) Plot of peak currents of PAR and B) Plot of peak currents of DA versus simultaneous increasing concentrations of PAR and DA, respectively

Table 4.9. The application results of various electrodes for the determination of PAR

Electrode	pH used	Linear range (μM)	Detection limit (nM)	Reference
C ₆₀ /GCE	7.2	50-1500	50000	(Goyal and Singh, 2006)
N-DHPB-MWCNT/CPE	7.0	15-270	10000	(Ensafi et al., 2011)
PANI-MWCNT/GCE	5.5	1-100	2500	(Li and Jing, 2007)
PAY/nano-TiO ₂ /GCE	7.0	12-120	2000	(Kumar et al., 2008)
PEDOT/SPE	5.0	4-400	1390	(Su and Cheng, 2010)
ZrO ₂ /CPE	7.0	1- 2500	912	(Mazloum-Ardakani et al., 2010)
C-Ni/GCE	3.0	2-230	600	(Wang et al., 2007)
f-MWCNT/GCE	8.0	3-300	600	(Alothman et al., 2010)
PR/MCPE	5.0	0.7-100	530	(Thomas et al., 2013)
IL/CNTPE	7.0	1-600	500	(Tavana et al., 2012)
PSS-PDDA/GE	7.0	25-400	500	(Manjunatha et al., 2011)
Poly(taurin)-MWCNT/GCE	7.3	1-100	500	(Wan et al., 2009)
CoOx/CCE	13	5-35	370	(Razmi and Habibi, 2010)
Carbon ionic liquid electrode	4.6	1-2000	300	(Shang-Guan et al., 2008)
Nafion/TiO ₂ -graphene	7.0	1-100	210	(Fan et al., 2011)
Chitosan-MWCNT/GCE	7.0	1-145	100	(Babaei et al., 2010)
Ppyox/AZ/Au	2.8	0.2-100	80	(Gholivand and Amiri, 2012)
MWCNT-ACS/GCE	9.0	0.05-2	50	(Lu and Tsai, 2011)
MWCNT/CPE	4.0	0.1 – 100	50	(Shahrokhian and Asadian, 2010)
Carbon NP/GCE	7.0	0.1-100	50	(Ghorbani-Bidkorbeh et al., 2010)
Graphite oxide/GCE	2.0	0.165-26.5	40	(Song et al., 2011)
SWCNT-DPF/GCE	6.5	0.1-20	40	(Sun and Zhang, 2007)
SWCNT-Graphene/GCE	7.0	0.05-64.5	38	(Chen et al., 2012)
Graphene/GCE	9.3	0.1-20	32	(Kang et al., 2010)
ISSM-CNT/PE	7.0	0.112– 69.4	25.8	(Sanghavi et al., 2010)
MWCNT/BPPGE	7.5	0.01-20	10	(Kachoosangi et al., 2008)
Poly(CCA)/GCE	6.0	0.1-10	10	(Liu et al., 2012)
D50wx2-GNP/GCPE	6.0	0.0334-45.5	4.71	(Sanghavi and Srivastava, 2011)
CoNPs/MWCNT/GCE	7.0	0.0052- 0.45	1	This work

Table 4.10. Analytical parameters of some modified electrodes for the determination of DA

Electrode	pH used	Linear range (μM)	Detection limit (nM)	Reference
HCNTs/GCE	4.5	2.5- 105	800	(Cui et al., 2012)
SDS/CPE	7.0	10-196	771	(Colín-Orozco et al., 2012)
CTAB/GNSPE	6.5	4-52	600	(Liu et al., 2012)
IMWCNT-CPE	7.0	1.9-771.9	520	(Nasirizadeh et al., 2013)
Poly(caffeic acid)/GCE	6.6	1-40	470	(Li et al., 2008)
C-Ni/GCE	13	0.1-18	290	(Yang et al., 2013)
Poly(CCDA) /GCE	4.0	5-280	290	(Ensafi et al., 2009)
SGN/NiPc	5.0	40-1080	260	(Barros et al., 2013)
Au/MWNTs/Nafion/GCE	6.0	006-8	40	(Yang et al., 2013)
PGE	7.0	0.3-150	33	(Alipour et al., 2013)
SWCNT/GCE	7.0	5-100	20	(Li et al., 2012)
Si-ZrPH/CPE	5.5	0.04-400	20	(Shams et al., 2009)
poly(Tyr)/MWCNT/GCE	7.4	0.1-30	20	(Wang et al., 2013)
CoNPs/MWCNT/GCE	7.0	0.05-30	15	This work

Overall facility of the proposed electrode for the simultaneous determination of DA and PAR was demonstrated in the presence of common coexisting species AA and UA. Figure 4.73. shows the voltammograms obtained for DA and PAR coexisting at various concentrations where the concentrations of AA and UA were kept constant. In the presence of constant concentrations of AA and UA, the voltammetric responses of both DA and PAR increased linearly with their concentrations as shown as inset in Figure 4.73. The results indicated that no evidence of interference of AA and UA was observed for the simultaneous determination of DA and PAR. It was remarkable that the excess amount of AA and UA did not interfere with the concentration of DA and PAR.

The proposed electrode was also applied to a mixture of simultaneously increasing concentrations of AA, DA, UA and PAR (Figure 4.74.). It clearly shows no interference from AA and UA on the determinations of DA and PAR as the peak currents of both DA and PAR are proportional to their concentrations as shown as inset in Figure 4.74.

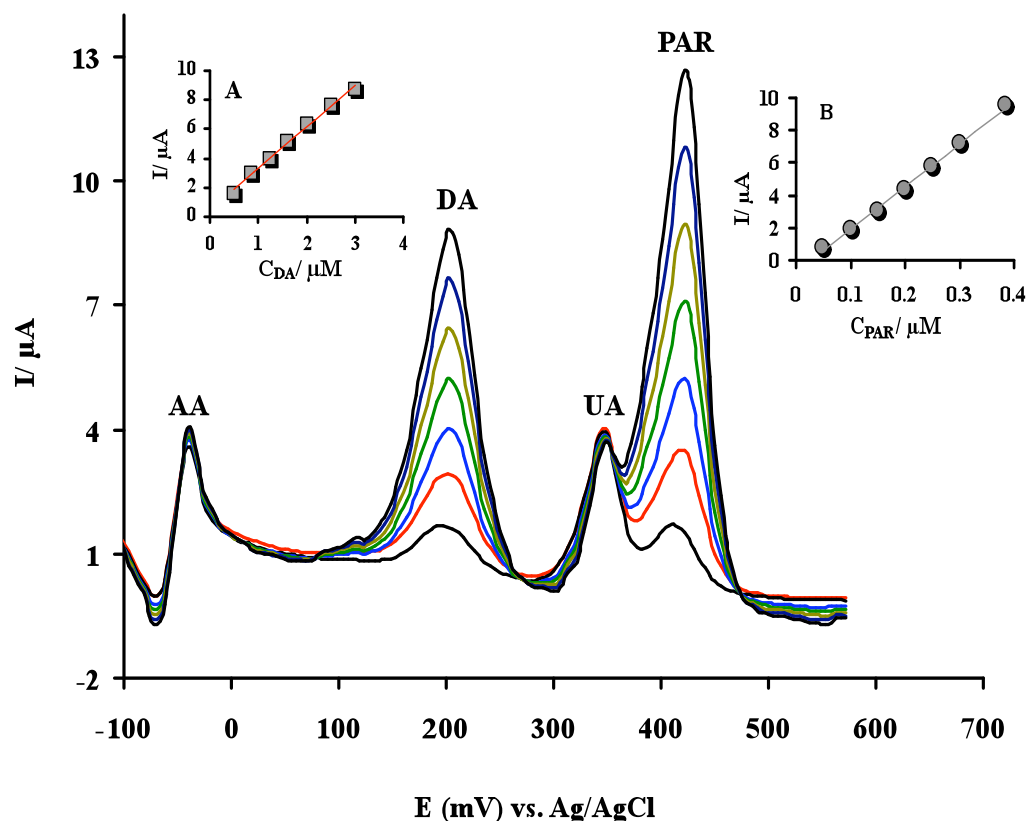


Figure 4.73. Square wave voltammograms of simultaneously increasing concentrations of DA and PAR in the presence of 1.0×10^{-4} M AA and 2.0×10^{-5} M UA at CoNPs/MWCNT/GCE in 0.1 M PBS at pH 7.0. DA concentrations: 5.0×10^{-7} M; 8.5×10^{-7} M; 1.25×10^{-6} M; 1.6×10^{-6} M; 2.0×10^{-6} M; 2.5×10^{-6} M; 3.0×10^{-6} M. PAR concentrations: 5.0×10^{-8} M; 1.0×10^{-7} M; 1.5×10^{-7} M; 2.0×10^{-7} M; 2.5×10^{-7} M; 3.0×10^{-7} M; 3.85×10^{-7} M. Frequency: 22 Hz. Step potential: 100 mV/s. Amplitude: 50 mV/s. Equilibrium time: 5 s. Inset A: A plot of peak currents versus the concentration of DA. Inset B: A plot of peak currents versus the concentration of PAR.

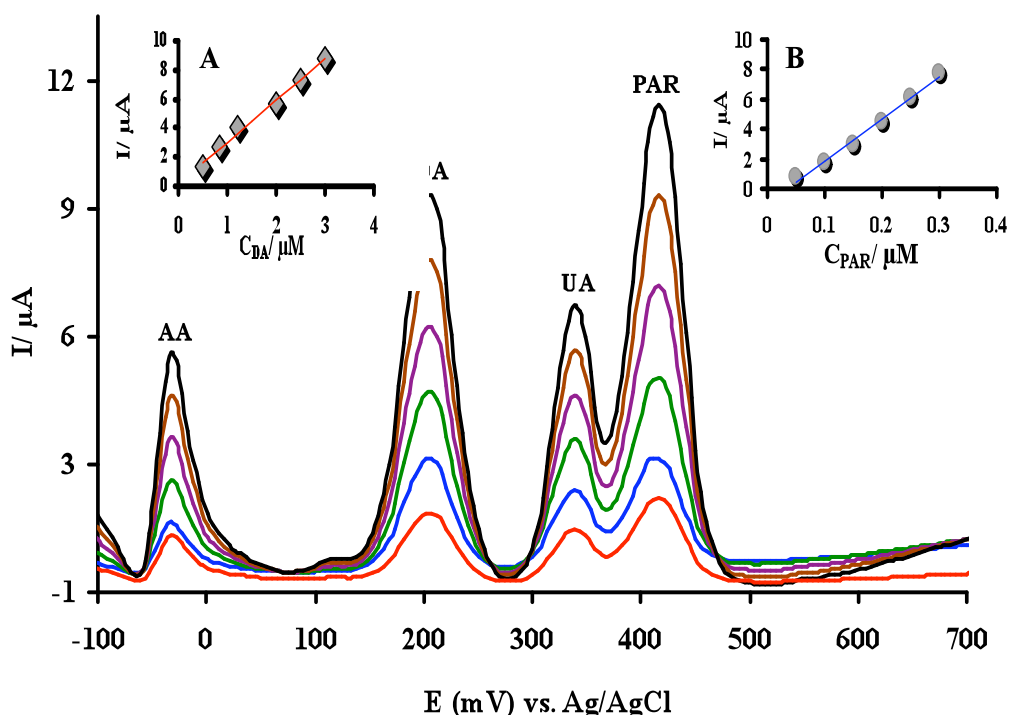


Figure 4.74. Square wave voltammograms of the mixture of simultaneously increasing concentrations of AA, DA, UA and PAR at CoNPs/MWCNT/GCE in 0.1 M PBS at pH 7.0. AA concentrations: 3.0×10^{-4} M; 3.5×10^{-4} M; 4.0×10^{-4} M; 4.5×10^{-4} M; 5.0×10^{-4} M; 5.5×10^{-4} M. DA concentrations: 5.0×10^{-7} M; 8.5×10^{-7} M; 1.25×10^{-6} M; 1.6×10^{-6} M; 2.5×10^{-6} M; 3.0×10^{-6} M. UA concentrations: 3.5×10^{-5} M; 4.0×10^{-5} M; 4.5×10^{-5} M; 5.0×10^{-5} M; 5.5×10^{-5} M; 6.0×10^{-5} M. PAR concentrations: 7.5×10^{-8} M; 1.0×10^{-7} M; 1.5×10^{-7} M; 2.0×10^{-7} M; 2.75×10^{-7} M; 3.25×10^{-7} M. Frequency: 22 Hz. Step potential: 100 mV/s. Amplitude: 50 mV/s. Equilibrium time: 5 s. Inset A: A plot of peak currents versus the concentration of DA. Inset B: A plot of peak currents versus the concentration of PAR.

4.5.4. Reproducibility, stability and repeatability of modified electrode

The relative standard deviation (RSD) of 10 successive scans was 2.3% for 2.7×10^{-8} M PAR and 1.5% for 2.4×10^{-7} M DA. This indicated that the reproducibility of the CoNPs/MWCNTs/GCE was excellent. Also, five different electrodes prepared by the proposed method were independently applied for the determination of 3.5×10^{-7} M DA and 4.5×10^{-8} M PAR in 0.1 M PBS at pH 7.0, and the RSDs

were 2.85 % and 3.0 % for DA and PAR, respectively. This also indicated that reproducibility of the proposed electrode was excellent. The stability of the proposed electrode was also tested by keeping the electrode in 0.1 M PBS at pH 7.0 for 3 weeks. Then, the voltammograms were recorded and compared with those obtained before immersion. The change in the peak current was only 5.5% with and RSD of 3.0% for DA and 4.9% with an RSD of 2.6% for PAR. A slight decrease in the peak current indicated that the proposed electrode has good stability. Also, the RSD of 6 measurements at time intervals of 30 min was 2.50% for 3.5×10^{-7} M DA and 2.25% for 4.5×10^{-8} M PAR indicating that the proposed electrode has good repeatability.

4.5.5. Determination of drugs in pharmaceutical preparations

Square wave voltammetric determination of PAR in Parol tablets using the proposed electrode was referred to the regression equation. The analysis of tablets using the proposed method was summarised in Table 4.11. A mean recovery of 99.7% with RSD of 1.3% was obtained using the proposed method for the voltammetric analysis of tablets. The results of the drug analysis obtained from the proposed method were in close agreement with the claimed value. The results obtained were also comparable with the results obtained from square wave voltammetry at multi-walled carbon nanotube-alumina coated silica nanocomposite electrode with a recovery of 98.2% (Lu and Tsai, 2011), differential pulse voltammetry at nafion/TiO₂-graphene modified electrode with a recovery of 98.6% (Fan et al., 2011).

The proposed method was also utilized for the determination of DA in pharmaceuticals. Dopamine hydrochloride samples were diluted with 0.1 M PBS. The injections were analysed by the standard addition method. The results were shown in Table 4.11. A mean recovery of 100.8% with RSD of 1.8% was obtained using the proposed method for the voltammetric analysis of dopamine hydrochloride injections. The data obtained at proposed electrode were in close agreement with the claimed value. The data were also in good agreement with certified value obtained

by British Pharmacopoeia non-aqueous titrimetry (British Pharmacopoeia, 2000), (average recovery of 98.0%).

Table 4.11. Results of the determination of PAR and DA in pharmaceuticals

Drug sample	Content	Found	Recovery %	R.S.D %
Paracetamol (mg)	500	498.6±6.3	99.7	1.3
Dopamine (mg/mL)	40	40.30±0.73	100.8	1.8

Mean ± standard deviation (n = 5)

Recovery measurements using the standard addition were also performed and the results are given in Table 4.12. Average recoveries varied from 98.9 to 100.3% and 99.3 to 101.5% for were obtained for PAR and DA, respectively. The satisfactory recoveries demonstrated that the proposed method was accurate.

Table 4.12. Results of recoveries of PAR and DA in pharmaceuticals

Samples	No	Content (µM)	Added (µM)	Found ^a (µM)	Recovery %	R.S.D %
PAR Tablet	1	0.20	0.10	0.2967	98.9	1.36
	2	0.20	0.20	0.4012	100.3	1.25
DA Ampoule	1	1.5	1.0	2.4825	99.3	1.90
	2	1.5	1.5	3.0450	101.5	1.60

^aAverage of six determinations

The determination of PAR and DA was also carried out in mixed samples prepared synthetically. For this purpose, different capacities of diluted PAR solution and standard DA solution were added and adjusted to the volume with 0.1 M PBS to a series of 10-mL measuring flasks, and to another series of 10-mL measuring flasks, different capacities of diluted DA solution and standard PAR solution were added and adjusted to the volume with 0.1 M PBS. The SWVs were then recorded and the relevant anodic peak currents were measured. The standard addition method was used for the calculation of the concentrations PAR and DA. The results are shown in Table 4.13.

Table 4.13. Determinations of PAR and DA in mixtures

Number	PAR tablet (μM)	DA added (μM)	PAR			DA		
			Found (μM)	Recovery %	R.S.D %	Found (μM)	Recovery %	R.S.D %
1	0.15	0.00	0.1484	98.9	1.9	-	-	-
2	0.15	1.00	0.1524	101.6	2.1	1.011	101.1	2.2
3	0.30	0.00	0.2991	99.7	1.5	-	-	-
4	0.30	2.00	0.3069	102.3	2.3	1.990	99.5	1.9
	DA ampoule (μM)	PAR added (μM)	DA			PAR		
			Found (μM)	Recovery %	R.S.D %	Found (μM)	Recovery %	R.S.D %
1	1.00	0.00	0.997	99.7	2.0	-	-	-
2	1.00	0.20	1.021	102.1	2.2	0.1976	98.8	1.8
3	2.00	0.00	2.010	100.5	1.8	-	-	-
4	2.00	0.40	2.050	102.5	2.4	0.4028	100.7	2.1

The validity of the proposed method was also assured by the recovery of both DA and PAR in urine samples (Table 4.14.). The recoveries and RSD (%) values obtained for both DA and PAR confirm that the proposed electrode is also precise and accurate for the determinations of DA and PAR in biological samples.

Table 4.14. Results of recoveries of PAR and DA in urine samples

Number	PAR added (μM)	DA added (μM)	PAR			DA		
			Found (μM)	Recovery %	R.S.D %	Found (μM)	Recovery %	R.S.D %
1	0.15	1.00	0.149	99.3	3.0	0.985	98.5	2.6
2	0.35	2.50	0.359	102.5	2.8	2.540	101.6	2.0
3	0.45	3.00	0.456	101.3	3.2	2.994	99.8	2.5

4.6. Simultaneous Determination of Cd(II) and Pb(II) at Chitosan-MWCNT modified Glassy Carbon Electrode by Square Wave Anodic Stripping Voltammetry

Heavy metals have been used in many different areas especially in industries for thousands of years. The pollution of lead and cadmium is one of the most serious environmental problems. The deposition of these heavy metals in soils, waters and plants has some quite dangerous threats to human health and ecosystem. These hazard metals have been extensively investigated and their effects on human health regularly reviewed by international bodies such as the WHO (Järup, 2003). The quantitative detection and the removal of the heavy metals are very important subject since they are very persistent in the environment. They are toxic even in trace amounts and their deposition in the biological cells can cause severe pathologies (Săndulescu et al., 2011).

Sensitive methods for the determination of trace amount of lead and cadmium have received much attention and many techniques have been employed for the determination of lead and cadmium. The most commonly used methods for the determination of various metal ions are atomic adsorption spectrometry (AAS) (Jr et al., 1999; Bulska et al., 1997), atomic emission spectrometry (AES) (Wensing et al., 1994) and mass spectrometry (MS). However, these techniques have some disadvantages, such as complicated operation, high cost of maintenance, expensive apparatus and requiring well-controlled experimental conditions.

Electrochemical method is one of the most favorable techniques for the determination of heavy metal ions, including lead(II) and cadmium(II), because of its low cost, high sensitivity, easy operation and the ability of analyzing element speciation. In previous works the determination of heavy metal ions were mostly carried out at mercury electrodes (Fischer and Berg, 1999; Yang and Sun, 1998; Lu et al., 1999; Zen and Ting, 1996) . A number of electrodes have been published in the literature on the use of chemically modified glassy carbon electrodes for the determination of Cd(II) and Pb(II) such as diacetyldioxime modified carbon paste

electrode CMCPE (Hu et al., 2003), multi-walled carbon nanotube modified glassy carbon electrode (Wu et al., 2003), MWCNTs-Nafion/bismuth composite electrode (Xu et al., 2008), bismuth-modified carbon nanotube electrode (Hwang et al., 2008), bismuth modified carbon nanotubes (CNTs)-poly(sodium 4-styrenesulfonate) composite film electrode (CNTs-PSS/Bi), (Jia et al., 2010).

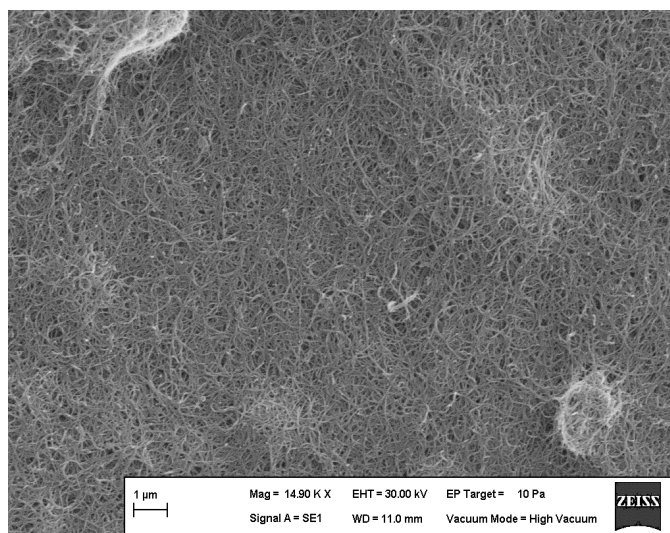
Chitosan (CTS) is a polysaccharide derived by deacetylation of chitin that displays excellent film-forming ability, good adhesion, high mechanical strength, and susceptibility to chemical modifications due to the presence of reactive hydroxyl and amino functional groups (Zhang et al., 2004). CTS as a popular bio-polymer has been used for protein immobilization and for the development of biosensors (Zhang et al., 2004; Zhou et al., 2007; Tan et al., 2009). In addition, because CTS has a high content of hydroxyl and amino groups along its chains and possesses a high metal-chelating ability, it is widely studied as a material for wastewater treatment (Bailet et al., 1999; Guibal, 2004), and electrochemical determinations of metals ions in aqueous solutions (Marcolino-Junior et al., 2007; Janegitza et al., 2009). Moreover, the chemical modifications of CTS can introduce new chelating groups along the CTS chains, which can not only prevent its dissolution in acidic solutions but also improve the adsorption capacity and selectivity of an existing group for a specific metal ion (Qu et al., 2009; Merrifield et al., 2004; Ngah et al., 2002). Carbon nanotubes (CNTs) as a kind of relatively new nanomaterial, which display attractive structural, mechanical, and electronic properties, including improved electrochemical activity (Haddon, 2002), have proven potential as superior sorbents for removing divalent metal ions from aqueous solution based on chemical interactions between the metal ions and the surface functional groups of the CNTs (Rao et al., 2007).

In this study, we aim to take the advantage of the combination of CTS and MWCNT in order to improve the adsorption capacity and selectivity of modified electrode for the simultaneous determination of Cd(II) and Pb(II) in aqueous solution using stripping voltammetry techniques.

4.6.1. SEM images of modified electrodes

The surface morphology of the modified electrodes was characterized by SEM. As shown in Figure 4.75A., a MWCNT layer without aggregation was observed on the electrode surface, indicating that the MWCNTs were homogeneously dispersed on the surface of the GCE. The morphology of the CTS-MWCNT nanocomposite was also examined by SEM, indicating that the MWCNTs are well coated by CTS in Figure 4.75B.

A)



B)

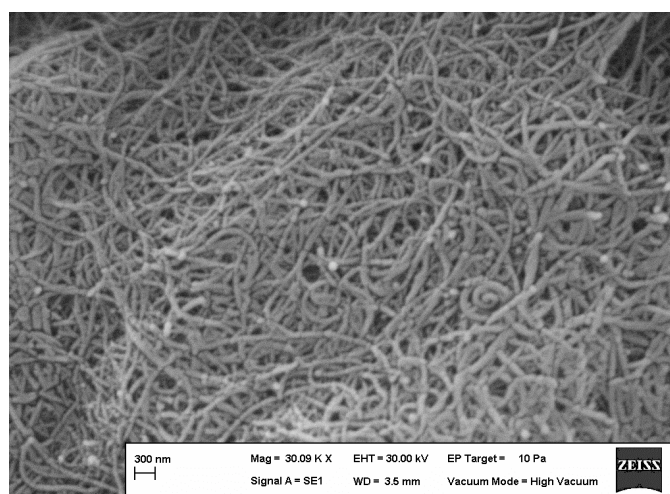


Figure 4.75. Sem images of MWCNT/GCE (A) and CTS-MWCNT/GCE (B) surfaces

4.6.2. Procedure of detection for Cd(II) and Pb(II)

All measurements were carried out in 0.1 M NaNO₃ solution at pH 7.0. A known volume of supporting electrolyte was added to an electrochemical cell, and then standard solution of Pb(II) and Cd(II) was added into the cell. A preconcentration potential of -1.2 V (vs. Ag/AgCl sat. KCl) was applied to the working electrode under the stirring conditions for 120 s. The stirring was stopped and after 5 s equilibration time, the square wave anodic stripping voltammograms were recorded from -1.25 V to chosen the positive direction (Frequency: 22 Hz, Step potential: 100 mV/s. Amplitude: 50 mV/s. Equilibrium time: 5 s. Two peaks were observed at -1.0 V and -0.72 V for Cd(II) and Pb(II) respectively. The same procedure was applied to real samples and the results were discussed below.

4.6.3. Working mechanism of the CTS-MWCNT modified GC electrodes

The performance of improved CTS-MWCNT modified glassy carbon electrode is based on the preconcentration of Cd(II) and Pb(II) from aqueous solution onto the surface of the modified electrode by forming complexes with the modifier as shown an illustration in Figure 4.76.

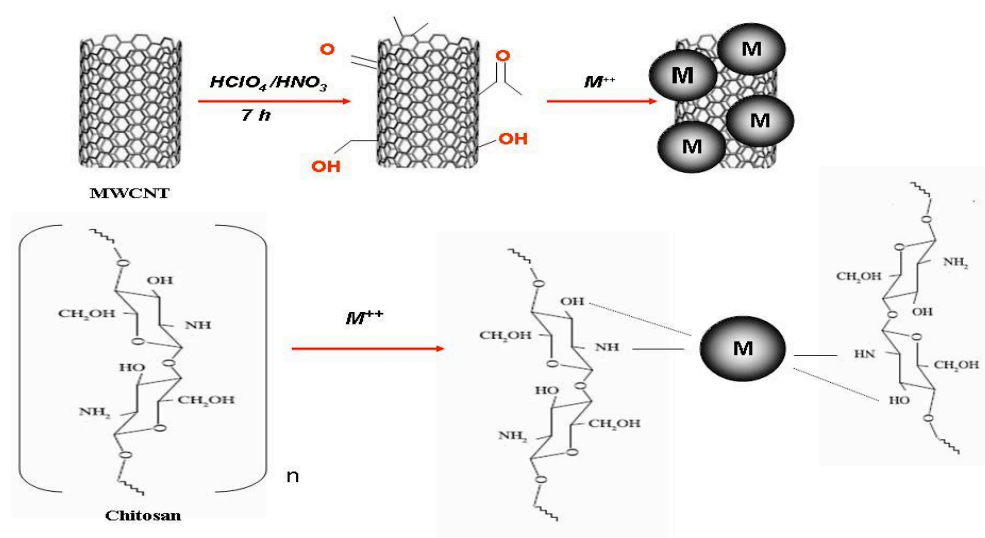


Figure 4.76. An illustration of CTS-MWCNT modifier acts as the ligand (L) and the metal ions (M²⁺)

The CTS-MWCNT modifier acts as the ligand (L) and the metal ions (M^{2+}) are the central atom. By this means, the surface concentrations of Cd(II) and Pb(II) are much larger than those of the unmodified electrode, and the sensitivity is greatly increased. The accumulated Cd(II) and Pb(II) were reduced at -1.2 V and the products were then oxidized in the stripping stage. The mechanism can be described as showed below (Hu et al., 2003):

Accumulation stage : $M^{2+}_{(solution)} + L_{(surface)} \rightarrow (M^{2+}-L)_{adsorption}$

The reduction stage: $(M^{2+}-L)_{adsorption} + 2e^{-} \rightarrow (M^0-L)_{adsorption}$

The stripping stage: $(M^0-L)_{adsorption} \rightarrow M^{2+}_{(solution)} + L_{(surface)} + 2e^{-}$

4.6.4. Effects of electrolyte and pH

The effects of some electrolytes, such as NaNO₃, KCl, KH₂PO₄, Na₂HPO₄, NaAc and KI on the anodic stripping peak currents of 2 nM Pb(II) and 2 nM Cd(II) were investigated. Cd(II) and Pb(II) shows different electrochemical responses in various electrolyte solutions. The results show that Pb(II) and Cd(II) have the best electrochemical responses in 0.1 M NaNO₃. The highest peak current and the best peak separation between Cd(II) and Pb(II) were obtained in 0.1 M NaNO₃.

The effect of pH on the detection of Pb(II) and Cd(II) was also investigated in the range of pH:3 to pH:8. As shown in Figure 4.77., the anodic peak currents of 2 nM Cd(II) and 2 nM Pb(II) increased linearly with increasing pH. The peak currents showed a maximum value at neutral pH (pH:7.0). Then the peak currents showed a decreasing with continuous increasing of pH. Thus 0.1 M NaNO₃ at pH 7.0 solution was chosen as suitable medium for detection of Cd(II) and Pb(II).

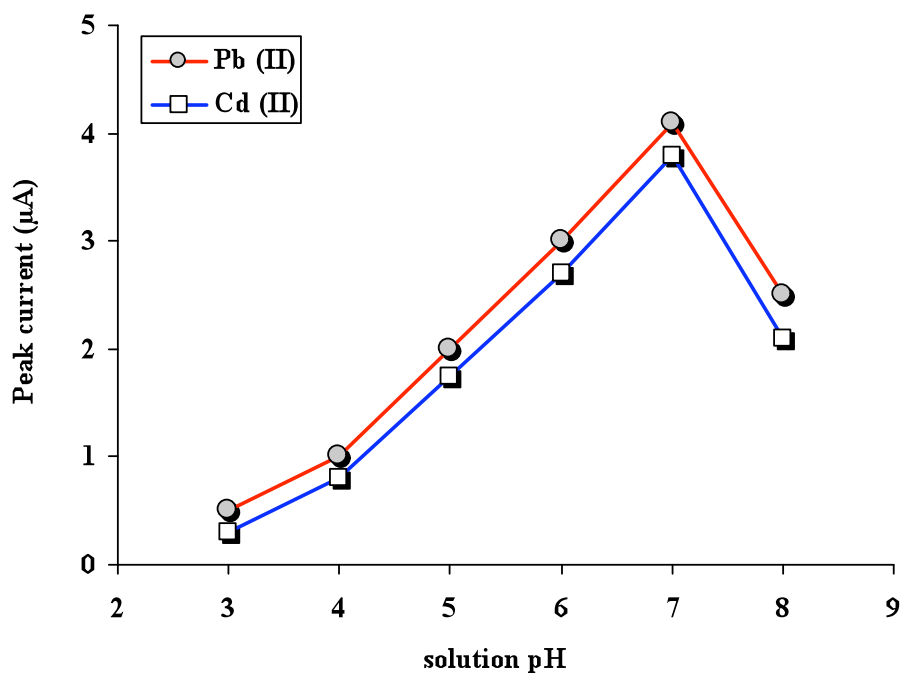


Figure 4.77. Effects of solution pH on anodic stripping peak currents of 2 nM Cd(II) and 2 nM Pb(II) in 100 mM NaNO₃ solution at CTS-MWCNT/GCE. Accumulation time: 120 s. Accumulation potential: -1.2 V. Frequency: 22 Hz. Step potential: 100 mV/s. Amplitude: 50 mV/s. Equilibrium time: 5 s

4.6.5. Effects of accumulation potential and accumulation time

Metal ions in the sample solution are preconcentrated into modified electrode during a given time period by application of a sufficient negative potential. These preconcentrated metals are then stripped (oxidized) out of the modified surface by scanning the applied potential in the positive direction. The resulting peak currents, i_p , are proportional to the concentration of each metal in the sample solution, with the position of the peak potential, E_p , specific to each metal. With more than one metal ion in the sample, the ASV signal may sometimes be complicated by formation of intermetallic compounds, such as ZnCu. This may shift or distort the stripping peaks for the metals of interest. These problems can often be avoided by adjusting the accumulation time or by changing the accumulation potential (Kounaves, 1987).

So, accumulation potential and accumulation time are important parameters for sensitive determination of Cd(II) and Pb(II) by anodic stripping techniques. When accumulation potentials are more negative than -1.2 V, the peak currents changes little. To prevent reducing some other metal ions at the same potential, the accumulation potential was chosen as -1.2 V in this study. As shown in Figure 4.78., the anodic peak currents of 2 nM Cd(II) and 2 nM Pb(II) increased versus different periods (20, 40, 60, 80, 100, 120 s). There is no important changes in peak currents of Cd(II) and Pb(II) than 120 s. Hence, the optimal accumulation time was employed as 120 s.

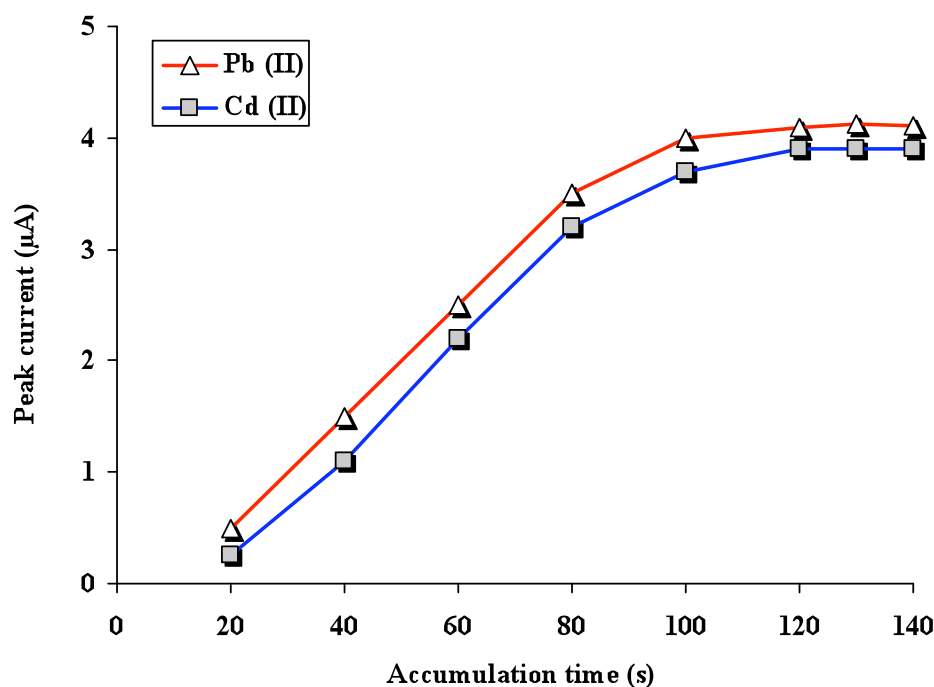


Figure 4.78. Effects of accumulation time on anodic stripping peak currents of 2 nM Cd(II) and 2 nM Pb(II) at pH 7.0 in 100 mM NaNO₃ solution at CTS-MWCNT/GCE. Accumulation potential: -1.2 V. Frequency: 22 Hz. Step potential: 100 mV/s. Amplitude: 50 mV/s. Equilibrium time: 5 s

4.6.6. Effect of the mass of the modifiers

The effect of the mass of modifiers on the electrode surface was examined. Figure 4.79. shows the influence of amount of modifier on the simultaneous determination of 2 nM Cd(II) and 2 nM Pb(II). As seen in Figure 4.79., the best

peak separation between Cd(II) and Pb(II) was obtained in 50% (w/w) CTS/CTS-MWCNT mixture. It is clearly shown that 50% (w/w) CTS/CTS-MWCNT mixture on the GCE surface exhibits an efficient electrocatalytic effect towards the oxidation of Cd(II) and Pb(II) with large peak separation. Therefore, the best ratio (50% CTS/CTS-MWCNT) mixture can be easily used for the simultaneous determination of Cd(II) and Pb(II).

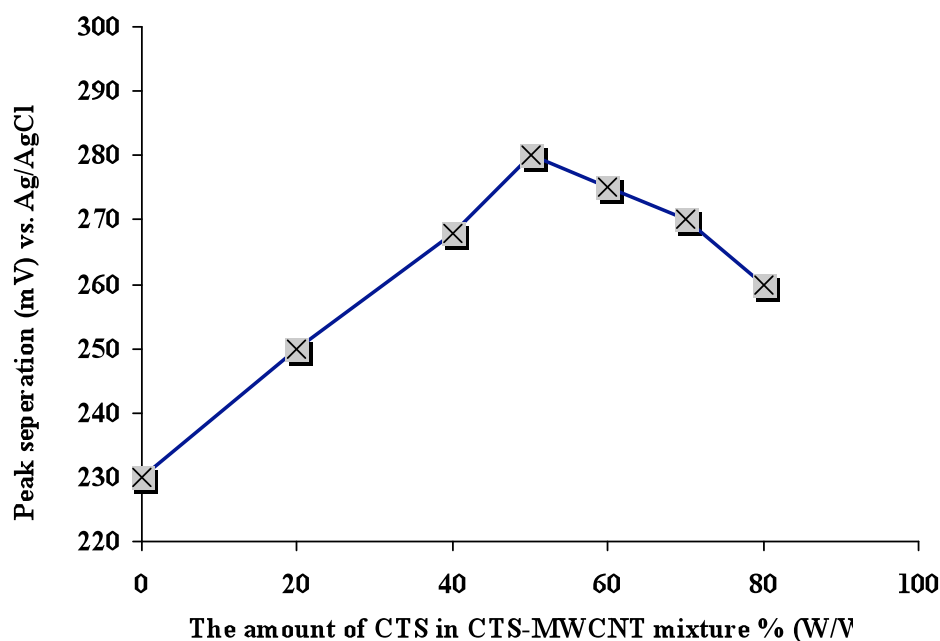


Figure 4.79. Effects of the amount of CTS in CTS-MWCNT mixture % (W/W) on the peak potential separations of 2 nM Cd (II) and 2 nM Pb (II) in 100 mM NaNO₃ solution at modified GCE. Accumulation time: 120 s. Accumulation potential: -1.2 V. Frequency: 22 Hz. Step potential: 100 mV/s. Amplitude: 50 mV/s. Equilibrium time: 5 s

4.6.7. Square wave anodic stripping voltammograms of Cd(II) and Pb(II)

The simultaneous determination of Cd(II) and Pb(II) in aqueous solution was carried out by SWASV at the MWCNT/GCE and CTS-MWCNT/GCE. The voltammograms are showed in Figure 4.80. In Figure 4.80B., two anodic peaks were appeared at -0.88 V and -0.65 V for Cd(II) and Pb(II) with a peak to peak separation of 230 mV at MWCNT/GCE. However, at CTS-MWCNT/GCE, Cd(II) and Pb(II)

exhibits two well-defined anodic peaks at -1.0 V and -0.72 V with a peak to peak separation of 280 mV (Figure 4.80A.). The separation of anodic peaks at CTS-MWCNT/GCE was large enough for simultaneous determination of Cd(II) and Pb(II) in a mixture. At bare GCE, no peaks appear at the same conditions for determination of Cd(II) and Pb(II) (data not shown). It is clearly shown that the CTS-MWCNT can greatly promote the preconcentration of Cd(II) and Pb(II) at GCE and significantly increase the sensitivity of the determination of Cd(II) and Pb(II) with sharp peaks and enhancement in current responses and also good selectivity with large peak separations between Cd(II) and Pb(II). This indicated that the electrochemical responses of Cd(II) and Pb(II) have greatly been increased at CTS-MWCNT/GCE. Intensive increases in peak currents of both Cd(II) and Pb(II) are observed owing to the improvement in the electron transfer process and the larger real area of the layer at the surface.

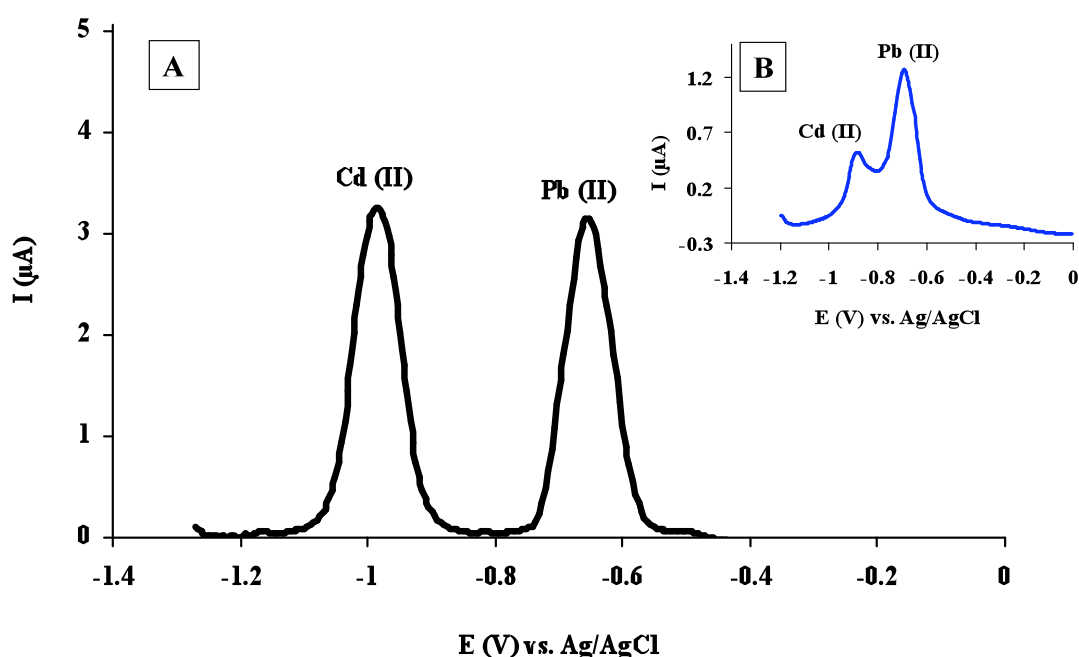


Figure 4.80. Square wave anodic stripping voltammograms (SWASV) of 1.7 nM Cd(II) and 1.2 nM Pb(II) at pH 7.0 in 100 mM NaNO₃ solution at A) CTS-MWCNT/GCE and B) MWCNT/GCE. Accumulation time: 120 s. Accumulation potential: -1.2 V. Frequency: 22 Hz. Step potential: 100 mV/s. Amplitude: 50 mV/s. Equilibrium time: 5 s

4.6.8. Calibration equation of Cd(II) in the absence of Pb(II)

The square wave anodic stripping voltammetric determination of the concentration of Cd(II) at glassy carbon electrodes modified with CTS-MWCNT was performed in 0.1 M NaNO₃ at pH 7.0 under the optimized working conditions described above as shown in Figure 4.81. The stripping peak currents were plotted against the concentration of Cd(II) in Figure 4.82. The response of stripping peak currents of Cd(II) at CTS-MWCNT/GCE was linear with the concentration of Cd(II) in the range of 0.1 nM ~ 2.5 nM. The linear regression equation was $I_p(\mu\text{A})=1.9240C(\text{nM})+0.0078$ with a correlation coefficient of 0.9986. The detection limit was 0.03 nM (S/N=3).

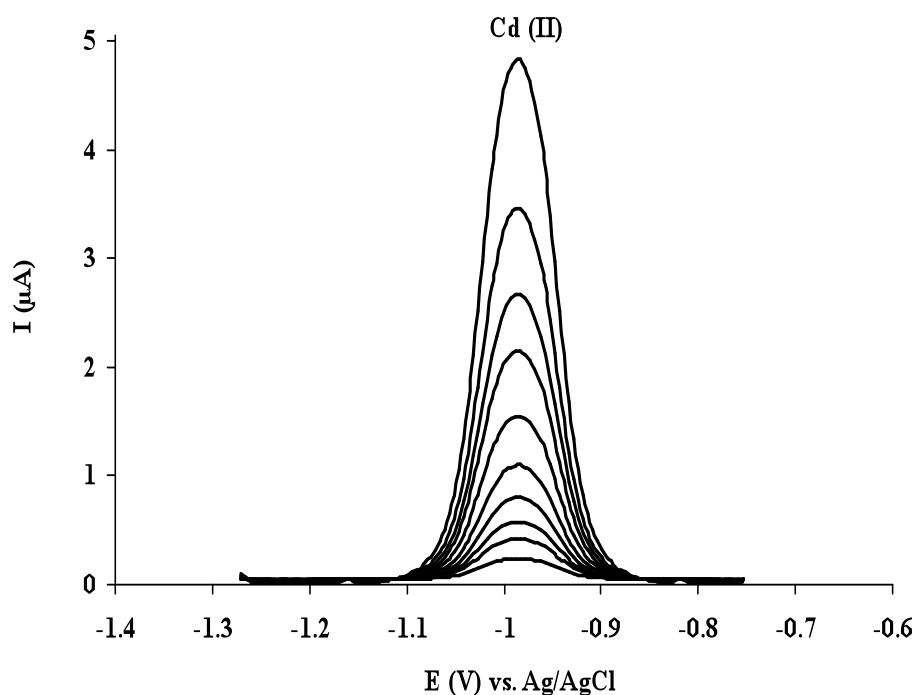


Figure 4.81. Square wave anodic stripping voltammograms (SWASV) of increasing concentrations of Cd(II) at pH 7.0 in 100 mM NaNO₃ solution at CTS-MWCNT/GCE. Accumulation time: 120 s. Accumulation potential: -1.2 V. Frequency: 22 Hz. Step potential: 100 mV/s. Amplitude: 50 mV/s. Equilibrium time: 5 s. Cd(II) concentrations: 0.1 nM; 0.2 nM; 0.25 nM; 0.3 nM; 0.5 nM; 0.7 nM; 1.0 nM; 1.3 nM; 1.8 nM; 2.5 nM

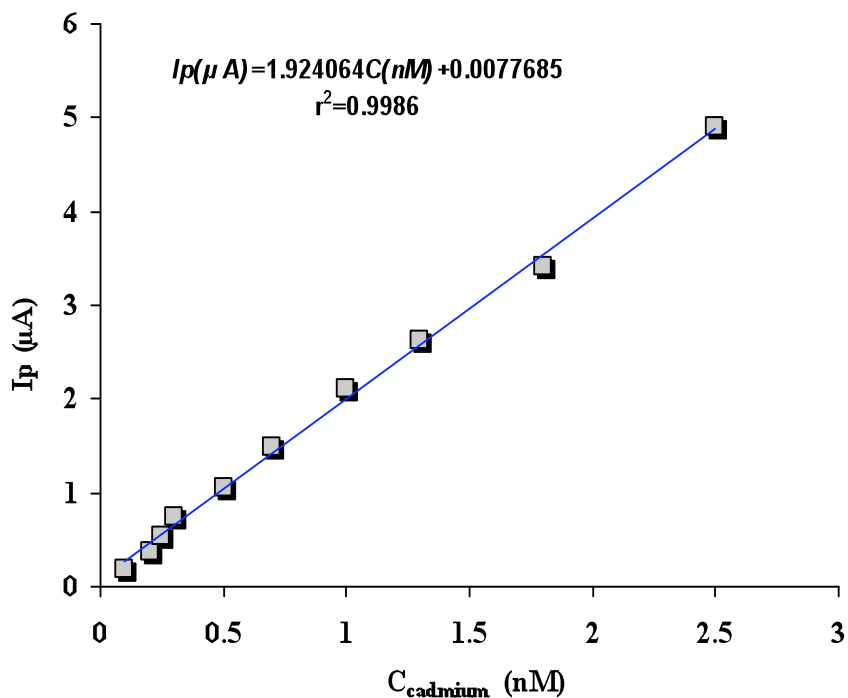


Figure 4.82. A plot of peak currents versus increasing concentrations of cadmium(II) in lead(II) free solution

4.6.9. Calibration equation of Pb(II) in the absence of Cd(II)

The square wave anodic stripping voltammograms (SWASV) determination of a series of standard Pb(II) solutions was performed in 0.1 M NaNO₃ at pH 7.0 under the optimal conditions as shown in Figure 4.83. The results show that stripping peak current has a linear relationship with concentration in the range of 0.1 nM~1.8 nM as shown in Figure 4.84. The linear regression equation was $I_p(\mu\text{A})=2.6270C(\text{nM})-0.0230$ with a correlation coefficient of 0.9990. The detection limit was 0.027 nM (S/N=3).

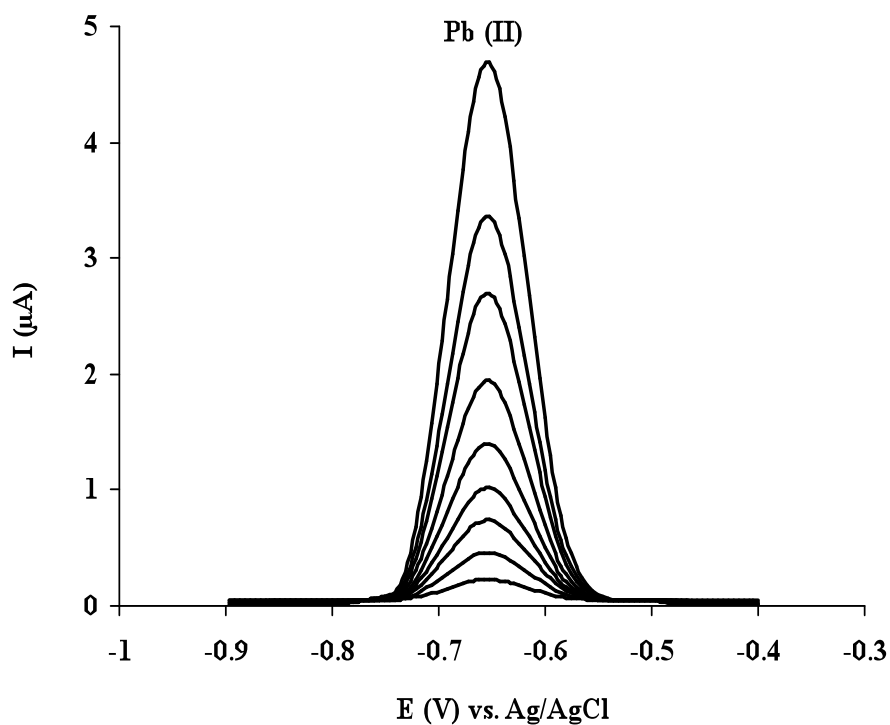


Figure 4.83. Square wave anodic stripping voltammograms (SWASV) of increasing concentrations of Pb(II) at pH 7.0 in 100 mM NaNO₃ solution at CTS-MWCNT/GCE. Accumulation time: 120 s. Accumulation potential: -1.2 V. Frequency: 22 Hz. Step potential: 100 mV/s. Amplitude: 50 mV/s. Equilibrium time: 5 s. Pb (II) concentrations: 0.1 nM; 0.2 nM; 0.25 nM; 0.3 nM; 0.5 nM; 0.7 nM; 1.0 nM; 1.3 nM; 1.8 nM

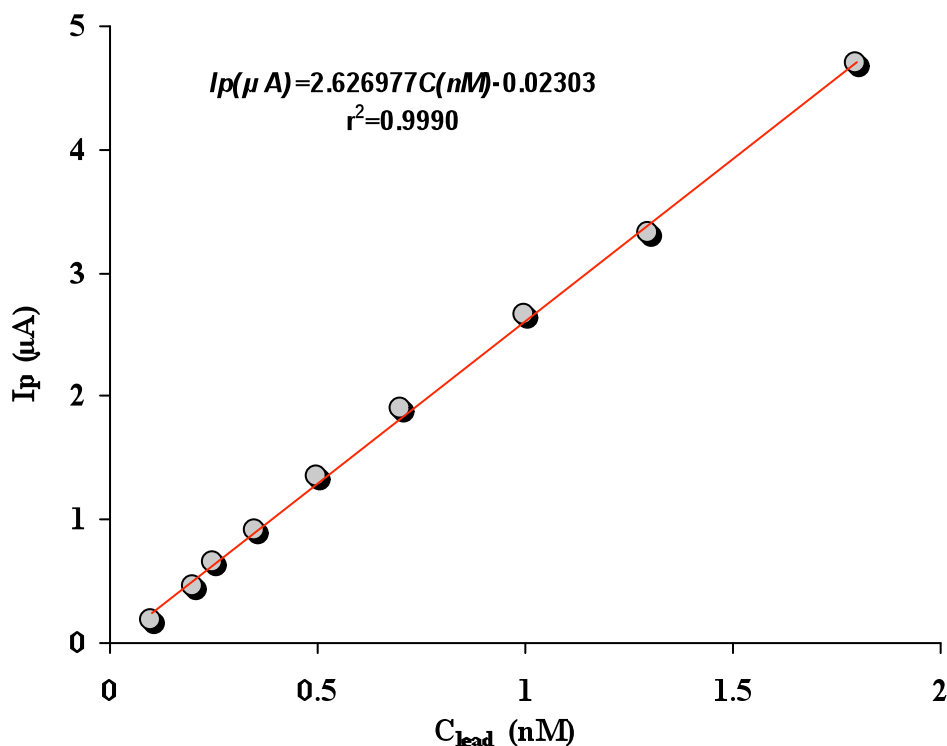


Figure 4.84. A plot of peak currents versus increasing concentrations of lead(II) in cadmium(II) free solution

4.6.10. Simultaneous determination of Cd(II) and Pb(II)

Figure 4.85. shows the square wave anodic stripping voltammograms (SWASV) of simultaneously increasing concentrations of Cd(II) and Pb(II) in 0.1 M NaNO_3 at pH 7.0. The electrochemical responses of both Cd(II) and Pb(II) have increased with their concentrations in Figure 4.86. and Figure 4.87. The results indicate that the proposed electrode enables the simultaneous determination of Cd(II) and Pb(II) owing to the large peak to peak separation. The results show that stripping peak current has a linear relationship with concentration in the range of 0.1 nM-2.5 nM for Cd(II) and 0.1 nM-1.8 nM for Pb(II) in the same solution. The linear regression equations were The linear correlation coefficients were 0.9980 and 0.9987 for Cd (II) and Pb(II) respectively. The detection limits were calculated as 0.035 nM for Cd (II) and 0.030 nM for Pb (II) when the S/N was 3. In addition, the results of the individually determination of Cd(II) and Pb(II) obtained from the proposed method are inclose aggrement with the simultaneous determination of

Cd(II) and Pb(II). Table 4.15. shows the analytical parameters of some modified electrodes for the simultaneous determination of Cd(II) and Pb(II).

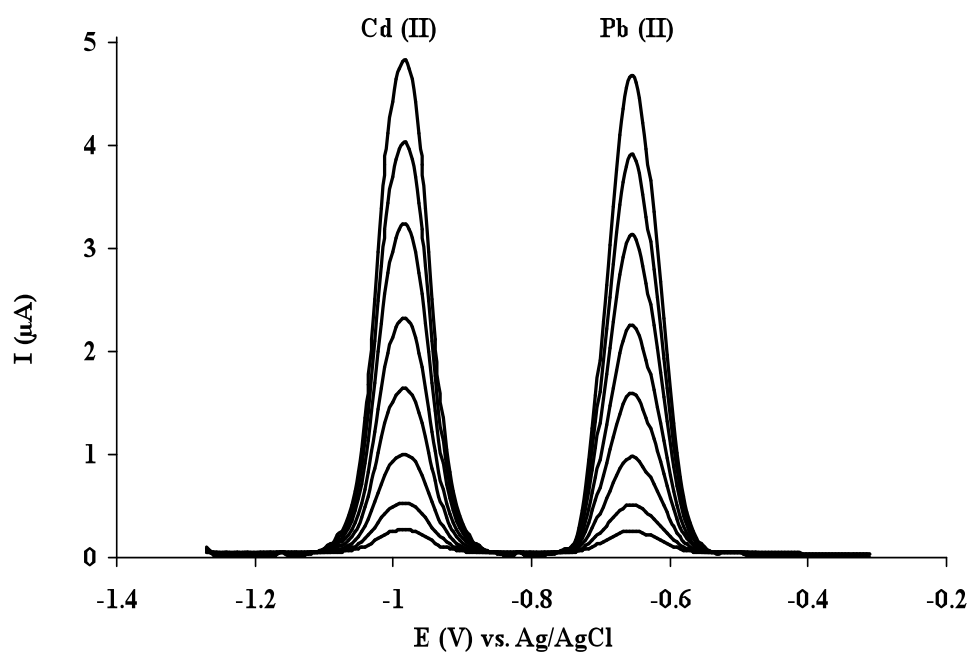


Figure 4.85. Square wave anodic stripping voltammograms (SWASV) of increasing concentrations of Cd(II) and Pb(II) at pH 7.0 in 100 mM NaNO₃ solution at CTS-MWCNT/GCE. Accumulation time: 120 s. Accumulation potential: -1.2 V. Frequency: 22 Hz. Step potential: 100 mV/s. Amplitude: 50 mV/s. Equilibrium time: 5 s. Cd (II) concentrations: 0.1 nM; 0.2 nM; 0.4 nM; 0.7 nM; 1.2 nM; 1.7 nM; 2.0 nM; 2.5 nM. Pb (II) concentrations: 0.1 nM; 0.15 nM; 0.3 nM; 0.6 nM; 0.9 nM; 1.2 nM; 1.5 nM; 1.8 nM

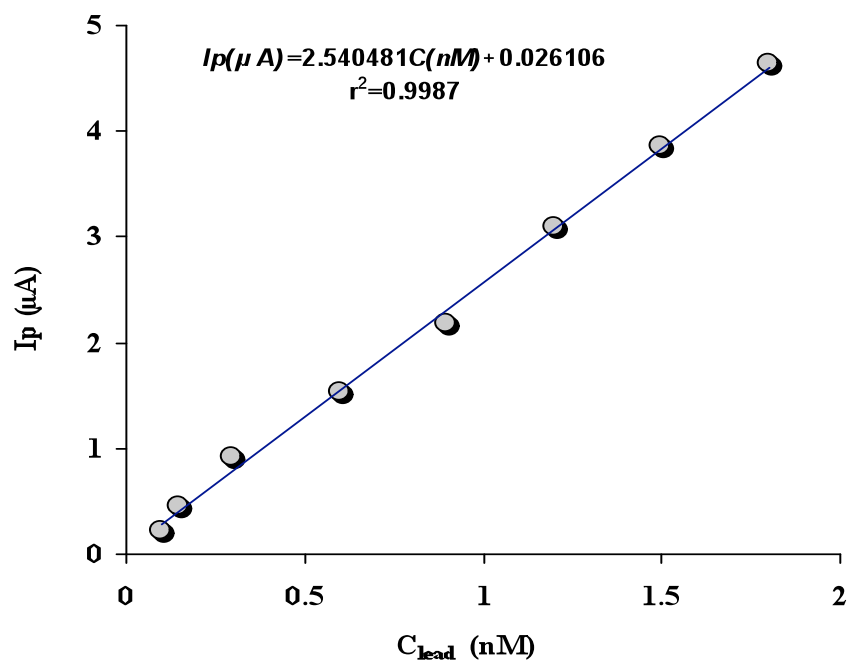


Figure 4.86. A plot of peak currents versus increasing concentrations of lead(II) in the presence of simultaneously increasing concentrations of cadmium(II)

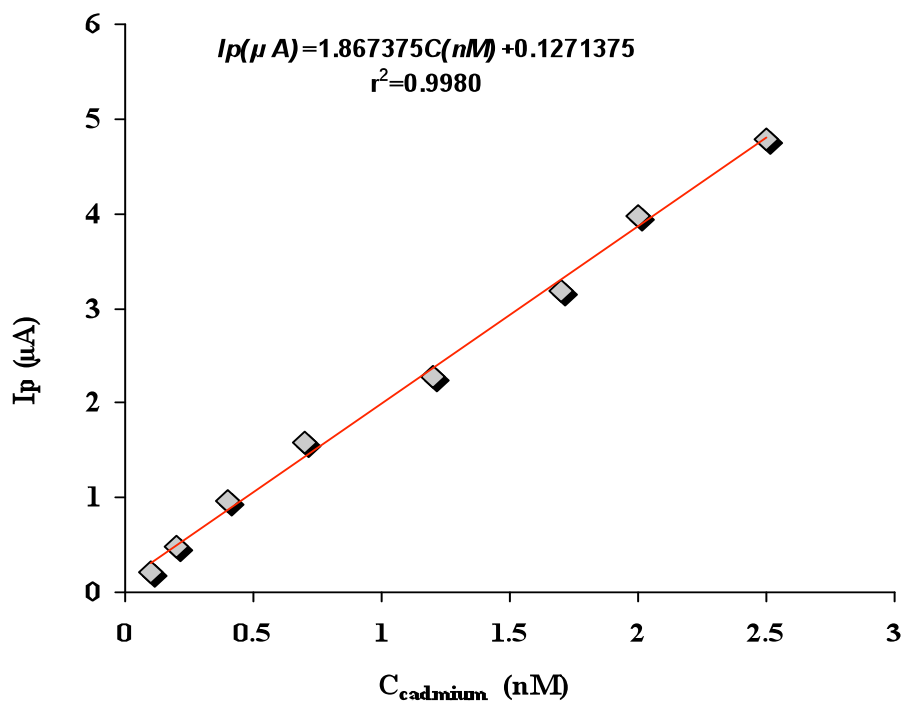


Figure 4.87. A plot of peak currents versus increasing concentrations of cadmium(II) in the presence of simultaneously increasing concentrations of lead(II)

Table 4.15. The application results of various electrodes for the determination of Cd(II) and Pb(II) simultaneously

Electrode	Used technique	Linear range (μM)		Detection limit (nM)		Reference
		Cd(II)	Pb(II)	Cd(II)	Pb(II)	
CMCPE	DPSV	0.25-25	0.1-15	10	40	(Hu et al., 2003).
MWCNT modified GCE	ASV	0.025-10	0.020-10	6	4	(Wu et al., 2003).
MWCNTs-Nafion/bismuth composite film electrode	DPASV	0.7-889.7	0.24-482.6	0.36	0.12	(Xu et al., 2008).
Bi-CNT electrode	ASV	0.018-0.890	0.0097-0.483	6.23	6.27	(Hwang et al., 2008).
CNTs-PSS/Bi composite film electrode	DPASV	0.004-0.44	0.004-0.43	0.178	0.193	(Jia et al., 2010).
CTS-MWCNT/GCE	ASSWV	0.0001-0.0025	0.0001-0.0018	0.035	0.030	This study

4.6.10. Stability, reproducibility and repeatability of CTS-MWCNT/GCE

The relative standard deviations (RSD)s of 10 successive measurements were 3.1 % for 2 nM Cd(II) and 2.8 % for 2 nM Pb(II). Five CTS-MWCNT/GCE examples fabricated independently were used to determine 2 nM Cd(II) and Pb(II), the RSDs were 3.5% and 3.0% respectively. The results indicated that the reproducibility of the CTS-MWCNT/GCE was excellent. However, the modified electrode should be well treated to maintain its reproducibility. Stability of the CTS-MWCNT/GCE was tested by keeping the electrode in 0.1 M NaNO₃ at pH 7.0 for 2 weeks and then recording ASSWVs for 2 nM Cd(II) and Pb(II) and comparing them with the results obtained in the same solution before immersion. The results obtained that peak current decreased only 3.5% for 2 nM Cd(II) and 3.3 % for 2 nM Pb(II) for the CTS-MWCNT/GCE, indicating that the CTS-MWCNT/GCE has good stability. To find the repeatability of the electrode, five measurement of 2 nM Cd(II) and Pb(II) were carried out using the CTS-MWCNT/GCE at intervals period of 30 min. The RSD was calculated to be 2.0 % and 1.8 % for Cd(II) and Pb(II), respectively. This indicated that the CTS-MWCNT/GCE has good repeatability.

4.6.11. Interference studies

In the interference study of CTS-MWCNT/GCE, any possible interference from common ions on the determination of Cd (II) and Pb (II) were also examined as shown in Table 4.16. Under the same experimental conditions, results have shown that 25-fold concentrations of Ca(II), Zn(II), Ni(II), Hg(II), Fe(II), Cu(II), Co(II), Mn(II) and Mg(II) had less than 3-3.5% influence on the peak current of Cd(II) and Pb(II), indicating good selectivity of the proposed method for the determination of Cd(II) and Pb(II).

Table 4.16. Possible interferences of some metal ions on the simultaneous determination of 2.0 nM cadmium(II) and 2.0 nM lead(II) with using the CTS-MWCNT/GCE

Possible interfering ions (each concentration: 50 nM)	Lead (II) Peak Current Change (%)	Cadmium (II) Peak Current Change (%)
Ca(II)	-	-
Zn(II)	2.1	1.9
Ni(II)	1.5	1.2
Hg(II)	2.2	2.3
Fe(II)	3.1	2.7
Cu(II)	2.5	2.2
Co(II)	1.8	1.3
Mn(II)	1.6	1.4
Mg(II)	-	-

4.6.12. Analytical Applications

The recovery studies were carried out with samples of water, human urine and nutrition. The different samples were spiked with known amount of Cd(II) and Pb (II) standard solution and the total concentration of Cd(II) and Pb(II) were analyzed using the CTS-MWCNT/GCE. The contents of cadmium(II) and lead(II) in different samples were determined referring to the regression equation. Table 4.17. summarizes the results obtained with the recovery studies. The mean recovery was

calculated as the ratio, expressed as a percentage, of the total Cd(II) and Pb(II) concentration found and the Cd(II) and Pb(II) concentration added to the samples. The recovery studies showed values in range 98%-103.5% and 98.3%-101.3% for Cd(II) and Pb(II) respectively. Consequently, the proposed electrode showed a good recoveries for both Cd(II) and Pb(II) in various samples.

Table 4.17. The recoveries of Cd(II) and Pb (II) in different samples using proposed method

Sample	Added $\times 10^{-10}$ (mol/L)		Found \pm s.d $\times 10^{-10}$ (mol/L)		R.S.D %		Recovery %	
	Cd (II)	Pb (II)	Cd (II)	Pb (II)	Cd (II)	Pb (II)	Cd (II)	Pb (II)
fizzy drink	1.00	1.00	1.013 \pm 0.025	1.008 \pm 0.032	2.5	3.2	101.3	100.8
	5.00	5.00	5.125 \pm 0.118	5.090 \pm 0.143	2.3	2.8	102.5	101.8
coke	1.00	1.00	0.980 \pm 0.030	0.983 \pm 0.028	3.1	2.8	98.0	98.3
	5.00	5.00	4.925 \pm 0.138	4.960 \pm 0.124	2.8	2.5	98.5	99.2
ice tea	1.00	1.00	0.985 \pm 0.027	0.990 \pm 0.029	2.7	2.9	98.5	99.0
	5.00	5.00	4.955 \pm 0.124	5.050 \pm 0.131	2.5	2.6	99.1	101.0
mixed juice	1.00	1.00	1.015 \pm 0.021	0.995 \pm 0.025	2.1	2.5	101.5	99.5
	5.00	5.00	5.105 \pm 0.092	5.015 \pm 0.100	1.8	2.0	102.1	100.3
milk	1.00	1.00	0.994 \pm 0.027	1.019 \pm 0.025	2.7	2.5	99.4	101.9
	5.00	5.00	5.010 \pm 0.125	5.025 \pm 0.116	2.5	2.3	100.2	100.5
mineral water	1.00	1.00	1.012 \pm 0.033	1.031 \pm 0.036	3.3	3.5	101.2	103.1
	5.00	5.00	5.175 \pm 0.155	5.080 \pm 0.157	3.0	3.1	103.5	101.6
tap water	1.00	1.00	1.009 \pm 0.030	1.013 \pm 0.033	3.0	3.3	100.9	101.3
	5.00	5.00	4.980 \pm 0.139	5.025 \pm 0.146	2.8	2.9	99.6	100.5
artificial lake water	1.00	1.00	1.033 \pm 0.033	1.013 \pm 0.035	3.2	3.5	103.3	101.3
	5.00	5.00	5.120 \pm 0.148	5.040 \pm 0.161	2.9	3.2	102.4	100.8
river water	1.00	1.00	1.032 \pm 0.035	1.020 \pm 0.038	3.4	3.7	103.2	102.0
	5.00	5.00	5.080 \pm 0.163	5.075 \pm 0.167	3.2	3.3	101.6	101.5
bottled water	1.00	1.00	0.985 \pm 0.025	0.991 \pm 0.030	2.5	3.0	98.5	99.1
	5.00	5.00	4.960 \pm 0.099	5.040 \pm 0.141	2.0	2.8	99.2	100.8
human urine	1.00	1.00	1.012 \pm 0.028	1.005 \pm 0.028	2.8	3.2	101.2	100.5
	5.00	5.00	5.155 \pm 0.124	5.110 \pm 0.124	2.4	2.7	103.1	102.2

5. CONCLUSION and SUGGESTIONS

In this thesis, a number of electrochemical sensors based on carbon nanotubes were fabricated for simple, sensitive and selective determination of various important drugs, molecules and ions in pharmaceuticals, food and environmental samples. The electrodes developed and results are summarized below.

A glassy carbon electrode (GCE) has been modified with multiwalled carbon nanotubes (MWCNTs) for the selective detection of paracetamol (PAR) in the presence of ascorbic acid (AA), dopamine (DA) and uric acid (UA). The oxidation of PAR shows a quasi-reversible response on a naked GCE at which an appreciable overpotential is required to drive the two electron oxidation. However, the peak-to-peak separation is seen to reduce and the electrochemical signal appears more reversible as the GCE is modified with an increasingly thick layer of MWCNTs. The results indicate that both anodic and cathodic peaks occur at lower overpotential with increasing layer thickness on the electrode surface, and that the overall peak-to-peak separation decreases as a result. The data are consistent with a transition from planar diffusion to a thin layer character as the potential required for the oxidation of PAR shifts to lower potentials. The experimental results show that the use of conducting porous layers on the surface of electrodes can be utilised to modify the mass transport regime from planar diffusion to a thin layer character that this alteration can also favourably facilitate the electrochemical discrimination between species which oxidise or reduce at similar potentials under planar diffusion conditions. The modified electrode was used for the determination of PAR using square wave voltammetry in 0.1 M phosphatebuffer solution (PBS) at pH 7.0. The results showed that the peak currents were proportional to the concentrations of PAR with a linear dynamic range of 2.0×10^{-10} M to 1.5×10^{-5} M and a detection limit of 9.0×10^{-11} M was obtained. The method has successfully been applied for the determination of PAR in pharmaceuticals.

A selective detection of albuterol has been carried out in pharmaceuticals for its therapeutic use and urine samples for doping control purposes using a glassy

carbon electrode (GCE) modified with multi-walled carbon nanotubes (MWCNT) and poly(pivalic acid) (PPA). The modified electrode (PPA/MWCNT/GCE) was applied for the detection of albuterol in the presence of uric acid (UA) since the urine samples contain excess amount of UA. The PPA/MWCNT/GCE showed a high electrocatalytic effect towards the oxidation of both albuterol and UA. Compared with a bare GCE and MWCNT/GCE, the PPA/MWCNT/GCE exhibits a distinct shift of the oxidation potential of albuterol and UA in the cathodic direction and a marked enhancement of the current response and also provides larger peak to peak separation between albuterol and UA for their easier simultaneous determination. The PPA/MWCNT/GCE was used for the determination of albuterol using square wave voltammetry in 0.1 M phosphate buffer solution (PBS) at pH 8.0. The peak current increased linearly with the concentration of albuterol in the range of 5.0×10^{-8} - 7.0×10^{-5} M with a detection limit of 1.2×10^{-8} M. The selective determination of albuterol makes the developed method of great interest for doping control purposes and monitoring its therapeutic use.

A reproducible voltammetric method is described for the determination of methimazole based on the modification of a glassy carbon electrode with multi-walled carbon nanotube/electro-copolymerized cobalt nanoparticles-poly(pivalic acid) composite. The modified electrode exhibited a highly electrocatalytic effect toward the oxidation of methimazole with a good reproducibility. Compared with a number of modified electrodes including a bare GCE, the poly(pivalic acid) CoNPs/MWCNT/GCE exhibits a distinct shift of the oxidation potential of methimazole in the cathodic direction and a marked enhancement of the current response. This enhancement was mainly contributed to the combination of the advantageous of multi-walled carbon nanotubes, cobalt nanoparticles and poly(pivalic acid) composites coated electrode. The results showed that methimazole exhibited a well defined oxidation peak at 255 mV. The modified electrode was used for the determination of methimazole in 0.1 M phosphate buffer solution (PBS) at pH 7.2. The peak current increased linearly with the concentration of methimazole in the range of 1.0×10^{-7} - 3.0×10^{-4} M with a correlation coefficient of 0.9996. The detection limit was 9.36×10^{-9} M (S/N=3). The relative standard deviation (RSD) of

10 successive scans was 1.6% for 20 μM methimazole. The proposed method was successfully applied to the determination of methimazole in thyramozol tablets.

Multi-walled carbon nanotubes (MWCNTs) functionalized by nickel nanoparticles were obtained using a single step chemical deposition method in an ultrasonic bath. The composite material was characterized by means of scanning electron microscopy (SEM) and energy dispersive X-ray analysis (EDX). The electroactivity of the nickel nanoparticle-functionalized MWCNTs was assessed in respect to the electrooxidation of bromhexine. Compared with a bare Pt and a bare Pt modified with MWNCTs, the nickel nanoparticle-functionalized MWCNTs modified Pt electrode exhibited a well-defined oxidation peak for bromhexine at 997 mV and a marked enhancement of the current response. The nanocomposite material modified Pt electrode has significantly improved the voltammetry of bromhexine and provided a highly reproducible detection. The modified electrode was used for the determination of bromhexine in 0.1 M phosphate buffer solution (PBS) at pH 4.0. The peak current increased linearly with the concentration of bromhexine in the range of 5.0×10^{-6} to 2.3×10^{-4} M with a correlation coefficient of 0.9999. The detection limit was 3.0×10^{-6} M (S/N=3). The proposed method was successfully applied to the determination of bromhexine in pharmaceutical formulations. The nanocomposite material modified Pt electrode has several advantageous such as providing improved voltammetric behavior, long-time stability and excellent reproducibility.

Multi-walled carbon nanotubes (MWCNTs) functionalized by cobalt nanoparticles were obtained using a single step chemical deposition method in an ultrasonic bath. The composite material was characterized by means of scanning electron microscopy (SEM) and energy dispersive X-ray analysis (EDX). The electroactivity of the cobalt-functionalized MWCNTs was assessed in respect to the electrooxidation of paracetamol (PAR) and dopamine (DA). It was found that the carbon nanotube supported cobalt nanoparticles have significantly higher catalytic properties. The proposed electrode has been applied for the simultaneous determination of PAR and DA. The modified electrode can resolve the overlapped

voltammetric waves of PAR and DA into two well-defined voltammetric peaks with peak to peak separation of about 203 mV. On the other hand, the presence of potential drug interfering compounds AA and UA does not affect the voltammetric responses of PAR and DA. The current of oxidation peaks showed a linear dependent on the concentrations of PAR and DA in the range of $5.2 \times 10^{-9} \sim 4.5 \times 10^{-7}$ M ($R^2 = 0.9987$) and $5.0 \times 10^{-8} \sim 3.0 \times 10^{-6}$ M ($R^2 = 0.9999$), respectively. The detection limits of 1.0×10^{-9} M and 1.5×10^{-8} M were obtained for PAR and DA, respectively. The proposed electrode showed good stability (peak current change: 4.9% with and RSD of %2.6 for PAR; 5.5% with and RSD of 3.0% for DA over 3 weeks), reproducibility (RSD 2.3% for PAR and RSD 1.5% for DA), repeatability (RSD 2.25% for PAR and RSD 2.50% for DA) and high recovery (%99.7 with an RSD of 1.3% for PAR; 100.8% with an RSD of 1.8% for DA). The proposed method was successfully applied to the determination of PAR and DA in pharmaceuticals.

A glassy carbon electrode modified with chitosan and multi-walled carbon nanotubes was also developed for a simple, sensitive and selective determination of Cd(II) and lead(II). Cd(II) and Pb(II) were preconcentrated on the surface of the modified electrode by complexing with CTS-MWCNT mixture and reduced at a negative potential (-1.2 V). Then the reduced products were oxidized by square wave anodic stripping voltammetry. The fact that two stripping peaks appeared on the voltammograms at the potentials of -1.0 V for Cd(II) and -0.72 V Pb(II) with a peak to peak separation of 280 mV demonstrates the possibility of simultaneous determination of Cd(II) and Pb(II). Under the optimized working conditions, peak currents were linear in the concentration ranges 0.1 nM-2.5 nM for Cd (II) and 0.1 nM-1.8 nM for Pb (II) in the same solution. The linear correlation coefficients were 0.9980 and 0.9987 for Cd (II) and Pb (II) respectively. The detection limits were calculated as 0.035 nM for Cd (II) and 0.030 nM for Pb (II) when the S/N was 3 for 120 s. preconcentration. The relative standard deviations (RSD)s of 10 successive measurements were 3.1 % for 2 nm Cd (II) and 2.8 % for 2 nm Pb (II). Five CTS-MWCNT/GCE examples fabricated independently were used to determine 2 nM Cd (II) and Pb (II), the RSDs were 3.5% and 3.0% respectively. The results indicated

that the reproducibility of the CTS-MWCNT/GCE was excellent. Interferences by some metals were investigated. The results indicated that 25-fold concentrations of Ca(II), Zn(II), Ni(II), Hg(II), Fe(II), Cu(II), Co(II), Mn(II) and Mg(II) had less than 3-3.5% influence on the peak current of Cd(II) and Pb(II), indicating good selectivity of the proposed method for the determination of Cd(II) and Pb(II). The recovery studies were also carried out with samples of water, human urine and nutrition.

REFERENCES

- ABDEL-GHANI, N. T., ISSA, Y. M. and AHMED, H. M., 2006. Potentiometric flow injection of bromhexine hydrochloride and its pharmaceutical preparation using conventional and coated wire ion selective electrodes. *Scientia Pharmaceutica*, 74:121–135.
- ABOUL-ENEIN, H. Y and AL-BADR, A. A., 1979. Analytical profile of methimazole. *Analytical Profiles of Drug Substances*, K. FLOREY (Ed.), Academic Press, New York, 8: 351-370.
- AJAYAN, P. M., 1999. Nanotubes from Carbon. *Chemical Review*, 99: 1787-1799.
- ALETRARI, M., KANARI, P., PARTASSIDES, D. and LOIZOU, E., 1998. Study of the British Pharmacopeia method on methimazole (thiamazole) content in carbimazole tablets. *Journal of Pharmaceutical and Biomedical Analysis*, 16: 785–792.
- ALIPOUR, E., MAJIDI, M. R., SAADATIRAD, A., GOLABI, S. M. and ALIZADEH, A. M., 2013. Simultaneous determination of dopamine and uric acid in biological samples on the pretreated pencil graphite electrode. *Electrochimica Acta*, 91: 36– 42.
- ALKIRE, R., KOLB, D. and LIPKOWSKI, J., 2009. Chemically modified electrodes, Germany: Wiley-VCH, Weinheim. Retrieved September 26, 2013, from: http://en.wikipedia.org/wiki/Chemically_modified_electrode.
- ALOTHMAN, Z. A., BUKHARI, N., WABAIDUR, S. M. and HAIDER, S., 2010. Simultaneous electrochemical determination of dopamine and acetaminophen using multiwall carbon nanotubes modified glassy carbon electrode. *Sensors and Actuators B*, 146: 314–320.
- AL-ZHOUBI, N., KOUNDOURELLIS, J. E. and MALAMATARIS, S., 2002. FT-IR and Raman spectroscopic methods for identification and quantitation of orthorhombic and monoclinic paracetamol in powder mixes. *Journal of Pharmaceutical and Biomedical Analysis*, 29: 459–467.
- Antithyroid agents, in: REYNOLDS, J. E. F. (Ed.), *Martindale, The Extra Pharmacopoeia*, 29th ed., The Pharmaceutical Press, London, 1989, pp. 682–688.
- ASLANOGLU, M. and PEKER, N., 2003. Potentiometric and voltammetric determination of methimazole. *Journal of Pharmaceutical and Biomedical Analysis*, 33: 1143–1147.
- ATTA, N. F., GALAL, A. and AHMED, R. A., 2011. Poly(3,4-ethylene-dioxythiophene) electrode for the selective determination of dopamine in presence of sodium dodecyl sulfate. *Bioelectrochemistry*, 80: 132-141.
- AVENDANO, C., ANGELES, G. A., SILVA, M. T. R., PINA, G. R., ROMO, M. R. and PARDAVE, M. P., 2007. On the electrochemistry of dopamine in aqueous solution. Part I: The role of [SDS] on the voltammetric behavior of dopamine on a carbon paste electrode. *Journal of Electroanalytical Chemistry*, 609: 17–26.
- BABAEI, A., AFRASIABI, M. and BABAZADEH, M., 2010. A glassy carbon electrode modified with multiwalled carbon nanotube/chitosan composite as a new sensor for simultaneous determination of acetaminophen and mefenamic

- acid in pharmaceutical preparations and biological samples. *Electroanalysis*, 22: 1743–1749.
- BAILEY, S. E., OLIN, T. J., BRICKA, R. M. and ADRIAN, D. D., 1999. A review of potentially low-cost sorbents for heavy metals. *Water Research*, 33: 2469–2479.
- BARROS, S. B. A., RAHIM, A., TANAKA, A. A., ARENAS, L. T., LANDERS, R. and GUSHIKEM, Y., 2013. In situ immobilization of nickel(II) phthalocyanine on mesoporous SiO₂/C carbon ceramic matrices prepared by the sol–gel method: Use in the simultaneous voltammetric determination of ascorbic acid and dopamine. *Electrochimica Acta*, 87: 140–147.
- BAZYLAK, G. and NAGELS, L. J., 2003. Simultaneous high-throughput determination of clenbuterol, ambroxol and bromhexine in pharmaceutical formulations by HPLC with potentiometric detection. *Journal of Pharmaceutical and Biomedical Analysis*, 32: 887–903.
- BEITOLLAHI, H. and SHEIKHSHOAIE, I., 2011. Electrocatalytic and simultaneous determination of isoproterenol, uric acid and folic acid at molybdenum (VI) complex-carbon nanotube paste electrode. *Electrochimica Acta*, 56: 10259–10263.
- BEITOLLAHI, H. and SHEIKHSHOAIE, I., 2012. Novel nanostructure-based electrochemical sensor for simultaneous determination of dopamine and acetaminophen. *Materials Science and Engineering: C*, 32: 375–380.
- BENVIDI, A., KAKOOLAKI, P., ZARE, H. R. and VAFAZADEH, R., 2011. Electrocatalytic oxidation of hydrazine at a Co(II) complex multi-wall carbon nanotube modified carbon paste electrode. *Electrochimica Acta*, 56: 2045–2050.
- BERKA, A., VELASEVIC, K. and NIKOLIC, K., 1989. Conductometric determination of methimazole. *Pharmazie*, 44: 499.
- British Pharmacopeia, 2000, Vol. 1, Version 4.0 Crown Copyright.
- BOYD, D., RODRIGUEZ, J. R. B., ORDIERES, A. J. M., BLANCO, P. T. and SMYTH, M. R., 1994. Voltammetric study of salbutamol, fenoterol and metaproterenol at unmodified and nafion-modified carbon-paste electrodes. *Analyst*, 119: 1979–1984.
- BRITTO, P. J., SANTHANAM, K. S. V. and AJAYAN, P. M., 1996. Carbon nanotube electrode for oxidation of dopamine. *Bioelectrochemistry and Bioenergetics*, 41:121–125.
- BULSKA, E. B., WALCERZ, M., JEDRAL, W. and HULANICK, A., 1997. On-line preconcentration of lead and cadmium for flame atomic absorption spectrometry using a flow-through electrochemical microcell. *Analytica Chimica Acta*, 357: 133–140.
- CAO, Q., ZHAO, H., YANG, Y., HE, Y., DING, N., WANG, J., ZHIJIAO, W., XIANG, K. and WANG, G., 2011. Electrochemical immunosensor for casein based on gold nanoparticles and poly(L-Arginine)/multi-walled carbon nanotubes composite film functionalized interface. *Biosensors and Bioelectronics*, 26: 3469–3474.
- CARVALHO, R. M. D., FREIRE, R. S., RATH, S. and KUBOTA, L. T., 2004. Effects of EDTA on signal stability during electrochemical detection of acetaminophen *Journal of Pharmaceutical and Biomedical Analysis*, 34 (5): 871–878.

- CASTILLO, J., GASPAR, S., LETH, S., NICULESCU, M., MORTARI, A., BONTIDEAN, I., SOUKHAREV, V., DORNEANU, S. A., RYABOV, A. D. and CSÖREGI, E., 2004. Biosensors for life quality design, development and applications. *Sensors and Actuators B-Chemical*, 102: 179-194.
- CHANDRA, U., KUMARA SWAMY, B. E., GILBERT, O. and SHERIGARA, B. S., 2010. voltammetric resolution of dopamine in the presence of ascorbic acid and uric acid at poly (calmagite) film coated carbon paste electrode. *Electrochimica Acta*, 55: 7166-7174.
- CHEN, X., ZHU, J., XI, Q. AND YANG, W., 2012. A high performance electrochemical sensor for acetaminophen based on single-walled carbon nanotube-graphene nanosheet hybrid films. *Sensors and Actuators B*, 161: 648–654.
- CHOW, E. and GOODING, J. J., 2006. Peptide modified electrodes as electrochemical metal ion sensors. *Electroanalysis*, 18: 1437–1448.
- COLIN-OROZCO, E., RAMÍREZ-SILVA, M. T., CORONA-AVENDANO, S., ROMERO-ROMO, M. and PALOMAR-PARDAVÉ, M., 2012. Electrochemical quantification of dopamine in the presence of ascorbic acid and uric acid using a simple carbon paste electrode modified with SDS micelles at pH 7. *Electrochimica Acta*, 85: 307– 313.
- CUI, R., WANG, X., ZHANG, G. and WANG, C., 2012. Simultaneous determination of dopamine, ascorbic acid, and uric acid using helical carbon nanotubes modified electrode. *Sensors and Actuators B*, 161: 1139– 1143.
- DENG, W., TAN, Y., LI, Y., WEN, Y., SU, Z., HUANG, Z., HUANG, S., MENG, Y., XIE, Q., LUO, Y. and YAO, S., 2010. Square wave voltammetric determination of Hg(II) using thiol functionalized chitosan-multiwalled carbon nanotubes nanocomposite film electrode. *Microchimica Acta*, 169: 367-373.
- DIAS, A. C. B., SANTOS, J. L. M., LIMA, J. L. F. C. and ZAGATTO, E. A. G., 2003. Multi-pumping flow system for spectrophotometric determination of bromhexine. *Analytica Chimica Acta*, 499: 107–113.
- DOL, I. and KNOCHEN, M., 2004. Flow-injection spectrophotometric determination of salbutamol with 4-aminoantipyrine. *Talanta*, 64: 1233–1236.
- DUAN, L. S., XIE, F., ZHOU, F. and WANG, S. F., 2007. The electrochemical behavior of acetaminophen on multi-walled carbon nanotubes modified electrode and its analytical application. *Analytical Letters*, 40: 2653–2663.
- EASWARAMOORTY, D., YU, Y. C. and HUANG, H. J., 2001. Chemiluminescence detection of paracetamol by a luminol-permanganate based reaction. *Analytica Chimica Acta*, 439: 95–100.
- EDWARD, A. C., 1992. Thyroid hormones and drugs that affect the thyroid, in: Smith, C. M., Reynard, A. M. (Eds.), *Text-Book of Pharmacology*, W.B. Saunders Company, Philadelphia, PA, pp. 652–656.
- ELBARDICY, M. G., ELSAHARTY, Y. S. AND TAWAKKOL, M. S., 1991. Determination of carbimazole and methimazole by first and third derivative spectrophotometry. *Spectroscopy Letters*, 24: 1079–1095.
- ELKAOUTIT, M., 2012. Application of Conducting Polymers in Electroanalysis, , Dr. Artur Motheo (Ed.), p: 43-66. InTech. Retrieved September 25, 2013, from: http://cdn.intechopen.com/pdfs/26618/InTech-Application_of_conducting_polymers_in_electroanalysis.pdf.

- EL-GINDY, A., EMARA, S. and SHAABAN, H., 2007. Development and validation of chemometrics-assisted spectrophotometric and liquid chromatographic methods for the simultaneous determination of two multicomponent mixtures containing bronchodilator drugs. *Journal of Pharmaceutical and Biomedical Analysis*, 43: 973–982.
- ENSAFI, A. A., KARIMI-MALEH, H., MALLAKPOUR, S. and HATAMI, M., 2011. Simultaneous determination of N-acetylcysteine and acetaminophen by voltammetric method using N-(3,4-dihydroxyphenethyl)-3,5-dinitrobenzamide modified multiwall carbon nanotubes paste electrode. *Sensors and Actuators B*, 155: 464–472.
- ENSAFI, A. A., TAEI, M. and KHAYAMIAN, T., 2009. Differential pulse voltammetric method for simultaneous determination of ascorbic acid, dopamine and uric acid using poly(3-(5-chloro-2-hydroxyphenylazo)-4,5-dihydroxynaphthalene-2,7-disulfonic acid) film modified glassy carbon electrode. *Journal of Electroanalytical Chemistry*, 633: 212–220.
- FAN, Y., LIU, J. H., LU, H. T. and ZANG, Q., 2011. Electrochemical behavior and voltammetric determination of paracetamol on Nafion/TiO₂-graphene modified glassy carbon electrode. *Colloids and Surfaces B: Biointerfaces*, 85: 289–292.
- FANJUL-BOLADO, P., LAMAS-ARDISANA, P. J., HERNANDEZ-SANTOS, D. And COSTA-GARCIA, A., 2009. Electrochemical study and flow injection analysis of paracetamol in pharmaceutical formulations based on screen-printed electrodes and carbon nanotubes. *Analytica Chimica Acta*, 638: 133–138.
- FATHIRAD, F., AFZALI, D., MOSTAFAVI, A., SHAMSPUR, T. and FOZOONI, S., 2013. Fabrication of a new carbon paste electrode modified with multi-walled carbon nanotube for stripping voltammetric determination of bismuth(III). *Electrochimica Acta*, 103: 206–210.
- FEI, J., WEN, X., YI, L., GE, F., ZHANG, Y., HUANG, M. and CHEN, X., 2008. Electrochemical determination diethylstilbestrol by a single-walled carbon nanotube/Platinum nanoparticle composite film electrode. *Journal of Applied Electrochemistry*, 38:1527–1533.
- FISCHER, E. and BERG, C. M. G., 1999. Anodic stripping voltammetry of lead and cadmium using a mercury film electrode and thiocyanate. *Analytica Chimica Acta*, 385: 273-280.
- GANJALI, M. R., NOROUZI, P., GHORBANI, M. and SEPEHRI, A., 2005. Fourier transform cyclic voltammetric technique for monitoring ultratrace amounts of salbutamol at gold ultra microelectrode in flowing solutions. *Talanta*, 66: 1225–1233.
- GAO, X., WEI, W., YANG, L. and GUO, M., 2006. Carbon nanotubes/poly(1,2-diaminobenzene) nanoporous composite film electrode prepared by multipulse potentiostatic electropolymerisation and its application to determination of trace heavy metal ions. *Electroanalysis* 18 (5): 485-492.
- GARCIA, M. S., ALBERO, M. I., SANCHEZPEDRENO, C. and TOBAL, L., 1995. Kinetic determination of carbimazole, methimazole and propylthiouracil in pharmaceuticals, animal feed and animal livers. *Analyst*, 120: 129–133.

- GETO, A., PITA, M., DE LACEY, A. L., TESSEMA, T. and ADMASSIE, S., 2013. Electrochemical determination of berberine at a multi-walled carbon nanotubes-modified glassy carbon electrode. *Sensors and Actuators-B*, 183 (5): 96–101.
- GHOLIVAND, M. B. and AMIRI, M., 2012. Simultaneous detection of dopamine and acetaminophen by modified gold electrode with polypyrrole/azophloxine film. *Journal of Electroanalytical Chemistry*, 676: 53–59.
- GHORBANI-BIDKORBEH, F., SHAHROKHIAN, S., MOHAMMAD, A. and DINARVAND, R., 2010. Simultaneous voltammetric determination of tramadol and acetaminophen using carbon nanoparticles modified glassy carbon electrode. *Electrochimica Acta*, 55: 2752–2759.
- GHORBANI-BIDKORBEH, F., SHAHROKHIAN, S., MOHAMMAD, A. and DINARVAND, R., 2010. Simultaneous voltammetric determination of tramadol and acetaminophen using carbon nanoparticles modified glassy carbon electrode. *Electrochimica Acta*, 55: 2752–2759.
- GOODING, J. J., 2005. Nanostructuring electrodes with carbon nanotubes: a review on electrochemistry and applications for sensing. *Electrochimica Acta*, 50: 3049–3060.
- GOODING, J. J., 2008. Advances in interfacial design for electrochemical biosensors and sensors: aryl diazonium salts for modifying carbon and metal electrodes. *Electroanalysis*, 20: 573–582.
- GÖRÖG, S., 2008. Drug safety, drug quality, drug analysis. *Journal of Pharmaceutical and Biomedical Analysis*, 48: 247–253.
- GOYAL, R. N., OYAMA, M., GUPTA, V. K., SINGH, S. P. and SHARMA, R. A., 2008. Sensors for 5-hydroxytryptamine and 5-hydroxyindole acetic acid based on nanomaterial modified electrodes. *Sensors and Actuators B: Chemical*, 134 (2): 816–821.
- GOYAL, R. N. and SINGH, S. P., 2006. Voltammetric determination of paracetamol at C60-modified glassy carbon electrode. *Electrochimica Acta*, 51: 3008–3012.
- GOYAL, R. N., KAUR, D., SINGH, S. P. and PANDEY, A. K., 2008. Effect of graphite and metallic impurities of C60 fullerene on determination of salbutamol in biological fluids. *Talanta*, 75: 63–69.
- GOYAL, R. N., BISHNOI, S. and AGRAWAL, B., 2011. Single-walled-carbon-nanotube-modified pyrolytic graphite electrode used as a simple sensor for the determination of salbutamol in urine. *International Journal of Electrochemistry*, <http://dx.doi.org/10.4061/2011/373498>.
- GOYAL, R. N., OYAMA, M. and SINGH, S.P., 2007. Fast determination of salbutamol, abused by athletes for doping, in pharmaceuticals and human biological fluids by square wave voltammetry. *Journal of Electroanalytical Chemistry*, 611: 140–148.
- GRANGE, J. M. and SNELL, N. J., 1996. Activity of bromhexine and ambroxol, semi-synthetic derivatives of vasicine from the Indian shrub *Adhatoda vasica*, against *Mycobacterium tuberculosis* in vitro. *Journal of Ethnopharmacology*, 50: 49–53.

- GRIESE, S., KAMPOURIS, D. K., KADARA, R. O. and BANKS, C. E., 2008. A critical review of the electrocatalysis reported at C-60 modified electrodes. *Electroanalysis*, 20: 1507–1512.
- GUIBAL, E., 2004. Interactions of metal ions with chitosan-based sorbents: A review. *Separation and Purification Technology*, 38: 43-74.
- GUPTA, V. K., JAIN, A. K. and SHOORA, S. K., 2013. Multiwall carbon nanotube modified glassy carbon electrode as voltammetric sensor for the simultaneous determination of ascorbic acid and caffeine. *Electrochimica Acta*, 93: 248–253.
- HABIB, I. H. I., HASSOUNA, M. E. M. and ZAKI, G. A., 2005. Simultaneous Spectrophotometric Determination of Salbutamol and .Bromhexine in Tablets II *Farmaco*, 60: 249–254.
- HABIBI, B., JAHANBAKHSI, M. and AZAR, M. H. P., 2011. Differential pulse voltammetric simultaneous determination of acetaminophen and ascorbic acid using single-walled carbon nanotube-modified carbon–ceramic electrode. *Analytical Biochemistry*, 411: 167–175.
- HABIBI, B., JAHANBAKHSI, M. and POURNAGHI-AZAR, M. H., 2011. Simultaneous determination of acetaminophen and dopamine using SWCNT modified carbon–ceramic electrode by differential pulse voltammetry. *Electrochimica Acta*, 56: 2888–2894.
- HADDON, R. C., 2002. Carbon nanotubes. *Accounts of Chemical Research*, 35: 977-981.
- HANAEE, J., 1997. Simultaneous determination of acetaminophen and codeine in pharmaceutical preparations by derivative spectrophotometry. *Pharmaceutica Acta Helveticae*, 72: 239–241.
- HARISH, S., MATHIYARASU, J., PHANI, K. L. N. and YEGNARAMAN, V., 2008. PEDOT/Palladium composite material: synthesis, characterization and application to simultaneous determination of dopamine and uric acid. *Journal of Applied Electrochemistry*, 38: 1583–1588.
- HENSTRIDGE, M. C., DICKINSON, E. J. F., ASLANOGLU, M., BATCHELOR-MCAULEY, C. and COMPTON, R. G., 2010. Voltammetric selectivity conferred by the modification of electrodes using conductive porous layers or films: The oxidation of dopamine on glassy carbon electrodes modified with multiwalled carbon nanotubes. *Sensors and Actuators B*, 145: 417–427.
- HRAPOVIC, S., MAJID, E., LIU, Y., MALE, K. and LUONG, J. H. T., 2006. Metallic nanoparticle-carbon nanotube composites for electrochemical determination of explosive nitroaromatic compounds. *Analytical Chemistry*, 78: 5504-5512.
- HU, C., WU, K., DAI, X. and HU, S., 2003. Simultaneous determination of lead(II) and cadmium(II) at a diacetyldioxime modified carbon paste electrode by differential pulse stripping voltammetry. *Talanta*, 60: 17-24.
- HU, Y. F., ZHANG, Z. H., ZHANG, H. B., LUO, L. J. and YAO, S. Z., 2011. Electrochemical determination of L-phenylalanine at polyaniline modified carbon electrode based on β -cyclodextrin incorporated carbon nanotube composite material and imprinted sol–gel film. *Talanta*, 84: 305–313.
- HU, Y., ZHANG, Z., LI, J., ZHANG, H., LUO, L. and YAO, S., 2012. Electrochemical imprinted sensor for determination of oleanic acid based on poly (sodium 4-styrenesulfonate-co-acrylic acid)-grafted multi-walled carbon

- nanotubes-chitosan and cobalt hexacyanoferrate nanoparticles. *Biosensors and Bioelectronics*, 31: 190-196.
- HUANG, K. J., LIU, X., XIE, W. Z. and YUAN, H. X., 2008. Electrochemical behavior and voltammetric determination of norfloxacin at glassy carbon electrode modified with multi walled carbon nanotubes/Nafion. *Colloids and Surfaces B: Biointerfaces* 64: 269-274.
- HUANG, J., LIN, Q., ZHANG, X., HE, X., XING, X., LIAN, W., ZUO, M. and ZHANG, Q., 2011. Electrochemical immunosensor based on polyaniline/poly (acrylic acid) and Au-hybrid graphene nanocomposite for sensitivity enhanced detection of salbutamol. *Food Research International*, 44: 92–97.
- HWANG, G. H., HAN, W. K., PARK, J. S. and KANG, S. G., 2008. Determination of trace metals by anodic stripping voltammetry using a bismuth-modified carbon nanotube electrode. *Talanta*, 76: 301-308.
- JAIN, R. and SHARMA, S., 2012. Glassy carbon electrode modified with multi-walled carbon nanotubes sensor for the quantification of antihistamine drug pheniramine in solubilized systems. *Journal of Pharmaceutical Analysis*, 2: 56–61.
- JANEGITZA, B. C., MARCOLINO-JUNIOR, B. L. H., CAMPANA-FILHOC, S. P., FARIAA, R. C. and FATIBELLO-FILHOA, O., 2009. Anodic stripping voltammetric determination of copper(II) using a functionalized carbon nanotubes paste electrode modified with crosslinked chitosan. *Sensors and Actuators- B*, 142: 260-266.
- JÄRUP, L., 2003. Hazards of heavy metal contamination. *British medical bulletin*, 68: 167-182.
- JENSEN, B. P., GAMMELGAARD, B., HANSEN, S. H. and ANDERSEN, J. V., 2005. HPLC-ICP-MS compared with radiochemical detection for metabolite profiling of 3H-bromohexine in rat urine and faeces. *Journal of Analytical Atomic Spectrometry*, 20: 204–209.
- JIA, X., LI, J. and WANG, E., 2010. High-sensitivity determination of Lead(II) and Cadmium(II) based on the CNTS-PSS/Bi composite film electrode. *Electroanalysis*, 22 (15): 1682-1687.
- JONES, S. E. W. and COMPTON, R. G., 2008. Fabrication and applications of nanoparticle-modified electrodes in stripping analysis. *Current Analytical Chemistry*, 4: 177-182.
- JR. BARBOSA, F., KRUG, F. J. and LIMA, E. C., 1999. On-line coupling of electrochemical preconcentration in tungsten coil electrothermal atomic absorption spectrometry for determination of lead in natural waters. *Spectrochimica Acta Part B: Atomic Spectroscopy*, 54: 1155-1166.
- KACHOOSANGI, R. T. and COMPTON, R. G., 2007. A simple electroanalytical methodology for the simultaneous determination of dopamine, serotonin and ascorbic acid using an unmodified edge plane pyrolytic graphite electrode. *Analytical and Bioanalytical Chemistry*, 387: 2793–2800.
- KACHOOSANGI, R. T., WILDGOOSE, G. G. and COMPTON, R. G., 2008. Carbon nanotube-based electrochemical sensors for quantifying the 'heat' of chilli peppers: the adsorptive stripping voltammetric determination of capsaicin. *Analyst*, 133: 888–895.

- KACHOOSANGI, R. T., WILDGOOSE, G. G. and COMPTON, R. G., 2008. Chemically modified carbon nanotubes for use in electroanalysis. *Analytica Chimica Acta*, 618: 54-60.
- KACHOOSANGI, R. T., WILDGOOSE, G. G. and COMPTON, R. G., 2008. Sensitive adsorptive stripping voltammetric determination of paracetamol at multiwalled carbon nanotube modified basal plane pyrolytic graphite electrode. *Analytica Chimica Acta*, 618: 54-60.
- KANG, X., WANG, J., WU, H., LIU, J., AKSAY, I. A. and LIN, Y., 2010. A graphene-based electrochemical sensor for sensitive detection of paracetamol. *Talanta*, 81: 754-759.
- KARUWAN, C., WISITSORAAT, A., MATUROS, T., PHOKHARATKUL, D., SAPPAT, A., JARUWON-GRUNGSEE, K., LOMAS, T. and TUANTRANONT, A., 2009. Flow injection based microfluidic device with carbon nanotube electrode for rapid salbutamol detection. *Talanta*, 79: 995-1000.
- KEELEY, G. P. and LYONS, M. E. G., 2009. The Effects of Thin Layer Diffusion at Glassy Carbon Electrodes Modified with Porous Films of Single-Walled Carbon Nanotubes. *International Journal of Electrochemical Science*, 4: 794-809.
- KNOCHEN, M., GIGLIO, J. and REIS, B. F., 2003. Flow-injection spectrophotometric determination of paracetamol in tablets and oral solutions. *Journal of Pharmaceutical and Biomedical Analysis*, 33: 191-197.
- KOOLE, A., BOSMAN, J., FRANKE, J. P. and DE-ZEEUN, R. A., 1999. On-column derivatization for the analysis of homocysteine and other thiols by capillary electrophoresis with laser-induced fluorescence detection. *Journal of Chromatography B*, 726: 149-156.
- KOUNAVES, S. P., *Voltammetric Techniques. Handbook of Instrumental Techniques for Analytical Chemistry*, Tufts University. Department of Chemistry, page: 701.
- KUMAR, S. A., TANG, C. F. and CHEN, S. M., 2008. Electroanalytical determination of acetaminophen using nano-TiO₂/polymer coated electrode in the presence of dopamine. *Talanta*, 76: 997-1005.
- LAI, G. S., ZHANG, H. L. and HAN, D. Y., 2008. Electrocatalytic oxidation and voltammetric determination of dopamine at a Nafion/carbon-coated iron nanoparticles-chitosan composite film modified electrode. *Microchimica Acta*, 160: 233-239.
- LAOCHAROENSUK, R., BULBARELLO, A., HOCEVAR, S. B., MANNINO, S., OGOREVC, B. and WANG, J., 2007. On-demand protection of electrochemical sensors based on adaptive nanowires. *Journal of the American Chemical Society*, 129: 7774-7775.
- LAU, O. W. and CHEUNG, Y. M., 1990. Simultaneous determination of some active ingredients in cough-cold syrups by gas-liquid chromatography. *Analyst*, 115: 1349-1353.
- LI, J., KUANG, D., FENG, Y., ZHANG, F. and LIU, M., 2011. Voltammetric determination of bisphenol-A in food package by a glassy carbon electrode modified with carboxylated multi-walled carbon nanotubes. *Microchimica Acta*, 172: 379-386.

- LI, M. and JING, L., 2007. Electrochemical behavior of acetaminophen and its detection on the PANI–MWCNTs composite modified electrode.
- LI, N. B., REN, W. and LUO, H. Q., 2008. Simultaneous voltammetric measurement of ascorbic acid and dopamine on poly (caffeic acid)-modified glassy carbon electrode. *Journal of Solid State Electrochemistry*, 12: 693-699.
- LI, X., CHEN, Z., ZHONG, Y., YANG, F., PAN, J. and LIANG, Y., 2012. Cobalt hexacyanoferrate modified multi-walled carbon nanotubes/ graphite composite electrode as electrochemical sensor on microfluidic chip *Analytica Chimica Acta*, 710: 118–124.
- LI, Y., DU, J., YANG, J., LIU, D., LU, X., LI, Y., DU, J., YANG, J., LIU, D. and LU, X., 2012. Electrocatalytic detection of dopamine in the presence of ascorbic acid and uric acid using single-walled carbon nanotubes modified electrode. *Colloids and Surfaces B*, 97: 32– 36.
- LIJIMA, S., 1991. Helical microtubules of graphitic carbon. *Nature*, 354: 56-58.
- LIJIMA, S. and ICHIHASHI, T., 1993. Single-shell carbon nanotubes of 1-nm diameter. *Nature*, 363: 603-605.
- LIJUN, L., LAIBO, Y., HAO, C., QIFENG, C., FENGMIN, W., TIAN, C., XIAOYONG, Z., HONGXING, K. and JIANLING, W., 2007. The determination of salbutamol sulfat based on a flow injection coupling irreversible biamperometry at poly(aminosulfonic acid) modified glassy carbon electrode. *Analytical Letters*, 40: 3290–3308.
- LIN, J., HE, C., ZHANG, L. and ZHANG, S., 2009. Sensitive amperometric immunosensor for α -fetoprotein based on carbon nanotube/gold nanoparticle doped chitosan film. *Analytical Biochemistry* 384: 130–135.
- LINDINO, A. and BULHOES, L. O. S., 2007. Determination of fenoterol and salbutamol in pharmaceutical formulations by electrogenerated chemiluminescence. *Talanta*, 72: 1746–1751.
- LIU, A. L., WANG, K., CHEN, W., GAO, F., CHAI, Y. S., LIN, X. H., CHEN, Y. Z. and XIA, X. H., 2012. Simultaneous and sensitive voltammetric determination of acetaminophen and its degradation product for pharmaceutical quality control and pharmacokinetic research by using ultrathin poly (calconcarboxylic acid) film modified glassy carbon electrode. *Electrochimica Acta*, 63: 161–168.
- LIU, H., WANG, G., CHEN, D., ZHANG, W., LI, C. and FANG, B., 2008. Fabrication of polythionine/NPAu/MWNTs modified electrode for simultaneous determination of adenine and guanine in DNA. *Sensors and Actuators B*, 128: 414-421.
- LIU, S. Q., SUN, W. H. and HU, F. T., 2012. Graphene nano sheet-fabricated electrochemical sensor for the determination of dopamine in the presence of ascorbic acid using cetyltrimethylammonium bromide as the discriminating agent. *Sensors and Actuators B*, 173: 497– 504.
- LOCKE, C. J., FOX, S. A., CALDWELL, G. A. and CALDWELL, K. A., 2008. Acetaminophen attenuates dopamine neuron degeneration in animal models of Parkinson's disease. *Neuroscience Letters*, 439: 129-133.
- LÛ, S., 2003. Voltammetric determination of 1-naphthylacetic acid in soil samples using carbon nanotubes film modified electrode. *Analytical Letters*, 36 (8): 1523-1534.

- LU, S., 2004. Electrochemical determination of 8-azaguanine in human urine at a multi-carbon nanotubes modified electrode. *Microchemical Journal*, 77: 37–42.
- LU, T. H., YANG, H. Y. and SUN, I. W., 1999. Square-wave anodic stripping voltammetric determination of thallium(I) at a Nafion/mercury film modified electrode. *Talanta*, 49: 59-68.
- LU, T. L. and TSAI, Y. C., 2011. Sensitive electrochemical determination of acetaminophen in pharmaceutical formulations at multiwalled carbon nanotube-alumina-coated silica nanocomposite modified electrode. *Sensors and Actuators B*, 153: 439–444.
- LUO, H., SHI, Z., LI, N., GU, Z. and ZHUANG, Q., 2001. Investigation of the electrochemical and electrocatalytic behavior of single-wall carbon nanotube film on a glassy carbon electrode. *Analytical Chemistry*, 73: 915-920.
- LUO, J. H., JIAO, X. X., LI, N. B. and LUO, H. Q., 2013. Sensitive determination of Cd(II) by square wave anodic stripping voltammetry with in situ bismuth-modified multiwalled carbon nanotubes doped carbon paste electrodes. *Journal of Electroanalytical Chemistry*, 689: 130–134.
- MANJUNATHA, R., NAGARAJU, D. H., SURESH, G. S., MELO, J. S., D'SOUZA, S. F. and VENKATE-SHA, T. V., 2011. Electrochemical detection of acetaminophen on the functionalized MWCNTs modified electrode using layer-by-layer technique. *Electrochimica Acta*, 56: 6619–6627.
- MANJUNATHA, R., NAGARAJU, D. H., SURESH, G. S., MELO, J. S., D'SOUZA, S. F. and VENKATESHA, T. V., 2011. Direct electrochemistry of cholesterol oxidase on MWCNTs. *Journal of Electroanalytical Chemistry*, 651: 24–29.
- MARCOLINO-JUNIOR, L. H., JANEGITZ, B. C., LOURENÇÃO, B. C. and FATIBELLO-FILHO, O., 2007. Anodic stripping voltammetric determination of mercury in water using a chitosan-modified carbon paste electrode. *Analytical Letters*, 40: 3119-3128.
- MARTIN, F. L. and MACLEAN, A. E., 1998. Comparison of paracetamol-induced hepatotoxicity in the rat in vivo with progression of cell injury in vitro in rat liver slices. *Drug and Chemical Toxicology*, 21: 477–494.
- MARTINEZ, N. A., MESSINA, G. A., BERTOLINO, F. A., SALINAS, E. and RABA, J., 2008. Screen-printed enzymatic biosensor modified with carbon nanotube for the methimazole determination in pharmaceuticals formulations. *Sensors and Actuators B*, 133: 256–262.
- MAZLOUM-ARDAKANI, M., BEITOLLAHI, H., AMINI, M. K., MIRKHALAF, F. and ABDOLLAHI-ALIBEIK, M., 2010. New strategy for simultaneous and selective voltammetric determination of norepinephrine, acetaminophen and folic acid using ZrO₂ nanoparticles-modified carbon paste electrode. *Sensors and Actuators B*, 151: 243-249.
- MERRIFIELD, J. D., DAVIDS, W. G., MACRAE, J. D. and AMIRBAHMAN, A., 2004. Uptake of mercury by thiol-grafted chitosan gel beads. *Water Research*, 38: 3132-3138.
- MORAES, F. C., CABRAL, M. F., MACHADO, S. A. S. and MASCARO, L. H., 2008. Electrocatalytic behavior of glassy carbon electrodes modified with multiwalled carbon nanotubes and cobalt phthalocyanine for selective analysis of dopamine in presence of ascorbic acid. *Electroanalysis*, 20: 851–857.

- MORETTI, G., BETTO, P., CAMMARATA, P., FRACASSI, F., GIAMBENEDETTI, M. and BORGHESE, A., 1993. Determination of thyreostatic residues in cattle plasma by high-performance liquid chromatography with ultraviolet detection. *Journal of Chromatography: Biomedical Applications*, 616: 291–296.
- MUSAMEH, M., WANG, J., MERKOCI, A. and LIN, Y., 2002. Low-potential stable NADH detection at carbon-nanotube-modified glassy carbon electrodes. *Electrochemistry Communications*, 4: 743–746.
- NASIRIZADEH, N., SHEKARI, Z., ZARE, H. R. and MAKAREM, S., 2013. Electrocatalytic determination of dopamine in the presence of uric acid using an indenedione derivative and multiwall carbon nanotubes spiked in carbon paste electrode. *Material and Science Engineering C*, 33: 1491–1497.
- NGAH, W. S. W., ENDUD, C. S. and MAYANAR, R., 2002. Removal of copper(II) ions from aqueous onto chitosan and crosslinked chitosan beads. *Reactive and Functional Polymer*, 50: 181-190.
- NIKOLIC, K. and VELASEVIC, K., 1987. Coulometric determination of methimazole. *Pharmazie*, 42: 698.
- ODOM, T. W., HUANG, J. L., KIM, P. and LIEBER, C. M., 1998. Atomic structure and electronic properties of single-walled carbon nanotubes. *Nature*, 391: 62-62.
- OHNUKI, Y., OHSAKA, T., MATSUDA, H. and OYAMA, N., 1983. Permselectivity of films prepared by electrochemical oxidation of phenol and amino-aromatic compounds. *Journal of Electroanalytical Chemistry*, 158: 55–67.
- OKAMOTO, H., NAKAJIMA, T., ITO, Y., AKETO, T., SHIMADA, K. and YAMATO, S., 2005. Simultaneous determination of ingredients in a cold medicine by cyclodextrin-modified microemulsion electrokinetic chromatography. *Journal of Pharmaceutical and Biomedical Analysis*, 37: 517–528.
- PADIGI, S. K., REDDY, R. K. K. and PRASAD, S., 2007. Carbon nanotube based aliphatic hydrocarbon sensor. *Biosensors and Bioelectronics*, 22: 829-837.
- PAN, M., FANG, G., DUAN, Z., KONG, L. and WANG, S., 2012. Electrochemical sensor using methimazole imprinted polymer sensitized with MWCNTs and Salen-Co(III) as recognition element. *Biosensors and Bioelectronics*, 31: 11–16.
- PARVEZ, L., VAIDYA, M., SAKHARDANDE, A., SUBBURAJ, S. and RAJAGOPALAN, T. G., 1996. Evaluation of antitussive agents in man. *Pulmonary Pharmacology*, 9: 299–308.
- PICHON, A., VENISSE, N., KRUPKA, E., PERAULT-POCHAT, M. C. and DENJEAN, A., 2006. Urinary and blood concentrations of beta-2-agonists in trained subject: comparison between routes of use. *International Journal of Sports Medicine*, 27: 187–192.
- PINZANTI, S., PAPESCHI, G. and LAPORTA, E., 1983. Potentiometric titration of thiols, cationic surfactants and halides using a solid-state silver-silver sulphide electrode. *Journal of Pharmaceutical and Biomedical Analysis*, 1: 47–53.
- POSPISILOVA, M., POLASEK, M. and JOKL, V. J., 2001. Determination of ambroxol or bromhexine in pharmaceuticals by capillary isotachopheresis. *Journal of Pharmaceutical and Biomedical Analysis*, 24: 421–428.

- QUITINO, M. S. M. and ANGNES, L., 2004. Bia-amperometric quantification of salbutamol in pharmaceutical products. *Talanta*, 62: 231–236.
- QU, R., SUN, C., MA, F., ZHANG, Y., JI, C., XU, Q., WANG, C. and CHEN, H., 2009. Removal and recovery of Hg(II) from aqueous solution using chitosan-coated cotton fibers. *Journal of Hazardous Materials*, 167: 717–727.
- QU, W., WU, K. and HU, S., 2004. Voltammetric determination of pyridoxine (Vitamin B6) by use of a chemically-modified glassy carbon electrode. *Journal of Pharmaceutical and Biomedical Analysis*, 36: 631–635.
- RAN, X. Q., YUAN, R., CHAI, Y. Q., HONG, C. L. and QIAN, X. Q., 2010. A sensitive amperometric immunosensor for alpha-fetoprotein based on carbon nanotube/DNA/Thi/nano-Au modified glassy carbon electrode. *Colloids and Surfaces B: Biointerfaces*, 79: 421–426.
- RAO, G. P., LU, C. and SU, F., 2007. Sorption of divalent metal ions from aqueous solution by carbon nanotubes: A review. *Separation and Purification Technology*, 58: 224–231.
- RAVINSANKAR, S., VASUDEVAN, M., GANDHIMATHI, M. and SURESH, B., 1998. Reversed-phase HPLC method for the estimation of acetaminophen, ibuprofen and chlorzoxazone in formulations. *Talanta*, 46: 1577–1581.
- RAZMI, H. and HABIBI, E., 2010. Amperometric detection of acetaminophen by an electrochemical sensor based on cobalt oxide nanoparticles in a flow injection system. *Electrochimica Acta*, 55: 8731–8737.
- REZAEI, B. and ZARE, Z. M., 2008. Modified glassy carbon electrode with multiwall carbon nanotubes as a voltammetric sensor for determination of leucine in biological and pharmaceutical samples. *Analytical Letters*, 41: 2267–2286.
- RODRIGUEZ, M. C., SANDOVAL, J., GALICIA, L., GUTIERREZ, S. and RIVAS, G. A., 2008. Highly selective determination of uric acid in the presence of ascorbic acid at glassy carbon electrodes modified with carbon nanotubes dispersed in polylysine. *Sensors and Actuators B*, 134: 559–565.
- ROY, P. R., OKAJIMA, T. and OHSAKA, T., 2003. Simultaneous electroanalysis of dopamine and ascorbic acid using poly (N,N-dimethylaniline)-modified electrodes. *Bioelectrochemistry*, 59: 11–19.
- RUBIANES, M. D. and RIVAS, G. A., 2007. Dispersion of multi-wall carbon nanotubes in polyethylenimine: a new alternative for preparing electrochemical sensors. *Electrochemistry Communications*, 9: 480–484.
- SAGAR, K. A., SMYTH, M. R. and MUNDEN, R., 1993. Voltammetric study of salbutamol and application to its determination in a tablet dosage form and dissolution profiles for the dosage form. *Journal of Pharmaceutical and Biomedical Analysis*, 11: 533–540.
- SALIMI, A., HALLAJ, R. and KHAYATIAN, G. R., 2005. Amperometric detection of morphine at preheated glassy carbon electrode modified with multiwall carbon nanotubes. *Electroanalysis*, 17 (10): 873–879.
- SANDULESCU, R., CRISTEA, C., HARCEAGA V. and BODOKI, E., 2011. Electrochemical sensors and biosensors for the pharmaceutical and environmental analysis. *Environmental Biosensors*, Prof. Vernon Somerset (Ed.), ISBN: 978-953-307-486-3 p:277:304. InTech. Retrieved September 25, 2013, from: <http://www.intechopen.com/books/environmental->

- biosensors/electrochemical-sensors-and-biosensors-for-the-pharmaceutical- and-environmental-analysis.
- SANGHAVI, B. J. and SRIVASTAVA, A. K., 2010. Simultaneous voltammetric determination of acetaminophen, aspirin and caffeine using an in situ surfactant-modified multiwalled carbon nanotube paste electrode. *Electrochimica Acta*, 55: 8338–8648.
- SANGHAVI, B. J. and SRIVASTAVA, A. K., 2011. Simultaneous voltammetric determination of acetaminophen and tramadol using Dowex50wx2 and gold nanoparticles modified glassy carbon paste electrode. *Analytica Chimica Acta*, 706: 246–254.
- SANCHEZPEDRENO, C., ALBERO, M. I., GARCIA, M. S. and RODENAS, V., 1995. Flow-injection spectrophotometric determination of carbimazole and methimazole. *Analytica Chimica Acta* 308: 457–461.
- SATINSKY, D., KARLICEK, R. and SVOBODA, A., 2002. Using on-line solid phase extraction for flow-injection spectrophotometric determination of salbutamol. *Analytica Chimica Acta*, 455: 103–109.
- SELVARAJU, T. and RAMARAJ, R., 2003. Simultaneous determination of dopamine and serotonin in the presence of ascorbic acid and uric acid at poly(o-phenylenediamine) modified electrode. *Journal of Applied Electrochemistry*, 33: 759–762.
- SHAHROKHIAN, S., GHALKHANI, M., ADELI, M. and AMINI, M. K., 2009. Multi-walled carbon nanotubes with immobilised cobalt nanoparticle for modification of glassy carbon electrode: Application to sensitive voltammetric determination of thioridazine. *Biosensors and Bioelectronics*, 24: 3235–3241.
- SHAHROKHIAN, S. and MEHRJARDI, H. R. Z., 2007. Simultaneous voltammetric determination of uric acid and ascorbic acid using a carbon-paste electrode modified with multi-walled carbon nanotubes/nafion and cobalt (II) nitrosalophen. *Electroanalysis*, 19 (21): 2234–2242.
- SHAHROKHIAN, S. and GHALKHANI, M., 2008. Voltammetric determination of methimazole using a carbon paste electrode modified with a schiff base complex of cobalt. *Electroanalysis*, 20: 1061–1066.
- SHAHROKHIAN, S. and ASADIAN, E., 2009. Electrochemical determination of L-dopa in the presence of ascorbic acid on the surface of the glassy carbon electrode modified by a bilayer of multi-walled carbon nanotube and polypyrrole doped with tiron. *Journal of Electroanalytical Chemistry*, 636:40–46.
- SHAHROKHIAN, S. and ASADIAN, E., 2010. Simultaneous voltammetric determination of ascorbic acid, acetaminophen and isoniazid using thionine immobilized multi-walled carbon nanotube modified carbon paste electrode. *Electrochimica Acta*, 55: 666–672.
- SHAMS, E., BABAEI, A., TAHERI, A. R. and KOOSHKI, M., 2009. Voltammetric determination of dopamine at a zirconium phosphated silica gel modified carbon paste electrode. *Bioelectrochemistry*, 75: 83–88.
- SHANGGUAN, X., ZHANG, H. and ZHENG, J., 2008. Investigation on electrochemical behaviors and differential pulse voltammetric determination of paracetamol at carbon ionic liquid electrode. *Analytical and Bioanalytical Chemistry*, 391: 1049–1055.

- SHEN, Q. and WANG, X., 2009. Simultaneous determination of adenine, guanine and thymine based on β -cyclodextrin/MWNTs modified electrode. *Journal of Electroanalytical Chemistry*, 632: 149–153.
- SILVA, M. L. S., GARCIA, M. B. Q., LIMA, J. L. F. C. and BARRADO, E., 2006. Flow system with electrochemical detection for determination of paracetamol in pharmaceutical preparations *Portugaliae Electrochimica Acta*, 24: 261–271.
- SILVA, M. L. S., GARCIA, M. B. Q., LIMA, J. L. F. C. and BARRADO, E., 2006. Modified tubular electrode in a multi-commutated flow system: Determination of acetaminophen in blood serum and pharmaceutical formulations. *Analytica Chimica Acta*, 573–574: 383–390.
- SINNOTT, S. B., 2002. Chemical functionalization of carbon nanotubes. *Journal of Nanoscience and Nanotechnology*, 2: 113–123.
- SIRICHAI, S. and KHANATHARANA, P., 2008. Rapid analysis of clenbuterol, salbutamol, procaterol, and fenoterol in pharmaceuticals and human urine by capillary electrophoresis. *Talanta*, 76: 1194–1198.
- SONG, J. C., YANG, J., ZENG, J. F., TAN, J. and ZHANG, L., 2011. Graphite oxide film-modified electrode as an electrochemical sensor for acetaminophen. *Sensors and Actuators B*, 155: 220–225.
- SPYRIDAKI, M. H., KIOUSI, P., VONAPARTI, A., VALAVANI, P., ZONARAS, V., ZAHARIOU, M., SIANOS, E., TSOUPRAS, G. and GEORGAKOPOULOS, C., 2006. Doping control analysis in human urine by liquid chromatography–electrospray ionization ion trap mass spectrometry for the Olympic Games Athens 2004: Determination of corticosteroids and quantification of ephedrine, salbutamol and morphine. *Analytica Chimica Acta*, 573: 242–249.
- STREETER, I., WILDGOOSE, G. G., SHAO, L. and COMPTON, R. G., 2008. Cyclic voltammetry on electrode surfaces covered with porous layers: An analysis of electron transfer kinetics at single-walled carbon nanotube modified electrodes. *Sensors and Actuators B-Chemical*, 133: 462–466.
- STREETER, I., XIAO, L., WILDGOOSE, G. G. and COMPTON, R. G., 2008. Gold nanoparticle-modified carbon nanotubes-modified electrodes. Using voltammetry to measure the total length of the nanotubes. *Journal of Physical Chemistry C*, 112: 1933–1937.
- SU, W. Y. and CHENG, S. H., 2010. electrochemical oxidation and sensitive determination of acetaminophen in pharmaceuticals at poly (3,4-ethylene-dioxythiophene)- modified screen- printed electrodes. *Electroanalysis*, 22: 707–714.
- SUN, D. and SUN, Z., 2008. Electrochemical determination of Pb^{2+} using a carbon nanotube/Nafion composite film-modified electrode. *Journal of Applied Electrochemistry*, 38: 1223–1227.
- SUN, D. and ZHANG, H. J., 2007. Electrochemical determination of acetaminophen using a glassy carbon electrode coated with a single-wall carbon nanotube-dicetyl phosphate film. *Microchimica Acta*, 158: 131–136.
- SUN, D., XIE, X., CAI, Y., ZHANG, H. and WU, K., 2007. Voltammetric determination of Cd^{2+} based on the bifunctionality of single-walled carbon nanotubes–Nafion film. *Analytica Chimica Acta*, 581: 27–31.
- TAN, Y., DENG, W., GE, B., XIE, Q., HUANG, J. and YAO, S., 2009. Biofuel cell and phenolic biosensor based on acid-resistant laccase/glutaraldehyde

- functionalized chitosan–multiwalled carbon nanotubes nanocomposite film. *Biosensors and Bioelectronic*, 24: 2225-2231.
- TASHKHOURIAN, J., HORMOZI NEZHAD, M. R., KHODAVESI, J. and JAVADI, S., 2009. Silver nanoparticles modified carbon nanotube paste electrode for simultaneous determination of dopamine and ascorbic acid. *Journal of Electroanalytical Chemistry*, 633: 85-91.
- TAVANA, T., KHALILZADEH, M. A., KARIMI-MALEH, H., ENSAFI, A. A., BEITOLLAHI, H. and ZAREYEE, D., 2012. Sensitive voltammetric determination of epinephrine in the presence of acetaminophen at a novel ionic liquid modified carbon nanotubes paste electrode. *Journal of Molecular Liquids*, 168: 69–74.
- The United States Pharmacopeia XXII Revision, Mack Printing Company, Easton, PA, 1990.
- THOMAS, T., MASCARENHAS, R. J., COTTA, F., GUHA, K. S., SWAMY, B. E. K., MARTIS, P. and MEKHALIF, Z., 2013. Poly(Patton and Reeder's reagent) modified carbon paste electrode for the sensitive detection of acetaminophen in biological fluid and pharmaceutical formulations. *Colloids and Surfaces B*, 101: 91–96.
- TIAN, Y. Q., LI, N. B. and LUO, H. Q., 2009. Simultaneous determination of trace Zinc(II) and Cadmium(II) by differential pulse anodic stripping voltammetry using a mwcnts–nadbs modified stannum film electrode. *Electroanalysis*, 21 (23): 2584-2589.
- TOLEDO, R. A., SANTOS, M. C. D., CAVALHEIRO, E. T. G. and MAZO, L. H., 2005. Determination of dopamine in synthetic cerebrospinal fluid by SWV with a graphite-polyurethane composite electrode. *Analytical and Bioanalytical Chemistry*, 381: 1161–1166.
- TU, X., YAN, L., LUO, X., LUO, S. and XIE, Q., 2009. Electroanalysis of bisphenol-A at a multiwalled carbon nanotubes-gold nanoparticles modified glassy carbon electrode. *Electroanalysis*, 21 (22): 2491- 2494.
- TURCHAN, M., JARA-ULLOA, P., BOLLO, S., NUNEZ-VERGARA, L. J., SQUELLA, J. A. A. and LVAREZ-LUEJE, A., 2007. Voltammetric behaviour of bromhexine and its determination in pharmaceuticals. *Talanta*, 73: 913–919.
- UBOH, C. E., RUDY, J. A., SOMA, L. R., FENNELL, M., MAY, L., SAMS, R., RAILING, F. A., SHEL-LENBERGER, J. and KAHLER, M., 1991. Characterization of bromhexine and ambroxol in equine urine: effect of furosemide on identification and confirmation. *Journal of Pharmaceutical and Biomedical Analysis*, 9: 33–39.
- VELA, J., YANES, E. G. and STALCUP, A. M., 2001. Quantitative determination of clenbuterol, salbutamol and tulobuterol enantiomers by capillary electrophoresis. *Fresenius Journal of Analytical Chemistry*, 362: 212–219.
- WALCARIUS, A., 2008. Electroanalytical applications of microporous zeolites and mesoporous (organo)silicas: recent trends. *Electroanalysis*, 20: 711–738.
- WALCARIUS, A., 2001. Electrochemical applications of silica-based organic-inorganic hybrid materials. *Chemistry of Materials*, 13: 3351–3372.
- WAN, Q., WANG, X., YU, F., WANG, X. and YANG, N., 2009. Poly(taurine)/MWNT-modified glassy carbon electrodes for the detection of acetaminophen. *Journal of Applied Electrochemistry*, 39: 785-790.

- WANG, A., ZHANG, L., ZHANG, S. and FANG, Y., 2000. Determination of thiols following their separation by CZE with amperometric detection at a carbon electrode. *Journal of Pharmaceutical and Biomedical Analysis*, 23: 429–436.
- WANG, C., LI, C., TING, LI, XU, X. and WANG, C., 2006. Application of a single-wall carbon nano-tube film electrode to the determination of trace amounts of folic acid. *Microchimica Acta*, 152:233–238.
- WANG, J., LI, M., SHI, Z., LI, N. and GU, Z., 2001. Electrocatalytic oxidation of 3,4-dihydroxyphenylacetic acid at a glassy carbon electrode modified with single-wall carbon nanotubes. *Electrochimica Acta*, 47: 651–657.
- WANG, J., 2005. Carbon nanotube based electrochemical biosensors: A review. *Electroanalysis*, 17: 7–14.
- WANG, J., MUSAMEH, M. and LAOCHAROENSUK, R., 2005. Magnetic catalytic nickel particles for on-demand control of electrocatalytic processes. *Electrochemistry Communications*, 7: 652–656.
- WANG, J., MUSAMEH, M., LAOCHAROENSUK, R., GONZALEZ-GARCIA, O., ONI, J. and GERVASIO, D., 2006. Pt/Ru-functionalized magnetic spheres for a magnetic-field stimulated methanol and oxygen redox processes: Towards on-demand activation of fuel cells. *Electrochemistry Communications* 8: 1106–1110.
- WANG, S. F., XIE, F. and HU, R. F., 2007. Carbon-coated nickel magnetic nanoparticles modified electrodes as a sensor for determination of acetaminophen. *Sensors and Actuators B*, 123: 495–500.
- WANG, Y., WANG, L., TIAN, T., YAO, G., HU, X., YANG, C. and XU, Q., 2012. A highly sensitive and automated method for the determination of hypoxanthine based on lab-on-valve approach using Fe₃O₄/MWCNTs/ β -CD modified electrode. *Talanta*, 99: 840–845.
- WANG, Y., LIU, H. and WANG, F. and GAO, Y., 2012. Electrochemical oxidation behavior of methotrexate at DNA/SWCNT/Nafion composite film-modified glassy carbon electrode. *Journal of Solid State Electrochemistry*, 16: 3227–3235.
- WANG, Y. and BI, C., 2013. Simultaneous electrochemical determination of ascorbic acid, dopamine and uric acid using poly (tyrosine)/functionalized multi-walled carbon nanotubes composite film modified electrode. *Journal of Molecular Liquids*, 177: 26–31.
- WEI, Y., HUANG, Q. A., LI, M. G., HUANG, X. J. FANG, B. and WANG, L., 2011. CeO₂ nanoparticles decorated multi-walled carbon nanotubes for electrochemical determination of guanine and adenine. *Electrochimica Acta*, 56: 8571–8575.
- WEI, Y., ZHANG, Q., SHAO, C., LI, C., ZHANG, L. and LI, X., 2010. Voltammetric determination of salbutamol on a glassy carbon electrode coated with a nanomaterial thin film. *Journal of Analytical Chemistry*, 65: 398–403.
- WENSING, M. W., LIU, D. Y., SMITH, B. W. and WINEFORDNER, J. D., 1994. Determination of lead in whole blood using a capacitively coupled 4wave plasma atomic emission spectrometer. *Analytica Chimica Acta*, 299: 1–7.
- WILDGOOSE, G. G., BANKS, C. E., LEVENTIS, H. C. and COMPTON, R. G., 2006. Chemically modified carbon nanotubes for use in electroanalysis. *Microchimica Acta*, 152:187–214.

- WU, F. H., ZHAO, G. C., WEI, X. W. and YANG, Z. S., 2004. Electrocatalysis of tryptophan at multi-walled carbon nanotube modified electrode. *Microchimica Acta*, 144: 243–247.
- WU, H. and YU, S., 2005. The fabrication of a colloidal gold–carbon nanotubes composite film on a gold electrode and its application for the determination of cytochrome c. *Colloids and Surfaces B: Biointerfaces* 41: 299–304.
- WU, K., FEI, J. and HU, S., 2003. Simultaneous determination of dopamine and serotonin on a glassy carbon electrode coated with a film of carbon nanotubes. *Analytical Biochemistry*, 318: 100–106.
- WU, K., HU, S., FEI, J. and BAI, W., 2003. Mercury-free simultaneous determination of cadmium and lead at a glassy carbon electrode modified with multi-wall carbon nanotubes. *Analytica Chimica Acta*, 489: 215–221.
- XI, X., MING, L. and LIU, J., 2011. Electrochemical determination of thiamazole at a multi-wall carbon nanotube modified glassy carbon electrode. *Journal of Applied Electrochemistry*, 40: 1449–1454.
- XIANG, C., ZOU, Y., XIE, J. and FEI, X., 2006. Voltammetric determination of L-dopa using a carbon nanotubes-nafion modified glassy carbon electrode. *Analytical Letters*, 39 (13): 2569–2579.
- XIAO, L., WILDGOOSE, G. G. and COMPTON, R. G., 2009. Exploring the origins of the apparent “electrocatalysis” observed at C60 film-modified electrodes. *Sensors and Actuators B*, 138: 524–531.
- XU, H., ZENG, L., XING, S., XIAN, Y., SHI, G. and JIN, L., 2008. Ultrasensitive voltammetric detection of trace lead(II) and cadmium(II) using MWCNTS-Nafion/Bismuth composite electrodes. *Electroanalysis*, 20 (24): 2655–2662.
- XU, Q. and WANG, S. F., 2005. Electrocatalytic oxidation and direct determination of L-tyrosine by square wave voltammetry at multi-wall carbon nanotubes modified glassy carbon electrodes. *Microchimica Acta*, 151: 47–52.
- XU, Y., WANG, F., WANG, L., ZHAO, F., YANG, B. and YE, B., 2012. Sensitive voltammetric sensor of dihydromyricetin based on Nafion/SWNT-modified glassy carbon electrode. *Journal of Solid State Electrochemistry*, 16: 1473–1480.
- XU, Z., CHEN, X., QU, X. and DONG, S., 2004. Electrocatalytic oxidation of catechol at multi-walled carbon nanotubes modified electrode. *Electroanalysis*, 16: 684–687.
- YANG, H. Y. and SUN, I. W., 1998. Cathodic stripping voltammetric determination of tellurium(IV) at a Nafion/8-quinolinol mercury film modified electrode. *Analytica Chimica Acta*, 358: 285–290.
- YANG, S., YIN, Y., LI, G., YANG, R., LI, J. and QU, L., 2013. Immobilization of gold nanoparticles on multi-wall carbon nanotubes as an enhanced material for selective voltammetric determination of dopamine. *Sensors and Actuators B*, 178: 217–221.
- YANG, G., YU, L., JIA, J. and ZHAO, Z., 2012. 4-Aminobenzoic acid covalently modified glassy carbon electrode for sensing paracetamol at different temperatures. *Journal of Solid State Electrochemistry*, 16: 1363–1368.
- YAZHEN, W., 2011. Electrochemical determination of methimazole based on the acetylene black/chitosan film electrode and its application to rat serum samples. *Bioelectrochemistry*, 81: 86–90.

- YE, J. S., WEN, Y., ZHANG, W. D., GAN, L. M., XU, G. Q. and SHEU, F. S., 2003. Selective voltammetric detection of uric acid in the presence of ascorbic acid at well-aligned carbon nanotube electrode. *Electroanalysis*, 15 (21): 1693-1698.
- YI, H., 2003. Anodic stripping voltammetric determination of mercury using multi-walled carbon nanotubes film coated glassy carbon electrode. *Analytical and Bioanalytical Chemistry*, 377: 770-774.
- YILMAZ, N., OZKAN, S. A., USLU, B., SENTURK, Z. and BIRYOL, I., 1998. Determination of terbutaline based on oxidation by voltammetry. *Turkish Journal of Chemistry*, 22: 175-182.
- YOGESWARAN, U., THIAGARAJAN, S. and CHEN, S. M., 2007. Nanocomposite of functionalized multiwall carbon nanotubes with nafion, nano Platinum, and nano gold biosensing film for simultaneous determination of ascorbic acid, epinephrine, and uric acid. *Analytical Biochemistry*, 365 :122-131.
- ZEN, J. M and TING, Y. S., 1996. Square-wave voltammetric stripping analysis of lead(II) at a Nafion®/copper-mercury film electrode. *Analytica Chimica Acta*, 332: 59-65.
- ZENG, B., WEI, S., XIAO, F. AND ZHAO, F., 2006. Voltammetric behavior and determination of rutin at a single-walled carbon nanotubes modified gold electrode. *Sensors and Actuators B- Chemical*, 115: 240-246.
- ZENG, Y., ZHOU, Y., KONG, L., ZHOU, T. and SHI, G., 2013. A novel composite of SiO₂-coated graphene oxide and molecularly imprinted polymers for electrochemical sensing dopamine. *Biosensors and Bioelectronics*, 45: 25-33.
- ZENGIN, H. and KALAYCI, G., 2010. Synthesis and characterization of polyaniline/activated carbon composites and preparation of conductive films. *Materials Chemistry and Physics*, 120: 46-53.
- ZHANG, H., ZHAO, J., LIU, H., LIU, R., WANG, H. and LIU, J., 2010. Electrochemical determination of diphenols and their mixtures at the multiwall carbon nanotubes/poly(3-methylthiophene) modified glassy carbon electrode. *Microchimica Acta*, 169: 277-282.
- ZHANG, M. G., SMITH, A. and GORSKI, W., 2004. Carbon nanotube-chitosan system for electrochemical sensing based on dehydrogenase enzymes. *Analytical Chemistry*, 76: 5045-5050.
- ZHANG, X., ZHAO, D., FENG, L., JIA, L. and WANG, S., 2010. Electrochemical sensor for procaine based on a glassy carbon electrode modified with poly-amidosulfonic acid and multi-walled carbon nanotubes. *Microchimica Acta*, 169:153-159.
- ZHANG, Y., KANG, T. F., WAN, Y. W. and CHEN, S. Y., 2009. Gold nanoparticles-carbon nanotubes modified sensor for electrochemical determination of organophosphate pesticides. *Microchimica Acta*, 165: 307-311.
- ZHANG, S., SUN, W., ZHANG, W., QI, W., JIN, L., YAMAMOTO, K., TAO, S. and JIN, J., 1999. Determination of thiocompounds by liquid chromatography with amperometric detection at a Nafion/indium hexacyanoferrate film modified electrode. *Analytica Chimica Acta*, 386: 21-30.

- ZHAO, S., BAI, W., YUAN, H. and XIAO, D., 2006. Detection of paracetamol by capillary electrophoresis with chemiluminescence detection. *Analytica Chimica Acta*, 559: 195–199.
- ZHOU, Q., XIE, Q., FU, Y., SU, Z., JIA, X. and YAO, S., 2007. Electrodeposition of carbon nanotubes-chitosan-glucose oxidase biosensing composite films triggered by reduction of p-benzoquinone or H₂O₂. *The Journal of Physical Chemistry B*, 111: 11276-11284.
- ZHU, Y. H., ZHANG, Z. L. and PANG, D. W., 2005. Electrochemical oxidation of theophylline at multi-wall carbon nanotube modified glassy carbon electrodes. *Journal of Electroanalytical Chemistry*, 581: 303–309.

CURRICULUM VITAE

PERSONAL INFORMATION

Name : Ayşegül KUTLUAY BAYTAK
Nationality : Turkish
Place of Birth and Date : Sanliurfa- August, 26, 1984
Phone Number : + 90 531 5822275
E-Mail : kutluay.aysegul@gmail.com

EDUCATION

High School : Sanliurfa Anatolian High School 1995-2002
BSc Degree : Harran University, Department of Chemistry 2002-2006
MSc Degree : Harran University, Department of Chemistry 2007-2009
PhD Degree : Harran University, Department of Chemistry 2010-2014

WORK EXPERINCE

2006- Harran University, Department of Chemistry Research Assistant

PUBLICATIONS

1. Aslanoglu M, Abbasoglu S, Karabulut S, **Kutluay A**, *Electrochemical determination of dopamine in the presence of ascorbic acid using a poly(3-acetylthiophene) modified glassy carbon electrode*. ACTA CHIMICA SLOVENICA, 54 (4): 834-839, **2007**.
2. Aslanoglu M, **Kutluay A**, Abbasoglu S, Karabulut S, *A poly(3-acetylthiophene) modified glassy carbon electrode for selective voltammetric measurement of uric*

acid in urine sample. CHEMICAL & PHARMACEUTICAL BULLETIN, 56 (3): 282-286, **2008**. DOI: 10.1248/cpb.56.282.

3. Aslanoglu M, **Kutluay A**, Karabulut S, Abbasoglu S, *Voltammetric determination of adrenaline using a poly(1-methylpyrrole) modified glassy carbon electrode*. JOURNAL OF THE CHINESE CHEMICAL SOCIETY, 55: (4) 794-800, **2008**.

4. Aslanoglu M, **Kutluay A**, Goktas S, Karabulut S, *Voltammetric behaviour of levodopa and its quantification in pharmaceuticals using a beta-cyclodextrine doped poly(2,5-diaminobenzenesulfonic acid) modified electrode*. JOURNAL OF CHEMICAL SCIENCES, 121 (2): 209-215, **2009**.

5. Aslanoglu M, Goktas S, Karabulut S, **Kutluay A**, *Cyclic Voltammetric Determination of Noradrenaline in Pharmaceuticals Using Poly(3-acetylthiophene)-Modified Glassy Carbon Electrode*. CHEMIA ANALITYCZNA, 54 (4): 643-653, **2009**.

6. **Kutluay A** and Aslanoglu M, *Electrocatalytic Oxidation of Isoproterenol and its Voltammetric Determination in Pharmaceuticals and Urine Samples Using a Poly(1-methylpyrrole)-DNA Modified Electrode*. ACTA CHIMICA SLOVENICA, 57 (1): 157-162, **2010**.

7. Kasumov V T, Koksal F, **Kutluay A**, *Spectroscopic and electron-transfer reactivity studies of bulky bis(N-cycloalkyl-3,5-Bu-t(2)-salicylaldiminato)copper(II) complexes: Generation of uncoordinated and coordinated phenoxyl radicals*. SPECTROCHIMICA ACTA PART A-MOLECULAR AND BIOMOLECULAR SPECTROSCOPY, 76(2): 99-106, **2010**. DOI: 10.1016/j.saa.2010.02.016.

8. **Kutluay A** and Aslanoglu M, *Multi-walled carbon nanotubes/electrocopolymerized nanocobalt- poly(pivalic acid) composite film coated glassy carbon electrode for the determination of methimazole*. SENSORS & ACTUATORS B: CHEMICAL, 171-172: 1216-1221, **2012**. DOI: 10.1016/j.snb.2012.06.083. **(produced from PhD Thesis)**

9. **Kutluay A** and Aslanoglu M, *Selective detection of albuterol in the presence of uric acid using a glassy carbon electrode modified with multi-walled carbon nanotubes and poly(pivalic acid)*. SENSORS & ACTUATORS B :CHEMICAL, 177: 703–709, **2013**. DOI:10.1016/j.snb.2012.11.081. **(produced from PhD Thesis)**

10. Kasumov V T, Yerli Y, **Kutluay A**, Aslanoglu M, *Synthesis, spectroscopy, magnetic and redox behaviors of copper(II) complexes with tert-butylated salen type ligands bearing bis(4-aminophenyl) ethane and bis(4-aminophenyl)amide backbones*. SPECTROCHIMICA ACTA PART A: MOLECULAR AND BIOMOLECULAR SPECTROSCOPY, 104:203–212, **2013**. DOI: 10.1016/j.saa.2012.11.061.

11. **Kutluay A** and Aslanoglu M, *Modification of electrodes using conductive porous layers to confer selectivity for the voltammetric detection of paracetamol in the presence of ascorbic acid, dopamine and uric acid*. SENSORS & ACTUATORS

B : CHEMICAL, 185: 398– 404, **2013**. DOI: 10.1016/j.snb.2013.05.025. **(produced from PhD Thesis)**

12. Kutluay A and Aslanoglu M, *Nickel nanoparticles functionalized multi-walled carbon nanotubes at Platinum electrodes for the detection of bromhexine*. SENSORS & ACTUATORS B : CHEMICAL, 192: 720-724, **2014**. DOI:10.1016/j.snb.2013.11.047. **(produced from PhD Thesis)**